

**Molecular characterisation of pigeon paramyxovirus and other  
viruses identified by deep sequencing in pigeons and doves in  
South Africa**

By

Michaela Catharine Hayes

Submitted in partial fulfilment of the requirements for the degree of Master of  
Science in the Department of Production Animal Studies in the Faculty of  
Veterinary Science, University of Pretoria

Date submitted: 31 October 2023

## **DECLARATION**

I, Michaela Catharine Hayes (student number 18120122), hereby declare that this dissertation, “Molecular characterisation of pigeon paramyxovirus and other viruses identified by deep sequencing in pigeons and doves in South Africa”, is submitted in accordance with the requirements for the Master of Science (MSc) degree at University of Pretoria, is my own original work and has not previously been submitted to any other institution of higher learning. All sources cited or quoted in the research paper are indicated and acknowledged with a comprehensive list of references.

---

Michaela Catharine Hayes

## **ETHICS STATEMENT**

The author, whose name appears on the title page of this thesis, has obtained, for the research described in this work, the applicable research ethics approval. The author declares that she has observed the ethical standards required in terms of the University of Pretoria's Code of ethics for researchers and the Policy guidelines for responsible research.

## ACKNOWLEDGEMENTS

*“I can do all things through Christ who strengthens me”*

First and foremost, I would want to praise and thank God, the Almighty, for bestowing upon me numerous benefits, knowledge, and opportunities that have enabled me to complete this project.

Aside from my efforts, the success of my project is heavily reliant on the support and guidance of many people. I'd want to take this opportunity to thank everyone who contributed to the successful completion of my project. I am at loss for words to convey my thanks, but I am grateful to everyone who helped me complete this project. It would be hard to identify everyone, but certain people deserve the heartfelt gratitude:

- I am extremely grateful for Professor Celia Abolnik (Supervisor), for whom I would like to give a very special thanks for her outstanding mentorship, continuous support, guidance, and expert advice, always giving me constructive feedback and helping me countlessly with encouragement throughout the research and writing of the project. Thank you, Prof, for the endless support and patience throughout the years and for granting me this opportunity. I truly appreciate everything!
- To my fiancé, thank you for being my unwavering source of support throughout my studies and bringing me tea during the numerous late nights. I couldn't have done it without you.
- To my caring, loving and supportive mother and sister, my deepest gratitude. Your words of encouragement, emotional and financial support when it was tough were really appreciated. Thank you.
- Agricultural Sector Education Training Authority (AgriSETA) and University of Pretoria (UP) Postgraduate Committee for the financial support throughout my studies.
- To Karen Ebersohn from the Department of Veterinary Tropical Diseases who offered invaluable support, guidance and help on the cell culture of QH9-2/1 cells used in this project.
- To Dr. Monakali for generously granting us permission to utilize the sequence data from sample S460-23.
- Friends and colleagues - for their friendship, and moral support.

## SUMMARY

By: Michaela Catharine Hayes  
Supervisor: Professor C. Abolnik  
Department: Production Animal Studies  
Degree: MSc

Pigeons, whether feral or bred for meat or sport like pigeon racing, are susceptible to a variety of diseases, many of which are caused by viral infections. Newcastle disease (ND) caused by *Orthoavulavirus javaense*, an avian paramyxovirus 1 (APMV1) virus is an example of a viral infection. Pigeon paramyxovirus (PPMV), a pigeon-specific variant of NDV that causes pigeon epidemics, is one of the most serious infectious illnesses within this host. The focus of the first part of the study was dedicated to investigating the molecular epidemiology of PPMVs in South Africa from 2012 onwards. A total of thirty-six field samples and isolated viruses were initially examined using real-time reverse transcriptase-polymerase chain reaction (RT-PCR) targeting a partial fragment of the M and F gene. Among these, it was observed that the kidneys from recent clinical cases exhibited the highest viral loads. Conventional RT-PCR, Sanger DNA sequencing, virus isolation in QH9/2-1 quail cells and Ion Torrent Next-Generation Sequencing (NGS) were applied, and the complete or partial genomes of twenty-one PPMVs were obtained for further analysis. Phylogenetic analysis grouped the recent South African viruses into subgenotypes VI.2.1.1.2.1 (VIj) and VI.2.1.1.2.2 (Vik). Based on a partial phylogenetic analysis of the fusion gene, these South African viruses displayed a close genetic relationship to PPMV strains sampled from pigeons in Switzerland and Belgium in 2005, 2007 and 2022. However, a phylogenetic analysis based on the complete fusion gene sequence revealed that the South Africa viruses were closely related to PPMV strains sampled from pigeons in Australia and Belgium in 2005, 2007 and 2011. South Africa PPMVs and other African PPMV strains included in a blast results analysis indicated no relatedness between each other, suggesting no intra-continental spread. The Ion Torrent reads obtained in the previous section were investigated further for the presence of other viruses by utilising a *de novo* assembly approach and BLAST analysis. Additional viruses detected included Autographacalifornica nucleopolyhedrovirus, Avian coronavirus (Pigeon coronavirus), Avian endogenous virus, Avian leukosis virus, Avian myeloblastosis virus, Avian orthoavula virus 1 (Pigeon

paramyxovirus), Avian sarcoma virus (Rous sarcoma virus), Bovine viral diarrhea virus, pigeon circovirus (PiCV), Human Gammaherpesvirus, Infectious bronchitis virus, porcine rotavirus, Semliki Forest virus, Tasmanian devil retrovirus, Torque teno virus (pigeon torque teno virus) and white spot syndrome virus. A phylogenetic analysis was performed with the three pigeon circovirus genomes discovered in a previous section through a metagenomic approach, plus eleven additional pigeon circovirus genome sequences previously detected during research at the University of Pretoria in recent years. The analysis of genotype classification yielded intriguing results, with 10 samples falling under the G genotype, two in the H genotype, and the final two in genotypes E and D, respectively. These samples displayed strong genetic association with PiCV strains obtained from pigeons in different countries, such as Belgium, Brazil, China, Germany, Italy, and Poland, from 2000 to 2021. This finding underscores the widespread distribution and genetic diversity of PiCV strains across international pigeon populations over the past two decades.

## TABLE OF CONTENTS

|   | <b>Page</b> |
|---|-------------|
| Declaration   | i           |
| Ethics Statement  | ii          |
| Acknowledgements  | iii         |
| Summary   | iv          |
| Table of Contents   | vi          |
| List of Tables  | xi          |
| List of Figures   | xiii        |
| List of Abbreviations and Symbols                         | xv          |
| <b>CHAPTER 1: LITERATURE REVIEW</b>                       | <b>1</b>    |
| 1.1 Introduction to Newcastle disease                     | 1           |
| 1.1.1 Pigeon Paramyxovirus                                | 2           |
| 1.1.1.1 History   | 2           |
| 1.1.1.2 Classification and nomenclature                   | 3           |
| 1.1.1.3 Morphology  | 7           |
| 1.1.1.4 Epidemiology                                      | 9           |
| 1.1.1.4.1 Host range                                      | 9           |
| 1.1.1.4.2 Transmission and spread                         | 10          |
| 1.1.1.4.3 Risk factors                                    | 11          |
| 1.1.1.4.4 Stability of the virus                          | 12          |
| 1.1.1.4.5 Lesions associated with the virus               | 12          |
| 1.1.1.4.5.1 Macroscopic lesions associated with the virus | 13          |
| 1.1.1.4.5.2 Microscopic lesions associated with the virus | 13          |
| 1.1.1.5 Viral replication cycle                           | 13          |
| 1.1.1.5.1 Nucleocapsid protein                            | 16          |
| 1.1.1.5.2 Phosphoprotein protein                          | 17          |
| 1.1.1.5.3 Matrix protein                                  | 18          |
| 1.1.1.5.4 Fusion protein                                  | 18          |
| 1.1.1.5.5 Hemagglutinin-neuraminidase protein             | 19          |
| 1.1.1.5.6 Large polymerase protein                        | 19          |
| 1.1.1.5.7 V protein                                       | 20          |

|   | <b>Page</b> |
|---|-------------|
| 1.1.1.5.8 W protein   | 20          |
| 1.1.1.6 Economic impact of NDV  | 20          |
| 1.1.1.7 Diagnosis of NDV  | 21          |
| 1.1.1.7.1 Clinical diagnosis  | 21          |
| 1.1.1.7.1.1 Velogenic viscerotropic   | 22          |
| 1.1.1.7.1.2 Velogenic neurotropic   | 22          |
| 1.1.1.7.1.3 Mesogenic   | 22          |
| 1.1.1.7.1.4 Lentogenic  | 23          |
| 1.1.1.7.2 Serological diagnosis   | 23          |
| 1.1.1.7.3 Virus isolation   | 24          |
| 1.1.1.7.4 Virus identification  | 24          |
| 1.1.1.7.5 <i>In vivo</i> and <i>In vitro</i>  | 26          |
| 1.1.1.8 Treatment and control strategies  | 27          |
| 1.1.1.9 History of Newcastle disease virus in South Africa                                    | 28          |
| 1.1.1.10 Previous findings for PPMV in South Africa with recent outbreaks and cases reported. | 32          |
| 1.2 Introduction to Circovirus  | 38          |
| 1.2.1 Pigeon circovirus   | 39          |
| 1.2.1.1 History   | 40          |
| 1.2.1.2 Morphology  | 40          |
| 1.2.2 Classification and nomenclature   | 43          |
| 1.2.3 Epidemiology  | 44          |
| 1.2.3.1 Host range  | 44          |
| 1.2.3.2 Transmission and spread   | 45          |
| 1.2.3.3 Stability of the virus  | 46          |
| 1.2.3.4 Lesions associated with the virus   | 46          |
| 1.2.4 Viral replication cycle   | 46          |
| 1.2.5 Diagnosis of Circovirus   | 47          |
| 1.2.5.1 Virus isolation   | 48          |
| 1.2.6 Treatment and control strategies  | 48          |
| 1.3 Other viruses associated with pigeons   | 49          |
| 1.3.1 <i>Astroviridae</i>   | 49          |



|  | <b>Page</b> |
|--|-------------|
| 1.3.2 <i>Picornaviridae</i>  | 50          |
| 1.3.3 <i>Coronaviridae</i>   | 51          |
| 1.3.4 <i>Reoviridae</i>  | 52          |
| 1.3.5 <i>Adenoviridae</i>  | 53          |
| 1.3.6 <i>Herpesviridae</i>   | 54          |
| 1.3.7 <i>Poxviridae</i>  | 55          |
| 1.3.8 <i>Retroviridae</i>  | 55          |
| 1.3.9 <i>Orthomyxoviridae</i>  | 57          |
| 1.3.10 <i>Nimaviridae</i>  | 57          |
| 1.3.11 <i>Togaviridae</i>  | 58          |
| 1.3.12 <i>Flaviviridae</i>   | 58          |
| 3.1.13. <i>Anelloviridae</i>   | 58          |
| <b>CHAPTER 2: MOLECULAR EPIDEMIOLOGY OF PIGEON<br/>PARAMYXOVIRUS IN SOUTH AFRICA FROM 2012 TO 2022</b> | <b>60</b>   |
| 2.1 Introduction   | 60          |
| 2.2 Aims and objectives of this study  | 64          |
| 2.3 Materials and methods  | 65          |
| 2.3.1 Ethical considerations   | 65          |
| 2.3.2 Samples  | 65          |
| 2.3.3 Sample processing  | 69          |
| 2.3.4 RNA extraction   | 70          |
| 2.3.5 Real-time RT-PCR   | 71          |
| 2.3.6 Conventional RT-PCR and Sanger DNA sequencing  | 72          |
| 2.3.7 Whole Transcriptome Amplification for Ion Torrent NGS  | 74          |
| 2.3.8 Bioinformatics analysis  | 75          |
| 2.3.9 Virus isolation  | 77          |
| 2.3.9.1 Preparation of cells   | 77          |
| 2.3.9.2 Trypsinization of cells  | 77          |
| 2.3.9.3 Splitting of cells for growth continuation   | 78          |
| 2.3.9.4 Counting and preparing cell plates   | 78          |
| 2.3.9.5 Infection of cell plates   | 79          |
| 2.3.9.6 Microscopic analysis   | 80          |
| 2.3.9.7 Further passage of infected cells  | 80          |

|   | <b>Page</b> |
|---|-------------|
| 2.3.9.8 Preparing passage samples for Ion Torrent NGS   | 81          |
| 2.3.8.9 Freezing of cells for storage   | 81          |
| 2.4 Results   | 82          |
| 2.4.1 Screening of field samples collected in 2022 by real-time RT-PCR  | 82          |
| 2.4.2 Conventional RT-PCR and sequence analysis   | 83          |
| 2.4.3 Virus isolation with cell culture   | 84          |
| 2.4.4 Bioinformatic analysis  | 90          |
| 2.4.5 Phylogenetic analysis   | 93          |
| 2.5 Discussion and Conclusion   | 102         |
| <b>CHAPTER 3: INVESTIGATION OF THE VIRAL METAGENOME OF PIGEONS INFECTED WITH PIGEON PARAMYXOVIRUS 1</b>                               | <b>105</b>  |
| 3.1 Introduction  | 105         |
| 3.2 Aims and objectives of this study   | 107         |
| 3.3 Materials and Methods   | 108         |
| 3.3.1 Samples   | 108         |
| 3.3.2 Viral metagenomics analysis   | 109         |
| 3.3.3 Phylogenetic analysis   | 110         |
| 3.4 Results   | 111         |
| 3.4.1 Viral metagenomic analysis  | 111         |
| 3.4.2 Phylogenetic analysis   | 117         |
| 3.4.2.1 Pigeon torque teno virus  | 117         |
| 3.4.2.2 Avian endogenous retrovirus   | 118         |
| 3.5 Discussion and Conclusion   | 120         |
| <b>CHAPTER 4: EPIDEMIOLOGICAL INSIGHTS INTO PIGEON CIRCOVIRUS VARIANTS IN SOUTH AFRICA: A MOLECULAR PERSPECTIVE FROM 2014 TO 2023</b> | <b>124</b>  |
| 4.1 Introduction  | 124         |
| 4.2 Aims and objectives of this study   | 125         |
| 4.3 Materials and Methods   | 126         |
| 4.3.1. Samples  | 126         |
| 4.3.2. Sample processing  | 126         |

|  | <b>Page</b> |
|--|-------------|
| 4.3.3. RNA extraction  | 127         |
| 4.3.4. Whole Transcriptome Amplification for Ion Torrent NGS | 127         |
| 4.3.5. Bioinformatic analysis                                | 127         |
| 4.4 Results  | 129         |
| 4.4.1. Collection of samples                                 | 129         |
| 4.4.2. Bioinformatic analysis                                | 129         |
| 4.4.3. Phylogenetic analysis                                 | 130         |
| 4.5 Discussion and Conclusion                                | 134         |
| <b>REFERENCES</b>  | 136         |
| <b>APPENDICES</b>  |             |
| Appendix A : Ethics Section 20                               | 165         |
| Appendix B : Animal Ethics Committee                         | 167         |
| Appendix C : Contigs blast results                           | 169         |
| Appendix D : Biosafety Level 3 Certificate of Compliance     | 170         |

## LIST OF TABLES

|                    |  | Page |
|--------------------|--|------|
| <b>Table 1.1:</b>  | The taxonomical division of the pigeon paramyxovirus type 1.   | 4    |
| <b>Table 1.2:</b>  | The updated consensus classification criteria.   | 6    |
| <b>Table 1.3:</b>  | Genome length characteristics of PPMV-1 isolates.  | 9    |
| <b>Table 1.4:</b>  | Summary of the genes involved in the virus replication cycle.  | 16   |
| <b>Table 1.5:</b>  | The values for measuring virulence for each different pathotype of NDV virus during <i>in vivo</i> testing.            | 27   |
| <b>Table 1.6:</b>  | Data necessary to report a disease/ outbreak for any species in general.   | 34   |
| <b>Table 1.7:</b>  | Number of ND cases reported for each South African province from 2010 to 2021.   | 36   |
| <b>Table 1.8:</b>  | Terminology and case definitions for Pigeon Circovirus-Related diseases, considering clinical and laboratory criteria. | 39   |
| <b>Table 2.1:</b>  | Samples analysed in this study.  | 67   |
| <b>Table 2.2:</b>  | Different samples and sample types analysed in this study with various methods.  | 69   |
| <b>Table 2.3:</b>  | Primers and probes used for real-time RT-PCR detection of NDV.   | 72   |
| <b>Table 2.4:</b>  | Primers used for conventional RT-PCR amplification of a partial region of the F gene.                                  | 73   |
| <b>Table 2.5:</b>  | Calculation of appropriate cell density to seed 6 well-plates.   | 77   |
| <b>Table 2.6:</b>  | Cycle threshold (Ct) values for PPMV detected by rRT-PCR in different organs of infected doves.                        | 82   |
| <b>Table 2.7:</b>  | Concentrations of purified RT-PCR amplicons for Sanger DNA sequencing.   | 83   |
| <b>Table 2.8:</b>  | Effects observed in the cells infected with the corresponding samples.   | 86   |
| <b>Table 2.9:</b>  | rRT-PCR results (CT values) of samples tested after each passage.  | 88   |
| <b>Table 2.10:</b> | Sequence data recovered for samples sequenced with Ion Torrent NGS.  | 91   |

|  | <b>Page</b> |
|--|-------------|
| <b>Table 2.11:</b> Consensus sequence data and percentage of indicated region (F gene/ Whole genome) recovered for samples sequenced with Ion Torrent NGS. | 92          |
| <b>Table 3.1:</b> Samples used in the study of the virome.   | 108         |
| <b>Table 3.2:</b> Viruses identified in the deep sequencing of samples from pigeons and doves.   | 112         |
| <b>Table 3.3:</b> Virome results for pigeon samples and percentage genome recovered of reads mapped.   | 116         |
| <b>Table 4.1:</b> Samples analysed in this study.  | 126         |
| <b>Table 4.2:</b> Sequence information obtained from samples subjected to Ion Torrent NGS.   | 129         |
| <b>Table 4.3:</b> Data on consensus sequences and the percentage of recovery for samples processed through Ion Torrent NGS.                                | 130         |

## LIST OF FIGURES

|   | <b>Page</b> |
|---|-------------|
| <b>Figure 1.1:</b> Diagram of the paramyxovirus structure.  | 7           |
| <b>Figure 1.2:</b> Illustration of the virus genome.  | 8           |
| <b>Figure 1.3:</b> Schematic representation of the virus replication cycle.   | 15          |
| <b>Figure 1.4:</b> Schematic diagram of the formation of the V and W protein by RNA editing.  | 17          |
| <b>Figure 1.5:</b> Molecular amplification of the F gene and sequential differentiation and pathotyping of the different strains of avian paramyxovirus -1 (APMV-1) and pigeon paramyxovirus -1 (PPMV-1). | 26          |
| <b>Figure 1.6:</b> A summary timeline of all the ND cases and various genotypes isolated in South Africa between 1994 and 2014.   | 30          |
| <b>Figure 1.7:</b> Newcastle disease and PPMV outbreaks reported by the Provincial Veterinary Services from 2015 to 2021 for each province in South Africa.   | 35          |
| <b>Figure 1.8:</b> Total ND cases reported for each province from 2010 to 2021.   | 37          |
| <b>Figure 1.9:</b> Diagram of the circovirus structure.   | 40          |
| <b>Figure 1.10:</b> Circovirus genome structure.  | 41          |
| <b>Figure 1.11:</b> Pigeon circovirus genome structure.   | 42          |
| <b>Figure 2.1:</b> Locations where samples were collected between February 2022 and September 2022, as indicated by the red stars.  | 66          |
| <b>Figure 2.2:</b> Agarose gel electrophoresis showing amplification of 580 bp fragments spanning the partial M and F genes of NDV.   | 83          |
| <b>Figure 2.3:</b> QH9-2/1 cell cultures after 24 and 96 hours seeding in a T-25 flask.   | 84          |
| <b>Figure 2.4:</b> Cell morphology during the passages.   | 87          |
| <b>Figure 2.5:</b> Negatively stained paramyxovirus particles and nucleocapsids of sample DOZA005M22.   | 89          |

|  | <b>Page</b> |
|--|-------------|
| <b>Figure 2.6:</b> Amino acid sequences at the F protein cleavage site (amino acids 112 - 117) for F gene sequences used.  | 93          |
| <b>Figure 2.7:</b> Maximum likelihood phylogenetic tree based on a partial fragment of the fusion gene (360 nt) of the dataset used for classification purposes.   | 94          |
| <b>Figure 2.8:</b> Maximum likelihood phylogenetic tree based on a partial fragment of the fusion gene (360 nt) of South African PPMVs sequenced in this study and the closest relatives in GenBank.   | 96          |
| <b>Figure 2.9:</b> Maximum likelihood phylogenetic tree based on a full fragment of the fusion gene (1700 nt) of South African PPMVs sequenced in this study and the closest relatives in GenBank.   | 98          |
| <b>Figure 2.10:</b> Maximum likelihood phylogenetic trees based on a partial fragment of the matrix and fusion gene (374 nt) of 14 South African PPMV samples sequenced in this study, previously South African-published PPMV samples and closest relatives in GenBank. | 100         |
| <b>Figure 3.1:</b> Summary of the steps used for the virome analysis of sequencing results for pigeon and dove samples.  | 109         |
| <b>Figure 3.2:</b> Maximum likelihood phylogenetic tree of PTTV based on partial genomes spanning over the <i>rep</i> and <i>cap</i> gene (539 nt) with different species of <i>Anelloviridae</i> family.  | 118         |
| <b>Figure 3.3:</b> Maximum likelihood phylogenetic tree of AERV based on partial genomes spanning over the <i>gag-env</i> gene (1577bp).   | 119         |
| <b>Figure 4.1:</b> Maximum likelihood phylogenetic tree of PiCV based on partial genomes spanning over the <i>rep</i> gene (880 nt).   | 131         |
| <b>Figure 4.2:</b> Dendrogram of the different PiCV genotypes based on a partial fragment of the <i>cap</i> gene (536 nt) used for genotype classification purposes.   | 133         |

## LIST OF ABBREVIATIONS AND SYMBOLS

### Abbreviations

|                  |  |
|------------------|--|
| aa:              | Amino acids  |
| AERV:            | Avian endogenous retrovirus                                  |
| AEV:             | Avian encephalitis virus                                     |
| ALV:             | Avian leukosis virus   |
| AML:             | Acute myeloblastic leukaemia                                 |
| AMV:             | Avian myeloblastosis virus                                   |
| APMV-1:          | Avian paramyxovirus 1  |
| BHQ:             | Black hole quencher  |
| bp:              | Base pairs   |
| BSL3:            | Biosafety Laboratory 3                                       |
| BVDV:            | Bovine viral diarrhea virus                                  |
| CAstV:           | Chicken astrovirus   |
| CD:              | Connecting domain  |
| CFM:             | Cryopreservation Media                                       |
| Ct:              | Cycle threshold  |
| CTD:             | C-terminal domain  |
| CPE:             | Cytopathic effects   |
| CPT:             | Cape Town  |
| DALRRD:          | Department of Agriculture, Land Reform and Rural Development |
| DAsV:            | Duck astrovirus  |
| DHAV-1:          | Duck hepatitis A virus 1                                     |
| DMSO:            | Dimethyl sulfoxide   |
| DNA:             | Deoxyribonucleotide acid                                     |
| dpi:             | Days post-infection  |
| EBV:             | Epstein-Barr virus   |
| EC:              | Eastern cape provinces                                       |
| ECes:            | Embryonated Chicken Eggs                                     |
| EDTA:            | Ethylenediaminetetraacetic acid                              |
| ELISA:           | Enzyme Linked Immuno Sorbent Assay                           |
| F:               | Fusion protein   |
| F <sub>0</sub> : | Fusion cleavage site   |
| FAM:             | Fluorescent dye  |
| FS:              | Free State province  |
| G:               | Guanine  |



|                      |  |
|----------------------|--|
| GFAsV:               | Guineafowl astrovirus                    |
| GoAsV:               | Goose astrovirus                         |
| GP:                  | Gauteng province                         |
| GTR:                 | General time-reversible                  |
| HA:                  | Haemagglutination assay                  |
| HI:                  | Haemagglutination inhibition test        |
| HN:                  | Hemagglutinin-neuramidase protein        |
| HPAI:                | High pathogenic avian influenza virus    |
| IAV:                 | Influenza A virus                        |
| IBV:                 | Infectious bronchitis virus              |
| ICPI:                | Intracerebral pathogenicity index        |
| IFN $\alpha/\beta$ : | Interferons alpha/ beta                  |
| IGS:                 | Intergenic sequences                     |
| IVPI:                | Intravenous pathogenicity index          |
| JHB:                 | Johannesburg                             |
| K:                   | Lysine                                   |
| Kb:                  | Kilobase                                 |
| kDa:                 | Kilodaltons                              |
| KZN:                 | KwaZulu-Natal                            |
| L:                   | Large polymerase protein                 |
| LP:                  | Limpopo province                         |
| LPAI:                | Low pathogenic avian influenza virus     |
| M:                   | Matrix protein                           |
| Mabs:                | Monoclonal antibodies                    |
| MDT:                 | Mean death time                          |
| MEGA:                | Molecular Evolutionary Genetics Analysis |
| MP:                  | Mpumalanga province                      |
| mRNA:                | Messenger ribonucleotide acid            |
| MTase:               | Methyltransferase                        |
| N:                   | Nucleocapsid protein                     |
| NA:                  | Neuraminidase                            |
| NC:                  | Northern Cape Province                   |
| ND:                  | Newcastle disease                        |
| NDV:                 | Newcastle disease virus                  |
| NGS:                 | Next-generation sequencing               |
| nt:                  | Nucleotide                               |
| NW:                  | North West province                      |

|          |   |
|----------|---|
| WOAH:    | World Organization for Animal Health                      |
| OP:      | Onderstepoort   |
| ORF:     | Open reading frame  |
| P:       | Phosphoprotein  |
| PAS:     | Department of Production Animal Studies                   |
| PBS:     | Phosphate buffered saline                                 |
| PE:      | Port Elizabeth  |
| PEC:     | Poult enteritis complex                                   |
| PEM:     | Poult enteritis mortality syndrome                        |
| Phe:     | Phenylalanine   |
| PHV:     | Pigeon Herpes virus                                       |
| PHEV:    | Pigeon Herpes encephalomyelitis virus                     |
| PiCV:    | Pigeon circovirus   |
| PiPV-A:  | Pigeon picornavirus A                                     |
| PiPV-B:  | Pigeon picornavirus B                                     |
| PKR:     | Pakistani rupee   |
| PPMV:    | Pigeon Paramyxovirus                                      |
| PPMV-1:  | Pigeon Paramyxovirus 1                                    |
| PRNTase: | Polyribonucleotidyltransferase                            |
| PTA:     | Pretoria  |
| PTTV:    | Pigeon torque teno virus                                  |
| R:       | Arginine  |
| RdRp:    | RNA-dependent RNA polymerase                              |
| RE:      | Restriction enzyme  |
| RFLP:    | Restriction fragment length polymorphism                  |
| RLV:     | Rauscher Leukaemia virus                                  |
| RNA:     | Ribonucleotide acid                                       |
| RNP:     | Ribonucleoprotein complex                                 |
| rRT-PCR: | Real-time reverse transcriptase-polymerase chain reaction |
| RSV:     | Rous sarcoma virus  |
| RT-PCR:  | Reverse transcriptase polymerase chain reaction           |
| RVA:     | Rotavirus A   |
| RVD:     | Rotavirus D   |
| RVF:     | Rotavirus F   |
| RVG:     | Rotavirus G   |
| SAN:     | Specific antibody negative                                |
| SAPA:    | South African Poultry Association                         |

|          |                                     |
|----------|-------------------------------------|
| SFM:     | Serum-free cell growth medium       |
| SFV:     | Semliki Forest virus                |
| SPF:     | Specific pathogen-free              |
| SU:      | Stellenbosch University             |
| TAE:     | Tris-Acetate EDTA                   |
| TAstV-1: | Turkey astrovirus                   |
| TEM:     | Transmission Electron Microscopy    |
| TM:      | Transmembrane                       |
| TTV:     | Torque teno virus                   |
| UK:      | United Kingdom                      |
| UP:      | University of Pretoria              |
| UTR:     | Untranslated region                 |
| USA:     | United States of America            |
| UV:      | Ultraviolet                         |
| VNT:     | Virus neutralisation test           |
| vRNP:    | Viral ribonucleoprotein             |
| WC:      | Western Cape province               |
| WPSA:    | World's Poultry Science Association |
| WSD:     | White spot disease                  |
| WSSV:    | White spot syndrome virus           |
| YPDS:    | Young pigeon disease syndrome       |

## **Symbols**

|     |                       |
|-----|-----------------------|
| %:  | Percentage            |
| °C: | Degrees Celsius       |
| cm: | Centimetre            |
| µL: | Microlitre            |
| µm: | Micrometre            |
| nm: | Nanometre             |
| mL: | Millilitre            |
| g:  | Grams                 |
| \$: | United States dollars |
| Γ:  | Gamma distribution    |

# CHAPTER 1

## Literature review

### 1.1. Introduction to Newcastle disease

Avian viral diseases are well known to cause significant economic losses to poultry production from which the most common and harmful avian viral disease is Newcastle Disease (ND), a virulent and easily transmissible viral disease with fatal consequences that is globally prevalent and subject to mandatory reporting to the World Organization for Animal Health (WOAH) and causes substantial mortality and morbidity rates (Pestka *et al.*, 2014; Ogali, 2018; Absalón *et al.* 2019; Mansour *et al.* 2021). The WOAH classifies virulent strains as viruses meeting specific criteria, including having an intracerebral pathogenicity index (ICPI) of 0.7 or higher, a fusion cleavage site (F<sub>0</sub>) with several basic amino acids such as <sup>112</sup>R/K-R-Q/K/R-K/R-R<sup>116</sup> located at the C-terminus of the F2 protein and phenylalanine at position 117, which corresponds to the N-terminus of the F1 protein (Dimitrov *et al.*, 2019; Dzogbema *et al.*, 2021). The term "expression of multiple basic amino acids" indicates the presence of at least three arginine or lysine residues falling between positions 113 and 116 (Dzogbema *et al.*, 2021). Clinical symptoms include (i) nervous symptoms such as neck twisting, paresis or paralysis, clonic spasms, tremors, torticollis, ataxia, and tremors; (ii) respiratory manifestations, including coughing, sneezing and tracheal rales; (iii) digestive symptoms, such as large amounts of green watery diarrhoea; and (iv) other symptoms such as eyelid oedema, cyanosis, and swollen heads (Akhtar, 2016; Abolnik, 2017). If an infection occurs during moulting, feather development issues such as deformed, poorly developed, and fragile feathers may occur (Pestka *et al.*, 2014). Clinical signs observed can differ based on the pathogenicity of the isolates, the bird's immune status, and the bird species. (Abolnik, 2017). Strains were initially classified into four pathotype groups which included: (i) Doyle, (ii) Beach, (iii) Beaudette and (iv) Hitchner (Cattoli *et al.*, 2011). Subsequently, these four groups were reclassified and renamed into five groups categorized by the distinct symptoms they provoke within the species (Abolnik, 2017). The five pathological groups include: (i) lentogenic strains (Hitchner) with low virulence and cause no clinical disease to subclinical disease or mild respiratory illness experiencing coughing, gasping, sneezing and rales; (ii) mesogenic strains (Beaudette) that cause acute respiratory disease and neurological symptoms, nonetheless, the mortality rate remains minimal, (iii) viscerotropic velogenic strains (Doyle) which is a highly pathogenic variant characterized by the presence of hemorrhagic intestinal lesions, (iv) neurotrophic

velogenic strains (Beach) induces severe systemic infections with high mortality rates and (v) subclinical strains which usually consists of subclinical enteric infections (Dimitrov *et al.*, 2016; Abolnik, 2017; Swayne and Brown, 2021). In addition to the cleavability of the fusion protein precursor (F<sub>0</sub>) and the presence of several basic residues in the fusion protein cleavage site, various other significant factors that influence the virus's pathogenicity encompass genetic elements like tissue or organ tropism, its capacity to evade the host's immune responses, and its replication efficiency (Ogali, 2018; Dortmans *et al.*, 2011). Newcastle disease has had a widespread influence, with 109 out of 200 countries officially reporting its presence to the WOAHP between 2014 and 2019 (Dimitrov *et al.*, 2019). During the period from 2006 to 2009, this disease held the position of the 8th most significant wildlife ailment (Dimitrov *et al.*, 2019).

### **1.1.1. Pigeon Paramyxovirus**

Pigeons are one of the dominant domesticated birds that humans keep for different purposes, such as hobbies that include racing, meat production in some countries or as pets (Rehan *et al.*, 2019). Pigeons are susceptible to various diseases, with viral infections being a predominant concern, among which Newcastle disease virus (NDV) stands out as one of the most significant (Liu *et al.*, 2003; Rehan *et al.*, 2019; He *et al.*, 2020). Newcastle disease is caused by pigeon paramyxovirus which is an antigenic pigeon form of the virus that is characterised by the frequent occurrence and recurrent outbreaks in pigeon populations (Absalón *et al.*, 2019; Chang *et al.*, 2020). It is believed that the antigenic pigeon form of the virus emerged because of the transmission of NDV strains from chickens to pigeons (Wei *et al.*, 2018).

#### **1.1.1.1. History**

Pigeon paramyxovirus causing ND in pigeons and doves was initially observed in 1926 in Java, Indonesia which made its way to England in 1927, when it was initially identified in chickens in Newcastle-upon-Tyne (Alexander, 2009; Pestka *et al.*, 2014). The disease was also described in Korea in 1926 (Dzoghbema *et al.*, 2021). Four panzootics occurred worldwide, between 1926 and 1981 (Dzoghbema *et al.*, 2021). Over 40 years, this disease rapidly disseminated throughout Asia, with the inaugural panzootic outbreak characterized by two distinct waves of transmission (Cross, 1995; Pestka *et al.*, 2014). The initial wave extended to Eastern Europe between 1926 and 1942, followed by a second wave encompassing Europe, Africa, and the Americas during the late 1940s and early 1950s (Cross, 1995; Pestka *et al.*, 2014). The relatively slow propagation of the virus during the first panzootic wave can be attributed to the underdeveloped state of the poultry industry, marked by minimal international trade (Cross,

1995). The second pandemic broke out during the late '60s, which caused the disease to spread throughout the Middle East and Europe (Cross, 1995). The disease was rapidly introduced into some countries by air transport of wild bird species such as international trade of psittacine species (Cross, 1995; Pestka *et al.*, 2014; Dzogbema *et al.*, 2021). The third panzootic disease outbreak was caused by the viscerotropic velogenic strain of the virus between 1968 and 1972 involving racing pigeons (*Columbia livia*) and Senegal Doves (*Streptopelia senegalensis*) (Cross, 1995; Dzogbema *et al.*, 2021). The fourth panzootic was documented from 1980 onwards, which mostly showed infections of racing pigeons, show pigeons, and domesticated pigeons, however, it later spread to wild pigeons and other poultry (Dzogbema *et al.*, 2021).

These infections hit worldwide during 1981 and 1985 due to a variant form of the classic NDV, using the basis of pathogenicity and monoclonal antibody binding studies, the virus was termed Pigeon Paramyxovirus (Naveen *et al.*, 2013). However, the first isolation of PPMV in various parts of South Africa was only documented during an outbreak in September 1986 (Abolnik *et al.*, 2008). Other PPMV outbreaks documented in Sweden, Estonia, France, Germany and United Kingdom (UK) suggested that PPMV in pigeons and other wild birds have a potential risk for the poultry industry (Hüppi *et al.*, 2020). The virus was classified in the family *Paramyxoviridae* and genus *Orthoavulavirus* where it has since become an WOAHA notifiable disease (Dzogbema *et al.*, 2021; Kuhn *et al.*, 2023). The disease is enzootic in 33 African countries to date and during 2019, the WOAHA documented 25 notifications of new outbreaks of this disease in 25 African countries (Dzogbema *et al.*, 2021).

#### **1.1.1.2. Classification and Nomenclature**

Viruses in vertebrates such as birds, reptiles, fish and mammals are classified under the family *Paramyxoviridae* (Fei *et al.*, 2019). The *Paramyxoviridae* family is further classified into subfamilies *Avulavirinae*, *Metaparamyxovirinae*, *Orthoparamyxovirinae* and *Rubulavirinae* referring to viruses characterized by a single-stranded RNA genome of negative polarity enclosed within a membrane that currently comprises further of three genera that include *Metaavulavirus*, *Orthoavulavirus* and *Paraavulavirus* (Fei *et al.*, 2019). Newcastle disease virus, also known as Avian orthoavulavirus 1 (AOaV-1) is taxonomically classified under the genus *Orthoavulavirus* with the remaining avian paramyxoviruses 2 – 9 (Yuan *et al.*, 2020). Pigeon Paramyxovirus is a host and antigenic variant of NDV or APMV-1 (Akhtar *et al.* 2016). Table 1.1 depicts the taxonomic classification of the pigeon paramyxovirus type 1:

**Table 1.1:** The taxonomical division of the pigeon paramyxovirus type 1 (Yuan *et al.*, 2020; Fei *et al.*, 2019; Akhtar *et al.*, 2016).

| Domain     | Virus  |
|------------|--|
| Order      | <i>Mononegaviriales</i>                                |
| Family     | <i>Paramyxoviridae</i>                                 |
| Subfamily  | <i>Avulavirinae</i>                                    |
| Genus      | <i>Orthoavulavirus</i>                                 |
| Virus      | Avian orthoavulavirus type 1 (Newcastle disease virus) |
| Class      | II   |
| Sublineage | Pigeon paramyxovirus VI.1.1                            |

Numerous molecular classification systems have been devised to follow NDV evolution and genetic diversity (Dimitrov *et al.*, 2019). Researchers from two independent studies in the late 1980s have found that three different NDV lineages (A, B, and C) can be identified based on F and HN gene sequence diversity (Dimitrov *et al.*, 2019). Nevertheless, Ballági-Pordani and colleagues suggested in 1996 that analysis of restriction fragment length polymorphism (RFLP) has revealed the presence of six unique genotypes, denoted as I to VI, among NDV isolates (Dimitrov *et al.*, 2019).

Phylogenetic analysis of the partial F gene sequence data allowed for further system improvements, ensuring the identification of additional genotypes (Dimitrov *et al.*, 2019). During a subsequent investigation employing full genome sequences, it was revealed that there are three distinct sizes for the genomes of NDV (Dimitrov *et al.*, 2019; He, 2020). Furthermore, NDV isolates were categorized into two primary classes, designated as class I and class II, and were subsequently subdivided into numerous genotypic variations (Dimitrov *et al.*, 2019; He, 2020). Class I comprises mainly lentogenic viruses primarily recovered from waterfowl, shorebirds and domestic poultry (Ogali *et al.*, 2018; Dzogbema *et al.*, 2021). Class II primarily comprises velogenic viruses which are predominantly obtained from domestic poultry and wild birds (Ogali *et al.*, 2018; Dzogbema *et al.*, 2021). Within the classification of Class II viruses, there are eight distinct genotypes, from which PPMV is categorized within genotype VI, a renowned lineage that specifically characterizes PPMV in pigeons which can further segment into nine subgenotypes, denoted as VIa, VIb, VIc, VIe, VIg, VIh, VIi, and VIj of which PPMV are placed in the genetic sublineage VIb that is generally also known as 4b depending on the nomenclature being used (Aldous *et al.*, 2014; Molini *et al.*, 2018; Mansour *et al.*, 2021). Class II is more diverse than class I as it encompasses viruses with varying levels of virulence, from non-harmful to highly pathogenic strains (Dimitrov *et al.*, 2019). Recent epidemiological

research has revealed that genotypes V, VI, and VII are the most commonly identified genotypes at present, with genotype VII being notably linked to numerous recent epidemics across Asia, Africa, the Middle East, and South America (Dzoghema *et al.*, 2021).

In 2003, Aldous and colleagues introduced an alternative approach to classifying NDV isolates, they used partial F gene analysis to delineate NDV isolates into six distinct lineages (1-6) and 13 sub-lineages (Dimitrov *et al.*, 2019), however, an additional lineage (7) was later proposed (Dimitrov *et al.*, 2019). While these classification systems yielded valuable insights into NDV evolution and genetic diversity, their differing methodologies led to inconsistencies in NDV classification (Dimitrov *et al.*, 2019). These variations made it challenging to compare and discuss findings across different studies, confusing existing and newly identified genetic groups (Dimitrov *et al.*, 2019). To address this issue, in 2012, a unified and objective NDV classification system was suggested, which involved the use of complete F gene coding sequences and the implementation of several objective criteria's for classification such as (i) the phylogenetic topology, (ii) inter-populational evolutionary nucleotide distances, (iii) branch support, and (iv) epidemiological independence, requiring at least four isolates per sub/genotype (Diel *et al.*, 2012; Dimitrov *et al.*, 2019). While the system proposed by Diel and colleagues in 2012 offered some objectivity in classification, the dynamic nature of NDV circulation and continuous evolution led to the almost simultaneous identification and naming of new genotypes without consistently applying all proposed criteria (Dimitrov *et al.*, 2019). In some instances, classification was conducted using limited sequence datasets rather than curated datasets of all available complete NDV F gene sequences (Dimitrov *et al.*, 2019). This approach resulted in inconsistencies in the nomenclature and classification of newly identified genotypes and sub-genotypes, with some bearing identical names despite representing different and unrelated viruses (Dimitrov *et al.*, 2019).

In 2019, a global consortium of scientists and collaborators conducted a comprehensive review of virus classification, aiming to address the challenges in categorizing these viruses (Dimitrov *et al.*, 2019). This endeavour resulted in the formulation of an updated classification system that introduced novel nomenclature criteria to resolve the existing issues and were primarily based on the guidelines outlined by Diel *et al.* (2012), which provided the fundamental framework for classifying NDV isolates. The outcome of this collaborative effort is succinctly presented in Table 1.2, summarizing the newly agreed-upon categorization criteria.



**Table 1.2:** The updated consensus classification criteria (Dimitrov *et al.*, 2019).

| Criterion | Description  |
|-----------|--|
| 1         | Assignment of viruses into new genotypes and sub-genotypes based on complete fusion gene phylogenetic analysis (sequences of at least 1645 nucleotides or longer).   |
| 2         | Assignment of viruses into new genotypes and sub-genotypes is done only utilizing a complete dataset of sequences from all existing genotypes. All classification criteria listed below need to be fulfilled for naming new genotypes and sub-genotypes.   |
| 3         | Sub-trees and pilot tree can be used for assigning new isolates to existing sub/genotypes.   |
| 4         | New genotypes or sub-genotypes are created only when four or more independent isolates, without a direct epidemiologic link (i.e. distinct outbreaks), are available.  |
| 5         | New genotypes and sub-genotypes are created based on the phylogenetic tree topology (need to cluster into monophyletic branches) using the Maximum Likelihood method and the general time-reversible (GTR) model with gamma distribution ( $\Gamma$ ) utilizing RaxML or a comparable tool.  |
| 6         | The mean nucleotide distance (evolutionary distances) between groups is inferred as the number of base substitutions per site from averaging over all sequence pairs between groups using Molecular Evolutionary Genetics Analysis (MEGA) v. 5/6/7 software (or a comparable tool) and utilizing the Maximum Composite Likelihood model with rate variation among sites that was modelled with a gamma distribution (shape parameter = 1). |
| 7         | Different genotypes have an average distance per site above 10% (0.1).   |
| 8         | Different sub-genotypes have an average distance per site above 5% (0.05).   |
| 9         | The bootstrap value at the genotype and sub-genotype defining node is 70% or above ( $\geq 70\%$ ).  |
| 10        | Viruses that do not fulfil all classification criteria are assigned to the lower order (closer to the root) sub/genotype   |

In the revised system, genotypes in class I were designated with Arabic numerals, while those in class II were identified with Roman numerals, marking a significant departure from the previous lowercase Latin letter system (Dimitrov *et al.*, 2019). Furthermore, they implemented a numerical-decimal system, replacing the Latin letters used for sub-genotype naming (Dimitrov *et al.*, 2019). A dichotomous splitting approach was adopted, using the numerals 1 and 2 to separate sub-genotypes at defining nodes (Dimitrov *et al.*, 2019).

As a result of this modified classification method, members of sub-genotype Va were reclassified into a new genotype, XIX, and five former sub-genotypes of genotype VI were divided into two new genotypes, XX and XXI (Dimitrov *et al.*, 2019). Consistent with previous classifications, several genotypes, including I, V, VI, VII, XII, XIII, XIV, and XVIII, were further subdivided into sub-genotypes (Dimitrov *et al.*, 2019).

The number of sub-genotypes within genotypes I, XIV, and XVIII remained unchanged, with four, two, and two sub-genotypes, respectively (Dimitrov *et al.*, 2019). Genotypes II, III, IV, VIII, IX, XI, XVI, XIX, and XX had no designated sub-genotypes (Dimitrov *et al.*, 2019). Notably, despite the creation of new genotypes XX and XXI from genotype VI, it remains the most diverse of all NDV genotypes (Dimitrov *et al.*, 2019). Former sub-genotypes VIa and VI<sub>n</sub> were merged into sub-genotype VI.2.1.1.1, while VI<sub>j</sub> and VI<sub>k</sub> were reclassified as VI.2.1.1.2.1 and VI.2.1.1.2.2, respectively (Dimitrov *et al.*, 2019). Other previously designated sub-genotypes VI<sub>b</sub>, VI<sub>e</sub>, VI<sub>f</sub>, and VI<sub>h</sub> were validated and renamed VI.1.1, VI.1.2.2.2, VI.1.2.1.2, and VI.1.2.1.2, respectively (Dimitrov *et al.*, 2019).

### 1.1.1.3. Morphology

Newcastle disease virus virions are 150 – 350 nm in diameter, generally pleomorphic, but usually have a spherical shape that can vary and present a filamentous form (Samal, 2008; Dzogbema *et al.*, 2021). This virion has a nucleocapsid surrounded by a lipid envelope (Samal, 2008). A diagram of a typical paramyxovirus is indicated in Figure 1.1 (Bello *et al.*, 2018).

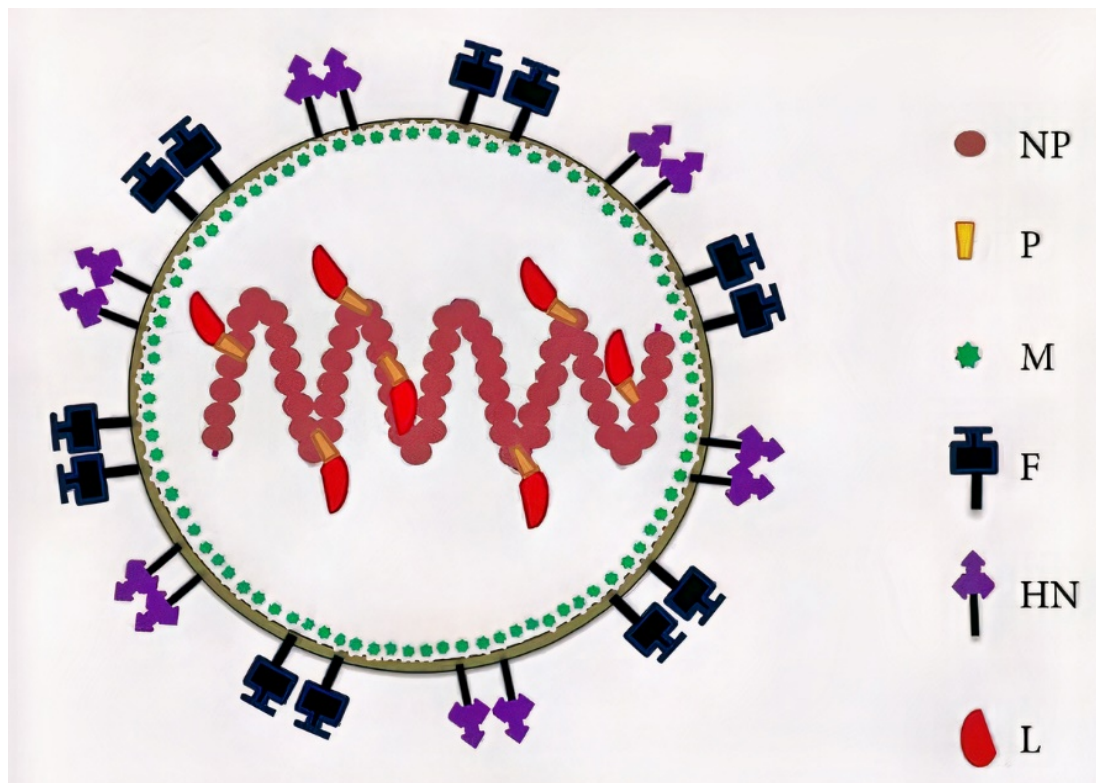


**Figure 1.1:** Diagram of the paramyxovirus structure (Bello *et al.*, 2018). No license required for reproduction of the figure.

The NDV genome is approximately 15.2 kb long and non-segmented (Qui, 2017). The core contains the single-stranded negative-sense RNA comprised of six transcriptional units 3'-NP-P-M-F-HN-L-5' ciphering structural proteins that include nucleocapsid protein (N), phosphoprotein (P), matrix protein (M), fusion protein (F), haemagglutinin-neuraminidase protein (HN) and large polymerase protein (L) (Qui, 2017). Proteins V and W, both non-structural proteins, are additionally produced through RNA editing originating from the P gene (Qui, 2017). The virus genome is depicted in Figure 1.2.

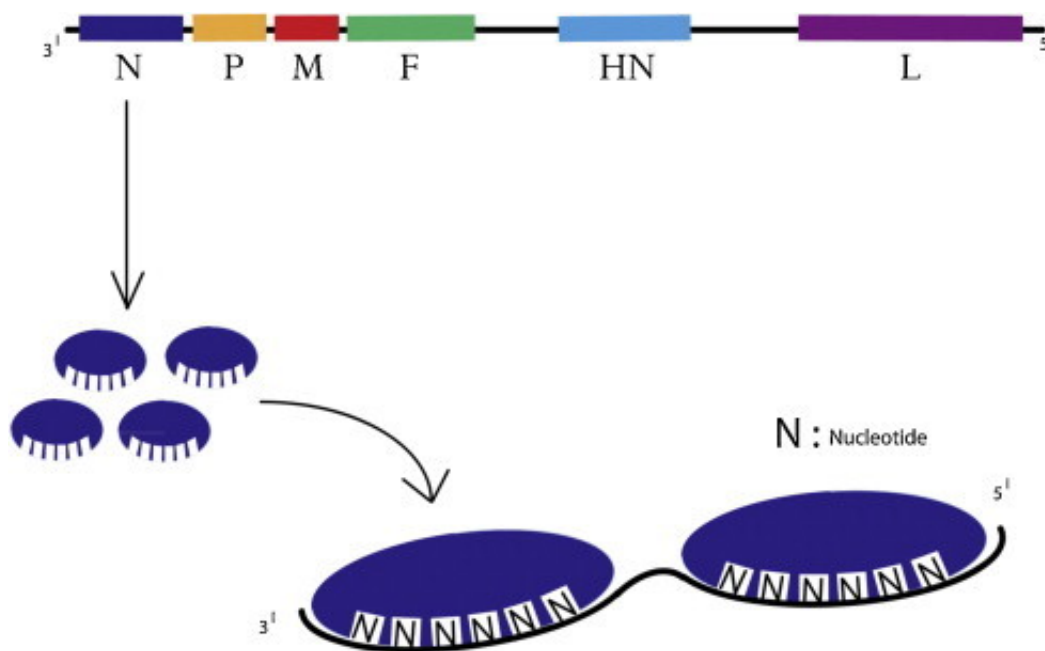


**Figure 1.2:** Illustration of the paramyxovirus genome emphasizing the significance of the rule of six, which implies that a nucleocapsid protein has optimal binding efficacy when interacting with a sequence of six nucleotides (Qui, 2017). Permission to reproduce under licence number 5700581183083.

The genome has a 55 nucleotide (nt) leader at its 3' end and 114 nt trailer at its 5' end as indicated in Table 1.3, which flanks six essential transcriptional units (Ganar *et al.*, 2014). Each of these six genes has gene start and end signals separated by intergenic sequences (IGS) that are represented in Figure 1.2 by the black lines between the genes and range in size from one to 47 nt (Ganar *et al.*, 2014). Each of the “N” subunits present in Figure 1.2 is associated with six nucleotides of genomic RNA which adheres to the “rule of six” of most paramyxoviruses, which explains why the genome size of all NDV is always a multiple of six (Dzogbema *et al.*,

2021). The virus is known to have a recognized virulence pattern <sup>112</sup>G/RRQKR↓ F<sup>117</sup> at the cleavage site located within the F protein (Wei *et al.*, 2018). Table 1.3 provides information regarding the genome length characteristics associated with PPMV-1 (Wang *et al.*, 2015).

**Table 1.3:** Genome length characteristics associated with PPMV-1 isolates (Wang *et al.*, 2015).

| Region         | Gene sequence | 3' UTR <sup>a</sup> | Coding sequence <sup>b</sup> | 5' UTR <sup>a</sup> | Intergenic region | Nucleotide length |
|----------------|---------------|---------------------|------------------------------|---------------------|-------------------|-------------------|
| <b>Leader</b>  | 1-55          |                     |                              |                     |                   | 55                |
| <b>NP</b>      | 56-1,808      | 66                  | 122-1,591                    | 217                 | 1                 | 1,753             |
| <b>P</b>       | 1,810-3,260   | 83                  | 1,893-3,080                  | 180                 | 1                 | 1,451             |
| <b>M</b>       | 3,262-4,502   | 34                  | 3,296-4,390                  | 112                 | 1                 | 1,241             |
| <b>F</b>       | 4,504-6,295   | 46                  | 4,550-6,211                  | 84                  | 31                | 1,792             |
| <b>HN</b>      | 6,327-8,328   | 91                  | 6,418-8,133                  | 195                 | 47                | 2,002             |
| <b>L</b>       | 8,376-15,078  | 11                  | 8,387-15,001                 | 77                  |                   | 6,703             |
| <b>Trailer</b> | 15,079-15,192 |                     |                              |                     |                   | 114               |

<sup>a</sup> untranslated region, <sup>b</sup> including the stop codon

The 5' untranslated regions (UTR) are documented to be longer than 3' UTRs (Wang *et al.*, 2015; Ogali *et al.*, 2020). The number of nucleotides in the UTRs may fluctuate across isolates due to genetic occurrences such as insertion (Wang *et al.*, 2015; Ogali *et al.*, 2020).

#### 1.1.1.4. Epidemiology

##### 1.1.1.4.1. Host range

PPMV, known to affect over 250 bird species, exhibits a wide host range and a global distribution (Samal, 2008; Bucko and Gieger, 2019). Among domestic species, susceptibility to PPMV is observed in various birds, including chickens (*Gallus gallus*), turkeys (*Meleagris gallapavo*), pheasants (*Phasianus colchicus*), guinea fowl (*Numida meleagris*), muscovy (*Cairina moschata*), domestic ducks (*Anas platyrhynchos*), and geese (*Anser anser*) (Bucko and Gieger, 2019). Crows, ravens, ostriches, and penguins are among the other general species thought to be susceptible (Bucko and Gieger, 2019). Considering that these viruses predominantly circulate within domestic pigeons (*Columba livia domestica*) or their closely related wild relatives, such as rock pigeons, Eurasian collared doves (*Streptopelia decaocto*), European turtle doves (*Streptopelia turtur*), feral pigeons (*Columbia livia*), California Condors (*Gymnogyps californianus*) and doves can function as animal reservoirs for Pigeon

Paramyxovirus (PPMV) (Lumeij and Stam, 1985; Kuiken *et al.*, 2018; Bucko and Gieger, 2019). Biological testing of the virus obtained from deceased pigeons for viral pathogenicity demonstrated that, while chickens are susceptible, they show little to no pathogenicity (He *et al.*, 2020). The virus mostly infects all birds and has two main reservoirs (Cross, 1995). Waterfowl are mainly associated with avirulent viruses, whereas tropical birds are more prone to highly virulent viruses (Cross, 1995). Some birds are highly susceptible to the virus, notably gallinaceous birds, pheasants, psittacine birds, ratite birds, pigeons, and doves (Cross, 1995). On the other hand, species with intermediate susceptibility include nocturnal and diurnal raptors, storks, penguins, and passeriform birds (Cross, 1995). Meanwhile, birds with minimal susceptibility to the virus comprise waterfowls, pelicans, shags, coots, gulls, and cranes (Cross, 1995).

Pigeon paramyxovirus, as a zoonotic pathogen, can induce conjunctivitis or flu-like symptoms in individuals with frequent exposure to infected birds such as farm workers, veterinarians or those that are engaged in veterinary disease diagnosis and associated laboratory research (Wang *et al.*, 2023). While the majority of cases reported are typically mild or self-restricting, fatal cases of PPMV infections in immunocompromised patients have been reported such as respiratory failure (Wang *et al.*, 2023). The first recorded instance of human infection with APMV-1 was documented in Australia in 1942 (Hurley *et al.*, 2023).

#### **1.1.1.4.2. Transmission and spread**

PPMV incubation time ranges from 2 to 15 days, with an average of 5 to 6 days, however, lengthier intervals of up to 4 weeks aren't considered uncommon (Hüppi *et al.*, 2020; Dzogbema *et al.*, 2021). The disease can be transmitted to healthy birds through various means, including direct contact or the indirect inhalation of dust from contaminated sources such as litter, food, drinking vessels, nest bowls, and utensils, all of which may be tainted with secretions and excretions from infected pigeons (Hüppi *et al.*, 2020; Lumeij and Stam, 1985). This is due to the fact that infected birds shed viruses in both faeces and respiratory secretions (Hüppi *et al.*, 2020; Lumeij and Stam, 1985). Furthermore, inadequate disinfection of infected facilities and transport vehicles can serve as potential transmission routes, as the virus can propagate in the air over short distances (Lumeij and Stam, 1985). It has been demonstrated that the virus may be transferred by aerosols over a distance of 64 meters (Hanson and Spalatin, 1978; Dzogbema *et al.*, 2021). Birds that have been immunized against the disease are capable of excreting viral particles for 4 to 12 months (Dzogbema *et al.*, 2021). Nonetheless, because

pigeons are non-migratory birds, the process by which these viruses propagate over great distances between regions and countries is unknown (He *et al.*, 2020).

Numerous theories have emerged regarding the potential role of migratory birds in the dissemination of PPMV, although the likelihood of these species serving as carriers of genotype VI viruses is considered minimal (He *et al.*, 2020). The contact between Columbiform birds in various scenarios, including racing pigeons in competitive flights, show pigeons during displays, and live bird markets featuring meat pigeons, as well as the extensive trade of these birds, offers a plausible explanation for the transmission of PPMV between regions and even across countries (He *et al.*, 2020). Furthermore, the dissemination of PPMV to other species might be attributed to the presence of laughing doves in farms and residential backyards, where they often come into close contact with free-ranging domestic poultry, sharing common feed lots and watering points, thereby elevating the risk of exposure and potential cross-transmission (Obanda *et al.*, 2016). Eradicating the virus proves challenging in traditional development systems due to the persistent interaction of domestic birds with potentially infected wild birds, presenting an ongoing and unforeseen risk of virus spread (Dzogbema *et al.*, 2021). It's worth noting that recorded morbidity rates for PPMV vary, ranging from 30% to 70%, while fatality rates span from 10% to 70% (Hüppi *et al.*, 2020).

#### **1.1.1.4.3. Risk factors**

Several factors are related to NDVs of pigeon origin, encompassing host characteristics, environmental conditions, co-infection circumstances, and the absence of proper hygiene protocols (Mansour *et al.*, 2021). Other risk factors for ND, specifically in poultry production, differ between developing and developed countries, while some are shared (Wiseman *et al.*, 2018). A 2015 study in West Malaysia examined the risk factors related to the high mortality rate connected with ND, and the following characteristics were examined: (i) flock characteristics, (ii) immunization programs, (iii) mortality and morbidity rates, (iv) age occurrence and (v) farm management parameters (Jaganathan *et al.*, 2015). Ethiopian risk factors encompassed several elements, including: (i) infrequent removal of poultry litter, (ii) procurement of replacement birds instead of on-farm hatching, (iii) flock size, and (iv) reliance on open water sources for poultry drinking (Wiseman *et al.*, 2018). Additionally, within rural African chicken production systems, other contributing factors encompassed: (i) seasonality, (ii) suboptimal physical condition of the birds, (iii) concurrent diseases, (iv) poultry breed, (v) a notable presence of young birds within the flock, (vi) the quality of poultry shelters, and (vii)

concerns related to environmental pollution (Wiseman *et al.*, 2018). The seasonality and environmental risk factors have been reported to have an effect on the virus's prevalence (Dzogbema *et al.*, 2021). The disease's incidence in tropical areas has been shown to be higher in dry seasons than in wet seasons, which include December, January, February, and March (Dzogbema *et al.*, 2021). Little is known about the features and factors that pose a risk for human infection with PPMV-1, however, zoonotic risks have been reported for all variants of this virus, resulting in transient conjunctivitis in individuals, such cases are mainly confined to laboratory personnel and vaccination teams exposed to substantial viral loads (Miller, 2014). However, the severity escalates in immunocompromised individuals, leading to lethal pneumonic cases and fatal encephalitis, particularly following blood stem cell or bone marrow transplantations (Hurley *et al.*, 2023; Wafaa, 2023). Instances of APMV-1-induced pneumonia and death have been reported, with cross-species transmission highlighted in cases involving close contact with live pigeons (Wafaa, 2023). The significance of this research in South Africa is underscored by the large population of immunocompromised individuals, particularly those with AIDS, who may be at elevated risk due to potential exposure to PPMV-1. Understanding and mitigating the risks associated with PPMV-1 transmission in such populations are crucial for public health.

#### **1.1.1.4.4. Stability of the virus**

The virus's thermal stability depends on the virus strain since heat and ultraviolet (UV) treatment reduces the virus's virulence or causes the virus to be inactivated (Dzogbema *et al.*, 2021). Lentogenic strains are inactivated at 56°C, whereas virulent bacteria are more resistant at this temperature (Dzogbema *et al.*, 2021). The most frequent temperature and period for virus inactivation are 56°C for 3 hours or 60°C for 30 minutes (Dzogbema *et al.*, 2021). Acidic pH such as  $\text{pH} \leq 2$  also induces virus inactivation because the virus is sensitive to certain substances such as ether, formalin, phenol, and 6% sodium hypochlorite (Dzogbema *et al.*, 2021).

#### **1.1.1.4.5. Lesions associated with the virus**

PPMV infection causes a variety of lesions; while most lesions are linked with specific strains, certain lesions are present in all cases. These lesions are categorised by macroscopic – and microscopic lesions.

#### **1.1.1.4.5.1. Macroscopic lesions associated with the virus**

Each organ's macroscopic alterations could include colour, shape, consistency, degeneration and necrosis, circulatory problems, inflammation, and exudation (Etriwati *et al.*, 2017). Birds infected with PPMV are prone to have an enlarged and mottled spleen, tracheal inflammation, emission of purulent exudates from the bronchioles and neuronal degeneration (Dzogbema *et al.*, 2021). Occasionally, haemorrhages on the pancreas, epicardium, liver, meninges and brain congestion are observed (Chowdhary *et al.*, 2020). Petechial haemorrhages are prevalent on the proventriculus mucosa and in the duodenal mucosa (Chowdhary *et al.*, 2020).

#### **1.1.1.4.5.2. Microscopic lesions associated with the virus**

Microscopic lesions associated with infection include degeneration and necrosis, haemorrhage, congestion, oedema, and inflammatory cell infiltration (Etriwati *et al.*, 2017). Birds that have been infected are susceptible to developing haemorrhagic lesions within their digestive system, affecting areas such as the proventriculus, small intestine, and caeca (Mehroon *et al.*, 2020; Dzogbema *et al.*, 2021). Additionally, they may exhibit tracheal and pulmonary congestion, along with bleeding in the lung and tracheal regions, and these infections can lead to lesions in the caudal central nervous system, involving the spinal cord and the brain stem (Mehroon *et al.*, 2020; Dzogbema *et al.*, 2021). Congestion of blood vessels, as well as oedema, are known to be present along the length of the trachea, with a number of infiltrating mononuclear cells found in the tracheal wall (Chowdhary *et al.*, 2020).

#### **1.1.1.5. Viral replication cycle**

To begin, the virus penetrates the target cell (Dzogbema *et al.*, 2021). The virus particle has two virus-encoded glycoproteins, embedded within its lipid membrane (Peeples, 1988; Dortmans *et al.*, 2011). These glycoproteins play a pivotal role in initiating viral infection by attaching the virion to surface proteins on the target cell (Peeples, 1988; Dortmans *et al.*, 2011). The virus envelope fuses with the host cell membrane through a pH-independent process, via receptor-mediated endocytosis or caveolae-dependent endocytosis (Cantin *et al.*, 2007; Ganar *et al.*, 2014). The virus's entry into respiratory epithelial cells relies on its interaction with sialic acid-containing molecules such as N-glycoprotein receptors and gangliosides, facilitated by its surface glycoprotein (HN protein) (Ganar *et al.*, 2014; Dzogbema *et al.*, 2021). This attachment event instigates the fusion of the viral envelope with the host cell's plasma membrane, a process promoted by the F protein (Dortmans *et al.*, 2011). The ribonucleoprotein complex (RNP), also known as the viral nucleocapsid, houses the RNA genome and is enclosed by N proteins that



are linked to the polymerase complex, composed of P and L proteins (Dortmans *et al.*, 2011). Once inside the host cell, the viral nucleocapsid separates from the M protein and enters the cytoplasm where the polymerase complex transcribes the negative-sense RNA genome into positive-sense messenger ribonucleotide acid (mRNA), which is essential for viral protein synthesis (Dortmans *et al.*, 2011; Ganar *et al.*, 2014). The resulting full-length positive-sense strand serves as a template for synthesising of the negative-sense RNA strand (Dortmans *et al.*, 2011). Upon sufficient production of viral proteins, a shift from transcription to genome replication takes place (Dortmans *et al.*, 2011). The budding process commences after the viral genome has completed its replication phase (Dzogbema *et al.*, 2021). Viral nucleocapsids assemble as NP proteins bind to newly produced genomic RNA and the polymerase complex (Dortmans *et al.*, 2011). All these viral components are transported to the plasma membrane, and the assembly is orchestrated by the M protein (Dortmans *et al.*, 2011). These virions are then liberated via the budding process and are separated from the host cell due to the HN protein's neuraminidase activity, which also eliminates the sialic acid residues to prevent self-aggregation (Dortmans *et al.*, 2011). Additionally, the virus can propagate within the host by creating syncytia, which are large multinucleated cells formed by the fusion of an infected cell expressing the HN and F proteins with adjacent cells (Dzogbema *et al.*, 2021). The entire viral reproduction process is visually depicted in Figure 1.3.

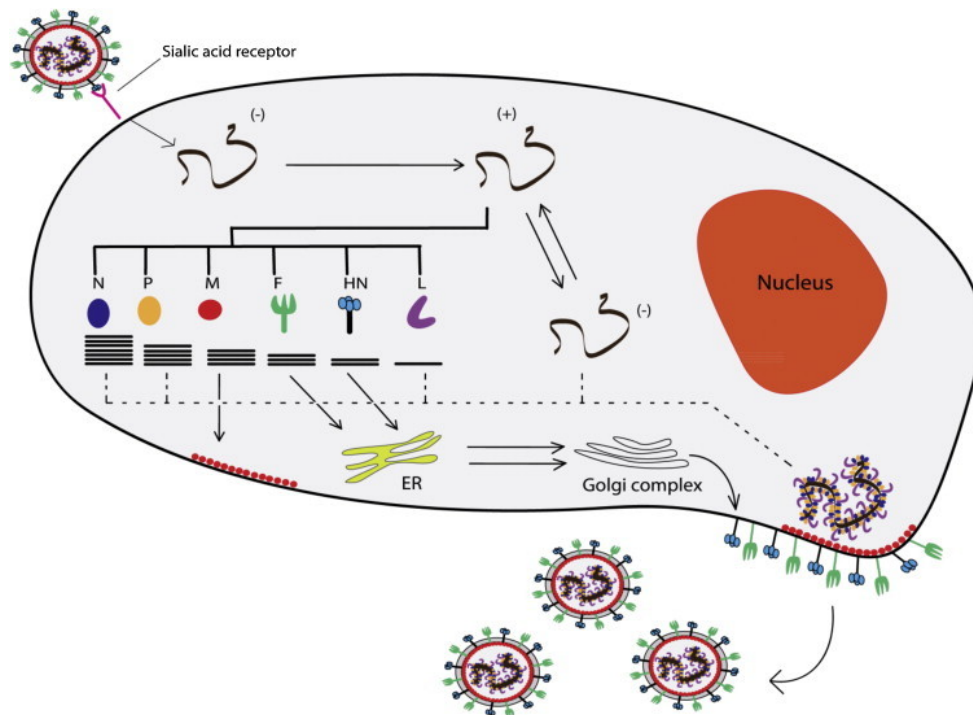


**Figure 1.3:** Schematic representation of the virus replication cycle (Dortmans *et al.*, 2011).  
 Permission to reproduce under licence number 5700581183083.

The several proteins involved in the virus's replication cycle are addressed below, and Table 1.4 summarises the fundamental information for each gene involved.

**Table 1.1:** Summary of the genes involved in the virus replication cycle (Ganar *et al.*, 2014).

|  | <b>Amino acids (aa)<sup>1</sup></b> | <b>Molecular weight (kDa)<sup>2</sup></b> | <b>Function</b>   |
|--|-------------------------------------|---|---|
| <b>Nucleocapsid protein</b>                | 489                                 | 55  | Protect the strands from nucleases, association with other proteins that act a template for RNA <sup>3</sup> synthesis  |
| <b>Phosphoprotein</b>                      | 395                                 | 50 - 55                                   | Role in viral replication and transcription, stabilises the L protein in the P-L complex and functions as viral RNA <sup>3</sup> -dependent RNA <sup>3</sup> polymerase |
| <b>Matrix protein</b>                      | 364                                 | 40  | Role in virus assembly and budding process. Controls RNA <sup>3</sup> synthesis, interacts with actin and maintains the spherical shape of the nucleocapsid.            |
| <b>Fusion protein</b>                      | 553                                 | 55  | Role in virus attachment and mediates fusion to the host cell membrane. Determinate virulence of strains by the cleavability of F <sub>0</sub> <sup>4</sup> .           |
| <b>Hemagglutinin-neuraminidase protein</b> | 571 - 616                           | 74  | Role in receptor recognition in the host cell, receptor removal, preventing self-assembly and interaction with F protein to promote fusion                              |
| <b>Large polymerase protein</b>            | 2204                                | 250                                       | Role in RNA <sup>3</sup> synthesis, capping, methylation and needs the P protein as a cofactor for in vivo RNA <sup>3</sup> synthesis                                   |
| <b>V protein</b>                           | 239                                 | 36  | Documented to be an additional virulence factor of the virus  |

<sup>1</sup>aa: Amino acids, <sup>2</sup>kDa: kilodalton, <sup>3</sup>RNA: ribonucleic acid, <sup>4</sup> F<sub>0</sub>: cleavage site.

#### 1.1.1.5.1. Nucleocapsid (N) protein

This protein is a polypeptide with a molecular weight of 55 kilodaltons (kDa) and 489 amino acids (aa) in length (Ganar *et al.*, 2014; Dzogbema *et al.*, 2021). It coats the entire length of the negative and positive strands to protect them from nucleases (Ganar *et al.*, 2014). It appears as a flexible helical structure that mimics a herringbone-like structure under negative-staining electron microscopy, with a diameter of 18 nm and a length of 1 µm. (Yusoff and Tan, 2001). It is thought to be the most abundant protein (Dzogbema *et al.*, 2021).

The N, P, and L proteins are found in conjunction with the RNP's genomic RNA, which serves as a template for RNA synthesis (Ganar *et al.*, 2014). The viral RNA binds with the N protein's amino terminus, assisting in the creation of the herringbone-like structure and the first few amino acids of the N protein's amino terminus form a soluble complex with the P protein (Ganar *et al.*, 2014). The carboxy-terminus of the N protein, on the other hand, is not necessary for any of the nucleocapsid assemblies but does play a regulatory function in nucleocapsid polymerization (Ganar *et al.*, 2014).

### 1.1.1.5.2. Phosphoprotein (P)

Because of the many phosphorylated forms, this protein has 395 aa and generates several bands with molecular weights varying from 50 to 55 kDa (Ganar *et al.*, 2014). The P protein, which works as a homo-oligomer, is phosphorylated at certain serine and threonine sites (Ganar *et al.*, 2014). It is involved in viral replication and transcription by stabilizing the L protein in the P-L complex and acting as a viral RNA-dependent RNA polymerase (Ganar *et al.*, 2014). The P-L complex is known to carry out genomic replication in order to create a full-length positive-sense strand that serves as a template for the negative-sense strand (Ganar *et al.*, 2014). A tetramer of P protein mediates the interaction between the L protein and the N-RNA template, acting as a chaperone to prevent random encapsidation of non-viral RNA by the N protein (Ganar *et al.*, 2014). The unassembled N protein creates a complex with the P proteins, assisting in the transition from transcription to replication (Ganar *et al.*, 2014). By introducing one to four non-templated guanine (G) nucleotides at position 484 in the mRNA that encodes the P protein, transcriptional modification may allow translation of two non-structural proteins, V and W, as shown in Figure 1.4. (Yusoff and Tan, 2001; Ganar *et al.*, 2014). The P protein's amino- and carboxy-terminals are both required for P-N interactions.

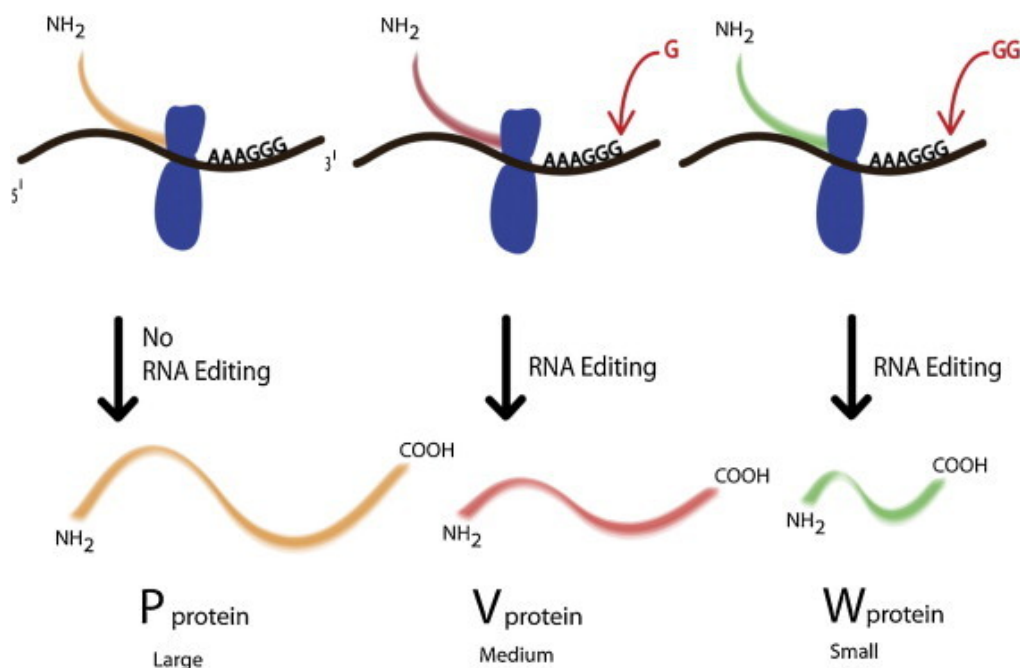


**Figure 1.4:** Schematic diagram of the formation of the V and W proteins by RNA editing (Ganar *et al.*, 2014). Permission to reproduce under licence number 5700581183083.

#### **1.1.1.5.3. Matrix (M) protein**

The M protein has 364 aa and a molecular weight of 40 kDa (Ganar *et al.*, 2014). It possesses a net positive charge that facilitates viral assembly by associating with the N protein (Ganar *et al.*, 2014). Between the nucleocapsid and the lipid membrane, the M protein has multiple conserved hydrophobic areas (Yusoff and Tan, 2001; Ganar *et al.*, 2014; Dzogbema *et al.*, 2021). This protein regulates viral RNA synthesis, interacts with actin, aids in virion assembly on the host cell, and contributes to virus budding as part of the ribonucleoprotein compaction process (Ganar *et al.*, 2014; Dzogbema *et al.*, 2021). As a result, this protein can prevent mRNA export while also inhibiting the expression of host cell genes (Dzogbema *et al.*, 2021). The M protein, which interacts with both the nucleocapsid and cytoplasmic domains of the HN and F proteins, has also been proposed to play a role in the spherical form of the nucleocapsid (Ganar *et al.*, 2014; Dzogbema *et al.*, 2021).

#### **1.1.1.5.4. Fusion (F) protein**

This protein is a surface glycoprotein with 553 aa and a molecular weight of 55 kDa that is found on the virus envelope and mediates virus-host cell membrane fusion when the virus enters the target cell (Yusoff and Tan, 2001; Ganar *et al.*, 2014; Dzogbema *et al.*, 2021). When the HN protein connects to the cellular receptors following activation, the virus-cell fusion occurs; this protein also fuses adjacent cells during the transfer of virions from cells to syncytium-forming cells (Dzogbema *et al.*, 2021). In the endoplasmic reticulum, the F protein is produced and glycosylated as an inactive precursor (F<sub>0</sub>) (Yusoff and Tan, 2001; Ganar *et al.*, 2014; Dzogbema *et al.*, 2021). This inactive precursor is cleaved at the peptide bond of residues 116 and 117 in the Golgi apparatus by specific cellular proteases, allowing disulphide-linked polypeptides, F<sub>1</sub> and F<sub>2</sub>, to form (Yusoff and Tan, 2001; Ganar *et al.*, 2014; Dzogbema *et al.*, 2021). The F protein is vital in the virulence of certain viral strains, and it is aided by the HN protein (Ganar *et al.*, 2014). The cleavability of F<sub>0</sub> is a crucial factor in a strain's pathogenicity (Yusoff and Tan, 2001). Mesogenic and Velogenic strains have cleavage sites created by at least three amino acids, arginine (R), lysine (K), and phenylalanine (Phe) at position 117. (Dzogbema *et al.*, 2021). In contrast to cleavage sites where two amino acids are solely cleaved by trypsin-like enzymes located in the digestive and respiratory mucosa, this type of cleavage site is cleaved by furin-like enzymes that are prevalent throughout the body (Dzogbema *et al.*, 2021). The many enzymes involved in cleavage explain why virulent strains are more invasive and cause systemic illness in infected organisms, as avirulent strains are activated by trypsin-like enzymes with a restricted distribution in the host and will be associated with localised or

focal infections, whereas virulent strains are activated by host proteases which cause infections to lead to systemic spread and disease (Fuller *et al.*, 2010; Dzogbema *et al.*, 2021). The transmembrane domain near the carboxy-terminus of the F protein anchors the protein (Yusoff and Tan, 2001).

#### **1.1.1.5.5. Hemagglutinin-neuraminidase protein (HN)**

The HN protein has a molecular weight of 74 kDa and is a type II integral membrane protein with the N-terminus fixed in the viral envelope (Ganar *et al.*, 2014; Dzogbema *et al.*, 2021). The protein has a homotetramer structure that is coupled with disulphide bonds within virus-infected cells (Yuan *et al.*, 2011; Ganar *et al.*, 2014). It has an N-terminal transmembrane domain, a stalk region, and an enzymatically active neuraminidase (NA) domain (Yuan *et al.*, 2011; Ganar *et al.*, 2014). This protein is thought to be a multifunctional protein since it recognizes receptors in the host cell, removes receptors, prevents self-assembly, and interacts with F protein to induce fusion (Takimoto *et al.*, 2002; Ganar *et al.*, 2014). This protein's NA activity contributes to the cleavage of the binding between hemagglutinin and sialic acid in the host cell, ensuring that viruses do not connect with their receptors at the producer level and can finish the dissemination step during the release of neosynthetic viruses (Dzogbema *et al.*, 2021). The F protein and HN protein are mutually dependent because co-expression and interaction between these two proteins are critical for virus fusion (Ganar *et al.*, 2014). The HN protein is responsible for virus infections and pathogenicity; it comprises 14 cysteine residues, 12 of which are conserved and form covalent connections for structural stability (Ganar *et al.*, 2014). As the position of the stop codon varies, the length of the HN protein varies; the shortest HN protein is reported to be 571 aa, while the longest HN protein is 616 aa (Ganar *et al.*, 2014). Other HN protein lengths are 577 and 581 aa (Dzogbema *et al.*, 2021). HN proteins with 616 aa are present in avirulent strains of the virus, while 581 and 577 aa are found in both avirulent and virulent strains (Dzogbema *et al.*, 2021). Only virulent strains have the HN protein with 571 aa (Dzogbema *et al.*, 2021).

#### **1.1.1.5.6. Large polymerase protein (L)**

The L protein is the largest and least abundant protein in the virus genome, with 2204 aa and a molecular weight of 250 kDa (Ganar *et al.*, 2014; Dzogbema *et al.*, 2021). This protein performs a variety of functions, including RNA synthesis, capping, and methylation, and it requires the P protein as a cofactor for *in vivo* RNA synthesis (Abdella *et al.*, 2020). This protein is also the last gene transcribed throughout the viral replication cycle and has been

shown to influence virus pathogenicity by boosting the rate of viral RNA synthesis during replication (Ganar *et al.*, 2014). The protein structure is made up of five conserved domains: RNA-dependent RNA polymerase (RdRp), poly-ribonucleotidyltransferase (PRNTase), connecting domain (CD), methyltransferase (MTase), and the C-terminal domain (CTD) (Abdella *et al.*, 2020). The interaction between the L protein and the P protein is critical for virus replication and transcription because the L protein provides all of the viral polymerase's catalytic activity (Abdella *et al.*, 2020; Dzogbema *et al.*, 2021).

#### **1.1.1.5.7. V protein**

This protein contains 239 aa and has a molecular weight of 36 kDa (Ganar *et al.*, 2014). When one G residue is introduced into the open reading frame (ORF) at a consensus sequence of the P protein during RNA editing, the V protein is encoded, while ensuring viral RNA replication modification by interacting with the N protein (Ganar *et al.*, 2014). This protein has been shown to be an additional virulence component of the virus because it inhibits the Interferons alpha/beta (IFN- $\alpha/\beta$ ) response (Ganar *et al.*, 2014; Tham *et al.*, 2019).

#### **1.1.1.5.8. W protein**

The W protein is created when two G residues are introduced into the P gene's RNA editing site (Ganar *et al.*, 2014). W protein mRNA has been detected in virus-infected cells, however, W protein has never been identified, and its function is unknown (Ganar *et al.*, 2014).

#### **1.1.1.6. Economic impact of NDV**

Newcastle disease is a worldwide infectious disease that is causing an increasing amount of economic damage (Xie *et al.*, 2020). Expenses for lengthy vaccination programs, performance losses owing to post-vaccination responses, monitoring assays, and supportive drugs are all examples of economic losses (Sandikli, 2021). Economic losses create annual costs in millions of dollars since ND is seen as a constraint on chicken goods due to its high mortality and trade restrictions (Susta *et al.*, 2011; Rehan *et al.*, 2019). The exportation of wild birds is a significant source of foreign currency revenues, with an estimated value in the international market of over eight billion United States dollars (\$) in 2002. (Sand, 2001). The mortality of around 4 million birds during the last significant outbreak observed in the United States of America (USA) of ND resulted in a loss of approximately \$162 million (Rehan *et al.*, 2019). Furthermore, NDV outbreaks in Pakistan commercial poultry observed in 2012 resulted in a massive loss of 45

million poultry birds alone, resulting in a loss of 6 billion Pakistani rupees (PKR) (Rehan *et al.*, 2019).

Pigeons and doves may play important roles in the transmission, epidemiology, and dispersal of new NDV strains, mostly by mechanical or fomite propagation (e.g. chicken manure carried on their feet). Because there is no evidence that Columbids may be infected with and disseminate NDV (other than PPMV) via the faecal-oral route, it is vital to track pigeons, particularly those near chicken farms (Mansour *et al.*, 2021). This disease has the potential to generate intercontinental endemicity, which can exacerbate economic crises due to the previously noted high morbidity and mortality, long-term restrictions on international trading operations, and increased veterinary management expenses (Mansour *et al.*, 2021). The identification of numerous elements involved in disease endemicity is critical for disease control (Rehan *et al.*, 2019). The southern ground hornbill (*Bucorvus leadbeateri*) is an endangered species in South Africa, Namibia, and Swaziland (Koeppel *et al.*, 2020). This species is reported to be highly affected by ND, which contributes to the extinction of this rare mammal as this disease is viewed as a threat to the animal (Koeppel *et al.*, 2020). Another potentially endangered species impacted by this virus is the Japanese Crested Ibis (*Nipponia nippon*), regularly found in China's Shaanxi province (Duan *et al.*, 2014).

#### **1.1.1.7. Diagnosis of NDV**

Despite breakthroughs in diagnostic methodologies, access to contemporary diagnostic tools is often limited to a small number of laboratories. Because of the importance of NDV categorization, a range of approaches for identification and differentiation have been developed (Dimitrov *et al.*, 2019). There are three major parts to ND diagnosis: (i) virus detection, (ii) virus characterisation, and (iii) epidemiology (Aldous and Alexander, 2001). The appeal of adopting molecular-based approaches has the potential to address all three components of ND diagnosis in a single test, swiftly and reliably (Aldous and Alexander, 2001). The detection and pathotyping of NDV is critical since the appearance of the virulent virus has major economic effects (Naveen *et al.*, 2013).

##### **1.1.1.7.1. Clinical diagnosis**

The clinical indicators of the disease, which could include prostration, depression, ruffling of feathers, leg and wing paralysis, and other neurologic abnormalities related to 100% mortality, are usually evaluated first during diagnosis of the disease (Hines and Miller, 2012). As a result,



developing nations with limited laboratory access employ an indeterminate diagnosis of NDV based on the clinical picture, which includes post-mortem lesions that detect haemorrhages in the proventriculus and caecal tonsils (Rehan *et al.*, 2019). The many post-mortem lesions linked with each pathotype are mentioned briefly below (Cattoli *et al.*, 2011).

#### **1.1.1.7.1.1. Velogenic viscerotropic**

The clinical indications associated with this strain become apparent only 2 days post-infection (dpi) (Cattoli *et al.*, 2011). Conjunctival swelling and reddening centered over the lymphoid patch located in the lower eyelid, anorexia, ruffled plumage, prostration, weakness, tremors, and diarrhoea are some of the prominent symptoms (Cattoli *et al.*, 2011). On the serosal surface of the intestines, there are multifocal haemorrhages, as well as multifocal areas of necrosis and ulcerations of the gut-associated lymphoid tissue (Cattoli *et al.*, 2011). The presence of disseminated necrosis foci in the spleen is strongly suggestive of this strain type infection (Cattoli *et al.*, 2011). The animal's spleens are swollen and extensively mottled, indicating necrosis (many foci of white to yellow discoloration) (Cattoli *et al.*, 2011). Animals infected through the conjunctiva exhibit eyelid oedema and haemorrhage (Cattoli *et al.*, 2011). The cortex of the thymus is completely necrotic, although the medulla has less severe lymphoid depletion (Cattoli *et al.*, 2011). This type of strain infection is usually accompanied by vascular alterations such as hydropic degeneration of the medium, hyalinization, and the development of hyaline thrombosis (Cattoli *et al.*, 2011). Necrosis also affects other organs such as the pancreas, liver, and gallbladder (Cattoli *et al.*, 2011).

#### **1.1.1.7.1.2. Velogenic neurotropic**

The most common clinical manifestations linked with this strain are neurological, such as head twitching, tremors, opisthotonos, and paralysis (Cattoli *et al.*, 2011). These indications are most commonly detected between 5 and 10 dpi (Cattoli *et al.*, 2011). In the early stages of the disease, splenic or proventricular congestion is prevalent (Cattoli *et al.*, 2011). There is multifocal mononuclear perivascular cuffing coupled with vascular endothelial hypertrophy or hyperplasia (Cattoli *et al.*, 2011). Lymphoid depletion and myocarditis have also been recorded as lesions (Cattoli *et al.*, 2011).

#### **1.1.1.7.1.3. Mesogenic**

This strain is known for causing minor clinical signs that are mostly respiratory in nature; nevertheless, on rare occasions, mesogenic infection might result in neurological symptoms

(Cattoli *et al.*, 2011). Concurrent viral and secondary bacterial infections are also common sequelae of this strain infection (Cattoli *et al.*, 2011). With this strain of infection, gross lesions are modest (Cattoli *et al.*, 2011). Myocarditis, splenic and pancreatic necrosis, perivascular cuffing, gliosis, chromatolysis, and neuronal necrosis can all occur in some species (Cattoli *et al.*, 2011).

#### **1.1.1.7.1.4. Lentogenic**

Some lentogenic strains cause respiratory problems, visible gross lesions, and persistent non-suppurative tracheitis (Cattoli *et al.*, 2011). Rales, coughing, anorexia, and depression are mild clinical symptoms linked with this strain infection between 2 and 12 dpi (Cattoli *et al.*, 2011). Other clinical indicators include lymphoid follicle hyperplasia in the spleen and air sacs, lymphoid follicle proliferation in the tracheal lamina propria, lymphocytic infiltration, cilia loss, and squamous metaplasia in the proximal trachea (Cattoli *et al.*, 2011).

#### **1.1.1.7.2. Serological diagnosis**

The inadequacy of characteristic clinical signs in different bird species poses a serious challenge for the rapid identification and diagnosis of this infection because these clinical signs are not always reliable measures, necessitating laboratory diagnosis for confirmation and pathotyping to rule out other diseases such as pigeon herpes virus (PHV) as the symptoms are very similar (Hines and Miller, 2012; Pestka *et al.*, 2014; Dzogbema *et al.*, 2021).

All indirect serological tests, such as haemagglutination inhibition test (HI) and Enzyme-linked immunosorbent assay (ELISA), are used to diagnose the disease (Dzogbema *et al.*, 2021). The haemagglutination assay (HA) can be used to detect NDV initially (the virus agglutinates red blood cells), and a conventional serological test such as HI can be performed for confirmation because it uses NDV specific antisera (Pestka *et al.*, 2014; Rehan *et al.*, 2019). The HI test with mouse monoclonal antibodies (MAbs), allows for rapid identification of NDV without the possibility of cross-reactions with other serotypes as it differentiates between APMV and PPMV; however, due to a wide range of genetic variation among PPMV members, the use of MAbs binding profiles is no longer regarded as an appealing option as it increases the possibility that a mutant is undetectable (Naveen *et al.*, 2013; Swayne and Brown, 2021).

The ELISA is commonly used to check post-vaccination levels because it quantifies antibodies (Dzogbema *et al.*, 2021; Swayne and Brown, 2021). A variety of commercial ELISA kits are

available, including indirect ELISA, sandwich ELISA, and competition ELISA (Dzogbema et al., 2021). However, serological assays for antibody detection have limited diagnostic relevance because they can identify specific antibodies for the virus but do not provide information on the viral strain and cannot distinguish between post-infection and post-vaccination antibodies (Pestka *et al.*, 2014; Dzogbema *et al.*, 2021).

Virus neutralisation test (VNT) is another serological test useful in determining the amount of neutralising antibodies, but requires the availability of cell cultures (Bello *et al.*, 2018). Detection of particular antibodies to the virus cannot be used to provide a diagnosis since it is difficult to separate field strain antibodies from vaccine strain antibodies due to the existence of a single serotype (Pestka *et al.*, 2014). As a result, rather than detecting specific antibodies, molecular techniques are often used (Pestka *et al.*, 2014).

#### **1.1.1.7.3. Virus isolation**

The first step towards correct diagnosis is virus isolation (Pestka *et al.*, 2014). This method is regarded as the gold standard method for definitive diagnosis and often validating the results from other detection methods (Bello *et al.*, 2018). Samples needed for virus isolation are determined by the sites of virus replication and routes of viral shedding (Bello *et al.*, 2018). Live bird samples should include tracheal or oropharyngeal and cloacal swabs in isotonic solution with or without antibiotics, but deceased bird samples should include swabs and organ pieces such as the lungs, kidneys, spleen, brain, liver, and intestines (Pestka *et al.*, 2014; Bello *et al.*, 2018). The WOAHA-recommended conventional procedure for virus isolation involves inoculating the virus into specific pathogen-free (SPF) embryonated chicken eggs or specific antibody-negative (SAN) eggs (Dzogbema *et al.*, 2021; Swayne and Brown, 2021). Samples used in SPF eggs for virus isolation may also be used for isolation in cell cultures, as the virus has the capability to replicate in a variety of cell cultures (Pestka *et al.*, 2014). However, some pigeon-adapted NDV strains known as PPMV-1 can only be isolated using cell cultures and not embryonated eggs (Bello *et al.*, 2018). Presence of the virus in the cell cultures allows cytopathic effects (CPE) which are shown by disruption of the monolayer, formation of syncytia, cell rounding and cell death (Pestka *et al.*, 2014; Bello *et al.*, 2018).

#### **1.1.1.7.4. Virus identification**

Technique-based molecular tools are used for more than only detection because they provide a quick genetic characterisation of the virus, with RT-PCR being the most sensitive technique

devised for NDV detection and *in vitro* differentiation (Rehan *et al.*, 2019). Amplification of the specific region of the genome can be done by utilising universal and specific primers for a given pathotype or antigenic variant of the virus (Pestka *et al.*, 2014). Two pairs of primers can also be used in a nested RT-PCR which allows for a higher sensitivity than the conventional RT-PCR (Pestka *et al.*, 2014). This conventional approach is followed by the application of real-time RT-PCR (rRT-PCR) (Dzogbema *et al.*, 2021). Real-time RT-PCR, with its higher sensitivity and ability to quantitatively measure viral RNA in samples, is increasingly replacing conventional RT-PCR. This method can be performed in a single tube, reducing reaction time and the risk of cross-contamination (Pestka *et al.*, 2014). Its preference for virus surveillance lies in enabling rapid sensitivity diagnosis at high throughputs (Swayne and Brown, 2021).

Molecular diagnosis of this virus can be accomplished in two ways: (i) by using particular primers against conserved parts of the genome such as the L, M, and NP genes, and (ii) by using the F gene region that includes the cleavage site to detect virulent NDV (Hoffmann *et al.*, 2009). Tracheal and oropharyngeal swabs are usually the best samples for this procedure because they do contain organic material such as cells, but they tend to be less contaminated with bacteria, yeast or other microbes that could hinder or obstruct the reconstruction and amplification of the virus RNA, as can be seen with cloacal swabs, faeces, or intestinal contents (Dzogbema *et al.*, 2021).

Naveen and colleagues (2013) reported a method for detecting, differentiating, and pathotyping PPMV simultaneously using RT-PCR and restriction enzyme (RE) digestion of a part of the F gene amplicon encoding the fusion protein cleavage site. The RT-PCR technique expanded by RFLP and sequencing of the gene fragment encoding the protein F cleavage site, not only allows the virulence of the virus to be partially determined, but also has a high educational value in epidemiological studies and phylogenetic analyses of the virus (Pestka *et al.*, 2014). A set of four restriction enzymes, including HhaI, MspI or HaeIII, MboI, and BglII, were successfully grouped into an assay to detect, differentiate, and pathotype APMV and PPMV viruses (Naveen *et al.*, 2013). These restriction enzymes are mapped out in Figure 1.5, illustrating the sequential manner for differentiation and pathotyping (Naveen *et al.*, 2013).

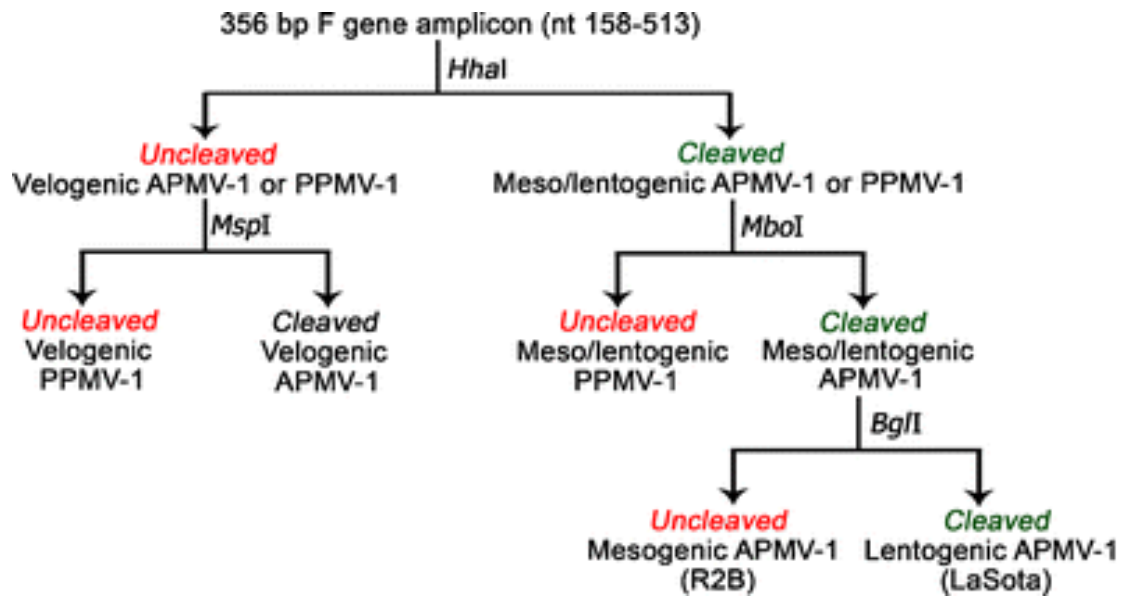


**Figure 1.5:** Molecular amplification of the F gene and sequential differentiation and pathotyping of the different strains of avian paramyxovirus -1 (APMV-1) and pigeon paramyxovirus -1 (PPMV-1) (Naveen *et al.*, 2013). Restriction enzymes: *HhaI*, *MspI*, *MboI* and *BglI*. Nt: nucleotides. Permission to reproduce under licence number 5700670374132.

Although the virus has significant genetic variety, viruses that share chronological, geographical, antigenic, and epidemiological features tend to clump into certain genetic lineages or genotypes (Swayne and Brown, 2021). As a result, it has proven useful in assessing both global epidemiology and local dissemination (Swayne and Brown, 2021). The implementation of a unified nomenclature and classification scheme based on phylogenetic analyses of the entire F gene and objective criteria splitting the viruses into genotypes and sub-genotypes allows for the categorization of new APMV-1. The Sanger sequencing approach is advised for the quick identification of a single target gene (F) to define virus virulence; however, by employing high throughput sequencing technology and using a variety of bioinformatics tools, a larger dataset can be generated (Swayne and Brown, 2021).

#### 1.1.1.7.5. *In vivo* and *in vitro* testing

*In vivo* and *in vitro* testing can determine the virus's pathogenicity (Dzogbema *et al.*, 2021). Mean death time (MDT) in embryonated chicken eggs, intravenous pathogenicity index (IVPI), and ICPI are other *in vivo* approaches (Hines and Miller, 2012; Dzogbema *et al.*, 2021). In the case of the ICPI test, the animal is given a score (0: normal; 1: sick; 2: dead) daily for an average of eight days (Dzogbema *et al.*, 2021). Table 1.5 shows the various values for

measuring virulence for each pathotype (Bilal *et al.*, 2014; Dey *et al.*, 2014; Dzogbema *et al.*, 2021).

**Table 1.2:** The values for measuring virulence for each different pathotype of Newcastle disease virus during *in vivo* testing (Bilal *et al.*, 2014; Dey *et al.*, 2014; Dzogbema *et al.*, 2021).

|                   | <b>ICPI<sup>1</sup></b> | <b>IVPI<sup>1</sup></b> | <b>MDT<sup>1</sup> (hours)</b> |
|-------------------|-------------------------|-------------------------|--------------------------------|
| <b>Velogenic</b>  | Above 1.5               | Greater than 2.5        | Less than 60                   |
| <b>Mesogenic</b>  | Between 0.7 and 1.5     | 0.55                    | Between 60 and 80              |
| <b>Lentogenic</b> | Below 0.7               | 0.00                    | Beyond 90                      |

<sup>1</sup> ICPI: Intracerebral pathogenicity index, IVPI: intravenous pathogenicity index, MDT: mean death time

During *in vitro* testing, the virus is known to produce the formation of plaques on cultured embryonic fibroblasts which vary in size and appearance depending on the strain's virulence (Dzogbema *et al.*, 2021). However, PPMV are known to have some difficulty when tested for pathogenicity *in vivo* using normal conventional *in vivo* pathogenicity tests (Naveen *et al.*, 2013).

#### **1.1.1.8. Treatment and control strategies**

Every year, ND outbreaks occur in various parts of the world due to a lack of vaccination coverage in backyard poultry production or a failure to elicit good protection in vaccinated farms (Bari, 2021). No specific treatment for PPMV has been established, however, supportive therapies are indicated and include: electrolytes, acidifying agents and probiotics (Palgen *et al.*, 2015; Bari, 2021). Controlling other disorders that may behave as comorbidities is also critical in the treatment of PPMV (Palgen *et al.*, 2015). The best control method remains immunization of flocks, combined with robust biosecurity regimes and hygienic culling of infected birds (Dzogbema *et al.*, 2021; Mansour *et al.*, 2021).

The production of conventional commercial vaccines is based on several virus strains that are separated into two groups: (i) lentogenic strains such as Hitchner-B1, LaSota, V4, NDW, and I2 strains and (ii) mesogenic strains such as Roakin, Mukteswar, and Komarov strains (Pestka *et al.*, 2014; Dzogbema *et al.*, 2021). Many vaccines are available, including live-attenuated

virus vaccines that can be administered via drinking water, aerosol, eye/nostril droplets, and beak dipping (Bucko and Gieger, 2019).

Inactivated virus vaccines, on the other hand, can only be injected, such as the paramyxovirus prophylaxis, which is administered via subcutaneous or intramuscular injection (Pestka *et al.*, 2014; Dzogbema *et al.*, 2021). As a result, inactivated vaccines cost more than live vaccines (Dzogbema *et al.*, 2021). Due to antigenic variations between vaccine and outbreak strains, vaccination against the virus does not prevent infection or even replication of the virus, it only inhibits the appearance of clinical syndromes for severe disease and death in infected birds (Pestka *et al.*, 2014; Mansour *et al.*, 2021; Peeters and Koch, 2021). Live vaccinations are also not utilized for paramyxovirus immunoprophylaxis because pigeons are less immunogenic and increase the risk of the vaccine virus spreading in the case of a carrier pigeon where the virus vaccination has not yet been applied (Pestka *et al.*, 2014). To limit the risk, sanitary prophylactic methods include correct carcass disposal, avoiding contact with birds of uncertain health state, and implementing biosecurity and disinfection measures for home flocks and staff (Bucko and Gieger, 2019). In some nations, compulsory vaccination of racing pigeons is considered a local act; nonetheless, management of this virus in wild pigeons is almost impossible (Mansour *et al.*, 2021). Documentation of the increasing frequency of outbreaks worldwide demonstrates that present immunization measures are insufficient to control the disease (Rehan *et al.*, 2019).

#### **1.1.1.9. History of Newcastle disease virus in South Africa.**

The earliest potential account of ND in South Africa dates back to a letter penned in 1892 to the Agricultural Journal and a letter to the Transvaal Agricultural Journal (1903) offering examples that hint at the possible existence of ND during this period. While it is acknowledged that many symptoms described in these cases do not conclusively point to ND, some features suggest Marek's disease infection. Collectively, these historical references suggest that ND may have been present in South Africa since the late 1800s.

In 1945, the formal diagnosis of ND in South Africa was established with the emergence of a severe poultry disease in KwaZulu-Natal (KZN) (Kaschula *et al.*, 1946). Employing serum neutralization tests for diagnostics, the investigation uncovered a striking similarity between the symptoms and post-mortem findings in Natal and those documented by Hudson in Mombasa, Kenya, in 1935 (Abolnik, 2017). Although widely assumed to be transmitted by a

ship from an East Coast harbour in Africa, the origins and distribution of the disease remained inadequately documented (Abolnik, 2017; Dzogbema *et al.*, 2021). The impact of the 1944/1945 outbreak documented in South Africa was almost predominantly confined to the sugarcane belt of Natal (Kaschula *et al.*, 1946).

In July 1949, instances of ND surfaced in Windermere Township, Cape Town (CPT), as reported by Abolnik (2017). Extending its impact to Port Elizabeth (PE) and De Aar, both within the Cape Province, the disease had already taken hold by September of that year. It wasn't until 1950 that Johannesburg (JHB) experienced its initial outbreak, followed by a recurrence in 1954. Subsequent outbreaks in Durban unfolded in 1951 and 1953. South Africa's virological scenario saw the identification of a mild lentogenic strain known as the "American type" in July 1960 with symptoms exceptionally mild (Kluge, 1964). Nevertheless, in August 1961 a resurgence of velogenic strains emerged in the northern outskirts of Pretoria (PTA). The severity of the situation escalated in 1967, manifesting as a severe epidemic on a farm in the Cape Flats near Cape Town. This outbreak had repercussions on adjacent areas like Belville and Stellenbosch. The World's Poultry Science Association (WPSA) South African branch reported that the strains responsible for this acute epidemic classified as the "Asian type" contrasted with the concurrent prevalence of the "American type" observed in the Transvaal (now known as Gauteng), Natal, and Eastern Cape (EC) provinces (Oosthuizen, 1979).

The prevailing belief was that ND was not enzootic in South Africa, and the restricted character of the outbreaks suggested that the infections likely originated from unidentified external sources and therefore were not deemed of significant concern as proposed by Kluge (1964) and De Almeida *et al.* (2013). Despite this, the poultry industry's notable expansion led to a considerable concentration of vulnerable chickens in South Africa, resulting in one of the most severe ND epidemics experienced from 1970 to 1972 resulting in the initial outbreak in Potgietersrus, followed by subsequent incidents in the suburbs of Pretoria (Abolnik, 2017). Towards the end of 1970, a notable commercial broiler operation in Johannesburg suffered the consequences of an ND outbreak, leading to considerable economic losses within the sector. The following year (1971), ND was assumed to be enzootic in South Africa, with outbreaks declining by 1974 and re-emerging exclusively in unvaccinated chickens (Abolnik, 2017). Responding to the impracticality of the previous eradication method in controlling ND, the Technical Advisory Committee of the South African Poultry Association (SAPA) introduced



a national strategy (Coetzee, 1980). Figure 1.6 illustrates a summary timeline of all the ND cases and various genotypes isolated in South Africa.

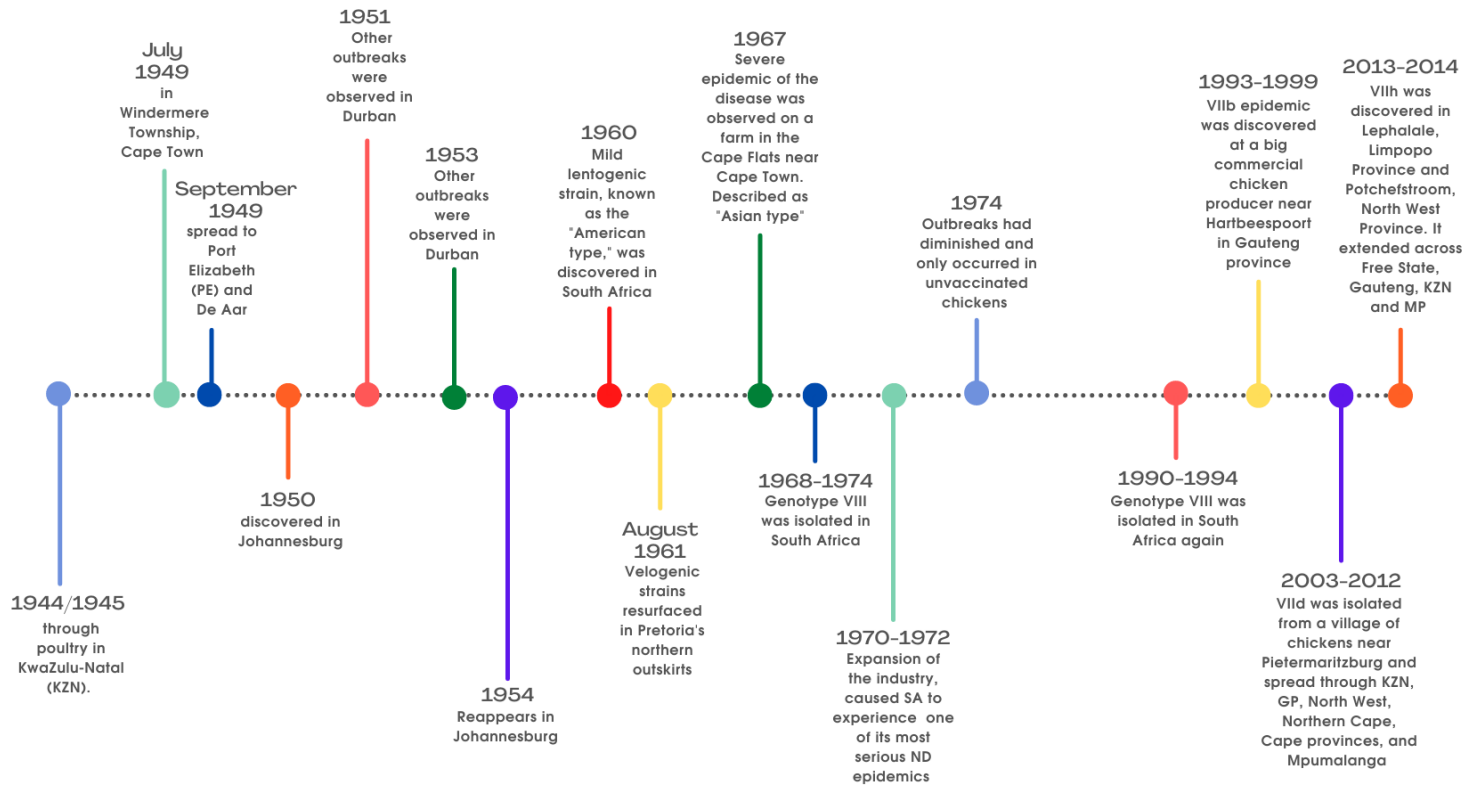


**Figure 1.6:** A summary timeline of all the Newcastle disease cases and various genotypes isolated in South Africa between 1944 and 2014 adapted from (Abolnik, 2017).

The genetic characterization of NDV strains in SA has been an ongoing challenge. Since the 1950s, the origins of sporadic Newcastle Disease (ND) outbreaks have persisted as an unresolved mystery, prompting the presumption that these intermittent incidents could potentially stem from spill-overs originating from an unidentified reservoir. Routine isolation of APMV-1 by the national veterinary laboratories in KZN, Western Cape, and the University of Pretoria (UP) from the national flock during outbreaks, played a crucial role in monitoring ND in South Africa. To delve into the molecular epidemiology of ND within the country, a comprehensive project was undertaken at the Onderstepoort Veterinary Institute in Pretoria by Abolnik (2007) subjecting all available APMV-1 isolates to RT-PCR amplification of a

segment of the F gene with subsequent steps of DNA sequencing and phylogenetic analysis. Identifying the strains accountable for sporadic poultry epidemics in SA unfolded as described below.

Genotype VIII, recognized as one of the smallest exotic groups of ND globally, made its initial appearance in SA between 1968 and 1974, re-emerging in the early 1990s until 1994 (Herczeg *et al.*, 1999). Despite rigorous active surveillance and continuous molecular epidemiological studies, the isolation of genotype VIII viruses remained absent from 1994 to 2000 as documented by Abolnik (2007) and no genotype VIII strains have been identified in South Africa since June 2000. An epidemic of genotype VIIb (VII.1.1) unfolded in June 1993 at a major commercial chicken producer near Hartbeespoort in Gauteng province (GP) (Abolnik, 2017). In just six months, ND swiftly spread throughout southern Africa, inflicting severe losses. In hindsight, the introduction of genotype VIIb into SA in the early 1990s coincided with the emergence of this pandemic strain in various parts of East Asia and Europe during the same period (Abolnik, 2017). Herczeg *et al.*, (1999) initially reported that the genotype VIIb (VII.1.1) strain responsible for the SA outbreaks had its origin in the Far East and some Western European countries, however extensive phylogenetic analysis revealed its origin in Southern Europe (Abolnik 2007). The possibility of multiple introductions of genotype VIIb (VII.1.1) into SA was suggested (Abolnik 2007). However, after 1999, genotype VIIb (VII.1.1) was not detected in SA (Abolnik 2007). In 1995, genotype XIII was discovered in an ostrich, and in 1999, lentogenic strains attributed to genotype II were acquired (Megahed *et al.*, 2020). These strains were suspected to originate from commercial vaccines, leading to the absence of genuine lentogenic wild type NDV strains during that period (Megahed *et al.*, 2020).

Between 1999 and 2000, a confined outbreak of velogenic viscerotropic NDV surfaced, impacting both a singular commercial flock and village chickens within the KZN province. The strain was identified as genotype VIIId, however, in the ensuing three years, no instances of ND outbreaks were documented. However, late in September 2003, a velogenic ND virus emerged among village chickens near Pietermaritzburg, close to the locations of the 1999 and 2000 outbreaks. Subsequent phylogenetic analysis by Abolnik *et al.*, (2004) unveiled that the 2003 genotype VIIId strain was intricately connected to the isolates from the 1999/2000 outbreaks.

An epidemic of genotype VIIId started in commercial flocks in the Camperdown/Richmond before spreading northwards through KZN, GP, and North West (NW) provinces (Abolnik, 2017). Over the following months, this genotype extended its reach to the Northern Cape (NC), Cape provinces, and Mpumalanga province (MP) (Abolnik, 2017). Post-2012, South Africa reported no cases of genotype VIIId (Abolnik, 2017). Throughout the epidemic affecting both commercial and backyard chickens, mortalities were documented in peafowl, hadeda ibis chicks, geese, ostriches, pheasants, and doves (Abolnik, 2007). In August 2013, genotype VIIh (VII.2) emerged in Lephalale, Limpopo Province (LP), and Potchefstroom, NW, spreading across Free State (FS) and GP throughout the remainder of 2013 (Abolnik, 2017). In 2014, genotype VIIh (VII.2) surfaced in KZN and MP (Abolnik, 2017). A recent addition to this genomic landscape is genotype XIIIa (XIII 1.1), isolated in 2020 (Megahed *et al.*, 2020). Exotic strains introduced at regular intervals were identified as the root cause of each epidemic in South Africa, with the unlawful importation of chickens, poultry products, or exotic birds considered the most likely source of infection (Abolnik, 2017).

#### **1.1.1.10. Previous findings for PPMV in South Africa with recent outbreaks and cases reported.**

Pigeon paramyxovirus type 1 (PPMV-1) has been active in South Africa since the mid-1980s, mostly affecting doves and pigeons, and has since spread (Abolnik *et al.*, 2008). The first isolation of PPMV from doves, however, occurred in September 1986 during an epidemic (Pienaar and Cilliers, 1987). Based on the presence of two distinct subgroups, 4bi and 4bii, that have been circulating in Europe and Japan since the early 1990s, phylogenetic data suggested that PPMV was imported into South Africa at least twice (Abolnik *et al.*, 2008). Since 2002, two incidences of PPMV infection in chickens have been reported in South Africa, one of these isolates was isolated from 28-week-old layers in December 2002, in the Mooi Rivier district (KZN) and corresponded to lineage 4bii, the second in chickens in Sibasa, near Polokwane in March 2006 from lineage 4bi (Abolnik *et al.*, 2008). Two other virus isolates were isolated from racing pigeons in Oudtshoorn during August 2004, and from doves in Darling (Cape Town) during March 2006 corresponding to lineage 4bii, where another isolate from a pigeon in Pretoria, corresponding to lineage 4bi, was discovered in May 2005. (Abolnik *et al.*, 2008). Between January 2005 and March 2006, viruses clustering in lineage 4bi were discovered in Kimberly (Northern Cape), Brits/Rustenburg, and Polokwane. (Limpopo). Lineage 4bii strains were isolated from pigeons and doves in Cape Town, Stellenbosch, Bellville, and Montagu (Western Cape) over six months from 2005 to 2006. (Abolnik *et al.*, 2008). In 2006, PPMV

infection was documented in an African ground hornbill (*Bucorvus leadbeateri*) (Abolnik *et al.*, 2008).

Disease reporting in South Africa is of vital importance because it assures a country's capacity to demonstrate to its trade partners that it can detect outbreaks or the existence of animal illnesses through a good passive monitoring system (de Klerk and Pienaar, 2022). When a farmer notices something wrong with his animals, he contacts an animal health technician, a state veterinarian, or a private veterinarian and notifies them (de Klerk and Pienaar, 2022). Occurrences must be recorded since they are a good indicator of a country's passive surveillance (de Klerk and Pienaar, 2022). Disease reporting is also critical for a country to detect epidemics of certain illnesses to respond to these outbreaks, where the spread of the disease can be prevented, control measures instituted, disease eradication, etc (de Klerk and Pienaar, 2022). Each province should determine which information should be obtained for each epidemic (de Klerk and Pienaar, 2022). The bare minimum of data necessary by the National Directorate of Animal Health, as well as how it should be sent to the Sub-directorate Epidemiology is listed briefly in Table 1.6 (de Klerk and Pienaar, 2022).

**Table 1.3:** Data necessary to report a disease/ outbreak for any species in general (de Klerk and Pienaar, 2022).

| <b>Data needed</b>   | <b>Description</b>  |
|--|---|
| <b>Date</b>  | Entered in the format YYYYMM <sup>1</sup> .   |
| <b>Provincial code, state veterinary area code, district code, disease code and species code</b> | These codes can be obtained from the lists of codes provided on the Department of Agriculture, Land Reform and Rural Development (DALRRD) website ( <a href="https://www.dalrrd.gov.za/Branches/Agricultural-Production-Health-Food-Safety/Animal-Health/Epidemiology/disease-reporting">https://www.dalrrd.gov.za/Branches/Agricultural-Production-Health-Food-Safety/Animal-Health/Epidemiology/disease-reporting</a> ) |
| <b>Farm ID</b>   | Registered number or name of farm.  |
| <b>Geographical location</b>   | Must be given in degrees, minutes and seconds EAST and degrees, minutes and seconds SOUTH.  |
| <b>Number of susceptible animals</b>   | Indication of the number of animals of the affected species in the affected epidemiological unit.   |
| <b>Number of outbreaks</b>   | The occurrence or not of a disease per geographic location.   |
| <b>Number of cases</b>   | Total number of animals for the disease reported (animals clinically affected and those that have died as a result of the disease).   |
| <b>Number dead</b>   | Total number of animals that died naturally as a result of being affected by the disease reported.  |
| <b>Number killed/ slaughtered</b>  | Total number of animals killed with and without salvage for human consumption.  |
| <b>Number treated</b>  | Total number of animals treated for a specific disease.   |
| <b>Number vaccinated</b>   | Total number of animals vaccinated for a specific disease.  |
| <b>Comments</b>  | To give any additional information to describe or identify the outbreak.  |

<sup>1</sup>YYYYMM: year and month.

Newcastle disease is classified as a Controlled Animal Disease under the Animal Diseases Act of 1984. (Act 35 of 1984) with disease codes of A160 and B314, respectively (de Klerk and Pienaar, 2022). Disease outbreaks for both have been reported across South Africa more so for NDV than PPMV - the latter predominantly reported in the more northern provinces (Figure 1.7).

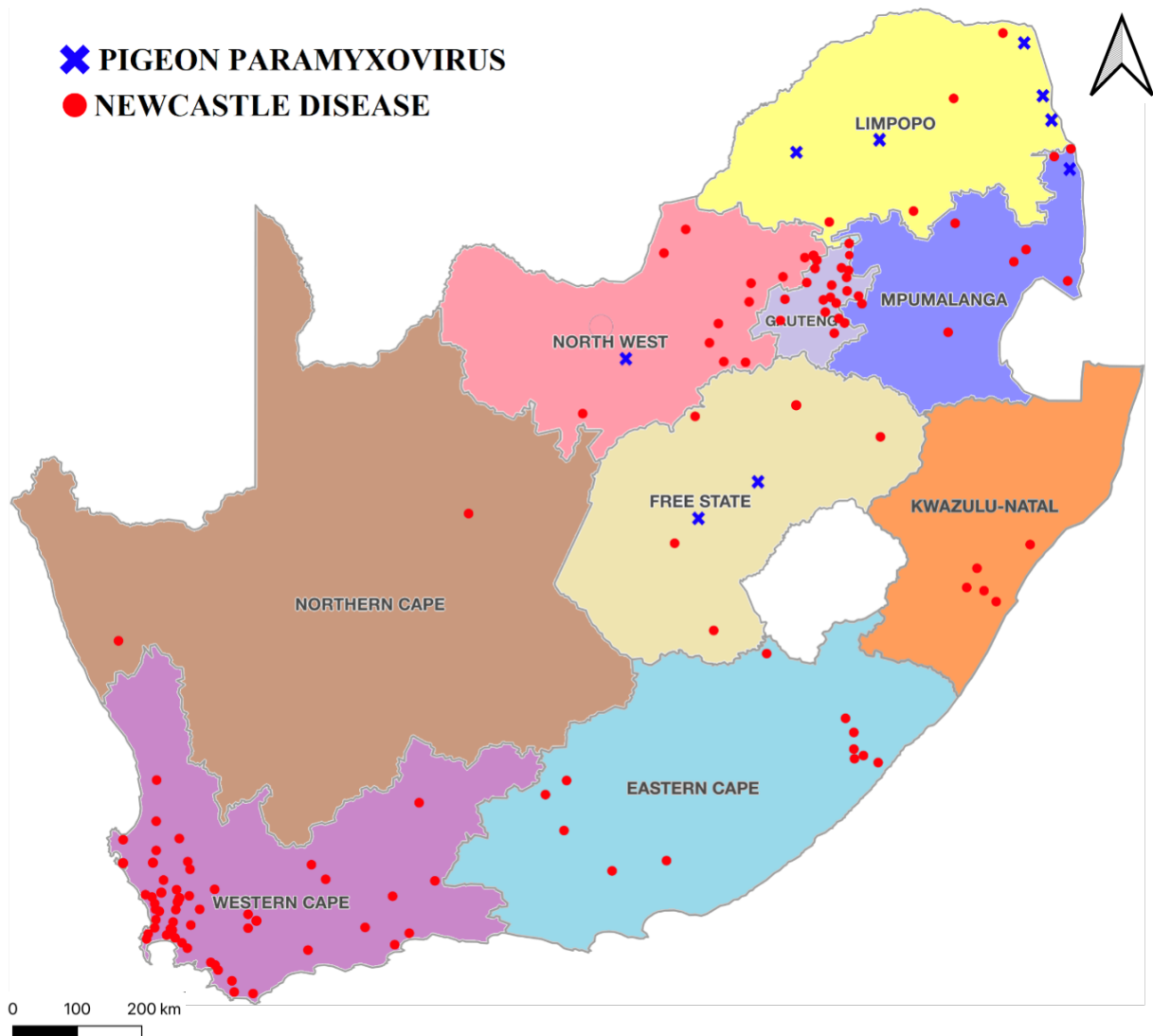


**Figure 1.7:** Newcastle disease and PPMV outbreaks reported by the Provincial Veterinary Services from 2015 to June 2022 for each province in South Africa (Department of Agriculture, 2022b).

Since the actual location of the PPMV outbreaks was not provided, the PPMV position on the South Africa map is only hypothetical in the province mentioned. In 2015, 45 ND outbreaks were recorded in South Africa which was the highest in comparison from 2016 to 2021, when the numbers were 23, 34, 31, 19, 15, and seven respectively. PPMV outbreaks have been recorded in 2017, 2018, and 2021. In 2017, there were eight PPMV outbreaks, one in 2018, and one in 2021. Up till June of 2022, nine ND outbreaks were observed. Gauteng and the Western Cape provinces had the most outbreaks recorded. Newcastle disease cases recorded

for each epidemic in South Africa's several provinces from 2010 to 2021 were acquired and summarized from DARLLD's disease database. Table 1.7 summarises the number of ND cases reported for each province during 2010 to 2021 (Department of Agriculture, 2022a).

**Table 1.4:** Number of ND cases reported for each South African province from 2010 to 2021 (Stats SA (South Africa), 2011; Department of Agriculture, 2022a).

|              |               | <b>PROVINCES<sup>1</sup></b> |             |            |                |             |           |               |             |            |
|--------------|---------------|------------------------------|-------------|------------|----------------|-------------|-----------|---------------|-------------|------------|
| <b>YEAR</b>  |               | <b>GAU</b>                   | <b>WC</b>   | <b>LP</b>  | <b>FS</b>      | <b>NW</b>   | <b>EC</b> | <b>NC</b>     | <b>MP</b>   | <b>KZN</b> |
|              | <b>2010</b>   | 635                          | 1113        | 0          | 0              | 101         | 1577      | 0             | 0           | 0          |
|              | <b>2011</b>   | 535                          | 3409        | 4          | 0              | 0           | 16        | 1             | 12          | 20         |
|              | <b>2012</b>   | 0                            | 47 951      | 0          | 0              | 39          | 250       | 0             | 3           | 21         |
|              | <b>2013</b>   | 13 224                       | 553         | 1          | 9              | 408 870     | 22        | 0             | 185         | 388        |
|              | <b>2014</b>   | 53 175                       | 242         | 27         | 15             | 27 638      | 79        | 1             | 2000        | 6296       |
|              | <b>2015</b>   | 2771                         | 1054        | 0          | 0              | 96          | 74        | 7             | 15 317      | 25         |
|              | <b>2016</b>   | 76                           | 197         | 0          | 0              | 51          | 274       | 0             | 0           | 1          |
|              | <b>2017</b>   | 460                          | 206         | 100        | 0              | 62          | 3         | 0             | 2           | 1          |
|              | <b>2018</b>   | 1                            | 318         | 2          | 7              | 0           | 0         | 0             | 44          | 0          |
|              | <b>2019</b>   | 502                          | 195         | 300        | 1              | 581         | 0         | 15            | 900         | 3          |
|              | <b>2020</b>   | 0                            | 278         | 1614       | 500            | 0           | 0         | 0             | 0           | 0          |
|              | <b>2021</b>   | 0                            | 58          | 0          | 9              | 640         | 0         | 0             | 0           | 0          |
| <b>TOTAL</b> | <b>71 379</b> | <b>55 574</b>                | <b>2048</b> | <b>541</b> | <b>438 078</b> | <b>2295</b> | <b>24</b> | <b>18 463</b> | <b>6755</b> |            |

<sup>1</sup> GAU - Gauteng, WC - Western Cape, LP – Limpopo, FS – Free State, NW – North West, EC – Eastern Cape, NC – Northern Cape, MP – Mpumalanga, KZN – KwaZulu-Natal

The total number of ND cases recorded for each year from 2010 to 2021, as shown in Table 1.7, is graphically represented in Figure 1.8 as colour provincial maps, allowing for easy comparison of various years throughout South Africa's provinces.

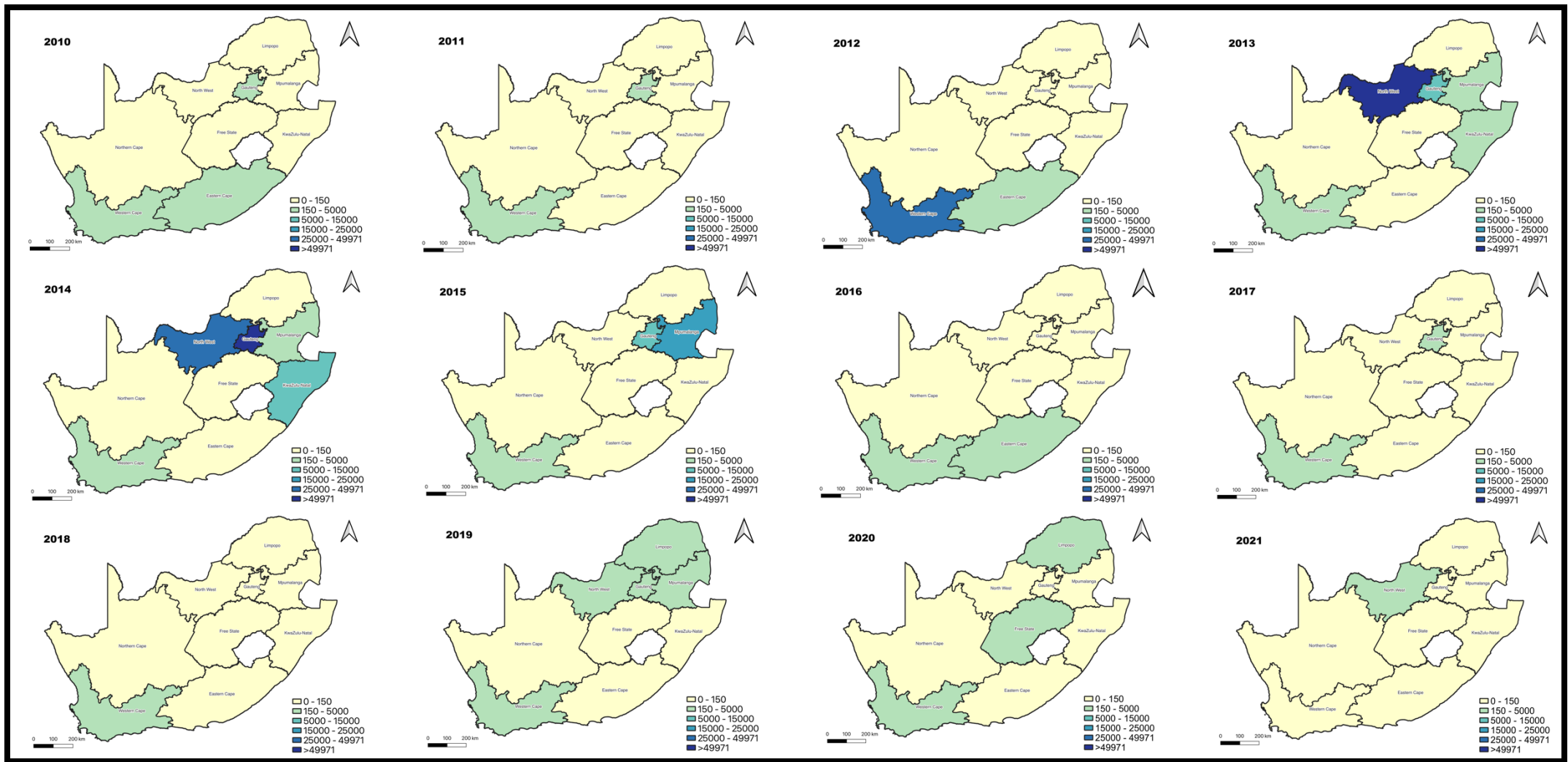


Figure 1.8: Total ND cases reported for each province from 2010 to 2021 (Department of Agriculture, 2022a), (Stats SA (South Africa), 2011).



## 1.2. Introduction to Circovirus

Circoviruses, which are exceptionally small, covalently closed, and circular single-stranded DNA viruses, have emerged as a major concern in the avian and pigeon industry because of their extensive and profound impact (Mankertz, 2008). It has been classified under the *Circoviridae* family and primarily impacts young pigeons during the summer months specifically between late May and early September in Europe (Stenzel and Konciki, 2017; (Loiko *et al.*, 2018; Khalifeh *et al.* 2021).

The prevalence of circovirus infections tends to peak during hot spells, trial flights, and the commencement of the first racing competitions (Stenzel and Konciki, 2017). At the outset, the symptoms of infection in pigeons are quite nonspecific as they first display unusual foraging behaviour, often lingering near feeders and pecking at food (Stenzel and Konciki, 2017). However, upon closer examination, it becomes evident that their crops are either empty or hold only a few seeds (Stenzel and Konciki, 2017). As the disease progresses, affected birds exhibit additional symptoms such as diarrhea and non-specific indicators like apathy, feather-ruffling, or reluctance to engage in training (Stenzel and Konciki, 2017). This rapid deterioration in the health of affected birds can lead to mortality rates reaching 20% to 50% in afflicted flocks. Initially, the syndrome - young pigeon disease syndrome (YPDS) was primarily observed in young domestic pigeons because they possess well-developed bursa of Fabricius (BF), which houses numerous target cells for PiCV (Stenzel and Konciki, 2017). Circovirus also affects other immune system organs, such as the thymus and spleen, and its genetic material has been detected in various other body parts, including the liver, kidneys, intestines, brain, and skin (Stenzel and Konciki, 2017). Circovirus infections have been observed in a diverse array of vertebrates and avian hosts, with passerines and species in non-passerine birds (Raidal, 2012; Kong *et al.*, 2021). Besides avian species, other vertebrates such as poultry and mammals are seen as natural hosts for circovirus infections. While PiCV has historically been predominantly identified in young pigeons with diseases, recent research has unveiled instances of PiCV infection in seemingly healthy adult birds (Daum *et al.*, 2009). This suggests that a significant number of PiCV infections may go unnoticed as subclinical cases (Daum *et al.*, 2009). These infections may persist, serving as potential sources of transmission to younger birds. However, the prevalence of PiCV infection, particularly in adult and recently hatched pigeons, remains poorly understood (Daum *et al.*, 2009). Global trade and pigeon racing have contributed to the widespread distribution of PiCV infection (Stenzel *et al.*, 2012).

### 1.2.1. Pigeon circovirus

Pigeon circovirus (PiCV), first described in the scientific literature during the early 1990s, stands as a pivotal infectious agent with profound implications for pigeon health (Silva *et al.*, 2022). It is one of four viruses grouped in the family *Circoviridae*, affecting young racing pigeons and pigeons raised for meat production globally (Zhang *et al.*, 2015; Duchatel *et al.*, 2006). The onset of immuno-suppression in infected birds is a significant aspect of the multifactorial disease known as young pigeon disease syndrome, where pigeon circovirus (PiCV) is recognized as a pivotal contributor to this phenomenon (Duchatel and Szeleszczuk, 2011). The pigeon industry sustained huge losses due to the high prevalence of PiCV in pigeons (Todd *et al.*, 2000; Santos *et al.*, 2020a). This mainly affected pigeon sports and the breeding of new stock which led to the production efficiency of pigeons to be highly affected (Todd *et al.*, 2000). Table 1.8 outlines the terminology and case definitions for diseases related to Pigeon circovirus, utilizing both clinical and laboratory criteria (Silva *et al.*, 2022).

**Table 1.8:** Terminology and case definitions for Pigeon Circovirus-Related diseases, considering clinical and laboratory criteria (Silva *et al.*, 2022).

| Pigeon Circovirus disease proposed name (acronym) | Main clinical sign                                       | Individual diagnostic criteria   |
|---|--|--|
| PiCV-subclinical infection (PiCV-SI)              | No clinical sign evident                                 | <ul style="list-style-type: none"> <li>• Sometimes presents with subtle clinical symptoms.</li> <li>• A few to no observable histological abnormalities in key lymphoid organs such as the bursa of Fabricius and spleen.</li> <li>• Reliably identified in fecal or cloacal swab samples through standard or quantitative PCR methods.</li> </ul> |
| PiCV-systemic disease (PiCV-SD)                   | Depression, weight loss, diarrhea, vomiting and lethargy | <ul style="list-style-type: none"> <li>• Clinical manifestations can be observed.</li> <li>• Distinctive viral inclusions, found primarily within the bursa and/or spleen, are evident in histological lesions, whether intranuclear or intracytoplasmic in nature.</li> </ul>   |

### 1.2.1.1. History

Pigeon circovirus was initially observed in 1993 in the United States where pigeons exhibited clinical signs such as lethargy, anorexia and poor racing performance (Santos *et al.*, 2020b). However, it was reported that the virus had been documented earlier in Canada, the USA, and Australia (Stenzel and Koncicki, 2017). It has since then been reported in several Asian (Iran, China, Japan, Taiwan, United Arab Emirates), African, America and European countries including Belgium, Czech Republic, England, France, Germany, Hungary, Italy, Northern Ireland, Poland and Slovenia (Zhang *et al.*, 2015; Santos *et al.*, 2020b).

### 1.2.1.2. Morphology

Circovirus virions are nonenveloped and have a spherical shape with a diameter of 15-25 nm that are extremely stable in the environment (Mankertz, 2008; Payne, 2017c). These virions have a smooth surface appearance (Payne, 2017c). A diagram of a typical circovirus is indicated in Figure 1.9 (Payne, 2017c).

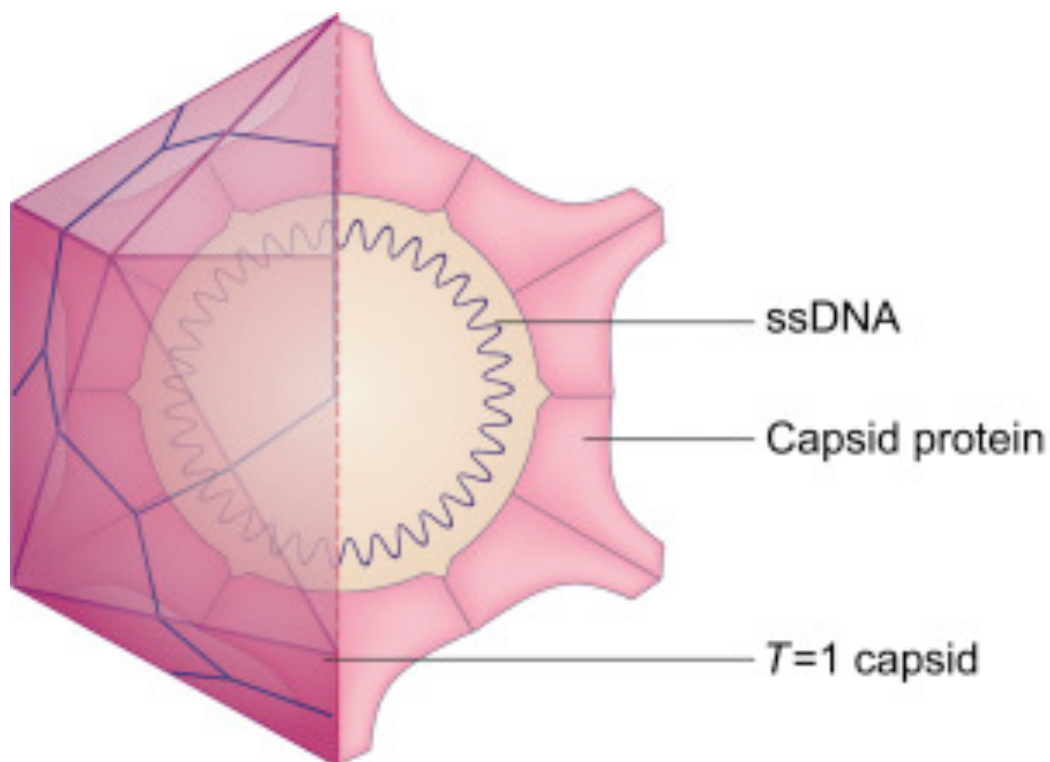


**Figure 1.9:** Diagram of the circovirus structure (Payne, 2017c). Permission to reproduce under licence number 5700700402314.

The circovirus genome is covalently closed and is approximately 2030 bp in length and consists of circular single-stranded spherical DNA (Stenzel and Koncicki, 2017). The viral capsid (T=1) consists of a single protein, called the capsid protein (Cap), which forms the protective shell and is assembled from 60 copies of the protein that has an approximate size of 28kDa (Payne, 2017c). The capsid protein self-assembles into icosahedral capsids which provides structural integrity to the virion (Stone *et al.*, 2019). Circovirus genomes consistently exhibit an ambisense organization with open reading frames (ORFs) distributed across distinct strands of the double-stranded replicative DNA (Stenzel and Koncicki, 2017). The virus genome is illustrated in Figure 1.10 (Payne, 2017c).

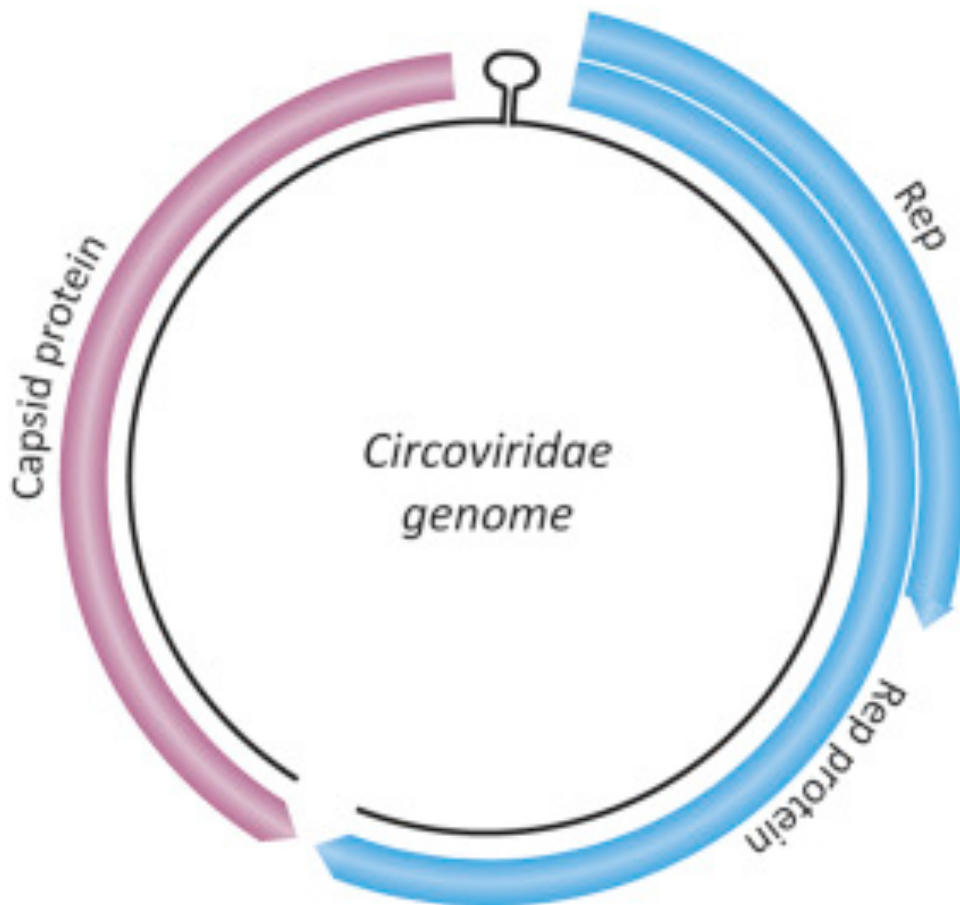


**Figure 1.10:** Circovirus genome structure (Payne, 2017c). Permission to reproduce under licence number 5700700628950.

All circoviruses have two major ORFs which transcribes in opposite directions from a single promoter site (Payne, 2017c; Stenzel and Koncicki, 2017). The largest ORF (V1) located on the virion sense strand encodes the non-structural replicase associated (Rep) protein responsible for viral replication, whereas the second largest ORF (C1) located on the complementary sense strand encodes the viral capsid protein (Cap) (Mankertz *et al.*, 2000; Todd *et al.*, 2001; Johne *et al.*, 2006, Todd *et al.*, 2008; Payne, 2017c; Stenzel and Koncicki, 2017). The ORF V1 also encodes the Rep' protein which is a product of mRNA splicing (Payne, 2017c). The Rep protein is 314 aa in length whereas the Rep' protein is 178 aa in length (Payne, 2017c). The Cap protein is 274 aa in length and is considered the only structural protein of the virion (Zhang *et al.*, 2015). All circovirus genomes also encode other ORFs, for instance, the PiCV genomes encode three additional ORFs that are located on the complementary sense strand for which the functions remain unknown (Todd *et al.*, 2008; Stenzel and Koncicki, 2017). Figure 1.11 depicts a diagram of a pigeon circovirus genome structure (Stenzel and Koncicki, 2017).

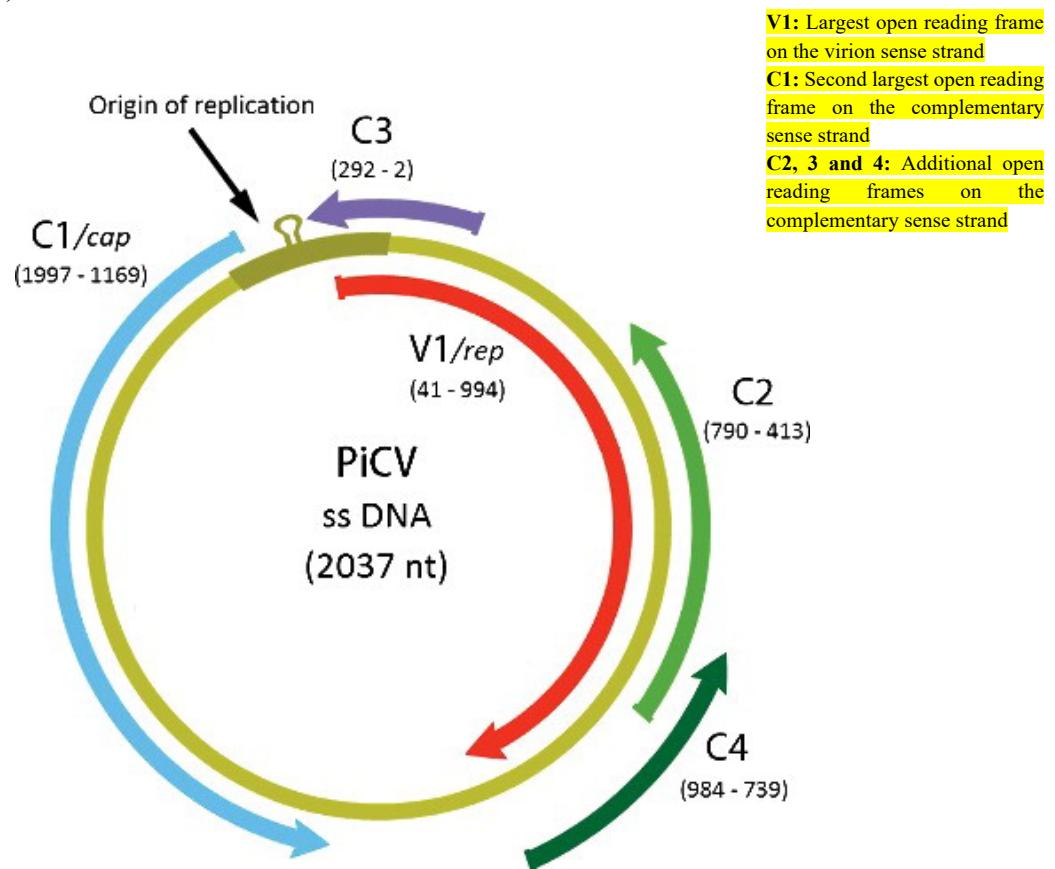


**Figure 1.11:** Pigeon circovirus genome structure (Stenzel and Koncicki, 2017). C1: capsid gene, C2 - C4: additional open reading frames, V1: replication gene, nt: nucleotides. No licence required for reproduction of the figure.

A conserved intergenic region is located between the start codons of the genes encoding Rep and Cap proteins for all circoviruses (Stenzel and Koncicki, 2017). The conserved intergenic region comprises a conserved nonanucleotide motif "(T/n)A(G/t)TATTAC," marking the origin of replication (*ori*) with the letter "n" which is found at the top of a potential stem-loop structure (Silva *et al.*, 2022). Unlike the gene encoding the Rep protein, the Cap gene is commonly mutated, according to research (Stenzel and Koncicki, 2017). Members of the genera *Circovirus* and *Cyclovirus* are discerned based on the location of the *ori*, within the genus *Circovirus*, the *ori* is positioned on the same strand as the Rep ORF, while in the genus *Cyclovirus*, the presumed *ori* is situated on the same strand as the Cap ORF (Breitbart *et al.*, 2017).

### 1.2.2. Classification and nomenclature

The *Circoviridae* family encompasses two distinct genera based on the different organization of their viral genome: (i) *Circovirus* and (ii) *Cyclovirus* which have recently been classified into the order *Cirivirales*, class *Arfiviricetes*, phylum *Cressnaviricota*, kingdom *Shotokuvirae* and realm *Monodnaviria* (Breitbart *et al.*, 2017; Vidovszky *et al.* 2023). Although *Circovirus* members have only been detected in vertebrates, *Cyclovirus* members have been detected in both vertebrates and invertebrates (Breitbart *et al.*, 2017). Pigeon circovirus is taxonomically classified under the species *Pigeon circovirus*, a member of the *Circoviridae* family formally recognised as a new member of the genus *Circovirus* in 2005 (Silva *et al.*, 2022).

The establishment of the *Circoviridae* family occurred in the mid-1990s when scientists recognized that animal viruses harbouring circular, single-stranded DNA (ssDNA) genomes represented a distinct group from other eukaryotic ssDNA viruses, which included plant viruses with circular genomes (*Geminiviridae*) and animal viruses with linear genomes (*Parvoviridae*) (Rosario *et al.*, 2017). Initially, all known animal viruses featuring covalently closed circular ssDNA genomes were placed under a single genus, *Circovirus*, within the *Circoviridae* family (Rosario *et al.*, 2017). However, it became apparent that animal viruses with circular ssDNA genomes exhibit remarkable diversity, and taxonomical classification extended beyond genome structures alone (Rosario *et al.*, 2017). The 9th report from the International Committee on Taxonomy of Viruses (ICTV), published in 2009, initially catalogued 12 viral species within the *Circoviridae* family and were categorized into two genera: *Circovirus*, comprising 11 species infecting birds and pigs, and *Gyrovirus*, which was solely represented by chicken anaemia virus (CAV) (Rosario *et al.*, 2017). However, as the discovery of new

genomic sequences similar to Circovirus members in various animals and environmental samples continued after the 9th report, a revision of the family's classification became necessary. Additionally, structural and genomic data suggested that CAV might belong to a distinct lineage of single-stranded DNA viruses, therefore the genus *Gyrovirus* was no longer considered part of the family *Circoviridae*. Instead, the genomic characteristics of CAV aligned more closely with single-stranded DNA viruses in the *Anelloviridae* family, leading to the reassignment of *Gyrovirus*.

Through viral metagenomic research and degenerate PCR, a group of viruses closely linked to circoviruses was discovered in 2010 (Rosario *et al.*, 2017). These viruses were discovered in human and chimp faeces samples and meat products from several animals (camels, chickens, cows, goats, and sheep) (Rosario *et al.*, 2017). These viruses were initially called cycloviruses to distinguish them from previously known circoviruses while still acknowledging the circular structure of their genomes. Although cycloviruses and circoviruses share genomic traits and are closely related, phylogenetic and genomic differences between the two prompted the establishment of a new taxonomic class which resulted in the creation of a new genus, *Cyclovirus*, inside the *Circoviridae* family (Rosario *et al.*, 2017).

### **1.2.3. Epidemiology**

#### **1.2.3.1. Host range**

Circoviruses exhibit a narrow host range or are host-specific, the majority of these infections have been observed in a wide array of avian hosts, both wild and domestic, spanning at least 18 different types of orders such as Columbiformes, Passeriformes, Anseriformes, Galliformes, Charidiiformes, and Struthioformes (King *et al.*, 2012; MacLachlan and Dubovi, 2017). These affected birds include passerines like canaries (*Serinus canaria*), common starlings (*Sturnus vulgaris*), gouldian finches (*Erythrura gouldiae*) and ravens (*Corvus coronoides*) (Raidal, 2012). Additionally, non-passerine birds, including anatids, lariids, and columbids, have also been affected, with circovirus species identified in diverse species of ducks, geese, ostriches, swans, gulls, pheasants and pigeons (King *et al.*, 2012; Raidal, 2012; MacLachlan and Dubovi, 2017; Loiko *et al.*, 2018). Besides avian species, other vertebrates such as poultry and mammals are seen as natural hosts for circovirus infections (Kong *et al.*, 2021). In Inner Mongolia, China, PiCV was discovered in ticks infesting both sheep and camels (Kong *et al.*, 2021). Through sequence comparison and phylogenetic analysis, it was determined that this

novel circovirus sequence is indeed a member of the PiCV family and was detected in two tick species, *Hyalomma asiaticum* and *Dermacentor nuttalli* (Kong *et al.*, 2021).

### **1.2.3.2. Transmission and spread**

Circoviruses employ diverse transmission pathways to disseminate within populations, and Pigeon circovirus, in particular, exhibits horizontal and vertical transmission routes (Khalifeh *et al.*, 2021; Silva *et al.*, 2022). The primary mode of transmission is direct contact between infected and susceptible hosts, with this mode being particularly prevalent in avian and swine populations (Todd, 2000). The virus has been detected in various avian anatomical sites, including the intestine, cloaca, and faeces, underscoring the potential for faecal-oral route transmission (Todd, 2000; Silva *et al.*, 2022). Furthermore, there is the intriguing possibility of respiratory transmission through the inhalation of faecal-contaminated materials, including feather dust (Silva *et al.*, 2022). Notably, the virus has previously been identified in the pharynx, trachea, and lungs, suggesting that these respiratory tissues could serve as sites for virus replication and persistence, particularly in older pigeons (Silva *et al.*, 2022).

In addition to these pathways, the trade and movement of infected animals play a substantial role in the regional and international dissemination of circoviruses (Woods *et al.*, 1993). Although the majority of infections primarily spread through the faecal-oral route, it's worth noting that vertical transmission has been conclusively demonstrated (Khalifeh *et al.*, 2021; Silva *et al.*, 2022). In 2006, Duchatel *et al.* aimed to investigate the transmission mechanisms of PiCV. Following the discovery of PiCV in semen and testes of breeding roosters and ovaries of hens, the possibility of vertical transmission was raised (Duchatel *et al.*, 2006). Notably no PiCV was detected in the oviducts of the hens. The detection of PiCV DNA in embryonic tissues further indicated the possibility of vertical transmission (Duchatel *et al.*, 2006). PiCV transmission in the rearing lofts of the pigeon breeders, were detected in 100% of the birds, however, before rearing only 20% PiCV detection was documented (Duchatel *et al.*, 2006). Swab samples taken from the bird's crop indicated no positive results, negating the possible transmission through crop milk (Duchatel *et al.*, 2006). The long-distance movement of PiCV could be facilitated by the international pigeon trade, pigeon exhibitions shows and pigeon racing competitions where in the lead-up to these races, the communal transportation, feeding, and watering of birds from various lofts may create optimal conditions for the transmission and widespread dissemination of PiCV (Stenzel *et al.*, 2014; Stenzel and Koncicki, 2017). This not



only brings together different PiCV lineages but also encourages mixed infections, potentially leading to the generation of new PiCV variants through recombination (Stenzel *et al.*, 2014).

#### **1.2.3.3. Stability of the virus**

Circoviruses, much like parvoviruses, exhibit remarkable environmental stability and are notorious for their resistance to inactivation (MacLachlan and Dubovi, 2017). Notably, they withstand heating at 60°C for 30 minutes and display high resistance to various disinfectants, often necessitating prolonged exposure to potent chemical sterilizers (MacLachlan and Dubovi, 2017).

#### **1.2.3.4. Lesions associated with the virus**

Circovirus infections typically lead to immunosuppression and developmental abnormalities, with the majority of cases occurring in young birds (MacLachlan and Dubovi, 2017). A range of clinical symptoms is associated with circovirus infections, including lethargy, weight loss, respiratory distress, ill thrift, diarrhea and poor racing performance, a condition commonly referred to as 'young pigeon disease syndrome' (YPDS) (Herdt and Pasmans, 2009; MacLachlan and Dubovi, 2017). However, it's essential to recognize that this syndrome, YPDS is typically multifactorial, often involving concurrent infections with a variety of viral, bacterial, and parasitic agents, which can complicate the assessment of circovirus's exact role (Herdt and Pasmans, 2009). Feather lesions and loss may be exhibited by infected doves, however, it is considered a rarity in racing pigeons (MacLachlan and Dubovi, 2017). A prominent pathological feature of circovirus infection is the acute-phase swelling and oedema of the bursa (Herdt and Pasmans, 2009). In cases of more chronic infections, atrophy of the bursa is often observed (Herdt and Pasmans, 2009; MacLachlan and Dubovi, 2017). Histologically, the lesions typically manifest as lymphocyte depletion in lymphoid tissue, along with the presence of characteristic intracytoplasmic basophilic inclusion bodies, primarily found in macrophages within the lymphoid tissue (Herdt and Pasmans, 2009).

#### **1.2.4. Viral replication cycle**

While the receptors facilitating cellular attachment of circoviruses remain insufficiently characterized, it is notable that certain circoviruses have the capacity to hemagglutinate erythrocytes, suggesting a probable interaction with sialic acid residues on the cell surface (MacLachlan and Dubovi, 2017). The internalization of virus particles into cells occurs through endocytosis, with clathrin-mediated endocytosis being a likely route, although the precise

mechanisms involved are not yet comprehensively elucidated (MacLachlan and Dubovi, 2017). Following the entry and localization of the virus within the endosome, the release of the virus from these compartments necessitates the involvement of a serine protease (MacLachlan and Dubovi, 2017). This implies that the uncoating process likely includes proteolytic cleavage of the capsid protein (Cap) (MacLachlan and Dubovi, 2017). Subsequent viral DNA replication takes place within the host cell nucleus and relies on cellular proteins and other components synthesized during the S phase of the cell cycle (MacLachlan and Dubovi, 2017; Payne, 2017c). The Rep protein is believed to initiate replication via the rolling circle replication (RCR) mechanism that commences at a stem-loop structure, instigating a nick in the virion-sense strand at positions 7 and 8 within the nonanucleotide motif (Breitbart *et al.*, 2017; Silva *et al.*, 2022). The RCR process entails the synthesis of a double-stranded DNA (dsDNA) replicative form with the assistance of host DNA polymerases, along with the generation of viral single-stranded DNA (ssDNA) from this replicative form template (Breitbart *et al.*, 2017). The ssDNA has dual potential outcomes, where it can undergo conversion into dsDNA to serve as a template for subsequent replication and transcription, or alternatively, it may be enclosed within the capsid protein to assemble into virions, eventually being released through cell lysis (Breitbart *et al.*, 2017). Notably, both circovirus and cyclovirus Rep proteins encompass conserved domains crucial for the RCR process (Breitbart *et al.*, 2017).

### **1.2.5. Diagnosis of Circovirus**

Diagnosing circovirus infections in pigeons involves various techniques. For live birds, molecular analyses are conducted on cloacal, blood, and serum samples (Stenzel and Konciki, 2017). Meanwhile, for deceased birds, samples from the bursa of Fabricius (BF) and spleen are analyzed (Stenzel and Konciki, 2017). However, it's important to note that the isolation of PiCV genetic material doesn't always indicate circovirus, given the high prevalence of subclinical infections (Stenzel and Konciki, 2017). A definitive diagnosis is made when birds exhibit disease symptoms, PiCV genetic material is detected in their immune organs, inclusion bodies are observed in lymphocytes within the BF and spleen via histopathological examination, and viral particles are identified under an electron scanning microscope (Todd *et al.*, 2001; Stenzel and Konciki, 2017). The original diagnostic methods, including electron microscopy, histology, dot blot hybridization, and in situ hybridization, are known to be time-consuming (Wang *et al.*, 2022). However, recent advancements in molecular biology techniques have revolutionized the detection of PiCV infections, offering a faster and more precise approach with conventional PCR, Real-time PCR, NGS techniques, loop-mediated

isothermal amplification and *in situ* hybridization (Wang *et al.*, 2022). Therefore PiCV infections are typically diagnosed through a combination of clinical symptom assessment and molecular analysis (Stenzel and Konciki, 2017; Santos *et al.*, 2020b).

#### **1.2.5.1. Virus isolation**

The difficulty of easily diagnosing PiCV forced many researchers to use histopathological and electron microscopy, whereas other authors used virus isolation in cell culture lines, but was limited and failed. (Daum *et al.*, 2009). A notable research challenge within the realm of PiCV studies revolves around the persistent struggle to establish a dependable and uniform approach for isolating this viral agent (Silva *et al.*, 2022). While many circoviruses are challenging to culture *in vitro*, there is an exception in the case of porcine circovirus (PCV), which can successfully propagate in PK-15 cells, as demonstrated by Stevenson and colleagues in 1999. Other well-documented instances in which PiCV propagation was successfully accomplished by introducing PiCV-positive tissue homogenates into embryonated chicken eggs that were free from specific pathogens was conducted by Van Borm *et al.*, and Sahindokuyucu *et al.*, in 2013 and 2022. Moreover, the advancement of high-throughput sequencing methods has led to the identification of a growing number of novel circovirus-like genomes in wild mammals and insects (Kong *et al.*, 2021).

#### **1.2.6. Treatment and control strategies**

A tailored protocol for protecting pigeons from PiCV infections has not been established because there are no vaccines available that target this specific pathogen, however, recent efforts have concentrated on developing a recombinant PiCV capsid protein for diagnostic assessments and creating a subunit vaccine for PiCV (Stenzel and Konciki, 2017). Regrettably, essential research in this field is still pending, leaving the effectiveness of PiCV vaccines in combating YPDS unverified (Stenzel and Konciki, 2017). Treatment for PiCV infections therefore primarily resolves around supportive care, as there are currently no specific antiviral medications or vaccines available. Various strategies are employed to manage and mitigate the effects of PiCV in infected pigeons. The symptoms accompanied by PiCV infection such as weight loss, respiratory distress or diarrhea should receive supportive care such as maintaining proper nutrition, hydration and warmth to bolster their immune system (Stenzel *et al.*, 2012). Stress has the potential to compromise the immune system, rendering pigeons more vulnerable to infections. Hence, it is imperative to implement stress reduction measures such as ensuring optimal housing conditions and minimizing environmental stressors (Stenzel *et al.*, 2017).

Alternative treatment approaches encompass the stabilization of vital organ tissues, along with the use of immunomodulating medications and compounds that hinder the growth of complicating factors in PiCV infections that include *Escherichia coli*, *Klebsiella pneumoniae*, *Riemerella sp.*, *Chlamydia psittaci*, and *Candida albicans* (Stenzel and Kochini, 2017).

Effectively addressing PiCV-induced diseases poses considerable challenges, primarily attributable to three key factors: (i) the continual trading, transportation, and racing of pigeons; (ii) the existence of a viral reservoir within wild pigeon populations; and (iii) the lack of a reliable means to diagnose the disease in live birds (Daum *et al.*, 2009). Given this context, a viable approach to curbing the dissemination of PiCV infections entails the selection of breeding stocks guided by routine serological and molecular testing outcomes (Stenzel and Kochini, 2017).

### **1.3. Other viruses associated with pigeons**

#### **1.3.1. Astroviridae**

Astroviruses were formerly thought to belong to the families *Picornaviridae* or *Caliciviridae* based on genetic similarities, however the virus was subsequently identified as a distinct family due to the lack of a helicase protein and usage of frameshifting event replication. (Moser and Shultz-Cherry, 2008; Tate and Bresee, 2012). Astroviruses are small, non-enveloped, single-stranded positive-sense RNA viruses with genomes ranging in size from 7kb to 9kb (Payne, 2017a). Astroviruses exhibit a distinct star-like appearance, characterized by spikes extending approximately 41 nm from the capsid's surface (Payne, 2017a). The genome comprises three overlapping ORFs encoding polyproteins, and while it lacks a cap, it does possess a poly A tail (Payne, 2017a).

Astroviruses exhibit a broad host range, with host-specific variants identified in several mammalian and avian species (Moser and Shultz-Cherry, 2008). Astrovirus infections can give rise to various types of diseases, with the specific outcomes largely contingent upon the infected organism (De Benedictis *et al.*, 2011). These outcomes encompass a spectrum of conditions, including diarrhea, interstitial nephritis, pyrexia, acute hepatitis, poult enteritis complex (PEC), poult enteritis mortality syndrome (PEMS), as well as symptoms like lethargy and anorexia (De Benedictis *et al.*, 2011). The *Astrovirus* genus includes duck astrovirus (DAstV), guineafowl astrovirus (GFAstV), goose astrovirus (GoAstV), turkey astrovirus (TAstV-1) and chicken astrovirus (CAstV) (Lukaszuk and Stenzel, 2020).

Avian Astroviruses (Avastroviruses) have been isolated from pigeons on four occasions according to reports in addition to their wide distribution in poultry (Phan *et al.*, 2013; Lukaszuk and Stenzel, 2020). In 2010, Zhao *et al.* identified one of the earliest Avastrovirus genera in pigeons, which was associated with a gastrointestinal illness that affected a population of pigeons in Shanghai (Lukaszuk and Stenzel, 2020). This discovery raises the likelihood of cross-infection occurring between pigeons and chickens (Lukaszuk and Stenzel, 2020). Another case of avastroviruses in pigeons entailed viruses that were not previously associated with poultry (Lukaszuk and Stenzel, 2020). Kofstad and Jonassen (2011) were the first to identify and describe feral pigeon astrovirus and wood pigeon astrovirus in Oslo, originating from feral pigeons (*Columba livia f. urbana*) and wood pigeons (*Columba palumbus*), respectively. The fourth instance of astroviruses detected in pigeons occurred when Phan *et al.* examined pigeon faecal samples collected from Hong Kong and Hungary in 2011 (Phan *et al.*, 2013). These four instances represent the sole documented findings of avastroviruses in pigeons to date. Due to the limited understanding of astrovirus pathogenesis in pigeons and their frequent isolation from poultry without clinical signs, it remains uncertain whether astroviruses are directly responsible for causing diarrhea in pigeons (Zhao *et al.*, 2011; Lukaszuk and Stenzel, 2020).

### **1.3.2. Picornaviridae**

Picornaviruses are members of the Picornaviridae family (Tuthill *et al.*, 2010). Picornavirus virions are icosahedral, non-enveloped small (22 to 30 nm) particles with capsid proteins encasing a positive-sense RNA strand genome with a size ranging from 7.2 to 9.1 kb (Yin-Murphy and Almond, 1996; Boros *et al.*, 2012). Picornaviruses mostly infect poultry but have also been isolated from pigeons.

Avian encephalitis virus (AEV), a member of the *Tremovirus* genus within the *Picornaviridae* family, was the first documented virus to infect pigeons and cause avian encephalomyelitis, suggesting the potential for cross-infection between chickens and pigeons (Lukaszuk and Stenzel, 2020). Another case in the *Avihepatovirus* genus involved duck hepatitis A virus 1 (DHAV-1), which was identified in pigeons from a Chinese farm that experienced a hepatitis outbreak with high mortality rates (Lukaszuk and Stenzel, 2020). In addition to these viruses, Kofstad and Jonassen made significant contributions by discovering two novel viruses in the *Picornaviridae* family, namely Pigeon picornavirus A (PiPV-A) and Pigeon picornavirus B (PiPV-B), underscoring the abundance of picornaviruses within feral pigeon populations

(Lukaszuk and Stenzel, 2020). Phan *et al.* further expanded our knowledge by detecting two additional picornaviruses, pigeon mesivirus 1 and pigeon mesivirus 2, during their research involving wild pigeon faecal samples from Hong Kong and Hungary (Lukaszuk and Stenzel, 2020). Despite picornaviruses being recognized as infectious agents responsible for enteric issues in commercial poultry, no picornavirus, aside from AEV, has been conclusively linked to enteric pathology in pigeons, indicating an absence of a clear correlation between picornavirus infection and pigeon health (Lukaszuk and Stenzel, 2020).

### **1.3.3. Coronaviridae**

Coronaviruses are members of the family *Coronaviridae* which is divided in two subfamilies *Letovirinae* and *Orthocoronavirinae* (Payne, 2017d; Lukaszuk and Stenzel, 2020; Zhou *et al.*, 2021). These viruses are single-stranded RNA viruses that are large, enveloped, and positive sensed (Payne, 2017d). They are the largest RNA viruses, with monopartite genomes ranging from 25 to 32 kb and virion diameters ranging from 118 to 136 nm (Payne, 2017d). The envelopes of the two subfamilies differ in their configuration, with the subfamily *Coronavirinae* having a flexible nucleocapsid and the subfamily *Torovirinae* having a doughnut-shaped nucleocapsid (Payne, 2017d).

Coronaviruses have diverse natural hosts, including bats, rodents, cats, wild birds, and marine animals (Zhou *et al.*, 2021). Among birds, there's a wide range of coronaviruses that effectively develop and spread, primarily belonging to the *Deltacoronavirus* and *Gammacoronavirus* families (Lukaszuk and Stenzel, 2020). These avian coronaviruses have been identified in various bird species, including domestic birds (Lukaszuk and Stenzel, 2020). Notably, racing pigeons and feral pigeons have been found to host pigeon coronaviruses, with studies by Jonassen *et al.*, Lau *et al.*, and Martini *et al.* detecting these viruses in feral pigeons during 2005 and 2018 (Martini *et al.*, 2018; Lukaszuk and Stenzel, 2020). Although these coronaviruses have been observed in other bird species, they predominantly circulate in pigeons (Lukaszuk and Stenzel, 2020). In a study by Domańska-Blicharz *et al.* (2021), coronaviruses were identified in 10 bird species, including pigeons, and the viruses isolated from pigeons formed a distinct "pigeon-like" group. This confirmed the high specificity of such coronaviruses in pigeons, supporting the idea proposed by Zhuang *et al.* (2020) that they constitute a distinct species within the Igacovirus subgenus (Zhuang *et al.*, 2020; Domańska-Blicharz *et al.*, 2021).

Infectious bronchitis virus (IBV), also known as the coronavirus of the chicken (*Gallus gallus*), is able to replicate at many non-respiratory epithelial surfaces (Cavanagh, 2007; Lukaszuk and Stenzel, 2020). Although chickens are considered the primary host of IBV, other bird species including pigeons, have been shown to play a role in the global spread of IBV strains (Adebiyi and Fagohun, 2017; Lukaszuk and Stenzel, 2020). In experimental inoculations of pigeons and chickens with the virus, distinct outcomes were observed (Adebiyi and Fagbohun, 2017; Lukaszuk and Stenzel, 2020). Chickens displayed signs of respiratory disease, and their IBV Hemagglutination Inhibition (HI) antibody levels showed an increase from  $2^0$  (prior to inoculation) to  $2^3$  and  $2^4$  at 18 days post-inoculation (dpi) (Adebiyi and Fagbohun, 2017; Lukaszuk and Stenzel, 2020). In contrast, pigeons did not exhibit any detectable IBV HI antibody levels following inoculation, as reported by Adebiyi and Fagbohun (2017) and Lukaszuk and Stenzel (2020). Adebiyi and Fagbohun concluded in a study conducted in 2017 that IBV is currently circulating in pigeons in Southwest Nigeria which indicates that these birds act as reservoirs for the propagation of IBV, however, the need for further studies has been indicated to determine the genotype and serotype of these IBV strains (Adebiyi and Fagbohun, 2017). The presence of IBV in pigeons could be attributed to the use of vaccination in poultry or the potential transmission of IBV between pigeons and chickens (Lukaszuk and Stenzel in 2020). A likely case of IBV transmission between pigeons and chickens occurred in 1985 in Australia, when IBV was isolated from a racing pigeon and a possible explanation offered by a racing pigeon worker was that pigeons are known to fly great distances and have been seen to seek refuge in open-sided caged-layer poultry barns when attacked by raptors, ensuring direct contact with chickens (Barr *et al.*, 1988).

#### **1.3.4. Reoviridae**

Rotaviruses, which belong to the family *Reoviridae* and the subfamily *Sedoreovirinae*, are characterized as double-stranded RNA viruses (Desselberger, 2014; Kapikan and Shope, 1996). They possess a genome of around 18.5 kb and exhibit a diameter of 75 nm (Desselberger, 2014; Kapikan and Shope, 1996). The genome comprises 11 segments of double-stranded RNA (dsRNA), encoding a total of 12 proteins — six structural and six non-structural (Desselberger, 2014). Rotaviruses have been identified in a wide array of bird species, with a notable presence in groups A, D, F, and G (RVA, RVD, RVF, RVG) (Lukaszuk and Stenzel, 2020).

In 1987, the initial isolation of rotavirus from pigeons in Japan was carried out by Minamoto *et al.* (Lukaszuk and Stenzel, 2020). Although little is known about the presence of rotaviruses in pigeons, avian RVA and RVD were discovered in healthy wild and domestic pigeons (Rubbenstroth *et al.*, 2018). However, the pathogenic potential of Rotavirus A (RVA) in domestic pigeons remained a mystery until the emergence of a pigeon-associated clade of RVA with genotype G18P[17] (Rubbenstroth *et al.*, 2020). This particular genotype was linked to fatal diseases in Europe and Australia, most notably a condition known as young pigeon disease syndrome (YPDS) (Rubbenstroth *et al.*, 2020). Young Pigeon Disease Syndrome has been recognized for almost three decades and is characterized by a seasonal pattern, predominantly affecting juvenile birds and typically arises during the racing season of homing pigeons in the summer and following ornamental pigeon displays in the winter (Rubbenstroth *et al.*, 2020). Rotavirus A genotype G18P[17] has been identified as a significant pathogen in juvenile domestic pigeons, leading to an acute illness that aligns with the presentation of YPDS. Notably, this genotype has not yet been detected in South Africa (Rubbenstroth *et al.*, 2020).

Rotavirus group D is usually found in turkeys, chickens, and pheasants, and is only seldom seen in guinea fowls, partridges, quails, pigeons, and ducks (Deol *et al.*, 2017). In 2013, the first pigeon RVG, distinct from the previously known chicken rotavirus, was identified by Phan *et al.* (Lukaszuk and Stenzel, 2020). Stucker *et al.* (2015) utilized sequence-independent amplification to obtain the initial complete genomic sequence of avian rotavirus group G (RVG) in South Africa that was acquired from a 5-month-old female chicken.

### **1.3.5. Adenoviridae**

Adenoviruses are characterized by their nonenveloped, icosahedral particles and linear double-stranded DNA genomes (Harrach, 2014; Kajon *et al.*, 2019). The genome is 26 kb to 48 kb in length with inverted terminal repeats ranging in size from 36 bp to 371 bp (Harrach, 2014). The *Adenoviridae* family is classified into two genera: (i) mastadenoviruses, which are mammalian adenoviruses, and (ii) aviadenoviruses, which are avian adenoviruses. (Doerfler, 1996).

Adenoviral infection in pigeons was first recorded in 1976, and was subsequently detected in Belgium in 1984 (Wan *et al.*, 2018; Sahindokuyucu *et al.*, 2022). It has since spread worldwide, driven by international trade in both wild-caught and captive-raised pet birds, as well as the global sale of racing pigeons (Wan *et al.*, 2018). Pigeon adenoviruses cause two separate



disease entities, both of which affect the pigeon population (Vereecken *et al.*, 1998). Type 1 adenovirus, also referred to as classic adenovirus or pigeon adenovirus 1, primarily affects young pigeons (Wan *et al.*, 2018). On the other hand, type 2 adenovirus, known as pigeon adenovirus 2, can afflict pigeons of all age groups (Wan *et al.*, 2018). Feral pigeons and waterfowl may serve as viral reservoirs for adenoviruses for other birds kept outside. (Greenacre, 2005).

### **1.3.6. Herpesviridae**

Herpesviruses belong to the *Herpesviridae* family and are characterized by their unique four-layered structure (Marlier and Vindevogel, 2006; Whitley, 1996). This distinctive structure consists of four key components: (i) a core that houses a large double-stranded DNA genome, (ii) an isosapentahedral capsid composed of capsomers that encloses this genome, (iii) an outer layer known as the tegument, made up of amorphous proteins, surrounding the capsid, and (iv) an outermost layer, an envelope bearing glycoproteins, that encases the tegument (Whitley, 1996). The molecular weight of herpesviruses varies, with genome sizes ranging from approximately 80 to 150 million or 120 to 250 kilobase pairs (Whitley, 1996).

Herpesviruses exhibit a wide host range, infecting various vertebrate hosts, ranging from humans, horses, cattle, mice, pigs, and chickens to turtles, lizards, fish, and even certain invertebrates like oysters (Roizman and Thayer, 2001). These viruses replicate within the nuclei of their diverse host organisms. (Roizman and Thayer, 2001). Pigeon herpesvirus 1 (PHV1), originally designated as Columbid herpesvirus 1, was initially grouped within the subfamily *Betaherpesvirinae* (Woźniakowski *et al.*, 2013). However, it was subsequently reclassified as an *Alphaherpesvirus*, primarily due to its strong association with the Marek's disease virus (MDV) in chickens (Woźniakowski *et al.*, 2013). Smadel *et al.* first characterized pigeon herpesvirus 1 as an agent infecting pigeons in 1940 (Woźniakowski *et al.*, 2013). Pigeons are natural hosts of PHV1, in a dormant state, from which it is believed that wild pigeons spread the virus to domestic pigeons (Marlier and Vindevogel, 2006; Woźniakowski *et al.*, 2013). Pigeon herpesvirus infection was reported and confirmed in South Africa by Pollard and Marais (1983) after a single pigeon was submitted from a flock of 60 showing clinical signs (Pollard and Marais, 1983). Pigeon herpesvirus infections have been documented often in young pigeons with respiratory illness symptoms such as rhinitis, which might be followed by conjunctivitis (Santos *et al.*, 2020b). Other symptoms do not always appear before death, but if they do, they may include depression, anorexia, oral and pharyngeal ulcers,

dyspnea, and diarrhea (Santos *et al.*, 2020b). Pigeons are associated with two distinct illnesses caused by Herpes viruses. One of these is pigeon Herpes encephalomyelitis virus (PHEV), which is relatively uncommon but can result in brain damage, paralysis, and impaired coordination. The other illness, known as inclusion body hepatitis, primarily affects the liver (Carranza *et al.*, 1986).

### **1.3.7. Poxviridae**

Poxviruses are double-stranded DNA viruses with very large genomes ranging from 130 kb to 360 kb in length (Hughes *et al.*, 2010). These viruses usually encode more than 150 genes per genome (Hughes *et al.*, 2010). All avian poxviruses (also called avipoxviruses) are classified to the genus *Avipoxvirus* and the subfamily *Chordopoxvirinae* of the *Poxviridae* family (Gyuranecz *et al.*, 2013). There are presently ten identified species of *Avipoxvirus*: (i) Fowlpox virus, (ii) Canarypox virus, (iii) Juncopox virus, (iv) Mynahpox virus, (v) Psittacinepox virus, (vi) Sparrowpox virus, (vii) Starlingpox virus, (viii) Pigeonpox virus, (ix) Turkeypox virus, and Quailpox virus (Gyuranecz *et al.*, 2013). Poxvirus infections have been discovered in at least 232 bird species representing 23 orders (Bwala *et al.*, 2015). The most common form of avian poxvirus affects the skin, where the development of dry crusty vesicles around featherless regions such as the face, legs and feet (cutaneous pox) and yellow plaques in the mouth (mucosal pox) form (Khan *et al.*, 2019). *Avipoxvirus*, which is extremely host-specific, does not provide protection against infection with other strains of poxvirus, as demonstrated by Chaves Hernández in 2014. These poxviruses are typically named based on the susceptible host species they infect, such as Fowlpox virus, Canarypox virus, Pigeonpox virus, Psittacinepox virus, Turkeypox virus, and others (Chaves Hernández, 2014). Host susceptibility and virulence of poxvirus vary with the strain of avipoxvirus (Harris and Oglesbee, 2006). Pigeonpox virus was detected in South Africa when a wild pigeon was found on the grounds of the Faculty of Veterinary Science, University of Pretoria, Onderstepoort (Bwala *et al.*, 2015).

### **1.3.8. Retroviridae**

Retroviruses are members of the *Alpharetrovirus* genus, *Orthoretrovirinae* subfamily and *Retroviridae* family are known to induce tumours (Nair, 2022). Retroviruses, which are characterized by their protein-enveloped structure, belong to the class of positive double-stranded RNA viruses (Gonda, 1999). What sets them apart is their possession of a distinctive enzyme known as reverse transcriptase which plays a crucial role in catalyzing the conversion

of genetic material from RNA to DNA (Gonda, 1999). These viruses are roughly 100 nm in diameter and have an RNA genome that is 7kb to 10kb in size (Ryu, 2017). Avian leukosis viruses (ALV), commonly referred to as RNA tumor viruses, pose a significant economic threat to the global poultry industry (Wang *et al.*, 2020). These infectious retroviral agents have full-length genome sequences spanning from 7200 to 7800 base pairs, organized as 5'LTR-leader-gag-pol-env-3'LTR (Wang *et al.*, 2020). Within this genome structure, the LTR is a non-structural gene, while the *gag*, *pol*, and *env* genes are considered structural genes (Li *et al.*, 2018). The *gag* gene is responsible for encoding ALV group-specific antigens and various other proteins, including matrix proteins and nucleocapsid proteins (Li *et al.*, 2018). On the other hand, the *pol* gene encodes reverse transcriptase and integrase, while the *env* gene encodes the gp37 transmembrane (TM) and the gp85 surface proteins (Li *et al.*, 2018).

Based on the viral envelope, ALV is classified into ten subgroups labeled A-J (Nair, 2022). These viruses are further classified based on their mechanism of transmission, which is either (i) exogenous (viruses being transmitted from bird to bird either through the egg or contact) or (ii) endogenous retroviruses (Nair, 2022). The hosts of ALV are mainly chickens, however previous reports have shown that ALV can infect budgerigars, canaries, coturnix quail ducks, game birds, geese, pheasants, pigeons and turkeys (Odend'Hal, 1983). Various symptoms associated with ALV infection include weight loss despite normal or increased appetite, reduced energy and activity levels, overall weakness and a weakened immune system making them more susceptible to secondary infections and diseases (Zeghdoudi *et al.*, 2017). Nine avian leukosis virus outbreaks was reported in chickens in the Eastern Cape, South Africa during the time 1999 to 2020 (Simbizi *et al.*, 2021).

Peyton Rous discovered the Rous sarcoma virus (RSV) in 1911 as a tumor-causing agent, and it is classified within the *Retroviridae* family of avian retroviruses (Ridky and Leis, 2013). The RSV stands out for its remarkably diverse host range, encompassing chickens, pheasants, guinea fowl, ducks, pigeons, Japanese quails, turkeys, and rock partridges (Kordadmehr *et al.*, 2017). Avian myeloblastosis virus (AMV), originally identified from RSV and Rauscher Leukaemia virus (RLV), is an alpha retrovirus that is responsible for acute myeloblastic leukaemia (AML) (Perbal, 2008). This virus is known to affect birds and transform myeloid hematopoietic cells *in vitro* leading to the development of myeloblastic leukaemia or lymphoid tumours (Gonda, 1999). It primarily affects the bone marrow and lymphoid tissues of infected pigeons, inducing the proliferation of immature myeloid cells or lymphocytes and triggering

uncontrolled cell division (Calnek *et al.*, 2003). Infiltration of leukemic cells in multiple tissues such as the liver, spleen, kidneys, lungs and intestines contributes to organ enlargement and dysfunction (Robinson *et al.*, 1997).

### **1.3.9. Orthomyxoviridae**

The family *Orthomyxoviridae* comprises a considerable number of human and animal diseases, including Influenza A virus (IAV) (Payne, 2017b). The IAV genome, as described by Ghedin *et al.* in 2005, consists of eight single-stranded negative-sense viral RNA segments, collectively spanning approximately 13.5 kb. Each of these segments encodes a total of 11 proteins and varies in length, ranging from 890 to 2,341 nucleotides (Ghedin *et al.*, 2005). These segments are housed in distinct viral ribonucleoprotein (vRNP) complexes, as highlighted by Dadonaite *et al.* in 2019, and are subsequently packaged together within single virus particles. Infecting a wide range of animals and birds, IAV replicates in the respiratory and gastrointestinal systems (Payne, 2017b). Recent findings on the identification of low pathogenic avian influenza viruses (LPAI) in healthy pigeons have focused attention on the possible role of pigeons and doves in avian influenza virus transmission (Abolnik, 2014). Pigeons and doves may play a role in the ecology of avian influenza by spreading viruses between poultry and migratory populations as fomite transmitters, as prior studies have suggested a global concern owing to the detection of a poultry-origin strain in healthy pigeons as well as mass wild pigeon and dove mortalities during high pathogenic avian influenza virus (HPAI) outbreaks in South Africa (Abolnik, 2014; Abolnik *et al.*, 2018).

### **1.3.10. Nimaviridae**

White spot syndrome virus (WSSV) is a double-stranded DNA virus with a large 280 kb genome, encoding 442 predicted genes (Kang *et al.*, 2013; Kumar *et al.*, 2018). This virus belongs to the genus *Whispovirus* within the *Nimaviridae* family, as identified by Onihary *et al.* in 2021. It serves as the causative agent of White Spot Disease (WSD), a major viral pathogen affecting cultured shrimp (Onihary *et al.*, 2021). The first case of WSD was reported in Taiwan in 1992 (Zhu *et al.*, 2019). The route of transmission of the White Spot Syndrome Virus (WSSV) to pigeons remains largely unknown, with limited literature offering comprehensive explanations. Existing studies on WSSV primarily focus on its impact on crustaceans, such as shrimp, and information regarding its transmission dynamics and detection in avian species, particularly pigeons, is notably scarce (Onihary *et al.*, 2021).

### **1.3.11. Togaviridae**

Semliki Forest virus (SFV) is an RNA virus classified within the *Alphavirus* genus and *Togaviridae* family (James D. Cherry MD *et al.*, 2019). Semliki Forest virus (SFV), which was first isolated from mosquitoes in Uganda's Semliki Forest in 1942, has a genome estimated to be around 11,442 nucleotides in length (Kääriäinen *et al.*, 1987). This genome possesses a 5' cap-structure and a 3' poly(A) tail consisting of 100 residues (Kääriäinen *et al.*, 1987).

### **1.3.12. Flaviviridae**

Bovine viral diarrhea virus (BVDV) is a positive-stranded RNA virus which belongs to the genus *Pestivirus* and in the family *Flaviviridae* (Yu *et al.*, 1999; Al-Kubati *et al.*, 2021). The genome of BVDV, approximately 12.3 kb in size, contains a single open reading frame and untranslated regions at the 5' and 3' ends (Yu *et al.*, 1999; Al-Kubati *et al.*, 2021). BVDV particles exhibit a spherical to semi-spherical shape with a diameter ranging from 40 nm to 60 nm (Al-Kubati *et al.*, 2021). Initially identified in the United States of America (USA) within a herd of cattle, BVDV has since become a prominent viral pathogen affecting cattle in various regions worldwide (Al-Kubati *et al.*, 2021).

### **1.3.13. Anelloviridae**

Torque teno viruses (TTV) are globally distributed small, nonenveloped, single-stranded, negative-sense circular DNA viruses (Zhang *et al.*, 2013; Agnihotri *et al.*, 2021). These viruses are classified as *Alphatorqueviruses* and belong to the *Anelloviridae* family (Agnihotri *et al.*, 2021). The genomic size of Torque teno virus (TTV) ranges from 3.6kb to 3.8kb, and it has been observed to affect a wide range of species, including humans, nonhuman primates, tupaia, and domestic animals (cats, chickens, cattle, dogs, sheep and pigs) (Hussain *et al.*, 2012; Zhang *et al.*, 2013). Given the prevalence of species-specific TTVs in both domestic and wild animal populations across the globe, there is a possibility that TTVs have co-evolved with their respective hosts, as some animals are naturally infected with TTVs specific to their species (Manzin *et al.*, 2015). Different infections for vertebrate species reveal varying genome lengths and sequence variations (Zhang *et al.*, 2013).

Torque teno viruses have been reported to infect pigeons, from which a species-specific pigeon torque teno virus (PTTV) was isolated in China in 2012 (Agnihotri *et al.*, 2021). Pigeons infected with PTTV, as reported by Agnihotri *et al.* in 2021, exhibit clinical signs such as respiratory issues, weight loss, and diarrhea. Zhang *et al.* (2013) documented that the genomic

size of PTTV falls within the range of 1,584 to 1,585 base pairs. This genome consists of two open reading frames (ORFs), namely ORF V1, which encodes the Rep replication protein, and ORF C1, which encodes the Cap coat protein (Zhang *et al.*, 2013). In Zhang's study, it was further revealed that there exists a short overlapping region between these two ORFs, and translation commences in single-stranded DNA.

## CHAPTER 2

### Molecular epidemiology of Pigeon paramyxovirus in South Africa from 2012 to 2022

#### 2.1. Introduction

Pigeon paramyxovirus 1 (PPMV-1) belongs to the *Paramyxoviridae* family and is classified in the genus *Orthoavulavirus* (Fei *et al.*, 2019). It is an antigenic form of the Newcastle disease virus (NDV) that causes regular outbreaks in domestic and wild pigeons and doves in many countries (Dortmans *et al.*, 2011; Absalón *et al.* 2019; Chang *et al.*, 2020). PPMVs have also been isolated from other bird species such as sparrows (*Passer domesticus*), crows (*Corvus*), kestrels (*Falco sparverius*), budgerigars (*Melopsittacus undulatus*), falcons (*Falco*), swans (*Cygnus*), pheasants (*Phasianus colchicus*), cockatoos (*Cacatuidae*), robins (*Turdus migratorius*) and African Ground Hornbills (*Bucorvus* spp.) (Abolnik *et al.*, 2007; Abolnik *et al.*, 2008, Aldous *et al.*, 2003, Alexander *et al.*, 1985; Bucko and Gieger, 2019; Johnston and Key, 1992; Kaleta 1992; Lister *et al.*, 1986; Monne *et al.*, 2006; Werner *et al.*, 1999; Zhu *et al.*, 2010). Pigeons and doves show clinical signs of infection including neurological signs such as neck twisting, torticollis, leg and wing paralysis (Hines and Miller, 2012). Other key clinical symptoms associated with virus infection include large amounts of green watery diarrhea, coughing or sneezing and ruffling of the feathers (Hines and Miller, 2012; Akhtar, 2016; Abolnik, 2017). PPMV-1 can be transmitted through direct contact with infected birds, their secretions and excretions, contact with contaminated surfaces or indirect inhalation of dust from litter (Hüppi *et al.*, 2020; Lumeij and Stam, 1985). The close interaction between pigeons from different regions and the congregation of birds during races creates a favourable environment for the spread of PPMV (He *et al.*, 2020). Outbreaks of PPMV can result in quarantine restrictions and trade bans, significantly impacting the racing industry's economic sustainability.

Various early techniques have been used to identify and differentiate isolates of NDV based on their biological properties including assessing pathogenicity, plaque formation, thermostability, analysing structural polypeptides, and employing hemagglutination inhibition patterns using monoclonal antibodies (Dimitrov *et al.*, 2019). Extensive research and monitoring efforts have enhanced the classification and identifying distinct subtypes and genotypes based on genetic sequencing and antigenic characteristics (Lamb *et al.*, 2018). The

virulence of PPMV subtypes varies, with certain strains generating substantial morbidity and fatality rates in pigeons (Fuller *et al.*, 2010). Phylogenetic analysis classified PPMVs into a discrete subgenotype VIb, which is also known as 4b and has been reclassified in 2019 as VI.1.1 (Aldous *et al.*, 2014; Molini *et al.*, 2018; Dimitrov *et al.*, 2019; Mansour *et al.*, 2021). International live bird movements (pigeon races and exhibitions) and pigeon migration likely contributed to the global spread of PPMV. Humans also keep pigeons for a variety of other reasons, including meat production in relevant nations, and even pets.

Outbreaks have been documented in Korea, India, Sri Lanka, Canada, Japan, Australia, Egypt, Philippines, United Kingdom, Belgium, Germany, the Netherlands, and South Africa (Abolnik, 2007; Ganar *et al.*, 2014). PPMV-1 are enzootic in 33 African countries to date, including South Africa and neighbouring countries (Dzogbema *et al.*, 2021). Twelve outbreaks of NDV were reported in Namibia between July and November 2016 along the Angolan border, (Molini *et al.*, 2018). PPMV-1 strains were initially documented in 1986 in South Africa and were further reported during 2002 to 2006 (Abolnik *et al.*, 2008). Phylogenetic data suggested that PPMV-type viruses were imported into South Africa at least twice, based on the presence of two distinct subgroups (4bi and 4bii) that have been circulating in Europe and Japan since the early 1990s (Abolnik, 2007). PPMV genotypes detected in Southern African countries include I, II, VI (VIa, VIb, VIk), VII (VIIb, VIId, VIIh), VIII, XI, XIII and lineage 4bii (Herczeg *et al.*, 1999; Aldous *et al.*, 2003; Abolnik *et al.*, 2008; Snoeck *et al.*, 2009; Snoeck *et al.*, 2013; Abolnik, 2017; Molini *et al.*, 2017; Megahed *et al.*, 2020). Lineage 4bii was further split into VIe, VIf, VIh, VIj and VIk (Dimitrov *et al.*, 2019). Genotype VIII strains are geographically confined viruses that emerged in South Africa for decades and were found in 1960 and in the period 1990 to 1995, however no record of isolation of this genotype has been published after 2000 (Herczeg *et al.*, 1999; Abolnik, 2007; Megahed *et al.*, 2020).

Although a few studies are available about virus shedding in asymptomatic pigeons, the increasing global interconnection of the pigeon racing industry and the possibility of asymptomatic carriers as documented by Wang *et al.*, 2015 and Anaheim *et al.*, 2022, a possible mechanism by which PPMV might be transmitted across borders (He *et al.*, 2020). The absence of clinical symptoms in infected pigeons can be attributed to antigenic variations between vaccine and outbreak strains, which reduces the effectiveness of vaccination and does not prevent infection or even replication of the virus, although no prior studies have provided



conclusive evidence proving this theory (Pestka *et al.*, 2014; Mansour *et al.*, 2021; Peeters and Koch, 2021).

After the first isolation of PPMV-1 from doves during an outbreak in September 1986 from various parts of the Republic of South Africa, significant dove and pigeon die-offs have sporadically been reported in different areas of South Africa (Abolnik *et al.*, 2008). Pigeon racing has a rich history in South Africa, dating back to the late 1800s. The sport gained popularity among breeders and enthusiasts, who established local racing clubs and participated in national and international competitions (South African Million Dollar Pigeon Race, 2021). The previous molecular study of PPMV isolated from pigeons, and chickens, conducted in different regions of South Africa from 2001 to 2006 shed light on the genetic diversity and epidemiology of PPMV strains circulating within the country. Twenty-one PPMV samples from various areas of South Africa (Gauteng, Mpumalanga, North-West, Limpopo, Northern Cape, Western Cape, and Kwazulu-Natal) were found to be split between two lineages 4bi and 4bii, showing the presence of multiple lineages within the local population (Abolnik *et al.*, 2008).

Moreover, it was established that PPMV infection may be lethal to species other than doves and pigeons and potentially threaten the biodiversity of wild birds (Abolnik *et al.*, 2008). Ehlers Smith *et al.* (2021), highlighted that while African Ground Hornbills can harbour PPMV, they may not exhibit overt clinical signs of the disease, complicating disease surveillance and control efforts. Pigeon racing breeders employ vaccination as a preventative measure to reduce losses caused by PPMV, however, despite these efforts, losses still occur. Several factors might contribute to this inadequate protection, including virus genetic diversity, which can result in the emergence of new strains or variations against which the vaccination may not give adequate protection (Alexander, 2000). Another factor is the effectiveness of the vaccination program, proper vaccine storage, handling and administration, all crucial for vaccine efficacy (Brown, 2000). If breeders do not follow recommended vaccination protocols, the vaccine's effectiveness can be compromised, leaving pigeons vulnerable to infection (Brown, 2000). While vaccination is a valuable tool in reducing losses, it is not foolproof and multiple factors can contribute to losses despite vaccination efforts.

Genetic drift, also known as the "Sewall Wright effect" is a fundamental concept in population genetics that describes the random fluctuations in allele frequencies within a population over

time along with mutation, gene flow and natural selection (Honnay, 2008). Genetic drift can lead to the fixation of certain genetic variants and the loss of others, even in the absence of natural selection (Fisher, 1930). It is particularly relevant in viral populations, such as PPMV, since viruses have relatively high mutation rates and short generation times, allowing viruses to rapidly evolve and adapt to the host environment (Stern and Andino, 2016). In the case of PPMV, genetic drift can play a significant role in shaping the viral population structure, where PPMV strains can evolve and diversify over time through the accumulation of mutations, and genetic drift can influence which variants become dominant (Holmes, 2010). One key implication of genetic drift in PPMV populations is the potential for the emergence of novel strains with altered virus characteristics, including virulence and host specificity (Dimitrov *et al.*, 2019). Furthermore, genetic drift can lead to the persistence of older strains within a population, even if they are less adapted to the current host environment. Older strains may be able to persist, potentially causing sporadic outbreaks or serving as reservoirs for future infections (Abolnik *et al.*, 2007).

To gain a better understanding of the genetic diversity and evolution of PPMV in South Africa, ongoing research and surveillance are essential. Molecular epidemiology studies can determine the genetic diversity of PPMV strains circulating in the region, providing insights into whether older strains are still prevalent or if new strains have emerged or been introduced (Cattoli *et al.*, 2011). In the present study, the phylogenetic relationship of South African PPMV-1 viruses isolated from feral doves, and pigeons from 2011 to 2022 was investigated.

## **2.2. Aims and objectives of this study**

The aim of this chapter was to determine and update the molecular epidemiology of pigeon paramyxoviruses (PPMV) in South Africa from 2012 to 2022.

The objectives were:

- To perform molecular techniques on new field samples collected in 2022 for the presence of PPMV.
- To sequence and assemble the full virus genomes where possible, or at least fusion gene sequences.
- To perform phylogenetic analysis and determine the genetic diversity.
- To determine whether QH9-2/1 Quail cell cultures would be a suitable alternative to SPF eggs for virus isolation.

## **2.3. Materials and Methods**

### **2.3.1. Ethical considerations**

The general project was approved by the Faculty of Veterinary Science Research Ethics Committee, University of Pretoria (UP). Prior to the commencement of laboratory work, procedures were pre-approved by the Department of Agriculture, Forestry and Fisheries (DAFF) (Reference number: 12/11/1/1/8 (2280LH) (Appendix A) and the Animal Ethics Committee (AEC) of UP (Reference number: REC013-22) (Appendix B).

### **2.3.2. Samples**

Samples from the University of Pretoria's (UP) repository (n=18) were available for analysis and were already sequenced, but the data had not yet been fully analysed or published. In addition, ten new samples submitted to the University by national veterinary laboratories in Western Cape for sequencing and eight samples collected in Gauteng during the study period were included as listed in Table 2.1. Species included general wild dove species (*Columbiformes*), Laughing dove (*Spilopelia senegalensis*), Pigeon (*Columba livia*) and Feral pigeon (*Columba livia domestica*). A total of 36 cases of PPMV were analysed in this study, comprising of 18 samples obtained from the University of Pretoria's repository, and 18 samples collected between February 2022 and September 2022 from various locations in Gauteng and Western Cape provinces (Figure 2.1, Table 2.1). The field cases in Gauteng were collected near the Department of Production Animal Studies (PAS), University of Pretoria, Onderstepoort Campus, especially in the vicinity of trees. The organs of the eight samples collected in Gauteng were methodically removed and individually stored in separate tubes. Departing from the conventional method of pooling tissues, in this study, I pursued a more refined approach with the samples collected in Gauteng where each organ and tissue from the eight fresh dove carcasses collected in this study was extracted and tested individually, allowing one to discern the viral load among them.

The first dove (DOZA000M22) was located immediately outside the Department of Production Animal Studies laboratory, and it had a full crop, suggesting recent feeding. The second dove (DOZA001M22) was also discovered outside the Department of Production Animal Studies building in a less intact state, having been scavenged by cats and lacking a head. Following that, the third (DOZA002M22), fourth (DOZA003M22), fifth (DOZA004M22), sixth (DOZA005M22), and seventh (DOZA006M22) doves were found early in the morning from several sites on the Onderstepoort campus outside the Department of Production Animal

Studies building. Finally, an eighth dove was collected near a tree in close proximity to the Veterinary Genetics Laboratory building. Samples collected by Western Cape Provincial Veterinary Laboratory (WCPVL) were submitted as RNA samples and indicated that initial sample types were organ pools. Specific details regarding the collection environment and any contextual information for the samples collected in the Western Cape region are unknown.



**Figure 2.1:** Locations where samples were collected between February 2022 and September 2022, as indicated by the red stars.

**Table 2.1:** Samples analysed in this study.

| Sample                    | Host          | Sample type <sup>1</sup> | Sampling date | Location <sup>2</sup>        | Source          |
|---------------------------|---------------|--------------------------|---------------|------------------------------|-----------------|
| N1775                     | Laughing dove | Organ pool               | 11 Jul 2012   | OP Campus, Pretoria, GAU     | UP repository   |
| 20200121_087_6102A        | Laughing dove | Organ pool               | 23 Dec 2019   | Oudtshoorn, WC               | UP repository   |
| 20200121_087_6102/613923B | Laughing dove | Organ pool               | 23 Dec 2019   | Oudtshoorn, WC               | UP repository   |
| OP04-2020/PRL01-2020      | Laughing dove | Egg-culture isolate      | 21 Apr 2020   | OP Campus, Pretoria, GAU     | UP repository   |
| PRL02-2020                | Laughing dove | Organ pool               | 07 May 2020   | OP Campus, Pretoria, GAU     | UP repository   |
| PRL03-2020                | Laughing dove | Organ pool               | 07 May 2020   | OP Campus, Pretoria, GAU     | UP repository   |
| PRL04-2020                | Laughing dove | Organ pool               | 08 May 2020   | OP Campus, Pretoria, GAU     | UP repository   |
| PRL05-2020                | Laughing dove | Organ pool               | 08 May 2020   | OP Campus, Pretoria, GAU     | UP repository   |
| 20100411                  | Pigeon        | Egg-culture isolate      | 27 Oct 2020   | Graafwater, Vredendal, WC    | UP repository   |
| 20110039                  | Laughing dove | Egg-culture isolate      | 04 Nov 2020   | Montagu, Worcester, WC       | UP repository   |
| PD_01/06                  | Feral pigeon  | Organ pool               | 25 May 2021   | Robin Hills, Randburg, GAU   | UP repository   |
| PD_02/06                  | Feral pigeon  | Organ pool               | 25 May 2021   | Robin Hills, Randburg, GAU   | UP repository   |
| S2021/06_0218             | Laughing dove | Egg-culture isolate      | 10 Jun 2021   | Tableview, Cape Town, WC     | UP repository   |
| S2021/06_0251             | Laughing dove | Egg-culture isolate      | 11 Jun 2021   | Edgemead, Cape Town, WC      | UP repository   |
| 21070306                  | Laughing dove | Egg-culture isolate      | 15 Jul 2021   | Porterville, WC              | UP repository   |
| 21070474                  | Laughing dove | Egg-culture isolate      | 22 Jul 2021   | Swellendam, WC               | UP repository   |
| 21070476                  | Laughing dove | Organ pool               | 23 Jul 2021   | Misverstand, Morreesberg, WC | UP repository   |
| 21090443                  | Laughing dove | Organ pool               | 23 Sep 2021   | Riversdal, WC                | UP repository   |
| DOZA000M22                | Laughing Dove | Multiple organs          | 12 May 2022   | OP Campus, Pretoria, GAU     | Collected at UP |
| DOZA001M22                | Laughing Dove | Multiple organs          | 18 May 2022   | OP Campus, Pretoria, GAU     | Collected at UP |
| DOZA002M22                | Laughing Dove | Multiple organs          | 24 May 2022   | OP Campus, Pretoria, GAU     | Collected at UP |
| DOZA003M22                | Laughing Dove | Multiple organs          | 30 May 2022   | OP Campus, Pretoria, GAU     | Collected at UP |
| DOZA004M22                | Laughing Dove | Multiple organs          | 30 May 2022   | OP Campus, Pretoria, GAU     | Collected at UP |
| DOZA005M22                | Laughing Dove | Multiple organs          | 01 Jun 2022   | OP Campus, Pretoria, GAU     | Collected at UP |
| DOZA006M22                | Laughing Dove | Multiple organs          | 01 Jun 2022   | OP Campus, Pretoria, GAU     | Collected at UP |
| DOZA007M22                | Laughing Dove | Multiple organs          | 04 Jun 2022   | OP Campus, Pretoria, GAU     | Collected at UP |
| 22030045                  | Pigeon        | Organ pool               | 01 Mar 2022   | Malmesbury, Boland, WC       | WCPVL           |
| 22040247                  | Pigeon        | Organ pool               | 20 Apr 2022   | Moorreesburg, Malmesbury, WC | WCPVL           |
| 22040244                  | Dove          | Organ pool               | 19 Apr 2022   | Langebaan, Vredendal, WC     | WCPVL           |
| 22060338                  | Domestic Dove | Organ pool               | 20 Jun 2022   | Constantia, Boland, WC       | WCPVL           |
| 22060412                  | Wild Dove     | Organ pool               | 23 Jun 2022   | Durbanville, Boland, WC      | WCPVL           |
| 22060471                  | Dove          | Organ pool               | 27 Jun 2022   | Durbanville, Boland, WC      | WCPVL           |
| 22070111                  | Laughing dove | Organ pool               | 08 Jul 2022   | Bellville, Boland, WC        | WCPVL           |
| 22080021                  | Dove          | Organ pool               | 03 Aug 2022   | Stanford, Swellendam, WC     | WCPVL           |
| 22080566                  | Dove          | Organ pool               | 01 Sep 2022   | Cape Town, Boland, WC        | WCPVL           |
| 22090303                  | Pigeons       | Organ pool               | 19 Sep 2022   | Stellenbosch, Boland, WC     | WCPVL           |

<sup>1</sup> RNA was extracted directly from tissues and alantoic fluid (egg-culture isolates.), which was stored at -80°C.<sup>2</sup> GAU - Gauteng province, OP - Onderstepoort, WC – Western Cape province, WCPVL - Western Cape Provincial Veterinary Laboratory

Out of the total 36 cases analyzed in this study, only the eight samples that were collected in Gauteng during 2022 were subjected to screening by real-time RT-PCR. The remaining 28 samples, obtained from the University's Repository and Western Cape Provincial Veterinary Laboratory, were not included in the screening process as they were previously diagnosed as NDV-positive. The eight samples collected in Gauteng underwent Conventional RT-PCR. Among these, only four samples were sent for Sanger sequencing due to challenges in amplification. Simultaneously, all eight Gauteng samples were subjected to virus isolation on QH9-2/1 cells. Subsequently, seven cell culture samples and five organ tissue samples were extracted and forwarded for Ion Torrent Next Generation Sequencing (NGS). This comprehensive approach of different sample types for NGS aimed to facilitate optimal analysis and address any gaps that may arise. The different approaches for each sample and sample type are indicated in Table 2.2

**Table 2.2:** Different samples and sample types analysed in this study with various methods.

| Sample     | Real-time RT-PCR <sup>2</sup> | Conventional RT-PCR <sup>2</sup> | Sanger sequencing <sup>2</sup> | Virus isolation | Ion Torrent NGS <sup>1,2</sup>                 |
|------------|-------------------------------|----------------------------------|--------------------------------|-----------------|--|
| DOZA000M22 | ×<br>Multiple organs          | ×<br>Lung                        | ×<br>Lung                      | ×<br>Lung       | ×<br>Lung                                      |
| DOZA001M22 | ×<br>Multiple organs          | ×<br>Stomach                     |                                | ×<br>Stomach    | ×<br>Stomach and QH9-2/1 cell cultured isolate |
| DOZA002M22 | ×<br>Multiple organs          | ×<br>Heart                       | ×<br>Heart                     | ×<br>Heart      | ×<br>Heart and QH9-2/1 cell cultured isolate   |
| DOZA003M22 | ×<br>Multiple organs          | ×<br>GIT                         |                                | ×<br>GIT        | ×<br>QH9-2/1 cell cultured isolate             |
| DOZA004M22 | ×<br>Multiple organs          | ×<br>Kidney                      |                                | ×<br>Kidney     | ×<br>Kidney and QH9-2/1 cell cultured isolate  |
| DOZA005M22 | ×<br>Multiple organs          | ×<br>Kidney                      | ×<br>Kidney                    | ×<br>Kidney     | ×<br>Kidney and QH9-2/1 cell cultured isolate  |
| DOZA006M22 | ×<br>Multiple organs          | ×<br>Kidney                      | ×<br>Kidney                    | ×<br>Kidney     | ×<br>QH9-2/1 cell cultured isolate             |
| DOZA007M22 | ×<br>Multiple organs          | ×<br>Kidney                      |                                | ×<br>Kidney     | ×<br>QH9-2/1 cell cultured isolate             |
| 22030045   |                               |                                  |                                |                 | ×<br>Organ pool                                |
| 22040247   |                               |                                  |                                |                 | ×<br>Organ pool                                |
| 22040244   |                               |                                  |                                |                 | ×<br>Organ pool                                |
| 22060338   |                               |                                  |                                |                 | ×<br>Organ pool                                |
| 22060412   |                               |                                  |                                |                 | ×<br>Organ pool                                |
| 22060471   |                               |                                  |                                |                 | ×<br>Organ pool                                |
| 22070111   |                               |                                  |                                |                 | ×<br>Organ pool                                |
| 22080021   |                               |                                  |                                |                 | ×<br>Organ pool                                |
| 22080566   |                               |                                  |                                |                 | ×<br>Organ pool                                |
| 22090303   |                               |                                  |                                |                 | ×<br>Organ pool                                |

<sup>1</sup> More than one sample type if indicated, was submitted for Ion Torrent NGS and compared for optimal analysis, <sup>2</sup> RNA was extracted from indicated sample type and used.

### 2.3.3. Sample processing

Tissue samples that potentially contained live viruses were handled and stored in the Poultry Biosafety Laboratory 3 (BSL3) (Compliance number: #DAH-CQ06) (Appendix D) facility at -80 °C. Various tissue samples of organs including brain, gastrointestinal tract, kidney, lung, stomach, trachea, heart and liver were collected from deceased pigeons by means of necropsy and individually placed into TRIzol LS reagent (ThermoFisher Scientific, USA), which



effectively inactivated the viruses before further processing and testing in the Poultry Research Laboratory was conducted. For extraction of nucleic acids and virus isolation, a tissue sample from the different tissue samples of organs ( $\pm 0.5\text{cm} \times 0.5\text{cm}$ ) placed in TRIzol with 1 ml of PBS (Phosphate-Buffered Saline)(Sigma-Aldrich, USA) with double the normal concentration of gentamycin (Virbac, South Africa)(100  $\mu\text{g}/\text{mL}$  to 200  $\mu\text{g}/\text{mL}$ ) and fungizone (Omega Scientific Inc, USA)(5  $\mu\text{g}/\text{mL}$  to 10  $\mu\text{g}/\text{mL}$ ) was macerated using homogenizer bead tubes (Roche, Germany) in the Omni International Bead Ruptor 4 homogenizer (Sigma-Aldrich, USA). The mixture was thoroughly vortexed and then centrifuged at 13 000 rpm for 1 minute (Sigma 1-14 microcentrifuge, Whitehead Scientific, Nest Biotechnology, China). Following centrifugation, the supernatant was carefully transferred to a clean Eppendorf tube, labelled and stored thereafter at  $-80\text{ }^{\circ}\text{C}$  until extraction of genetic material and virus isolation.

Cell culture samples in 6-well plates were transferred to a  $-80\text{ }^{\circ}\text{C}$  freezer to rapidly freeze for 24 hours once the majority of the cells had detached from the plate surface. Subsequently, the frozen cell culture samples in the 6-well plates were thawed at room temperature for cell lysis and the release of intracellular contents. After thawing, the infection media was carefully removed and 250  $\mu\text{l}$  of the lysate was used for extraction of genetic material. The remaining lysate was used to infect newly prepared 6-well plates for subsequent passages.

#### **2.3.4. RNA extraction**

To ensure the retrieval of optimal RNA for analysis, diverse approaches were employed, encompassing both manual and automatic extraction methods. This comprehensive strategy aimed to maximize the chances of obtaining high-quality RNA samples. RNA was extracted from tissue homogenates or cell culture samples in TRIzol LS reagent (ThermoFisher Scientific, USA) or total nucleic acids were extracted with a robotic IndiMag 48 platform.

For TRIzol RNA extraction, 750  $\mu\text{l}$  of TRIzol (ThermoFisher Scientific, USA) was aliquoted to a 1.5 ml microcentrifuge tube (Merck, Germany) which contained 250  $\mu\text{l}$  of the sample. The tube was then vortexed (VX-200 Vortex Mixer, Labnet, USA) thoroughly and left for 5 minutes. Chloroform (200  $\mu\text{l}$ ) (Merck, Germany) was added to the tube (Merck, Germany), shaken to emulsify and incubated on the bench for 10 minutes. The solution was centrifuged (Sigma 1-14 Microcentrifuge, Lasec, Cape Town) at 13 000 rpm for 15 minutes, after which the upper clear phase ( $\sim 650\text{ }\mu\text{l}$ ) was transferred to a clean labelled 1.5ml tube (Merck,

Germany). An equal volume (~650 µl) of isopropanol (Merck, Germany) was added to the tube (Merck, Germany). The RNA was precipitated on the bench for 15 minutes. The tubes (Merck, Germany) were centrifuged (Sigma 1-14 Microcentrifuge, Lasec, Cape Town) at 13 000 rpm for 15 minutes. All the isopropanol was carefully removed to not disturb the pellet. 70 % ethanol (500 µl) (Merck, Germany) was then added to the pellet, vortexed (VX-200 Vortex Mixer, Labnet, USA) briefly and centrifuged (Sigma 1-14 Microcentrifuge, Lasec, Cape Town) for 5 minutes at maximum speed. All the ethanol was removed carefully to not disturb the pellet. The tube (Merck, Germany) was air-dried upright and open for 5 minutes to ensure the ethanol evaporated. Ultrapure Nuclease-Free Water (50 µl) (Omega Bio-tek, USA) was added to the pellet, resuspended using a micropipette and left for 5 minutes. RNA was then tested immediately and stored thereafter at -80 °C.

For the robotic IndiMag extraction, an IndiMag<sup>®</sup> Pathogen Kit w/o plastics (384) (Indical Bioscience, Germany) was used according to the manufacturer's recommended procedure. Briefly, Wash Buffer 1 (700 µl), Wash Buffer 2 (700 µl) and Elution Buffer (100 µl) were added into wells 2, 3 and 4 separately. The following master mix was prepared with Buffer VXL (100 µl), Buffer ACB (400 µl), MagAttract Suspension (25 µl) and Carrier RNA (1 µl) from which 500 µl were added into the sample rows alongside 200 µl of the sample and Proteinase K (20 µl). The prepared plates were loaded into the IndiMag 48 with the disposable sterile plastic rod cover strips over the relevant magnetic rods. Total nucleic acid (100 µl) was removed from the last well and transferred to individually marked 1.5 ml microcentrifuge tubes, (Merck, Germany) tested immediately and stored thereafter at -80 °C.

RNA submitted by Western Cape samples had previously been extracted with Nucleospin<sup>®</sup> RNA Virus Kits (Macherey-Nagel GmbH & Co. KG) or a QIAcube HT<sup>®</sup> automated extraction system using the Cador<sup>®</sup> Pathogen 96 QIAcube<sup>®</sup>HT kit (QIAGEN SA [Pty] Ltd), and the presence of NDV was confirmed by real-time RT-PCR according to the WCPVL's accredited diagnostic test for the detection of Newcastle disease virus (B. Pevrot, personal communication).

### **2.3.5. Real-time RT-PCR**

Real-time RT-PCRs were carried out for screening the field samples collected (indicated in Table 2.2) using the VetMAX –Plus One-Step RT-PCR kit (Applied Biosystems, USA), PCR-

grade water and a set of primers and probes (Table 2.3) (synthesized at ThermoFisher Scientific, USA) optimized for targeting the L gene (142 bp region) for detection of all Avian avulavirus (APMV-1) lineages (Fuller *et al.*, 2010). As APMV-1 is known for its genetic variability, which results in a wide range of strains circulating in avian populations, this assay contains two probes for increased detection sensitivity (Fuller *et al.*, 2010). The probes were labelled with a 5' fluorescent dye (FAM) and a 3' black hole quencher (BHQ).

**Table 2.3: Primers and probes used for real-time RT-PCR detection of NDV (Fuller *et al.*, 2010).**

|                     |  |
|---------------------|--|
| Forward primer: NDF | 5'- GAGCTAATGAACATTCTTTC-3'  |
| Reverse primer: NDR | 5'-AATAGGCGGACCACATCTG-3'  |
| Probe: NDpro1       | 5'[FAM] <sup>1</sup> - TCATTCTTTATAGAGGTATCTTCATCATA-[BHQ] <sup>1</sup> 3' |
| Probe: NDpro2       | 5'[FAM] <sup>1</sup> -TCATACACTATTATGGCGTCATTCTT-[BHQ] <sup>1</sup> 3'     |

<sup>1</sup>FAM: Fluorescein amidite, BHQ: Black hole quencher.

The reaction mixture for each real-time RT-PCR assay consisted of the following: 1.2 µL PCR-grade water, 6 µL of 2 X RT-PCR buffer, 0.5 µL RT Enzyme mix, 0.5 µL of 10pmol/µl forward (NDF) and reverse (NDR) primers, respectively and 0.15 µL of 5pmol/µl probe 1 (NDpro1) and probe 2 (NDpro2). In each real-time RT-PCR assay run, a previously confirmed NDV-positive sample and two no-template negative controls (PCR-grade water) were incorporated. Nucleic acid (4 µl) (sample/ positive control - PPMV UP 2020 [121.3 ng/ µl] of water (negative control) was added to each corresponding sample well. The real-time RT-PCRs were carried out in Applied Biosystems Verti 96 well thermal cycler (ThermoFisher, Scientific, USA) and the cycling conditions were as follows: 1 cycle at 48°C for 10 minutes, 1 cycle of 95°C for 10 minutes, 40 cycles of 95°C for 15 seconds and a final cycle of 53°C for 45 seconds.

### 2.3.6. Conventional RT-PCR and Sanger DNA sequencing

Conventional RT-PCRs were performed on positive samples using the tissue material with the highest virus levels to confirm virus identity using 2 x Phusion Flash master mix (ThermoFisher, USA), MMLV-RT (Invitrogen, USA) RNase Inhibitors (Applied Biosystems, USA) and a set of primers that were modified to bind specifically for PPMV detection from the published primers by Abolnik *et al.*, (2004) which resulted in the amplification of a 580 bp

fragment that spans the F<sub>0</sub> cleavage site (Table 2.4). Primers were synthesized by Inqaba Biotech (Pty) Ltd (Inqaba, South Africa).

**Table 2.4: Primers used for conventional RT-PCR amplification of a partial region spanning the M and F genes.**

|                            |                                 |
|----------------------------|---------------------------------|
| Forward primer: PPMV-F FOR | 5'- CGGGTAGAAGAGTCTGGATCTCGG-3' |
| Reverse primer: F581-DEG   | 5'-CYGCCACTGCTAGYTYGATAAKCC-3'  |

The reaction mixture for each RT-PCR assay consisted of the following: 10 µL of 2 x Phusion Flash Master Mix, 1 µL of 10pmol/ µL forward (PPMV-F FOR) and reverse (F581-DEG) primers, respectively, 0.3 µL MMLV (Moloney Murine Leukemia Virus; Invitrogen, USA), 0.2 µL RNase Inhibitor, 2.5 µL Water and 5 µL nucleic acid/ water (negative control). In each RT-PCR assay run, a previously confirmed NDV positive sample and negative control was incorporated. The RT-PCRs was carried out in Applied Biosystems Verti 96 well thermal cycler with the following optimised conditions: 1 cycle at 37°C for 20 minutes, 35 cycles of 98°C for 10 seconds, 98°C for 5 seconds, 54°C for 15 seconds, 72°C for 30 seconds and 1 cycle at 72°C for 1 minute.

The amplification products of the RT-PCR assays were detected by agarose gel electrophoresis using a 1% (m/v) agarose gel (Meridian Bioscience, UK) stained with 8 µl ethidium bromide (Merck, Germany) using a gel electrophoresis horizontal tank and a powerpac power supply (Bio-Rad, USA) at 90 V for 75 minutes. A 1x Tris-Acetate-Ethylenediaminetetraacetic acid (EDTA)(TAE) (Merck, Germany) buffer was utilised for electrophoresis. Loading dye (2 µl) (Lonza Bioscience, USA) along with the amplified products of the RT-PCR (15 µl) were loaded into the wells. A 1 Kb DNA ladder (ThermoFisher Scientific, USA) was included to determine the size of the amplified products. A UV transilluminator (Spectroline™ Slimline™, Sigma-Aldrich, USA) was used to visualize bands after electrophoresis was completed. Amplicons excised from 1% agarose gels underwent purification using the QIAquick Gel Extraction Kit (Qiagen, Germany) through the following steps: Initially, 300 µl of Buffer QC was introduced to the excised fragments within a 1.5ml Eppendorf tube, followed by incubation for 10 minutes at 50°C. Throughout the incubation, the tube was vortexed every 2 to 3 minutes to facilitate gel dissolution. Subsequently, 100 µl of isopropanol was added to the sample, and thorough mixing was achieved through inversion. The processed sample was loaded into a

QIAquick spin column placed in a 2ml collection tube, and then centrifuged (Sigma 1-14 Microcentrifuge, Lasec, Cape Town) for 1 minute at 13 000 rpm. The resulting flow-through was discarded, and the QIAquick column was returned to the collection tube. For successive washing steps, 500  $\mu$ l of Buffer QG and 750  $\mu$ l of Buffer PE were separately added to the QIAquick column and subjected to centrifugation (Sigma 1-14 Microcentrifuge, Lasec, Cape Town) for 1 minute at 13 000 rpm. After discarding the flow-through, the QIAquick column was carefully placed inside a clean 1.5ml Eppendorf tube, appropriately labelled. The elution of DNA was achieved by adding 50  $\mu$ l of nuclease-free water to the centre of the QIAquick membrane, followed by centrifugation (Sigma 1-14 Microcentrifuge, Lasec, Cape Town) for 1 minute at 13 000 rpm. The quantification of purified DNA occurred using a NanoDrop spectrophotometer through the following steps: Initially, the software settings were adjusted to the relevant sample source, such as DNA. Subsequently, 1-2  $\mu$ l of nuclease-free water was carefully pipetted onto the lower measurement pedestal, and the sampling arm was lowered to initiate a blank measurement for calibration using the PC software. Once the calibration was completed, both the upper and lower pedestals were wiped clean with a dry, lint-free laboratory wipe. Following this, each DNA sample was pipetted onto the lower measurement pedestal, and the sampling arm was lowered to initiate a spectral measurement. The concentrations and ratios of each sample were tabulated and subsequently submitted, along with the forward and reverse primers for Sanger DNA sequencing, to Inqaba Biotech (Pty) Ltd.

### **2.3.7. Whole Transcriptome Amplification for Ion Torrent NGS**

The RNA or total nucleic acids extracted from samples (organ material and QH9-2/1 cell culture isolates as indicated in Table 2.2) were used to prepare transcriptome libraries with a Complete Whole Transcriptome Amplification Kit (Sigma-Aldrich, USA) according to the manufacturer's recommended procedure as follows. The Library Synthesis Buffer, Library Synthesis Solution, Library Synthesis Enzyme and Nuclease-Free water were thawed, 14  $\mu$ l of the sample was added with 2.5  $\mu$ l Library Synthesis Solution and nuclease-free water to a total of 16.6  $\mu$ l. The solution was gently mixed and incubated in a thermocycler for 5 minutes at 70  $^{\circ}$ C and then cooled to 18  $^{\circ}$ C. Library Synthesis Buffer (2.5  $\mu$ l), Water (3.9  $\mu$ l) and Library Synthesis Enzyme (2 $\mu$ l) were added to the cooled-primed RNA solution which was incubated under the following conditions: 18  $^{\circ}$ C for 10 minutes, 25  $^{\circ}$ C for 10 minutes, 37  $^{\circ}$ C for 30 minutes, 42  $^{\circ}$ C for 10 minutes, 70  $^{\circ}$ C for 20 minutes and held at 4  $^{\circ}$ C. The following master mix was prepared containing nuclease-free water (301  $\mu$ l), amplification mix (37.5  $\mu$ l), WTA

dNTP Mix (7.5 µl) and amplification enzyme (3.75 µl) also supplied in the kit. The library synthesis reaction (25 µl) from the previous step was added to the master mix solution, and the total volume was divided into five (75 µl) reactions in separate tubes. A reaction volume of less than 75 µl for the last aliquot, is not critical as stated per protocol. The reactions were incubated in a thermocycler (Applied Biosystems Veriti 96 well, ThermoFisher, Scientific, USA) using the following conditions: 94 °C for 2 minutes, 94 °C for 30 seconds, and 70 °C for 5 minutes for 17 cycles.

The PCR products were purified with a High Pure PCR Product Purification Kit (Roche, Germany) according to the manufacturer's recommended procedure. The five 75 µl reactions were pooled and added into an 5 ml Eppendorf tube containing Binding buffer (1750 µl). A High Pure Filter Tube was inserted into a collection tube, to which the sample (a maximum of 750 µl) was transferred and centrifuged (Sigma 1-14 Microcentrifuge, Lasec, Cape Town) at maximum speed (13 000 rpm) for 30 to 60 seconds. The entire volume of PCR product in the binding buffer was centrifuged in successive rounds through the same tube, discarding the flow through each time. 500 µl of Wash Buffer was added to the filter tube containing the bound DNA, centrifuged (Sigma 1-14 Microcentrifuge, Lasec, Cape Town) for 1 minute at 13 000 rpm and then the flow-through solution was discarded. Wash Buffer (200 µl) was added, centrifuged (Sigma 1-14 Microcentrifuge, Lasec, Cape Town) for 1 minute at maximum speed (13 000 rpm) and the flow-through was discarded. 55 µl of Nuclease-Free Water was added and allowed to stand for 1 minute on the bench. The tubes were centrifuged at 13 000 rpm for 1 minute to collect the eluted DNA.

The PCR products were quantified on a NanoDrop spectrophotometer (minimum concentration of 10ng per sample needed) and shipped in a polystyrene cooler with ice packs to the Central Analytical Facility at Stellenbosch University (SU) for Ion Torrent NGS.

### **2.3.8. Bioinformatic analysis**

The conventional RT-PCR forward and reverse sequences were visually analysed in Chromas Lite (v.2.1) (Technelysium, Queensland, Australia) to identify differences such as base-call errors, ambiguous bases, or low-quality areas. The sequences were trimmed to remove errors and ensure high-quality areas. The forward and reverse sequences (the latter reverse-complemented) were aligned in BioEdit (v.7.2) (Hall, 1999) from which a consensus sequence

was generated and exported in FASTA format for further analysis. The consensus sequences exported for further analysis were rigorously validated by subjecting the sequences to a BLAST search on the National Centre for Biotechnology Information (NCBI) database to distinguish true positives from any potential non-specific amplification or contamination from control samples. Consensus sequences generated from Sanger sequencing data were used in conjunction with sequences generated from Ion torrent data to compare and fill gaps, if necessary.

Ion torrent reads (.bam files) were downloaded by FTP from the SU server and imported into CLC Genomic Workbench V11.0.1 for genome assembly using a combination of assemble-to-reference and *de novo* assembly approaches. The default parameters used for *de novo* assembly included mismatch cost 2, insertion cost 3, deletion cost 3, length fraction 0,5 and similarity fraction 0,8. The Pigeon paramyxovirus reference sequences used for assemble-to-reference was JX901110.1, retrieved from the GenBank database (<https://www.ncbi.nlm.nih.gov/genbank/>). The F gene sequence was also extracted from this strain. After read mapping, the consensus sequences for each sample were exported. Full F gene sequences were annotated and submitted to Genbank.

The NDV classification dataset generated by Dimitrov *et al.*, 2019 was downloaded from GenBank (<https://www.ncbi.nlm.nih.gov/genbank/>) and used for genotype identification. The F gene sequences generated in this study were blasted against the GenBank nucleotide sequence database (<https://www.ncbi.nlm.nih.gov/genbank/>) to retrieve closely-related PPMV sequences from other regions. Multiple sequence alignments were prepared in BioEdit (Hall, 1999) and MAFFT (<https://mafft.cbrc.jp/alignment/server/>) open-source software programs.

Phylogenetic trees of metagenomic datasets were reconstructed in IQ tree (<http://iqtree.cibiv.univie.ac.at/>) using the maximum likelihood method with 1000 bootstrap replicates. The substitution model in IQ tree database was selected as auto, with maximum iterations of 1000, minimum correlation coefficient 0.99, perturbation strength 0.5 and the IQ-TREE stopping rule 100. The phylogenetic trees generated were visualised in FigTree (v1.4.4) (<http://tree.bio.ed.ac.uk/software/figtree/>) and edited in Inkscape (v1.2.2) (<https://inkscape.org>). Suitable outgroups were used for each phylogenetic tree constructed.

### **2.3.9. Virus isolation**

Confluent monolayers of QH9-2/1 Quail cells (Nuvonis Technologies, Austria) were prepared in tissue flasks (Whitehead Scientific, Nest Biotechnology, China) according to the supplier's protocol, as described below. The supernatant obtained from the tissue homogenate as described in section 2.3.2 for eight samples (DOZA000M22, DOZA001M22, DOZA002M22, DOZA003M22, DOZA004M22, DOZA005M22, DOZA006M22 and DOZA007M22) was inoculated (0.2 - 0.5 ml) onto the cell culture and incubated at 37 °C for 24 hours. For control purposes, each 6-well plate contained a positive virus (Avian orthoavulavirus 1 isolate turkey/ South Africa/ N2057/ 2013 - KR815908.1; diluted with PBS) and a negative sample. Observations for any cytopathic changes were recorded daily after each passage with an inverted microscope at 10x magnification (ZEISS Primovert, Axiology Labs, South Africa).

#### **2.3.9.1. Preparation of cells**

The QH9-2/1 Quail cells (Nuvonis Technologies, Austria) stored in 1 ml cryovials at -80 °C were thawed in a 37 °C water bath before being transferred into a T25 flask (Whitehead Scientific, NEST Biotechnology, China) containing 10 ml Serum-Free cell growth Medium (SFM) (Gibco, ThermoFisher Scientific, USA) previously equilibrated to 37 °C in a 5% CO<sub>2</sub> incubator (Midi 40, Labotec, ThermoFisher Scientific, USA). The cells were incubated at 37 °C for 24 hours in a 5% CO<sub>2</sub> incubator (Midi 40, Labotec, ThermoFisher Scientific, USA).

#### **2.3.9.2. Trypsinization of cells**

The cells in the T25 flask (Whitehead Scientific, NEST Biotechnology, China) were trypsinized to break up any cell clumps and transferred to a new T25 flask (Whitehead Scientific, NEST Biotechnology, China), as follows. The old medium was removed with a 10 ml serological glass pipette from the T25 flask (Whitehead Scientific, NEST Biotechnology, China) after 24 hours where the cells were washed with 5 ml PBS (Gibco, ThermoFisher Scientific, USA). 1xTrypLE (3 ml)(Gibco, ThermoFisher Scientific, USA) was added to the flask and incubated for 6-8 minutes at 37 °C until the cells appeared rounded. 8 ml of SFM was added to the mixture and was rinsed by pipetting, whereafter the cell suspension was carefully transferred with a pipette into a sterile conical bottom 50 ml centrifuge tube. An additional 8 ml of SFM was used to rinse the flask and added to the centrifuge tube. The tube was centrifuged for 10 minutes at 310 x g and 22 °C in an Eppendorf 5804 R centrifuge (Eppendorf, Germany). The supernatant was removed and the cells were resuspended in 2 ml SFM and



transferred to a new T25 flask (Whitehead Scientific, NEST Biotechnology, China) containing 8 ml of fresh SFM. The cells were incubated at 37 °C in the CO<sub>2</sub> incubator until ideal confluence of 75% was acquired ( $\pm$  3 days).

#### **2.3.9.3. Splitting of cells for growth continuation**

After ideal confluence was achieved, the cells in the T25 flask (Whitehead Scientific, NEST Biotechnology, China) were trypsinized as previously described in section 2.2.6.2 to split the cell suspension into a T75 and T25 flask (Whitehead Scientific, NEST Biotechnology, China) for growth continuation. After the centrifugation of the conical bottom centrifuge tube and the removal of the supernatant, the cells were resuspended in 3 ml of fresh SFM. 2 ml of the cell suspension was added to a T75 flask (Whitehead Scientific, NEST Biotechnology, China) containing 28 ml of fresh SFM and the remaining 1 ml of cell suspension was added to a T25 flask (Whitehead Scientific, NEST Biotechnology, China) containing 9 ml of fresh SFM. These T25 and T75 flasks (Whitehead Scientific, NEST Biotechnology, China) were incubated at 37 °C in the CO<sub>2</sub> incubator until confluent monolayers formed.

#### **2.3.9.4. Counting and preparing cell plates**

To seed 6 well-plates with the appropriate cell density, the cells in the T25 and T75 flasks (Whitehead Scientific, NEST Biotechnology, China) were trypsinized as previously described in section 2.2.6.2. After centrifugation of the conical bottom centrifuge tube at 310 x g for 10 minutes and the removal of the supernatant, the cells were resuspended in 6 ml of fresh SFM, and 100  $\mu$ l of this cell suspension was placed in a 1.5 ml centrifuge tube. 10  $\mu$ l of cell suspension were added to each of the two chambers of a NucleoCounter slide (Marienfeld, Germany) where the number of cells present was counted to determine the number of cells per ml. The calculations for cell density were done as follows (Table 2.5):

**Table 2.5: Calculation of appropriate cell density to seed 6 well-plates.**

| <b>Cell Calculation</b>  |   |
|--|---|
| <b>Calculation:</b>  | Block 1: 175  |
|  | Block 2: 142  |
| <b>Total cells in all 2 blocks:</b>                                | 317   |
| <b>Average cells in one block:</b>                                 | $317/2 = 158.5$   |
| <b>Total cells per 1ml:</b>  | $158.5 \times 10\ 000 = 1\ 585\ 000$  |
| <b>Dilution factor (Cells present/<br/>Cells required):</b>        | $1\ 585\ 000\ \text{cells per ml} / 200\ 000\ \text{cells per ml} = 7.925$<br>$7.925 - 1 = 6.925$ |
| <b>Volume of media used to<br/>resuspend cells to count</b>        | 6 ml  |
| <b>Volume of media you need to<br/>add to get the final volume</b> | $6.925 \times 6\ \text{ml} = 41.55\ \text{ml media added}$  |

Therefore, from the example above, to ensure a cell density of 200 000 cells/ml to seed 6 well plates, the number of cells present in blocks 1 and 2 was added and divided by two to get the average number of cells present which was multiplied by 10 000, to calculate the total number of cells present per 1ml (1ml = 1000  $\mu$ l, as 10  $\mu$ l was added per block). The dilution factor was determined by dividing the total cells per 1ml with the cells density required per 1ml, from which 1 is subtracted, giving a dilution factor of 6.925. The dilution factor is then multiplied by the volume of media the cells were resuspended in before counting, in this instance 6ml. Giving a total of 41.55 ml of media that was added to the cell suspension where two 6 well-plates were seeded with 3 ml of the cell suspension media in each well (Gibco, ThermoFisher Scientific, USA) and incubated at 37 °C for 24 hours. The remainder of the cell suspension was seeded into a T25 and T75 flask (Whitehead Scientific, NEST Biotechnology, China) where an additional SFM was used to ensure the correct volume. The flasks were incubated at 37 °C in a CO<sub>2</sub> incubator for 24 hours to allow for optimal cell growth. The cell suspensions in the flasks were split again and subsequently seeded into additional 6-well plates and flasks. This sequential process was repeated until an adequate number of 6-well plates was seeded for the passages. Any remaining cells after that were collected, preserved, and stored at -80°C as described in section 2.3.6.7.

### **2.3.9.5. Infection of cell plates**

The medium was removed from the 6-well plates and the cells were washed twice with 5 ml of PBS (Gibco, ThermoFisher Scientific, USA). 1 ml of the medium (supernatant collected for

one tissue sample with the highest virus titre for the eight samples, DOZA000M22 to DOZA007M22) used for infection was pipetted into each well. The 6-well plates were then incubated at 37 °C in the CO<sub>2</sub> incubator. After one hour, the medium was removed and 1.5 ml of SFM was added to each well and incubated at 37 °C in the CO<sub>2</sub> incubator. Cells were observed daily for any cytopathic effects (CPE) after infection until a majority of the cells detached from the surface.

#### **2.3.9.6. Microscopic analysis**

Following infection, QH9-2/1 cells were carefully monitored using an inverted light microscope under 10x magnification (ZEISS Primovert, Axiology Labs, South Africa) to observe morphological changes indicative of viral CPE. Images were captured at various time points post-infection to document alterations in cell morphology, including cell rounding, detachment, and the formation of syncytia. To confirm infection, infected QH9-2/1 cells were processed for transmission electron microscopy. Briefly, cells were fixed, embedded, and sectioned before examination under a transmission electron microscope. This allowed for the visualization of intracellular viral particles and other ultrastructural changes associated with PPMV infection.

#### **2.3.9.7. Further passage of infected cells**

Samples that presented with CPE, were further passaged. When 75% - 100% of the cell monolayer showed any changes or had detached from the surface due to degeneration, the cells and the supernatant were used for further passages. Further passages consisted of the cells being freeze-thawed and harvested, cells and supernatant of the initial 6 well-plate were transferred to newly prepared 6 well-plates as follows: For transfer, the initial 6 well-plates were frozen at -80°C while new 6 well-plates were prepared (as described in section 2.3.6.1 and 2.3.6.2) for another passage of the samples. The frozen 6 well-plates were defrosted and harvested into 1.5 ml collection tubes once the newly prepared 6 well-plates were ready for infection. Harvested cells and supernatant were filtered with a 0.45 µm syringe filter before inoculation (200 µl) onto freshly prepared cell monolayers. This was done to ensure that any toxicity in the media was removed and to filter media samples that have signs of bacteria (black spots) and yeast (strings) prior to proceeding with subsequent passages, this precautionary step aimed to eliminate potential contamination such as microbial or particulate matter that may affect the integrity of the cell culture. Some of the remaining harvested cells and supernatants of each

passage that was not used for inoculation were tested for the presence of PPMV by rRT-PCR as described in section 2.3.5 to confirm the presence of NDV/PPMV. Virus isolates were stored with Dimethyl sulfoxide (DMSO) with a final cell density of 7.5 mio/ml and concentration of 7.5% (v/v) (ThermoFisher Scientific, USA) at -80 °C in the BSL3 facility.

#### **2.3.9.8. Preparing passage samples for Ion Torrent NGS**

Harvested cells and supernatants for passage three were meticulously processed for Ion Torrent NGS following the procedures outlined in section 2.3.7. This sequence data will be employed in conjunction with organ material that have also been sent for Ion Torrent NGS processing. By combining the genetic information obtained from both harvested cells and organ material for the different samples, this integrated approach aims to provide a comprehensive and detailed bioinformatic analysis.

#### **2.3.9.9. Freezing of cells for storage**

The day before freezing, CoolCell LX cell freezing containers (Corning, Sigma Aldrich, USA) were pre-cooled at temperatures ranging from 2 °C to 8 °C. On the day of freezing, a sufficient quantity of SFM and 2x Cryopreservation Media (CFM; 5.1 ml SFM + 900 µl DMSO) was prepared in advance. The media was then cooled on ice for a minimum of one hour. Subsequently, the cell culture flasks were trypsinized, and the resulting cell suspension was centrifuged for 10 minutes at 310 g. After removing the supernatant, the appropriate volumes of SFM and 2xCFM were added to each cryovial (Greiner, Sigma Aldrich, USA) based on predetermined calculations (0.5 ml SFM and 0.5 ml 2xCFM per vial). Homogenisation of the cell suspension was performed with inversion, and 1 ml aliquots were subsequently transferred into cryovials. The cryovials were then placed inside pre-cooled CoolCell LX cell freezing containers. These containers were subsequently stored at -80 °C for a period of 16 to 24 hours to facilitate controlled slow freezing of the cells. The day after freezing, the cryovials were transferred to a container at -80 °C for long-term storage, ensuring the preservation of the cells for future use and experimentation.

## 2.4. Results

### 2.4.1. Screening of field samples collected in 2022 by real-time RT-PCR

All collected doves during 2022 in the Gauteng region tested positive for PPMV. Sample DOZA001M22 was found to be decapitated, rendering it impossible to collect brain tissue. Similarly, sample DOZA000M22 presented challenges as certain organs could not be accurately identified due to their mangled state. The Cycle threshold (Ct) values from different tissues documented are tabulated in Table 2.6.

**Table 2.6:** Cycle threshold (Ct) values for PPMV detected by rRT-PCR in different organs of infected doves.

| SAMPLE     | ORGAN <sup>1</sup> |                  |        |       |       |         |         |       |
|------------|--------------------|------------------|--------|-------|-------|---------|---------|-------|
|            | BRAIN              | GIT <sup>2</sup> | KIDNEY | LIVER | LUNG  | STOMACH | TRACHEA | HEART |
| DOZA000M22 | 25,48              | 0                | 20,73  | 22,65 | 20,07 | 32,37   | 23,72   | NC    |
| DOZA001M22 | NC                 | NC               | NC     | 27,41 | NC    | 32,35   | NC      | NC    |
| DOZA002M22 | 27,56              | 24,79            | 36,88  | 28,88 | 23,96 | 0       | 31,99   | 23,48 |
| DOZA003M22 | 33,95              | 26,87            | 0      | 29,18 | 0     | 31,45   | 34,82   | 27,95 |
| DOZA004M22 | 27,96              | 26,62            | 23,10  | 28,37 | 27,85 | 30,23   | 31,67   | 25,74 |
| DOZA005M22 | 25,95              | 28,38            | 21,90  | 33,57 | 24,13 | 29,35   | 30,78   | 26,27 |
| DOZA006M22 | 0                  | 23,53            | 22,80  | 27,77 | 24,25 | 26,77   | 34,97   | 28,10 |
| DOZA007M22 | 28,72              | 22,65            | 20,45  | 25,21 | 25,79 | 26,46   | 31,26   | 26,15 |

<sup>1</sup> NC – Not collected, 0 - Undetermined; Ct > 40, Highlighted values - Highest viral loads of sample

<sup>2</sup> GIT – Gastrointestinal tract

The virus detection rate in the kidney was generally the highest among the organs tested as it had the lowest Ct value most frequently (Table 2.6).

### 2.4.2. Conventional RT-PCR and sequence analysis

The RNA extracted from tissues of the eight samples (one tissue type per sample) with the highest virus levels as determined were further analysed using conventional RT-PCR. Four of the eight samples analysed (DOZA000M22, DOZA002M22, DOZA005M22 and DOZA006M22) produced the expected 580 amplicon spanning the partial M and F genes (Figure 2.2).

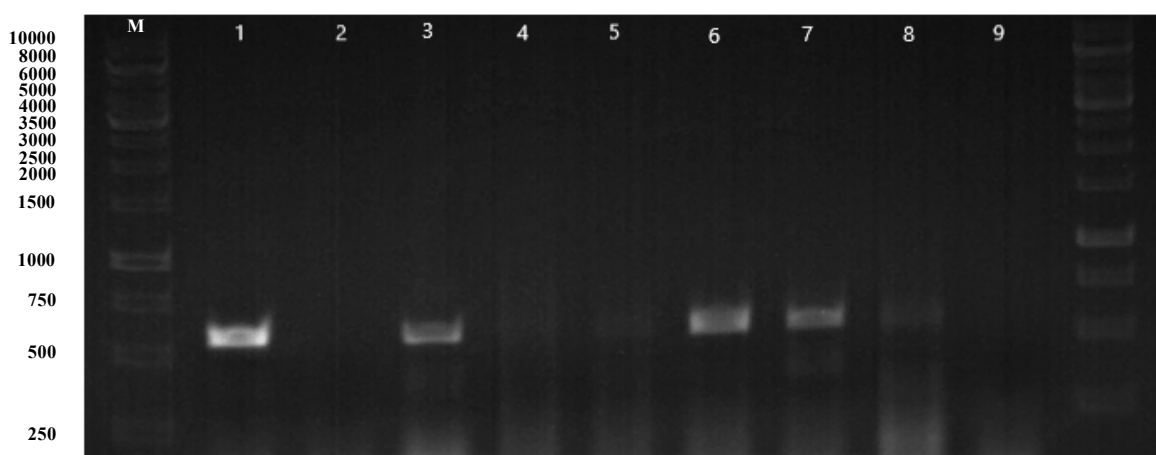


**Figure 2.1:** Agarose gel electrophoresis showing amplification of 580 bp fragments spanning the partial M and F genes of NDV. M: Ladder (1Kb), Lane 1 (DOZA000M22 Lung), 3 (DOZA002M22 Heart), 6 (DOZA005M22 Kidney) and 7 (DOZA006M22 Kidney): Positive amplification of partial M and F gene for NDV, Lane 2 (DOZA001M22 Stomach), 4 (DOZA003M22 Gastrointestinal tract) and 5 (DOZA004M22 Kidney): Negative amplification of partial M and F gene for NDV, Lane 8: Positive control. Lane 9: Negative control.

Sample DOZA007M22 was analysed on a separate gel, however amplification difficulties persisted resulting in no amplification. The 580 bp amplicons visible in Figure 2.2 were excised, purified and the concentrations were determined as per Table 2.7:

**Table 2.7:** Concentrations of purified RT-PCR amplicons for Sanger DNA sequencing.

|            | Concentration ng/μl | A <sub>260</sub> | A <sub>280</sub> | A <sub>260</sub> /A <sub>280</sub> |
|------------|---------------------|------------------|------------------|------------------------------------|
| DOZA000M22 | [-3.6]              | -0.073           | -0.032           | 2.30                               |
| DOZA002M22 | [5.0]               | 0.100            | 0.024            | 4.17                               |
| DOZA005M22 | [6.7]               | 0.134            | 0.043            | 3.14                               |
| DOZA006M22 | [7.8]               | 0.157            | 0.057            | 2.73                               |

DNA concentrations of between 5 and 7.8 ng/ $\mu$ l were obtained for the partial region spanning the M and F gene amplified by conventional RT-PCR, but a negative value was obtained for sample DOZA000M22. Sample runs had been repeated numerous times, however amplification difficulties persisted. A negative DNA concentration reading using a Nanodrop spectrophotometer (Thermo Fisher Scientific, Wilmington, DE, USA), suggests the presence of chemical contaminants from the extraction procedures or impurities in the sample, such as proteins, salts, or organic solvents, which can interfere with the accurate measurement of DNA (Matlock, 2015). Sequences were subjected to blast confirmation before any further analysis; however, these results were not tabulated and presented each time in interest of keeping the chapter short. Sequences produced were utilized to compare with Ion Torrent NGS data to fill sequence gaps if any were present.

#### 2.4.3. Virus isolation with cell culture

Successful isolation of PPMV from quail cells attests to their efficacy as a viable alternative for virus isolation other than SPF eggs. The cell morphology during the different seeding phases is presented in Figure 2.3.

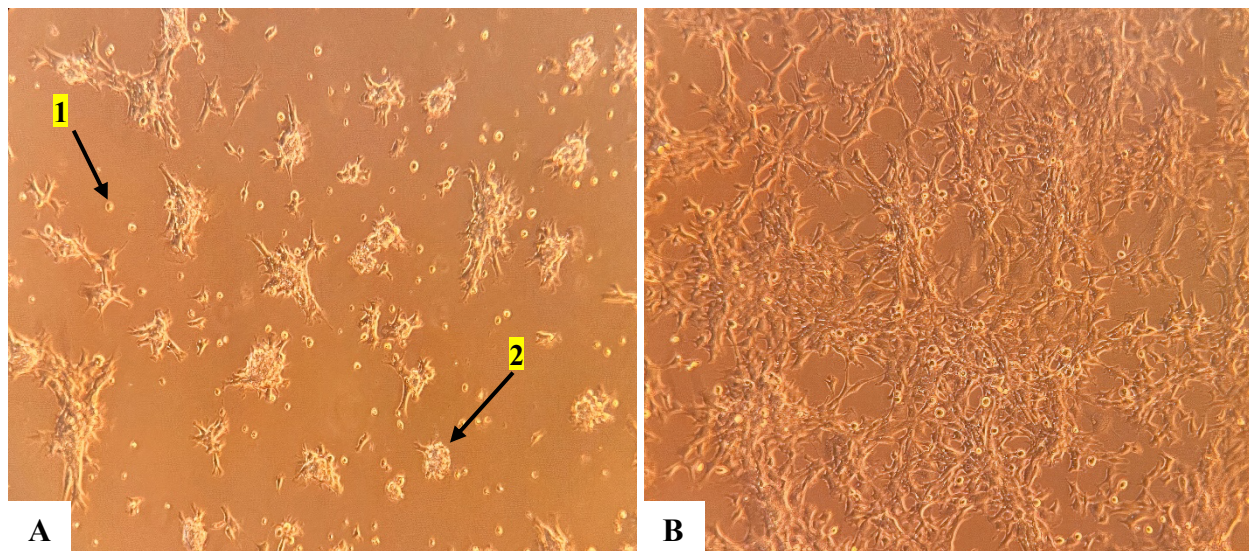


**Figure 2.3:** QH9-2/1 cell cultures after 24 hours (A) and 96 hours (B) seeding in a T-25 flask. 1: Single cell, 2: Cluster of cells (numerous cells aggregated together).

For the initial passage, the cells for most of the samples the day after infection (day 1) (Table 2.8) appeared viable and no cytopathic effects were present, however, two samples (DOZA000M22 and DOZA007M22) showed signs of subtotal cell destruction that are characterized by the detachment of a few cells but not all the cells of the monolayer. Sample

DOZA002M22 and the positive control had indications of focal degeneration which includes cells becoming enlarged, rounded, are seen more easily (refractile) and eventually detach from the growth surface leaving clear areas surrounded by rounded cells. A second passage on all the samples was performed. Most of the cells were still in good condition after 24 hours of the second passage with no cytopathic effects observed, while four samples (DOZA001M22, DOZA003M22, DOZA005M22 and DOZA006M22) had shown indications of subtotal cell destruction. The positive sample indicated signs of focal degeneration. On day 2 of the second passage, more samples showed effects of focal degeneration while sample DOZA000M22 had effects of subtotal cell destruction, sample DOZA003M22 also had effects of subtotal cell destruction, however, contained discoloration which are only numerous cells on top of each other. Sample DOZA004M22 showed signs of a ballooning effect where cells are enlarged and rounded and give a swollen or balloon-like effect. The effects continued to be observed on day three the same as it was on day two for the second passage. A third passage was performed on all the samples. After 24 hours, all the samples exhibited effects of focal degeneration and the negative control had no cytopathic effects observed. The positive control was removed on day 1 after infection for the third passage and stored until all the samples were subjected to a fourth passage. On day two of the third passage all the samples exhibited the exact same signs as observed for day 1 of passage 3. A fourth passage was undertaken, and the majority samples exhibited effects of focal degeneration, two samples (DOZA001M22 and DOZA002M22) showed effects of swelling and clumping that is characterized by enlarged and rounded cells that clump together like "grape-like" clusters before detaching. Cell morphology observed during the different passages are shown in Figure 2.4. Signs of contamination including bacteria (black spots) and yeast (strings) have been observed for samples DOZA003M22, DOZA005M22 and the positive control one day after inoculation on passage 1, these samples were passed through a filter to remove resulting bacteria and yeast before the next inoculation occurred as suggested by Sykes and Rankin (2013). Contamination may manifest through a cloudy appearance in the media.

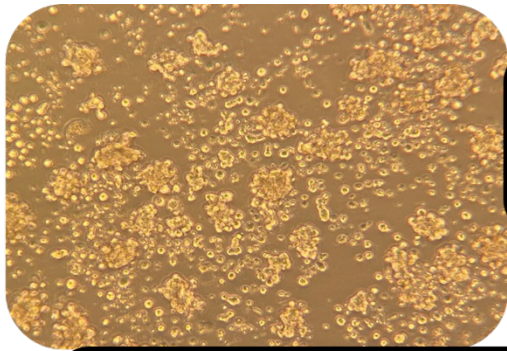
Different Ct values for each sample were measured after each passage to see if the virus replicated in the cell, increasing virus titration levels. The different titration levels after each passage were tabulated as seen in Table 2.9.



**Table 2.8:** Effects observed in the cells infected with the corresponding samples.

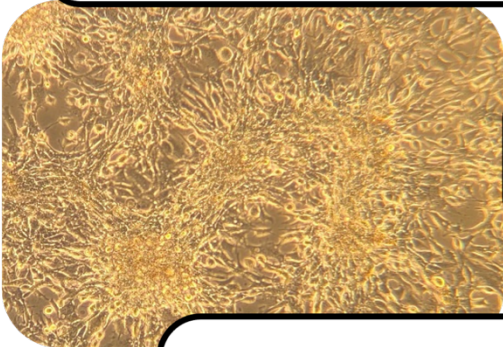
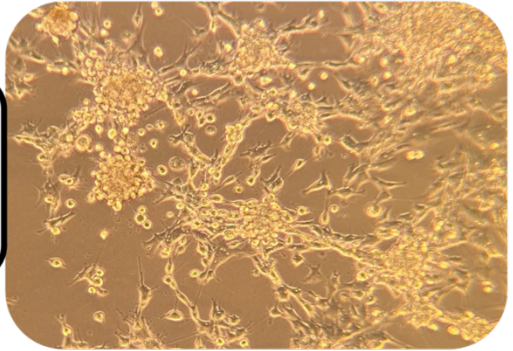
| Days                          | Samples    |            |            |            |            |            |            |            |          |          |
|-------------------------------|------------|------------|------------|------------|------------|------------|------------|------------|----------|----------|
|                               | DOZA000M22 | DOZA001M22 | DOZA002M22 | DOZA003M22 | DOZA004M22 | DOZA005M22 | DOZA006M22 | DOZA007M22 | POSITIVE | NEGATIVE |
| Day 1                         | !          | \$         | &          | \$         | &          | &          | &          | !          | \$       | &        |
| <b>2<sup>nd</sup> Passage</b> |            |            |            |            |            |            |            |            |          |          |
| Day 1                         | &          | !          | &          | !          | &          | !          | !          | &          | \$       | &        |
| Day 2                         | !          | \$         | %          | \$         | #          | \$         | \$         | \$         | \$       | &        |
| Day 3                         | !          | \$         | %          | \$         | #          | \$         | \$         | \$         | \$       | &        |
| <b>3<sup>rd</sup> Passage</b> |            |            |            |            |            |            |            |            |          |          |
| Day 1                         | \$         | \$         | \$         | \$         | \$         | \$         | \$         | \$         | \$       | &        |
| Day 2                         | \$         | \$         | \$         | \$         | \$         | \$         | \$         | \$         | @        | &        |
| <b>4<sup>th</sup> Passage</b> |            |            |            |            |            |            |            |            |          |          |
| Day 1                         | \$         | +          | +          | \$         | \$         | *          | \$         | \$         | \$       | &        |

<sup>1</sup> &: No cytopathic effects observed, !: Subtotal cell destruction, #: Ballooning, \$: Focal degeneration, %: Subtotal cell destruction with discoloration, @: Taken off the previous day, \*: Cell fusion, +: Swelling and clumping



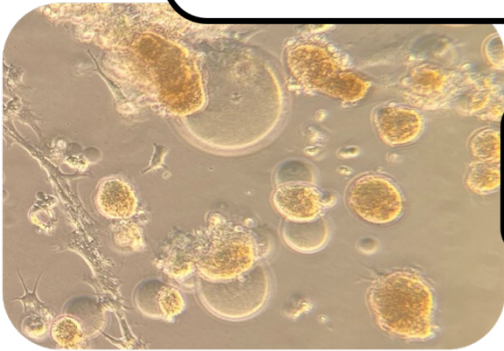
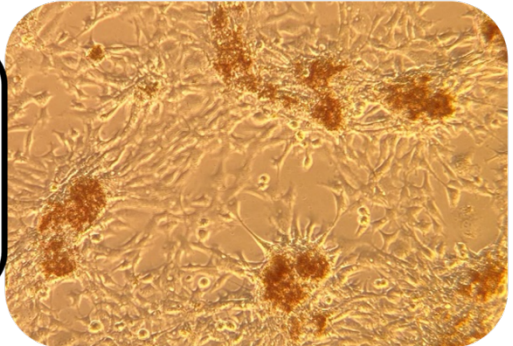
**SWELLING AND CLUMPING:** Enlarged cells that are rounded and clump together like "grape-like" clusters.

**FOCAL DEGENERATION:** Cells become enlarged, rounded, and are seen more easily (refractile), then eventually detach from the growth surface leaving clear areas surrounded by rounded up cells.



**SUBTOTAL CELL DESTRUCTION:** Some cells start to detach but not all the cells in the monolayer.

**SUBTOTAL CELL DESTRUCTION WITH DISCOLORATION:** Some cells start to detach but not all the cells in the monolayer. Cells have a strange discoloration in the middle which is only a lot of cells on top of each other.



**BALLOONING (GIANT CELL):** Cells are enlarged and rounded, giving a swollen or balloon-like appearance.

**CELL FUSION:** Syncytium formed due to fusion of plasma membranes of four or more cells to produce enlarged cells with four or more nuclei (indicated by black circle).

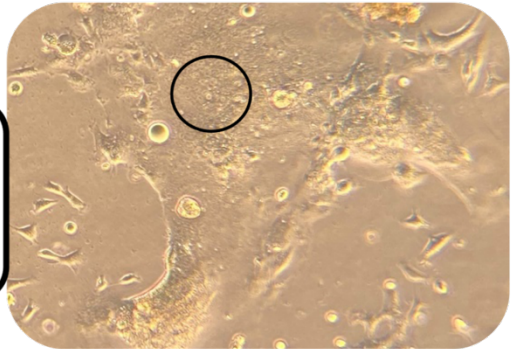


**Figure 2.4:** Cell morphology observed during the passages.

**Table 2.9:** rRT-PCR results (Ct values) of samples tested after each passage.

| Passage | Samples        |                |                |                |                |                |                |                |          |
|---------|----------------|----------------|----------------|----------------|----------------|----------------|----------------|----------------|----------|
|         | DOZA000M<br>22 | DOZA001<br>M22 | DOZA002<br>M22 | DOZA003<br>M22 | DOZA004<br>M22 | DOZA005<br>M22 | DOZA006<br>M22 | DOZA007<br>M22 | POSITIVE |
| 1       | 24.05          | 24.09          | 26.71          | 29.75          | 21.75          | 18.60          | 20.77          | 19.54          | 23.04    |
| 2       | 28.59          | 28.25          | 20.69          | 25.99          | 18.16          | 21.92          | 18.06          | 19.84          | 22.54    |
| 3       | 22.71          | 26.81          | 20.54          | 21.01          | 14.93          | 18.86          | 19.49          | 17.04          | 22.38    |
| 4       | 16.22          | 22.13          | 20.71          | 17.23          | 16.56          | 14.57          | 20.24          | 18.52          | 17.70    |

As shown in Table 2.9, the highest Ct value among all the isolates was 29.75, indicative of the lowest viral load among the samples. The lowest Ct value was 14.57, indicating the highest viral load. For all samples, the viral titer increased with the use of passages, as expected, and confirmed successful virus isolation by rRT-PCR which prompted the exploration of alternative methods for virus isolation. In comparison to traditional egg cultures, utilizing QH9-2/1 cells as a viable alternative not only demonstrated effectiveness in virus isolation but also offered the advantage of being less invasive and more humane. The choice to use QH9-2/1 cells represents a conscious effort to balance efficiency in virus isolation with ethical considerations in laboratory practices. The reason for the fluctuation of the Ct values for each passage is unknown. The interpretation of Ct values in the context of virus growth progression in cell culture with each passage reveals valuable insights into the dynamics of viral replication. As the passage number increases, a decrease in Ct values is indicative of an elevated viral load, suggesting efficient virus replication within the cell culture. Lower Ct values correspond to higher amounts of viral genetic material detected during rRT-PCR, implying an accelerated rate of virus growth.

The cell culture supernatant harvested for DOZA005M22 was submitted to the Faculty of Veterinary Science's Transmission Electron Microscopy (TEM) Unit and the presence of NDV-like particles was confirmed (Figure 2.5). The TEM results confirmed the successful isolation of PPMV in QH9-2/1 cell culture.

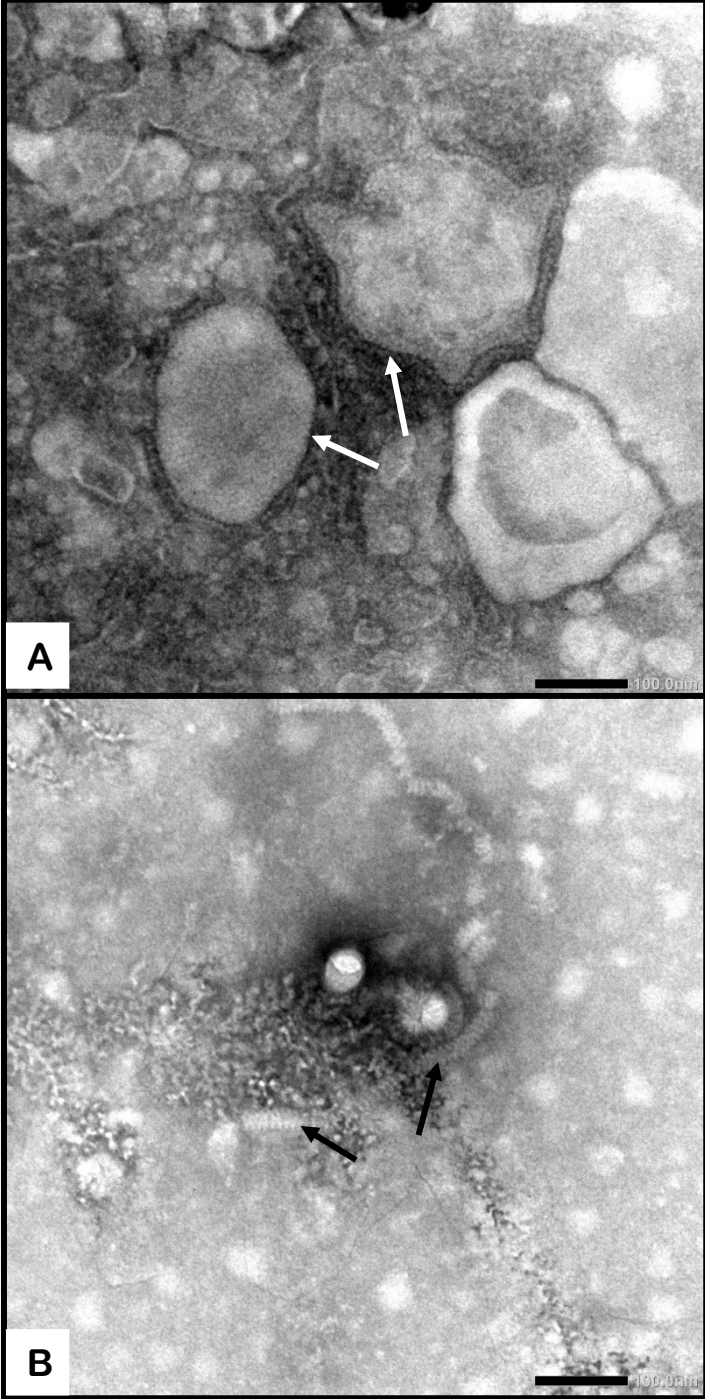


**Figure 2.5:** Negatively stained paramyxovirus particles and nucleocapsids of sample DOZA005M22. A arrows: Virus envelope studded with virus-encoded glycoproteins, B arrows: Helical ribonucleoprotein capsid that has a “herringbone” appearance.

#### **2.4.4. Bioinformatic analysis**

In our Ion Torrent NGS data (Table 2.10), we observed notable variations among the samples in terms of read metrics. The range of total reads obtained across the samples spanned from 195,217 bp to 540,410,427 bp showcasing the diversity in sequencing depth. The average read lengths demonstrated some consistency across the dataset, however, some outliers were present, with average lengths between 70 bp and 185 bp.

Pigeon paramyxovirus sequences generated from DOZA001M22, DOZA002M22 and DOZA003M22 were determined to be contaminants from the positive control used (100% sequence homology) and were excluded from all subsequent PPMV phylogenetic analysis in Chapter 2 and not submitted to GenBank. After consensus sequences from the different approaches (Sanger sequencing and Ion Torrent NGS) were compared to fill gaps, only 14 of the 31 samples (Table 2.11) produced complete F gene sequences, two samples had complete whole genomes and 10 samples recovered >95% of the whole genome. Sample DM299713's F gene sequence could not be recovered. Sequences were submitted for PPMV to the GenBank nucleotide sequence database under the accession numbers OR681891, OQ745932, OQ745933, OQ745934, OR681890, OQ745935, OQ745937, OR681888, OQ745938 and OR681889.

**Table 2.10:** Sequence data recovered for samples sequenced with Ion Torrent NGS.

| <b>Lab/ sample no.</b>    | <b>Bases</b>  | <b>Total Reads</b> | <b>Average read length (bp)</b> |
|---------------------------|---------------|--------------------|---------------------------------|
| N1775                     | 13,766,467    | 195,217            | 70                              |
| 20200121_087_6102A        | 350,921,167   | 2,082,282          | 168                             |
| 20200121_087_6102/613923B | 647,282,862   | 540,410,427        | 164                             |
| 20100411                  | 1,142,492,457 | 6,581,748          | 173                             |
| 20110039                  | 1,313,304,490 | 8,948,420          | 146                             |
| OP04-2020/PRL01-2020      | 3,449,528,474 | 19,869,458         | 173                             |
| S2021/06_0251             | 1,188,647,887 | 6,447,774          | 184                             |
| S2021/06_0218             | 1,370,657,196 | 7,715,476          | 177                             |
| 21070306                  | 1,388,058,884 | 7,751,218          | 179                             |
| 21070474                  | 1,215,625,044 | 6,725,231          | 180                             |
| 21070476                  | 1,024,404,836 | 5,729,160          | 178                             |
| 21090443                  | 1,189,114,129 | 6,415,453          | 185                             |
| DOZA000M22                | 341,510,215   | 4,060,293          | 84                              |
| DOZA001M22                | 615,173,611   | 3,788,380          | 162                             |
| DOZA002M22                | 296,433,453   | 1,763,906          | 168                             |
| DOZA003M22                | 641,668,811   | 4,023,110          | 159                             |
| DOZA004M22                | 576,705,811   | 3,543,438          | 162                             |
| DOZA005M22                | 494,329,349   | 3,043,301          | 162                             |
| DOZA006M22                | 1,642,387,422 | 10,134,890         | 162                             |
| DOZA007M22                | 307,429,500   | 1,734,647          | 177                             |
| 22030045                  | 840,234,134   | 5,147,135          | 163                             |
| 22040096                  | 513,810,470   | 3,091,555          | 166                             |
| 22040247                  | 475,103,886   | 3,060,591          | 155                             |
| 22040244                  | 1,040,510,685 | 7,247,640          | 143                             |
| 22060338                  | 308,607,677   | 2,241,406          | 137                             |
| 22060412                  | 1,205,362,190 | 7,484,285          | 161                             |
| 22060471                  | 691,378,075   | 4,588,010          | 150                             |
| 22070111                  | 753,230,797   | 5,384,611          | 139                             |
| 22080021                  | 969,776,494   | 6,269,391          | 154                             |
| 22080566                  | 644,952,641   | 4,406,300          | 146                             |
| 22090303                  | 413,212,824   | 2,910,826          | 141                             |

**Table 2.11:** Consensus sequence data and percentage of indicated region (F gene/ Whole genome) recovered for samples sequenced with Ion Torrent NGS.

| Lab/sample no.            | Sample type                            | Consensus sequence length         |                                   | Accession number <sup>1</sup> |
|---------------------------|--|-----------------------------------|-----------------------------------|-------------------------------|
|                           |  | F gene recovery (nt) <sup>2</sup> | Genome recovery (nt) <sup>2</sup> |                               |
| N1775                     | Organ pool                             | 1791 (100%)                       | 14789 (97.4%)                     | OR681891                      |
| 20200121_087_6102A        | Organ pool                             | 177 (9.8%)                        | 400 (2.6%)                        |                               |
| 20200121_087_6102/613923B | Organ pool                             | 1687 (94.2%)                      | 10374 (68.3%)                     |                               |
| 20100411                  | Egg-cultured isolate                   | 1791 (100%)                       | 15192 (100%)                      | OQ745932                      |
| 20110039                  | Egg-cultured isolate                   | 1791 (100%)                       | 15192 (100%)                      | OQ745933                      |
| OP04-2020/PRL01-2020      | Egg-cultured isolate                   | 1791 (100%)                       | 15165 (99.8%)                     | OQ745934                      |
| S2021/06_0251             | Egg-cultured isolate                   | 1791 (100%)                       | 14789 (97.4%)                     | OR681890                      |
| S2021/06_0218             | Egg-cultured isolate                   | 1791 (100%)                       | 15180 (99.9%)                     | OQ745935                      |
| 21070306                  | Egg-cultured isolate                   | 1187 (66.3%)                      | 12212 (80.4%)                     |                               |
| 21070474                  | Egg-cultured isolate                   | 992 (55.4%)                       | 10884 (71.6%)                     |                               |
| 21070476                  | Organ pool                             | 344 (19.2%)                       | 2109 (13.9%)                      |                               |
| 21090443                  | Organ pool                             | 604 (33.7%)                       | 2610 (17.2%)                      |                               |
| DOZA000M22                | Lung                                   | 1459 (81.5%)                      | 13383 (88.1%)                     |                               |
| DOZA001M22                | Stomach/ QH9-2/1 cell cultured isolate | 1791 (100%)                       | 15002 (98.8%)                     | *                             |
| DOZA002M22                | Heart/ QH9-2/1 cell cultured isolate   | 1791 (100%)                       | 14023 (92.3%)                     | *                             |
| DOZA003M22                | QH9-2/1 cell cultured isolate          | 1791 (100%)                       | 15143 (99.7%)                     | *                             |
| DOZA004M22                | Kidney/ QH9-2/1 cell cultured isolate  | 1791 (100%)                       | 15190 (99.9%)                     | OQ745937                      |
| DOZA005M22                | Kidney/ QH9-2/1 cell cultured isolate  | 1791 (100%)                       | 15181 (99.9%)                     |                               |
| DOZA006M22                | QH9-2/1 cell cultured isolate          | 1791 (100%)                       | 15030 (98.9%)                     | OR681888                      |
| DOZA007M22                | QH9-2/1 cell cultured isolate          | 1791 (100%)                       | 15164 (99.8%)                     | OQ745938                      |
| 22030045                  | Organ pool                             | 928 (51.8%)                       | 8322 (54.8%)                      |                               |
| 22040096                  | Organ pool                             | 165 (9.2%)                        | 341 (2.2%)                        |                               |
| 22040247                  | Organ pool                             | 263 (14.7%)                       | 1800 (11.9%)                      |                               |
| 22040244                  | Organ pool                             | 1791 (100%)                       | 14297 (94.1%)                     | OR681889                      |
| 22060338                  | Organ pool                             | 144 (8%)                          | 2637 (17.4%)                      |                               |
| 22060412                  | Organ pool                             | 1394 (77.8%)                      | 9409 (61.9%)                      |                               |
| 22060471                  | Organ pool                             | 1366 (76.3%)                      | 11537 (75.9%)                     |                               |
| 22070111                  | Organ pool                             | 1725 (96.3%)                      | 13971 (91.9%)                     |                               |
| 22080021                  | Organ pool                             | 1676 (93.6%)                      | 14337 (94.4%)                     |                               |
| 22080566                  | Organ pool                             | 1124 (62.8%)                      | 9726 (64%)                        |                               |
| 22090303                  | Organ pool                             | 1390 (77.6%)                      | 10587 (69.7%)                     |                               |

<sup>1</sup> Sequences submitted to Genbank, <sup>2</sup> nt: Nucleotide \* Excluded from any further phylogenetic and bioinformatic analysis due to contamination with positive control.

The region spanning the F<sub>0</sub> cleavage site was recovered for 13 of the 28 F gene sequences (excluding the three samples contaminated with the positive control) as depicted in Figure 2.6. The analysis of cleavage sites faced challenges due to the presence of gaps in the sequenced data. These gaps hindered the accurate determination of cleavage sites as amino acid sequences struggled to provide consecutive information in the presence of interruptions. While minor gaps could be filled or adjusted to some extent, larger gaps posed a significant challenge, impeding the seamless identification and characterization of cleavage sites within the protein sequences. A single amino acid motif was present for the 13 different isolates, consisting of <sup>112</sup>RRQKRF<sup>117</sup>, which is a characteristic of virulent NDV strains.

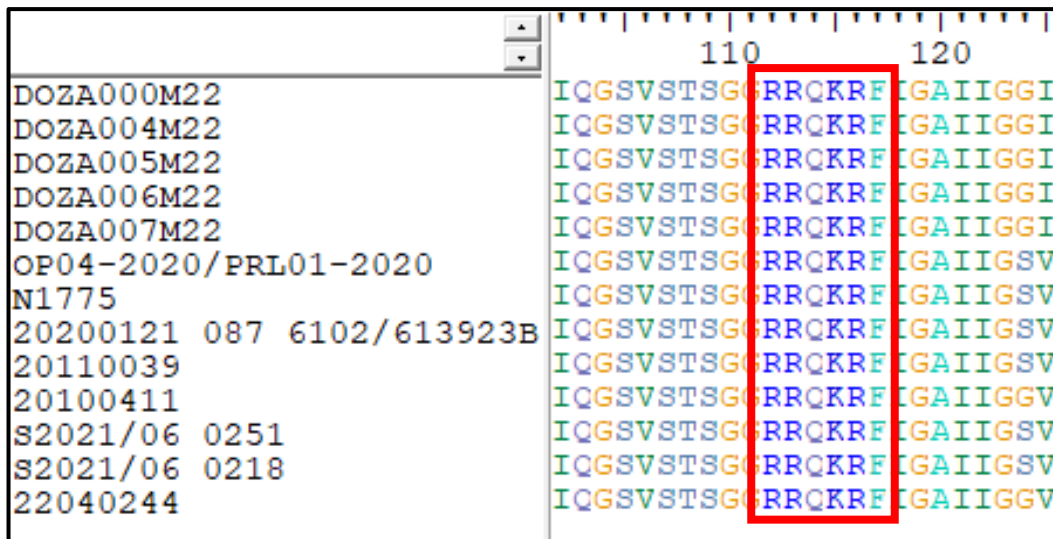


**Figure 2.6:** Amino acid sequences at the F protein cleavage site (amino acids 112 – 117) for F gene sequences used.

#### 2.4.5. Phylogenetic analysis

A 360 nt region spanning over the F gene region including nucleotides (1301 to 1661) of the PPMV genome for 21 of the 28 PPMVs sequenced in Table 2.11 was used for the phylogenetic analysis for genotype classification purposes. This available region utilized was not available for seven of the samples, namely 22040247, 20200121\_087\_6102A, 22040096, 22060338, DOZA000M22, 21070476 and 22030045. Figure 2.7 was constructed using a pilot dataset developed for classification purposes by Dimitrov *et al.*, 2019 with the partial F gene fragment of the 21 samples sequenced in this study.



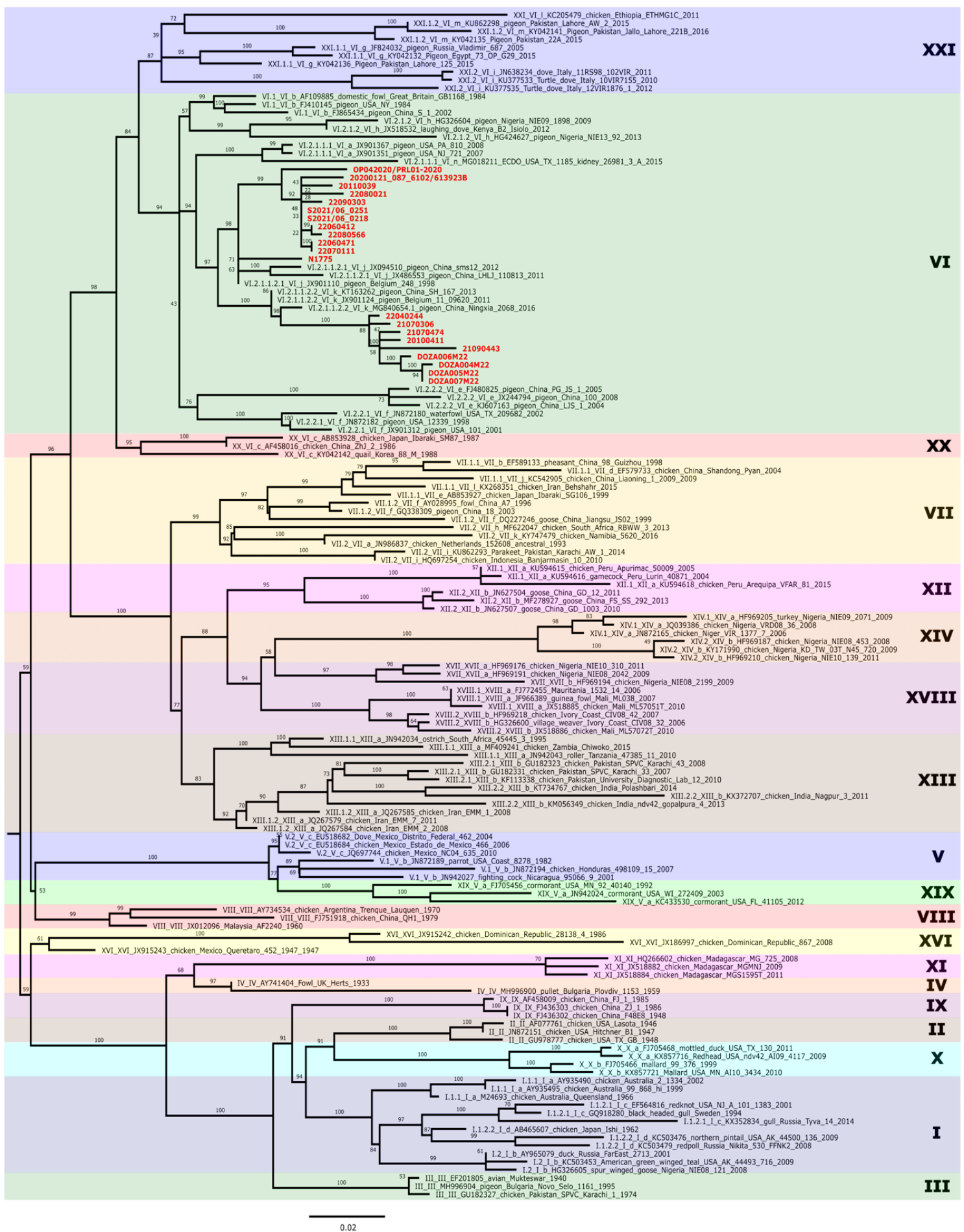


**Figure 2.7:** Maximum likelihood phylogenetic tree based on a partial fragment of the fusion gene (360 nt) of the dataset used for classification purposes. Isolates generated in this study are highlighted in red font. The trees are rooted and drawn to scale, with branch lengths measured in the number of substitutions per site.

The classification analysis (Figure 2.7) revealed that all of the South African strains sequenced in this study grouped in genotype VI, confirming them to be PPMV strains. The South African viruses sampled between 2012 and 2022 were further grouped into two distinct sub-lineages. DOZA007M22, DOZA005M22, DOZA004M22, DOZA006M22, 21090443, 20100411, 21070474, 21070306 and 22040244 grouped into subgenotype VI.2.1.1.2.2 (VIk), whereas OP04-2020/PRL01-2020, 20200121\_087\_6102/613923B, 22090303, 20110039, S2021/06\_0251, S2021/06\_0218, 22060471, 22070111, 22080021, 22060412, 22080566 and N1775 grouped into subgenotype VI.2.1.1.2.1 (VIj).

Phylogenetic analysis (Figure 2.8) was reiterated with the 360 nt region spanning over a partial region of the F gene of the PPMV genome, this time including the closest relative PPMV sequences retrieved from the GenBank database. Out of the 28 PPMV samples sequenced, data from 21 samples were included in this examination due to the availability of overlapping regions for sequences in this study and those available on GenBank. Genotypes in brackets of sequences included in this analysis were limited to those provided on GenBank database or in published articles.

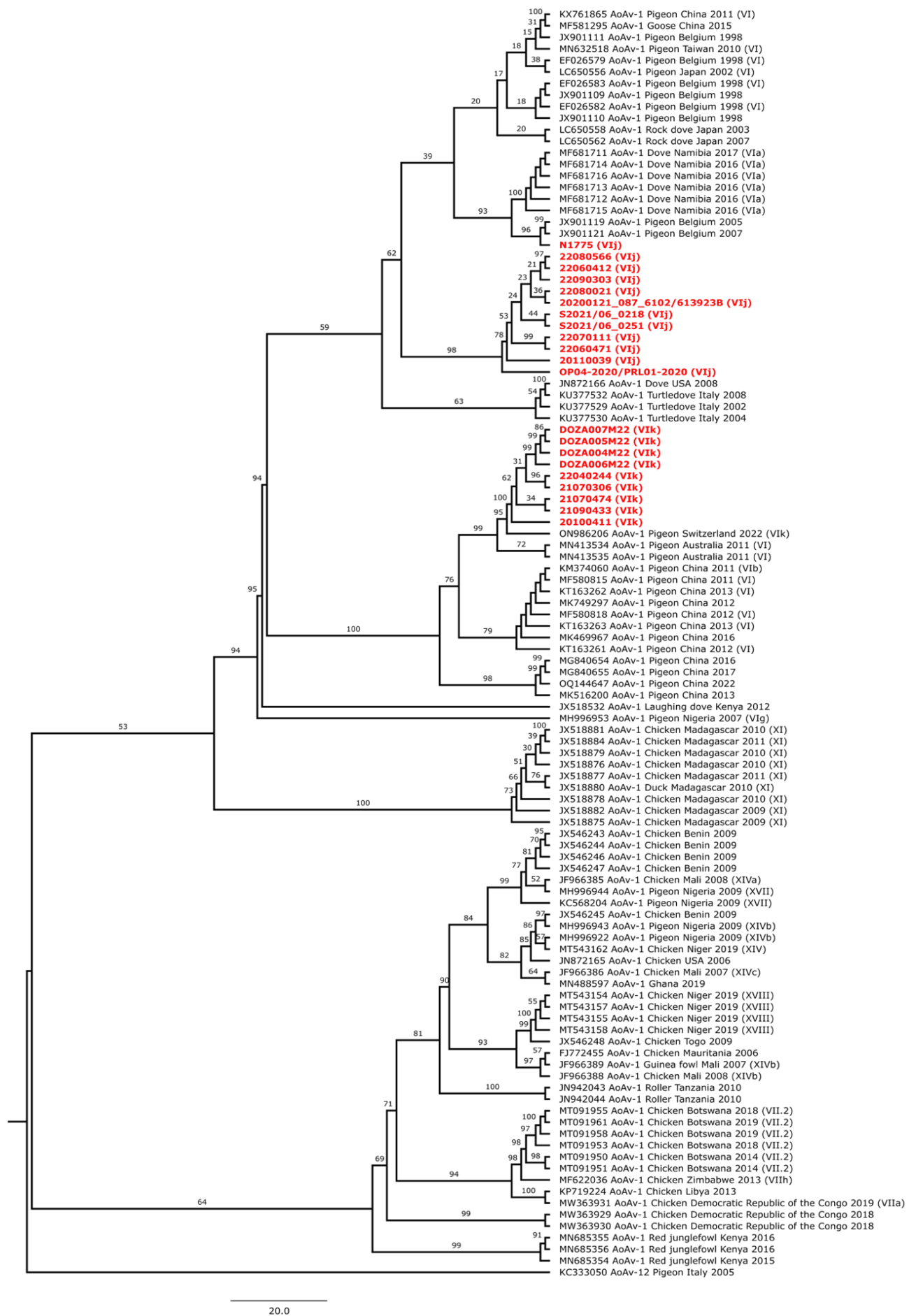


**Figure 2.8:** Maximum likelihood phylogenetic tree based on a partial fragment of the fusion gene (360 nt) of South African PPMVs sequenced in this study and the closest relatives in Genbank. Sequences generated in this study are highlighted in red font. Genotypes/subgenotypes of sequences are provided in brackets. The trees are rooted and drawn to scale, with branch lengths measured in the number of substitutions per site. Sequence KC333050 (Avian orthoavulavirus 12) was used as an outgroup.

The phylogenetic analysis (Figure 2.8) revealed that samples DOZA005M22, DOZA007M22, DOZA004M22, DOZA006M22, 21070474, 22040244, 21070306, 21090443 and 20100411 clustered together with a PPMV strain sampled from a pigeon in Switzerland during 2022 with a bootstrap value of 95% and sub-genotype VIk. The PPMV strain found in a pigeon in Switzerland was part of an epidemic that impacted laying hens and feral pigeons on a farm (Annaheim *et al.*, 2022). Samples 22070111, 22060471, 22080566, 22060412, S2021/06\_0218, S2021/06\_0251, 22090303, 22080021, 20110039, 20200121\_087\_6102/613923B and OP04-2020/PRL01-2020 formed a separate clade on its own. The remaining sample, N1775 clustered together with an PPMV sampled from pigeons in Belgium during 2005 and 2007 with a bootstrap value of 96%. These viruses sampled from pigeons were according to routine virus isolation procedures of the Belgian reference laboratory for avian influenza and Newcastle disease.

Phylogenetic analysis (Figure 2.9) was then conducted using the closest relative PPMV sequences derived from the GenBank database based on the full F gene for 11 PPMV samples from this study. In the context of this analysis, we encountered instances where only a small partial region of certain epidemiologically significant viruses was available for most samples. Recognizing the importance of obtaining a more comprehensive phylogenetic understanding, we expanded our approach by including the larger region of the F gene encompassing other available viruses, however fewer sequences of this study was utilized due to availability of the full F gene. This strategic inclusion aimed to enhance the resolution of our phylogenetic analysis, ensuring a more robust interpretation of the relationships among these viruses. The genotypes/sub-genotypes in brackets of the sequences included in this study were restricted to those found in the Genbank database or in published studies.

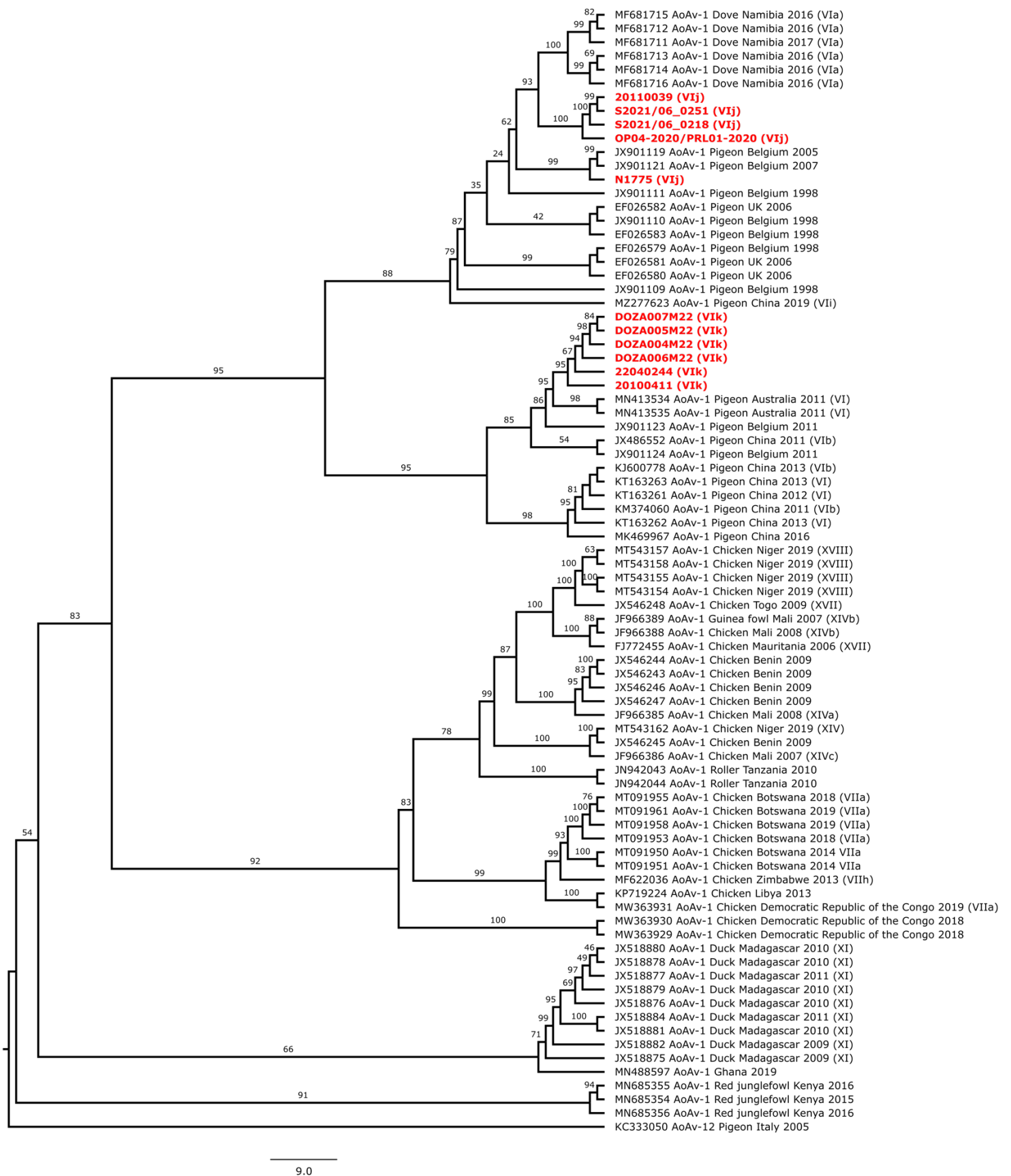


**Figure 2.9:** Maximum likelihood phylogenetic tree based on a full fragment of the fusion gene (1700 nt) of South African PPMVs sequenced in this study and the closest relatives in Genbank. Sequences generated in this study are highlighted in red font. Genotypes/sub-genotypes of sequences available are provided in brackets. The trees are rooted and drawn to scale, with branch lengths measured in the number of substitutions per site. Sequence KC333050 (Avian orthoavulavirus 12) was used as an outgroup.

Phylogenetic analysis (Figure 2.9) revealed that samples DOZA005M22, DOZA007M22, DOZA004M22, DOZA006M22, 22040244 and 20100411 clustered together with PPMV strains sampled from pigeons in Australia during 2011 with a bootstrap value of 95% and genotype VI. No outbreak information were available in a published article for the viruses sampled from pigeons in Australia. Samples S2021/06\_0218, S2021/06\_0251, 20110039 and OP04-2020/PRL01-2020 formed a separate clade on its own, however, formed within a larger clade containing PPMV strains collected from doves in Namibia in 2016 with a bootstrap value of 93%. Twelve separate outbreaks of NDV were reported in the north of the country along the Angolan border between July and November 2016 from which samples were collected as part of the control and prevention program implemented by the Namibian government (Molini *et al.*, 2017; Molini *et al.*, 2018). The feral birds were found dead or dying in the gardens of private houses (Molini *et al.*, 2018). The remaining sample, N1775 clustered together with an PPMV sampled from pigeons in Belgium during 2005 and 2007 with a bootstrap value of 99%.

Next, the previous South African PPMV sequences from 2002 to 2006 (Abolnik *et al.*, 2008), a 374 nt region that spans the 3' end of the M and the 5' end of the F gene, with intergenic region, that was commonly used for phylogenetic analysis in the past, were retrieved and phylogenetically compared to the 14 samples from 2012 to 2022 along with previously published Namibia PPMV sequences and closest relatives retrieved from GenBank. The results are shown in Figure 2.10.

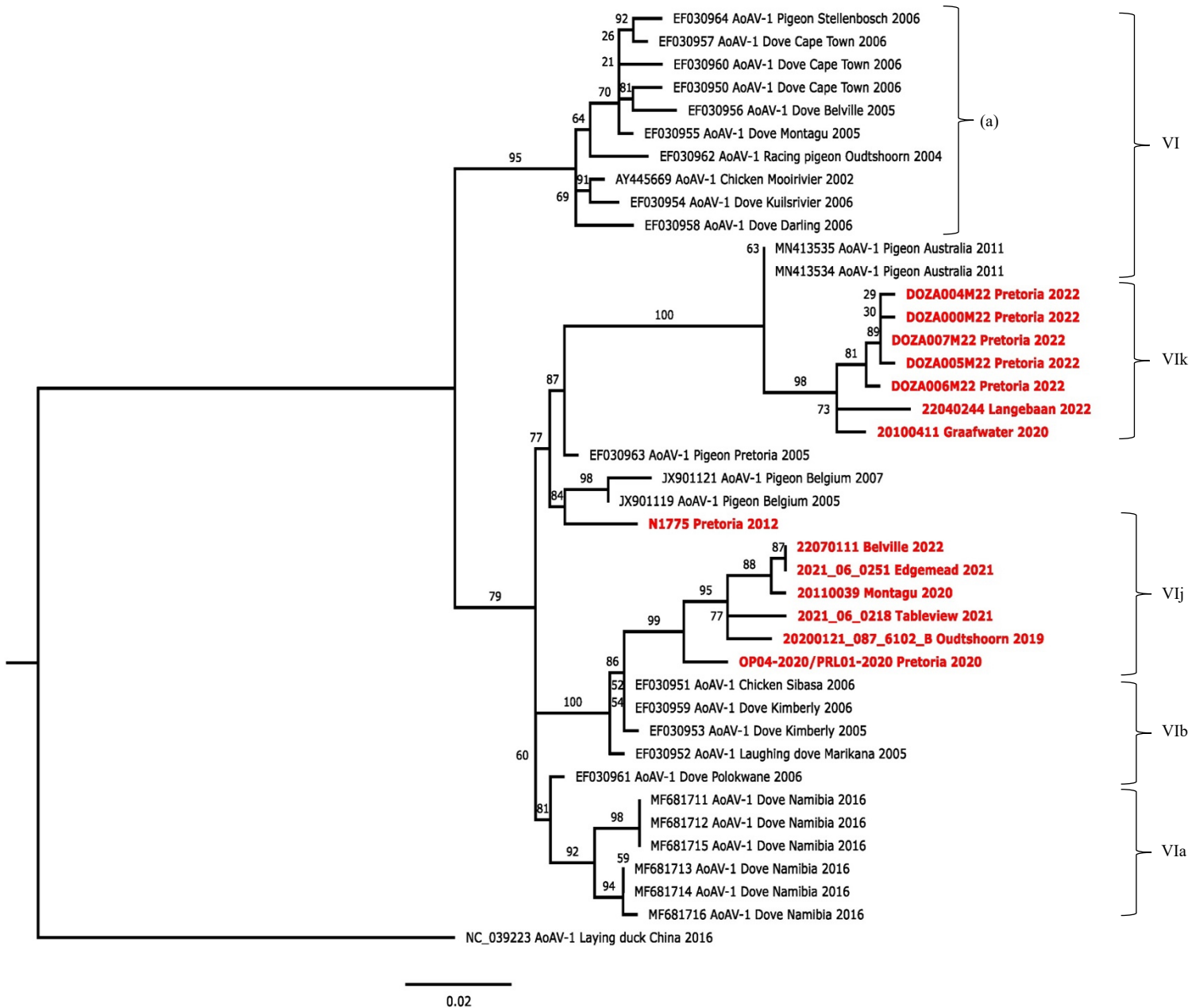


**Figure 2.10:** Maximum likelihood phylogenetic trees based on a partial fragment of the matrix and fusion gene (374 nt) of 14 South African PPMV samples sequenced in this study, previously South African- and Namibia-published PPMV samples and closest relatives in GenBank. Samples generated in this study are highlighted in red font. The trees are mid-rooted, nodes placed in increasing order, drawn to scale and branch lengths are measured in terms of the number of substitutions per site. Genotypes/ sub-genotypes are indicated. Sequence NC\_039223 was used as an outgroup.

Figure 2.10 shows that samples 22070111, 2021\_06\_0251, 20110039, 2021\_06\_0218, 20200121\_087\_6102\_613923B and OP04-2020\_PRL01-2020 clustered together in a monophyletic branch with samples collected from doves and chickens in Kimberly and Sibasa during 2005 and 2006 with a bootstrap value of 86%. The monophyletic branch containing samples DOZA004M22, DOZA000M22, DOZA007M22, DOZA005M22, DOZA006M22, 22040244 and 20100411 clustered together with PPMV sampled from pigeons in Australia during 2011 with a bootstrap value of 100%. Sample N1775 clustered together with PPMV samples collected from pigeons in Belgium during 2005 and 2007 with a bootstrap value of 84%. Samples 22040244, 20100411, 2021\_06\_0218 and 20200121\_087\_6102\_B formed polytomies within this tree, indicating not enough information for bifurcation. Close relatives from Australia, Belgium, and Namibia included with diverse South African strains, do not form separate outgroups. Instead, they are nested within the tree, indicating a more recent epidemiological connection between these countries and the respective outbreaks. Genotypes/sub-genotypes are indicated, however, the clade labelled (a) initially designated as VI was previously annotated as 4bii. However, after a reclassification update in 2019, the subgroup 4bii underwent further subdivision into several distinct sub-genotypes. Consequently, it could not be annotated using the revised classification due to the absence of provided designations for these newly identified sub-genotypes.



## 2.5. Discussion and Conclusion

PPMV viruses were collected from feral doves and pigeons that were found dead in Gauteng and Western Cape between 2012 and 2022. This study found that kidneys were the best source of virus in PPMV-infected pigeons and doves, suggesting kidneys to be the best-suited sample type for routine testing when samples are brought in. A similar study conducted in North-eastern Brazil examined various tissue samples, including kidney, brain, liver, proventriculus, lungs, heart, spleen, gizzard, intestine, air sac, trachea, and spinal cord, collected from five free-living pigeons (Pereira *et al.*, 2022). The lowest average Ct value of 34.62 was obtained from brain samples, while the highest average Ct value was 37.06 obtained from a lung sample (Pereira *et al.*, 2022). The kidney ranked second with an average Ct value of 35 (Pereira *et al.*, 2022).

Eight viruses collected in Gauteng (2022) were successfully isolated in QH9/2-1 quail cells, yielding optimal viral RNA with which to generate partial to almost complete genome sequences. The isolation of these viruses in the QH9/2-1 quail cells was visually confirmed with Transmission Electron Microscopy (TEM) indicating distinct features of paramyxovirus. The use of quail cell lines as an alternative to Embryonated Chicken Eggs (ECEs) for isolating PPMVs is valuable due to several benefits. Quail cell lines have been suggested to be effective for isolating and propagating various avian viruses and once established, can be readily available and reproducible, unlike ECEs, which require a constant supply of fertile eggs. Using quail cell lines aligns with ethical considerations in animal research where it eliminates the need for the use of embryonated chicken eggs, which addresses concerns related to animal welfare. While quail cell lines show promise as a suitable alternative to ECEs for PPMV isolation, it's essential to consider that their effectiveness depending on specific strains isolated is still unknown.

In the context of the F gene of PPMV, the terms monobasic and multibasic refer to the composition of the cleavage site, the number of basic amino acids (positively charged amino acids) in the cleavage site influences the protease specificity and, consequently, the virulence of the virus. Lentogenic strains are usually associated with monobasic cleavage sites whereas mesogenic and velogenic strains are associated with multibasic cleavage sites (Panda *et al.*, 2004). The amino acid motif <sup>112</sup>RRQKRF<sup>117</sup> was consistently identified across all 13 isolates, a characteristic associated with virulent NDV, however, it is of importance for the final confirmation of pathogenicity to test *in vivo* (Choi *et al.*, 2010; Molini *et al.*, 2018). The

presence of a multibasic cleavage site is often associated with enhanced pathogenicity because the multibasic cleavage site can be recognized and cleaved by a broader range of host proteases, allowing the virus to replicate in a wider range of tissues and causing more severe disease (Panda *et al.*, 2004). Understanding the cleavage site composition is crucial for assessing the virulence potential of paramyxoviruses and implementing effective control measures.

Genotype classification was conducted using a comprehensive dataset created by Dimitrov *et al.*, 2019. This comprehensive dataset consists of genetic and phenotypic information from NDV strains collected worldwide. The dataset allows for the identification and classification of NDV strains into distinct genotypes, sub-genotypes and lineages, providing valuable insights into the genetic diversity and evolution of NDV (Dimitrov *et al.*, 2019). Genotype classification analysis revealed that the 21 samples grouped into genotype VI of which twelve samples were grouped into sub-genotype VI.2.1.1.2.1 (VIj) and the remaining nine samples were grouped into sub-genotype VI.2.1.1.2.2 (VIk). Subgenotype VIj, as designated by Xue *et al.* (2017), was previously designated as VIi by De Almeida *et al.* (2013), which was associated with North American strains, however, it varied from the subgenotype VIi reported by Snoeck *et al.* (2013). Bayesian analysis conducted by Xie and colleagues (2020), revealed that subgenotype VIk (VI.2.1.1.2.2) viruses might have originated in Europe. Subgenotypes VIj and VIk, reassigned as VI.2.1.1.2.1 and VI.2.1.1.2.2 have been reported from pigeons, doves, ducks, rosellas and occasionally chicken in Pakistan, Belgium, USA, China, Luxembourg and Italy from 1998 to 2015 (Xue *et al.*, 2017; Dimitrov *et al.*, 2019).

The phylogenetic analysis of the blast results based on a partial fragment of the fusion gene indicated that the 21 samples clustered within three distinct clades. These samples were closely related to PPMV strains sampled from pigeons in Switzerland and Belgium in 2005, 2007 and 2022. Phylogenetic analysis of the blast results based on the full fusion gene indicated that 11 samples clustered within three distinct clades. These samples were closely related to PPMV strains sampled from pigeons in Australia and Belgium in 2005, 2007 and 2011. South Africa PPMVs and other African PPMV strains included in the blast results analysis indicated no relatedness suggesting no intra-continental spread. The phylogenetic comparison to the viruses that circulated in South Africa in past decades with other African and closely related PPMV strains, revealed that the samples collected in Western Cape and Gauteng from 2019 to 2022 were closely related to Avian orthoavulavirus strains sampled from doves and chickens in Kimberly and Sibasa in 2005 and 2006. Other samples collected in Western Cape and Gauteng

in 2020 and 2022 were closely related to an Avian orthoavulavirus strain sampled from pigeons in Australia in 2011 and clustered together within a bigger clade with an Avian orthoavulavirus strain collected from a pigeon in Pretoria in 2005. A sample collected in Gauteng in 2012 was closely related to Avian orthoavulavirus strains sampled from pigeons in Belgium in 2005 and 2007. It's noteworthy that close relatives from Australia, Belgium, and Namibia included with the diverse South African strains, do not emerge as distinct outgroups. Rather, they are integrated within the tree's structure, which implies a more recent epidemiological linkage between these countries and the specific outbreak events.

Previously annotated sub-genotypes VIb (4bi) grouped with a bigger clade with this study's samples identified as VIj and VIk. However, the clade labelled as (a) presented in Figure 2.10 previously annotated as 4bii clustered on its own suggesting that it has since disappeared. Several factors may contribute to the disappearance of some sub-genotypes. Sub-genotypes which are less adapted to their current ecological niche or host populations may face selective pressure and reduced fitness and become less prevalent or even disappear over time (Holmes, 2009). Changes in host populations, host immune responses or environmental conditions may also affect the fitness of sub-genotypes (Woolhouse and Gowtage-Sequeria, 2005).

The various results revealed the presence of multiple sub-genotypes of PPMV-1, suggesting ongoing viral evolution and the potential introduction of new strains through international trade and the movement of infected birds. Additionally, the phylogenetic analysis provided evidence of local and regional clustering of PPMV-1 strains within clades, indicating possible geographic factors influencing virus transmission. These findings contribute to the broader field of molecular epidemiology and enhance our understanding of the genetic diversity and dynamics of PPMV-1 in South Africa. One of the primary limitations of this study is the relatively small sample size from different provinces, collecting data from a restricted number of cases in different provinces may not fully represent the diversity of strains circulating in South Africa.

The insights gained from this study can inform disease surveillance and control strategies, facilitating the development of targeted interventions to mitigate the spread and impact of PPMV-1 among pigeon populations and safeguarding both pigeon and wild bird biodiversity. Given that the virus's evolving nature enables novel strains to exist, pigeon paramyxovirus presents a significant threat to the Southern African racing industry and the biodiversity of wild bird populations; therefore, continued surveillance is important.

## CHAPTER 3

### Investigation of the viral metagenome of pigeons infected with Pigeon paramyxovirus 1

#### 3.1. Introduction

Without the need for pure cultures, metagenomics is a molecular technique that analyses DNA from clinical samples to study the diversity of microorganisms present (Ghosh *et al.*, 2019). The advancement of high-throughput sequencing technology has resulted in studies of microbial and viral communities, also known as microbiomes and viromes, respectively spanning several host species (Francois and Pybus, 2020). Metagenomic analysis delves into the complete genetic composition of microbial populations, shedding light on the biochemical constitution of microorganisms residing in unconventional environments and their intricate interactions with other environmental factors (Dash and Das, 2018). The term metagenomics, also known as environmental or community genomics, was first introduced 1998 by the Jo Handelsman Group (Fadiji and Babalola, 2020). This term referred to the evaluation of all genetic materials isolated directly from environmental samples (Fadiji and Babalola, 2020). Initially, laboratory studies necessitated the isolation of viruses from clinical or environmental samples through propagation and isolation on cell cultures (Roux *et al.*, 2021). Nonetheless, this approach demonstrated biases and posed challenges when employed on a larger scale. Many viruses depend on specific host cells that are intricate to maintain as clonal cultures within the laboratory setting. Furthermore, even if these cells are accessible, viruses might demand propagation conditions distinct from those typically utilized in laboratory settings (Roux *et al.*, 2021). Metagenomics for virus detection and characterization offers a powerful approach for the discovery, survey, and analysis of novel viruses. It does so by bypassing the need for cultivation and instead relies on the direct sequencing of viral genomic material extracted from a given sample. (Vibin *et al.*, 2018; Roux *et al.*, 2021). This technique is relatively novel, leveraging the sensitivity of next-generation sequencing (NGS) while maintaining a broad, non-specific approach to detect any virus that may be present in a given sample (Vibin *et al.*, 2018). Recent advancements in bioinformatics have empowered us to reconstruct individual virus genome sequences from metagenomes, offering the ability to identify and conduct further studies on naturally occurring viruses.

Most metagenomic workflows consist of five basic steps which include: (i) pre-processing, (ii) filtering, (iii) assembly, (iv) searching and (v) post-processing (Nooij *et al.*, 2018). *De novo* assembly is frequently considered the method of choice in viral metagenomics approaches (Nooij *et al.*, 2018).

Poultry biomass accounts for 70% of total bird biomass globally; because of the potential relevance of bird populations to the poultry industry in terms of disease transmission, virome studies on bird populations are common among the various host species (Francois and Pybus, 2020). Because many significant infections of domesticated birds originate in wild bird populations, wild bird viromes are likewise crucial to poultry (Francois and Pybus, 2020). A significant hindrance in the study of viral communities within hosts is the prevalence of unnamed viral species. This has limited our ability to delve into viral ecology across multi-host systems, confining our understanding to the dynamics of individual viruses, especially within vertebrate systems (Wille *et al.*, 2019).

The racing pigeon industry, a multimillion-rand sport, faces concerns due to pigeons being identified as reservoirs for various pathogens, potentially posing risks to other species (Lukaszuk and Stenzel, 2020). Racing pigeon performance hinges on factors grouped into three main categories: health, training, and breeding (Kastelic *et al.*, 2021). Stressors or adverse conditions significantly hamper a pigeon's race performance, ultimately affecting the economic aspects of the sport (Kastelic *et al.*, 2021). Extensive insights into the health of domestic pigeons in their roles as racing pigeons have been gained through documented performance effects linked to infections (Marlier and Vindevogel, 2006). Over time, various viruses isolated from pigeons have demonstrated diverse impacts on their digestive and respiratory tracts, immune system, and nervous system. Regrettably, pigeon diseases often perplex veterinarians, leading to misdiagnoses and flawed preventive strategies (Marlier and Vindevogel, 2006). Furthermore, despite the classification of pigeons as poultry in some countries, our knowledge regarding the epidemiology and progression of diseases that impact the *Columbidae* family remains quite limited (Lukaszuk and Stenzal, 2020).

Expanding our understanding of pigeon diseases becomes especially critical when contemplating the potential economic ramifications within the racing pigeon industry (Lukaszuk and Stenzel, 2020). Pigeons, whether in the wild or domestic settings, can serve as viral hosts, creating opportunities for evolution and recombination, potentially resulting in the

emergence of novel viral variants with diverse levels of pathogenicity (Lukaszuk and Stenzel, 2020). It is vital to monitor pigeon pathogens, as they are often poorly described and exhibit subtle or absent clinical signs during infection (Lukaszuk and Stenzel, 2020). This lack of clear symptoms hinders effective prevention and treatment efforts (Lukaszuk and Stenzel, 2020). Pigeons, due to their frequent interactions with various species, could potentially pose a risk to other species (Lukaszuk and Stenzel, 2020). However, understanding the causes, modes of transmission and treatments of disease in valuable birds like show and racing pigeons is also important. Aside from PPMV-1, the most common virus isolated in pigeons, several other viruses have been detected in pigeons, for which pigeons are either natural hosts for or susceptible to the virus where cross infection occurs (Lukaszuk and Stenzel, 2020).

Viruses from the families *Astroviridae*, *Adenoviridae*, *Anelloviridae*, *Circoviridae*, *Coronaviridae*, *Herpesviridae*, *Paramyxoviruses*, *Parvoviridae*, *Picornaviridae*, and *Reoviridae* have all been linked to and shown to infect pigeons and were briefly discussed in Chapter 1 (Lukaszuk and Stenzel, 2020; Khalifeh *et al.*, 2021).

In this chapter, the Ion Torrent reads obtained in Chapter 2 were analysed for the presence of other viruses using *de novo* assembly and BLAST analysis, followed by phylogenetic analysis where sufficient data was recovered.

### **3.2. Aims and objectives of this study**

The aim of this chapter was to analyse the Ion Torrent reads obtained in Chapter 2 from samples in the University's repository, samples received from the Western Cape Provincial Veterinary Laboratory, as well as new field samples collected in 2022.

The objectives were:

- To analyse the data for the presence of other viruses using *de novo* assembly and BLAST analysis
- To perform phylogenetic analysis where sufficient data was recovered.

### 3.3. Materials and Methods

#### 3.3.1. Samples

For the viral analysis in this investigation, 21 samples (Table 3.1) were employed, including virus isolates and clinical samples. These samples were sequenced in Chapter 2, and their data were combined with previously sequenced information from UP. A sample (S460-23) submitted from the national veterinary laboratory, testing positive for the presence of pigeon torque teno virus and pigeon circovirus, was included in the analysis and forms part of the 21 samples.

**Table 3.1:** Samples used in the study for virome analysis.

| Sample <sup>2</sup>            | Host          | Sample type                                   | Sampling date | Location <sup>1</sup>        |
|--------------------------------|---------------|---|---------------|------------------------------|
| N1775*                         | Laughing dove | Organ pool                                    | 11 Jul 2012   | OP Campus, Pretoria, GP      |
| 20200121_087_6102A*            | Laughing dove | Organ pool                                    | 23 Dec 2019   | Oudtshoorn, WC               |
| 20200121_087_6102/61392<br>3B* | Laughing dove | Organ pool                                    | 23 Dec 2019   | Oudtshoorn, WC               |
| OP04-2020/PRL01-2020*          | Laughing dove | Egg-cultured isolate                          | 21 Apr 2020   | OP Campus, Pretoria, GP      |
| 20100411*                      | Pigeon        | Egg-cultured isolate                          | 27 Oct 2020   | Graafwater, Vredendal, WC    |
| 20110039*                      | Laughing dove | Egg-cultured isolate                          | 04 Nov 2020   | Montagu, Worcester, WC       |
| S2021/06_0218*                 | Laughing dove | Egg-cultured isolate                          | 10 Jun 2021   | Tableview, Cape Town, WC     |
| S2021/06_0251*                 | Laughing dove | Egg-cultured isolate                          | 11 Jun 2021   | Edgemead, Cape Town, WC      |
| 21070306*                      | Laughing dove | Organ pool                                    | 15 Jul 2021   | Porterville, WC              |
| 21070474*                      | Laughing dove | Organ pool                                    | 22 Jul 2021   | Swellendam, WC               |
| 21070476*                      | Laughing dove | Organ pool                                    | 23 Jul 2021   | Misverstand, Morreesberg, WC |
| 21090443*                      | Laughing dove | Organ pool                                    | 23 Sep 2021   | Riversdal, WC                |
| DOZA000M22 <sup>#</sup>        | Laughing Dove | Lung/ QH9-2/1 cell cultures                   | 12 May 2022   | OP Campus, Pretoria. GP      |
| DOZA001M22 <sup>#</sup>        | Laughing Dove | Stomach/ QH9-2/1 cell cultures                | 18 May 2022   | OP Campus, Pretoria, GP      |
| DOZA002M22 <sup>#</sup>        | Laughing Dove | Heart/ QH9-2/1 cell cultures                  | 24 May 2022   | OP Campus, Pretoria, GP      |
| DOZA003M22 <sup>#</sup>        | Laughing Dove | Gastrointestinal tract/ QH9-2/1 cell cultures | 30 May 2022   | OP Campus, Pretoria. GP      |
| DOZA004M22 <sup>#</sup>        | Laughing Dove | Kidney/ QH9-2/1 cell cultures                 | 30 May 2022   | OP Campus, Pretoria, GP      |
| DOZA005M22 <sup>#</sup>        | Laughing Dove | Kidney/ QH9-2/1 cell cultures                 | 01 Jun 2022   | OP Campus, Pretoria, GP      |
| DOZA006M22 <sup>#</sup>        | Laughing Dove | QH9-2/1 cell cultures                         | 01 Jun 2022   | OP Campus, Pretoria. GP      |
| DOZA007M22 <sup>#</sup>        | Laughing Dove | QH9-2/1 cell cultures                         | 04 Jun 2022   | OP Campus, Pretoria, GP      |
| S460-23 <sup>@</sup>           | Racing Pigeon | Organ pool                                    | 17 Feb 2023   | Not specified, FS            |

<sup>1</sup> GP - Gauteng, FS – Free State, OP - Onderstepoort, WC - Western Cape.

<sup>2</sup> Source of collection - \* UP repository, # Collected at UP, @ Submitted by national veterinary laboratory.

### 3.3.2. Viral metagenomics analysis

For the metagenomic analysis in this study (Figure 3.1), the next-generation sequencing data was imported into the CLC Workbench (v11.0.1), where *de novo* assemblies were performed with minimum contig length optimisation of (i) 1000, (ii) 700, (iii) 500 and (iv) 200 bp and *de novo* assembly default parameters with mismatch cost 2, insertion cost 3, deletion cost 3, length fraction 0.5 and similarity fraction 0.8 were used. Among the different minimum contig length optimisations (i.e., i-iv) the 500 bp threshold proved to be the most efficient to reduce redundant and non-specific detection of reads.

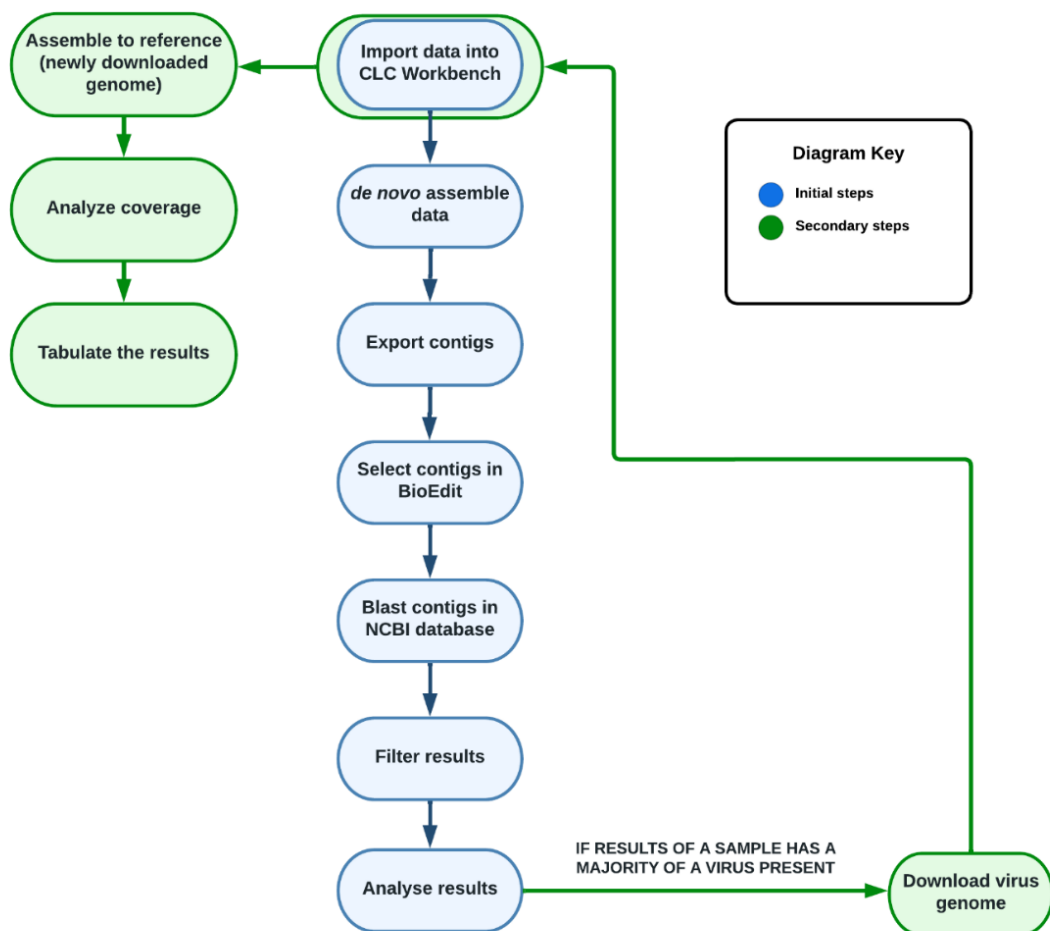


**Figure 3.1:** Summary of the steps used for the virome analysis of sequencing results for pigeon and dove samples.



The contig list for each sample was exported in fasta format into BioEdit (v.7.0.5.3)(Hall, 1999) and blasted in the NCBI database (<https://blast.ncbi.nlm.nih.gov/Blast.cgi>), set to search for viruses only with a query coverage of >70% and bacteriophages were excluded. The results were tabulated (Appendix C).

If a virus was abundantly (>40%) detected in the results, a reference genome of the respective virus was downloaded from GenBank in June 2022 (Table 3.2) and the sequence reads were reassembled against the more accurate reference genome to refine the results. The results were analyzed and tabulated (Table 3.2) with the length column showing the length for the specific virus reference sequence downloaded from GenBank. A consensus sequence was extracted from the mapped reads with parameters of match score 1, mismatch cost 2, linear gap cost, insertion cost 3, deletion cost 3, length fraction 0.5, similarity fraction 0.8 for each sample and the corresponding reference sequence of each virus, from which a sequence statistics report was performed in CLC Genomics Workbench (v11.0.1) to determine the coverage of the sequence (complete or partial).

### **3.3.3. Phylogenetic analysis**

To establish the phylogenetic relatedness of the above-mentioned mapped *de novo* assemblies (Table 3.1) a relatedness study with phylogenetic trees was performed with mapped *de novo* assemblies with sufficient coverage of at least 95% of the reference viral genome. A stringent cut-off threshold of 95% was established to prioritise nearly complete mapped reads. The map reads to reference approach was performed in CLC Genomics Workbench software v11.0.1 with corresponding reference sequences downloaded from GenBank in June 2022 (<https://www.ncbi.nlm.nih.gov/genbank/>). Multiple sequence alignments of the specified viral sequences with reference sequences retrieved by BLAST analysis (<https://blast.ncbi.nlm.nih.gov>) were constructed in BioEdit and MAFFT open-source software applications (<https://mafft.cbrc.jp/alignment/server/>). The Maximum likelihood method was used to reconstruct phylogenetic trees in IQ tree database with 1000 bootstrap replicates (<http://iqtree.cibiv.univie.ac.at/>). The substitution model in IQ tree database was selected as auto, with maximum iterations of 1000, minimum correlation coefficient 0.99, perturbation strength 0.5 and the IQ-TREE stopping rule 100. The SH-aLRT branch test was also selected with 1000 replicates. The phylogenetic trees generated were visualised in FigTree (v1.4.4) and edited in Inkscape (v1.2.2). Corresponding outgroups were used for each phylogenetic tree constructed.

### 3.4. Results

#### 3.4.1. Viral metagenomic analysis

A virome analysis was performed on 21 feral pigeons and dove samples submitted to the University of Pretoria's Poultry section from 2012 to 2023. The sequence analysis for all the corresponding map reads to reference sequence, is indicated in Table 3.2 and summarized in Table 3.3 with the quantity of genome recovered in percentages. Blast results are tabulated in Annexure C and are indicative of the closest related viruses. Full gene sequences were submitted for pigeon torque teno virus (PTTV) and pigeon circovirus (PiCV) to the GenBank nucleotide sequence database under the accession numbers OR681892 (PTTV), OR681893 (PiCV), OR681894 (PPTV) and OR681895 (PICV).

The viruses identified by the NCBI blast search in Table 3.3 among the 21 samples comprised of viruses from the families *Retroviridae*, *Paramyxoviridae*, *Orthomyxoviridae*, *Anelloviridae*, *Nimaviridae*, *Herpesviridae*, *Togaviridae*, *Baculoviridae*, *Coronaviridae*, *Circoviridae*, *Flaviviridae* and *Reoviridae*.

The duplication of blast hits (Table 3.2) for viruses associated with pigeons and other columbid species, may occur because the two terms could be used interchangeably in scientific literature or databases. For example, the term "columbid" is derived from the scientific family name "*Columbidae*," which includes pigeons and doves. Therefore, "columbid circovirus" is a broader term that encompasses circoviruses affecting all members of the *Columbidae* family, including both pigeons and doves. Researchers or authors may not always distinguish between the specific species within the *Columbidae* family when discussing circoviruses. As a result, the same virus might be referred to by both names, leading to duplicate hits in search results. The inclusion of both TTV and PTTV in the BLAST hit results is likely due to genetic closeness and relatedness between these two viruses, which are members of the *Anelloviridae* family and share significant genomic and structural traits. The same applies for the inclusion of Avian orthoavulavirus 1 and Pigeon paramyxovirus, even though they refer to the same virus, the dual naming is connected to the virus's historical categorization. The virus was initially identified and named for the epidemic area where it was originally isolated. However, when the virus was studied further, it was determined to impact a wide range of bird species, not only poultry, and its genetic diversity became clear. This resulted in the virus being reclassified into several lineages and genotypes.

**Table 3.2:** Viruses identified in the deep sequencing of samples from pigeons and doves.

| Reference genome (Family)                           | Accession number <sup>2</sup> | Reference genome length (bp) <sup>1</sup> | Total Ion Torrent/Illumina reads (average read length) <sup>1</sup> | Reads mapped (average read length) <sup>1</sup> |
|---|-------------------------------|---|---|---|
| <b>N1775</b>  |                               |   |   |   |
| Avian leukosis virus ( <i>Retroviridae</i> )        | KU375453.1                    | 7,746                                     | 195,217 (71)  | 1,592 (72)                                      |
| Avian myeloblastosis virus ( <i>Retroviridae</i> )  | L10922.1                      | 7,708                                     |   | 1,557 (72)                                      |
| Avian orthoavula virus 1 ( <i>Paramyxoviridae</i> ) | OP169005.1                    | 15,186                                    |   | 58,156 (76)                                     |
| Avian sarcoma virus ( <i>Retroviridae</i> )         | NC_008094.1                   | 5,188                                     |   | 771 (73)  |
| Pigeon paramyxovirus 1 ( <i>Paramyxoviridae</i> )   | ON637881.1                    | 15,290                                    |   | 109,917 (70)                                    |
| Rous sarcoma virus ( <i>Retroviridae</i> )          | NC_001407.1                   | 9,392                                     |   | 1,571 (72)                                      |
| Tasmanian devil retrovirus ( <i>Retroviridae</i> )  | KC894732.1                    | 3,189                                     |   | 1,286 (73)                                      |
| <b>20200121_087_6102A</b>                           |                               |   |   |   |
| White spot syndrome virus ( <i>Nimaviridae</i> )    | MG264599.1                    | 314,232                                   | 2,082,282 (168)   | 2,184 (104)                                     |
| Torque teno virus ( <i>Anelloviridae</i> )          | NC_015783.1                   | 3,725                                     |   | 16 (103)  |
| Pigeon torque teno virus ( <i>Anelloviridae</i> )   | MF576433.1                    | 1,574                                     |   | 219 (173)                                       |
| <b>20200121_087_6102/613923B</b>                    |                               |   |   |   |
| Avian orthoavula virus 1 ( <i>Paramyxoviridae</i> ) | OP169005.1                    | 15,186                                    | 3,941,919 (164)   | 215 (143)                                       |
| Pigeon paramyxovirus 1 ( <i>Paramyxoviridae</i> )   | ON637881.1                    | 15,290                                    |   | 238 (149)                                       |
| White spot syndrome virus ( <i>Nimaviridae</i> )    | MG264599.1                    | 314,232                                   |   | 4,703 (102)                                     |
| <b>20100411</b>                                     |                               |   |   |   |
| Avian orthoavula virus 1 ( <i>Paramyxoviridae</i> ) | OP169005.1                    | 15,186                                    | 6,581,748 (173)   | 1,260,914 (184)                                 |
| Avian sarcoma virus ( <i>Retroviridae</i> )         | NC_008094.1                   | 5,188                                     |   | 131 (164)                                       |
| Rous sarcoma virus ( <i>Retroviridae</i> )          | NC_001407.1                   | 9,392                                     |   | 247 (164)                                       |
| Avian leukosis virus ( <i>Retroviridae</i> )        | KU375453.1                    | 7,746                                     |   | 186 (167)                                       |
| Avian endogenous retrovirus ( <i>Retroviridae</i> ) | NC_005947.1                   | 4,302                                     |   | 1,136 (177)                                     |
| Pigeon paramyxovirus 1 ( <i>Paramyxoviridae</i> )   | ON637881.1                    | 15,290                                    |   | 1,711,496 (181)                                 |
| White spot syndrome virus ( <i>Nimaviridae</i> )    | MG264599.1                    | 314,232                                   |   | 8,096 (105)                                     |
| <b>20110039</b>                                     |                               |   |   |   |
| Avian orthoavula virus 1 ( <i>Paramyxoviridae</i> ) | OP169005.1                    | 15,186                                    | 8,948,420 (146)   | 568,735 (172)                                   |
| Avian endogenous retrovirus ( <i>Retroviridae</i> ) | NC_005947.1                   | 4,302                                     |   | 1,073 (160)                                     |
| White spot syndrome virus ( <i>Nimaviridae</i> )    | MG264599.1                    | 314,232                                   |   | 27,381 (91)                                     |
| Semliki forest virus ( <i>Togoviridae</i> )         | NC_003215.1                   | 11,442                                    |   | 176 (92)  |
| Pigeon paramyxovirus 1 ( <i>Paramyxoviridae</i> )   | ON637881.1                    | 15,290                                    |   | 813,549 (169)                                   |

<sup>1</sup> bp: Base pairs; <sup>2</sup> Downloaded from Genbank

**Table 3.2:** Viruses identified in the deep sequencing of samples from pigeons and doves (continued).

| Reference genome (Family)   | Accession numbers <sup>2</sup> | Reference genome length (bp) <sup>1</sup> | Total Ion Torrent reads (average read length) <sup>1</sup> | Reads mapped (average read length) <sup>1</sup> |
|---|--------------------------------|---|--|---|
| <b>OP04-2020/PRL01-2020</b>   |                                |   |  |   |
| Avian orthoavula virus 1 ( <i>Paramyxoviridae</i> )                 | OP169005.1                     | 15,186                                    | 19,863,458 (173)   | 3,856 (179)                                     |
| Human gammaherpesvirus 4 ( <i>Herpesviridae</i> )                   | LC573552.1                     | 183,865                                   |  | 51,177 (108)                                    |
| Pigeon paramyxovirus 1 ( <i>Paramyxoviridae</i> )                   | ON637881.1                     | 15,290                                    |  | 5,310 (179)                                     |
| White spot syndrome virus ( <i>Nimariviridae</i> )                  | MG264599.1                     | 314,232                                   |  | 13,537 (107)                                    |
| <b>S2021/06_0251</b>  |                                |   |  |   |
| Avian orthoavula virus 1 ( <i>Paramyxoviridae</i> )                 | OP169005.1                     | 15,186                                    | 6,447,774 (184)  | 671 (186)                                       |
| Pigeon paramyxovirus 1 ( <i>Paramyxoviridae</i> )                   | ON637881.1                     | 15,290                                    |  | 907 (186)                                       |
| Autographacalifornica nucleopolyhedrovirus ( <i>Baculoviridae</i> ) | KU697903.1                     | 138,991                                   |  | 985 (124)                                       |
| White spot syndrome virus ( <i>Nimariviridae</i> )                  | MG264599.1                     | 314,232                                   |  | 3,349 (119)                                     |
| <b>S2021/06_0218</b>  |                                |   |  |   |
| Avian orthoavula virus 1 ( <i>Paramyxoviridae</i> )                 | OP169005.1                     | 15,186                                    | 7,715,476 (177)  | 91,102 (186)                                    |
| White spot syndrome virus ( <i>Nimariviridae</i> )                  | MG264599.1                     | 314,232                                   |  | 3,573 (108)                                     |
| Avian leukosis virus ( <i>Retroviridae</i> )                        | KU375453.1                     | 7,746                                     |  | 213 (170)                                       |
| Avian endogenous retrovirus ( <i>Retroviridae</i> )                 | NC_005947.1                    | 4,302                                     |  | 723 (180)                                       |
| Pigeon paramyxovirus 1 ( <i>Paramyxoviridae</i> )                   | ON637881.1                     | 15,290                                    |  | 120,583 (184)                                   |
| <b>21070476</b>   |                                |   |  |   |
| Pigeon torque teno virus ( <i>Anelloviridae</i> )                   | MF576433.1                     | 1,574                                     | 5,729,160 (178)  | 340 (181)                                       |
| Torque teno virus ( <i>Anelloviridae</i> )                          | NC_015783.1                    | 3,725                                     |  | 28 (107)  |
| White spot syndrome virus ( <i>Nimariviridae</i> )                  | MG264599.1                     | 314,232                                   |  | 2,524 (112)                                     |
| <b>21070306</b>   |                                |   |  |   |
| Avian orthoavula virus 1 ( <i>Paramyxoviridae</i> )                 | OP169005.1                     | 15,186                                    | 7,751,218 (179)  | 588 (182)                                       |
| Pigeon paramyxovirus 1 ( <i>Paramyxoviridae</i> )                   | ON637881.1                     | 15,290                                    |  | 846 (177)                                       |
| Pigeon circovirus ( <i>Circoviridae</i> )                           | MW181985.1                     | 2,045                                     |  | 51 (177)  |
| Columbid circovirus ( <i>Circoviridae</i> )                         | KF738854.1                     | 2,043                                     |  | 45 (175)  |
| Torque teno virus ( <i>Anelloviridae</i> )                          | NC_015783.1                    | 3,725                                     |  | 43 (108)  |
| Pigeon torque teno virus ( <i>Anelloviridae</i> )                   | MF576433.1                     | 1,574                                     |  | 230 (181)                                       |
| Infectious bronchitis virus ( <i>Coronaviridae</i> )                | GCF_012271575.1                | 27,901                                    |  | 462 (152)                                       |
| White spot syndrome virus ( <i>Nimariviridae</i> )                  | MG264599.1                     | 314,232                                   |  | 3,878 (111)                                     |
| Avian coronavirus ( <i>Coronaviridae</i> )                          | NC_048213                      | 27,845                                    |  | 434 (157)                                       |
| Pigeon coronavirus ( <i>Coronaviridae</i> )                         | LC364344.1                     | 26,155                                    |  | 1,889 (110)                                     |

<sup>1</sup> bp: Base pairs; <sup>2</sup> Downloaded from Genbank

**Table 3.2:** Viruses identified in the deep sequencing of samples from pigeons and doves (continued).

| Reference genome (Family)                           | Accession numbers <sup>2</sup> | Reference genome length (bp) <sup>1</sup> | Total Ion Torrent reads (average read length) <sup>1</sup> | Reads mapped (average read length) <sup>1</sup> |
|---|--------------------------------|---|--|---|
| <b>21070474</b>                                     |                                |   |  |   |
| Avian orthoavula virus 1 ( <i>Paramyxoviridae</i> ) | OP169005.1                     | 15,186                                    | 6,752,23 (180)   | 261 (176)                                       |
| White spot syndrome virus ( <i>Nimariviridae</i> )  | MG264599.1                     | 314,232                                   |  | 3,219 (112)                                     |
| Pigeon paramyxovirus 1 ( <i>Paramyxoviridae</i> )   | ON637881.1                     | 15,290                                    |  | 358 (171)                                       |
| <b>21090443</b>                                     |                                |   |  |   |
| White spot syndrome virus ( <i>Nimariviridae</i> )  | MG264599.1                     | 314,232                                   | 6,415,453 (185)  | 2,827 (113)                                     |
| Torque teno virus ( <i>Anelloviridae</i> )          | NC_015783.1                    | 3,725                                     |  | 51 (111)  |
| Pigeon torque teno virus ( <i>Anelloviridae</i> )   | MF576433.1                     | 1,574                                     |  | 1,726 (189)                                     |
| <b>DOZA001M22</b>                                   |                                |   |  |   |
| Avian orthoavula virus 1 ( <i>Paramyxoviridae</i> ) | OP169005.1                     | 15,186                                    | 3,788,380 (162)  | 28,565 (177)                                    |
| Pigeon paramyxovirus 1 ( <i>Paramyxoviridae</i> )   | ON637881.1                     | 15,290                                    |  | 32,484 (178)                                    |
| White spot syndrome virus ( <i>Nimariviridae</i> )  | MG264599.1                     | 314,232                                   |  | 5,182 (100)                                     |
| Porcine rotavirus ( <i>Reoviridae</i> )             | D55717.1                       | 2,819                                     |  | 47 (118)  |
| Bovine viral diarrhea virus ( <i>Flaviviridae</i> ) | KX987157.1                     | 12,259                                    |  | 56 (99)   |
| <b>DOZA002M22</b>                                   |                                |   |  |   |
| Avian orthoavula virus 1 ( <i>Paramyxoviridae</i> ) | OP169005.1                     | 15,186                                    | 1,763,906 (168)  | 6,208 (177)                                     |
| White spot syndrome virus ( <i>Nimariviridae</i> )  | MG264599.1                     | 314,232                                   |  | 1,976 (103)                                     |
| <b>DOZA003M22</b>                                   |                                |   |  |   |
| Avian orthoavula virus 1 ( <i>Paramyxoviridae</i> ) | OP169005.1                     | 15,186                                    | 4,023,110 (159)  | 11,207 (175)                                    |
| Pigeon paramyxovirus 1 ( <i>Paramyxoviridae</i> )   | ON637881.1                     | 15,290                                    |  | 13,473 (174)                                    |
| Pigeon circovirus ( <i>Circoviridae</i> )           | MW181985.1                     | 2,045                                     |  | 137,379 (172)                                   |
| Columbid circovirus ( <i>Circoviridae</i> )         | KF738854.1                     | 2,043                                     |  | 130,924 (171)                                   |
| White spot syndrome virus ( <i>Nimariviridae</i> )  | MG264599.1                     | 314,232                                   |  | 5,635 (99)                                      |
| <b>DOZA004M22</b>                                   |                                |   |  |   |
| Avian orthoavula virus 1 ( <i>Paramyxoviridae</i> ) | OP169005.1                     | 15,186                                    | 3,543,438 (162)  | 13,894 (178)                                    |
| Pigeon paramyxovirus 1 ( <i>Paramyxoviridae</i> )   | ON637881.1                     | 15,290                                    |  | 22,606 (174)                                    |
| White spot syndrome virus ( <i>Nimariviridae</i> )  | MG264599.1                     | 314,232                                   |  | 4,681 (100)                                     |
| <b>DOZA005M22</b>                                   |                                |   |  |   |
| Avian orthoavula virus 1 ( <i>Paramyxoviridae</i> ) | OP169005.1                     | 15,186                                    | 3,043,301 (162)  | 1,049 (174)                                     |
| White spot syndrome virus ( <i>Nimariviridae</i> )  | MG264599.1                     | 314,232                                   |  | 3,596 (100)                                     |
| Pigeon paramyxovirus 1 ( <i>Paramyxoviridae</i> )   | ON637881.1                     | 15,290                                    |  | 1,863 (168)                                     |

<sup>1</sup> bp: Base pairs; <sup>2</sup> Downloaded from Genbank

**Table 3.2:** Viruses identified in the deep sequencing of samples from pigeons and doves (continued).

| Reference genome (Family)                           | Accession numbers <sup>2</sup> | Reference genome length (bp) <sup>1</sup> | Total Ion Torrent reads (average read length) <sup>1</sup> | Reads mapped (average read length) <sup>1</sup> |
|---|--------------------------------|---|--|---|
| <b>DOZA006M22</b>                                   |                                |   |  |   |
| Avian orthoavula virus 1 ( <i>Paramyxoviridae</i> ) | OP169005.1                     | 15,186                                    | 10,134,890 (162)   | 7,907 (173)                                     |
| White spot syndrome virus ( <i>Nimariviridae</i> )  | MG264599.1                     | 314,232                                   |  | 13,377 (100)                                    |
| Pigeon paramyxovirus 1 ( <i>Paramyxoviridae</i> )   | ON637881.1                     | 15,290                                    |  | 8,880 (172)                                     |
| <b>DOZA007M22</b>                                   |                                |   |  |   |
| Avian orthoavula virus 1 ( <i>Paramyxoviridae</i> ) | OP169005.1                     | 15,186                                    | 1,734,647 (177)  | 12,879 (187)                                    |
| Pigeon paramyxovirus 1 ( <i>Paramyxoviridae</i> )   | ON637881.1                     | 15,290                                    |  | 17,971 (185)                                    |
| White spot syndrome virus ( <i>Nimariviridae</i> )  | MG264599.1                     | 314,232                                   |  | 1,134 (109)                                     |
| <b>DOZA000M22</b>                                   |                                |   |  |   |
| Avian orthoavula virus 1 ( <i>Paramyxoviridae</i> ) | OP169005.1                     | 15,186                                    | 4,060,293 (84)   | 323 (89)  |
| White spot syndrome virus ( <i>Nimariviridae</i> )  | MG264599.1                     | 314,232                                   |  | 3,610 (61)                                      |
| Pigeon paramyxovirus 1 ( <i>Paramyxoviridae</i> )   | ON637881.1                     | 15,290                                    |  | 716 (84)  |
| <b>S460-23</b>                                      |                                |   |  |   |
| Pigeon circovirus ( <i>Circoviridae</i> )           | MW181985.1                     | 2,045                                     | 5,198,600 (166)  | 3,110 (176)                                     |
| Columbid circovirus ( <i>Circoviridae</i> )         | KF738854.1                     | 2,043                                     |  | 2,967 (175)                                     |
| White spot syndrome virus ( <i>Nimariviridae</i> )  | MG264599.1                     | 314,232                                   |  | 1,471 (102)                                     |
| Torque teno virus ( <i>Anelloviridae</i> )          | NC_015783.1                    | 3,725                                     |  | 0 (83)  |
| Pigeon torque teno virus ( <i>Anelloviridae</i> )   | MF576433.1                     | 1,574                                     |  | 1,186 (173)                                     |

<sup>1</sup> bp: Base pairs; <sup>2</sup> Downloaded from Genbank

**Table 3.3:** Virome results for pigeon samples and percentage of genome recovered of reads mapped.

| SAMPLES                   | VIRUSES                |                       |                   |                     |                    |                           |                             |                      |   |
|---------------------------|------------------------|-----------------------|-------------------|---------------------|--------------------|---------------------------|-----------------------------|----------------------|---|
|                           | Pigeon paramyxovirus 1 | Pigeon torqueno virus | Pigeon circovirus | Avian sarcoma virus | Pigeon coronavirus | White spot syndrome virus | Avian endogenous retrovirus | Avian leukosis virus | Other   |
| N1775                     | ✓ (96,8%)              |                       |                   | ✓ (32,2%)           |                    |                           |                             | ✓ (67,9%)            | <ul style="list-style-type: none"> <li>Avian myeloblastosis associated virus (66,5%)</li> <li>Tasmanian devil retrovirus (82,1%)</li> </ul> |
| 20200121_087_6102A        |                        | ✓ (97,8%)             |                   |                     |                    | ✓ (7,5%)                  |                             |                      |   |
| 20200121_087_6102/613923B | ✓ (67,5%)              |                       |                   |                     |                    | ✓ (13,6%)                 |                             |                      |   |
| OP04-2020/PRL01-2020      | ✓ (95%)                |                       |                   |                     |                    | ✓ (24%)                   |                             |                      | <ul style="list-style-type: none"> <li>Human gammaherpesvirus 4 (9,9%)</li> </ul>   |
| 20100411                  | ✓ (100%)               |                       |                   | ✓ (63,6%)           |                    | ✓ (6,5%)                  | ✓ (97,5%)                   | ✓ (69,3%)            |   |
| 20110039                  | ✓ (100%)               |                       |                   |                     |                    | ✓ (13,6%)                 | ✓ (97,1%)                   |                      | <ul style="list-style-type: none"> <li>Semliki forest virus (6,9%)</li> </ul>   |
| S2021/06_0218             | ✓ (99,5%)              |                       |                   |                     |                    | ✓ (7,6%)                  | ✓ (98,5%)                   | ✓ (66,3%)            |   |
| S2021/06_0251             | ✓ (84,8%)              |                       |                   |                     |                    | ✓ (8,1%)                  |                             |                      | <ul style="list-style-type: none"> <li>Autographa californica nucleopolyhedrovirus (6,8%)</li> </ul>  |
| 21070306                  | ✓ (79,1%)              | ✓ (100%)              | ✓ (71%)           |                     | ✓ (7,3%)           | ✓ (7,6%)                  |                             |                      | <ul style="list-style-type: none"> <li>Infectious bronchitis virus (31,5%)</li> </ul>   |
| 21070474                  | ✓ (71,1%)              |                       |                   |                     |                    | ✓ (8%)                    |                             |                      |   |
| 21070476                  |                        | ✓ (100%)              |                   |                     |                    | ✓ (7%)                    |                             |                      |   |
| 21090443                  |                        | ✓ (100%)              |                   |                     |                    | ✓ (9%)                    |                             |                      |   |
| DOZA000M22                | ✓ (88,9%)              |                       |                   |                     |                    | ✓ (3,6%)                  |                             |                      |   |
| DOZA001M22                | ✓ (97,3%)              |                       |                   |                     |                    | ✓ (7,1%)                  |                             |                      | <ul style="list-style-type: none"> <li>Bovine viral diarrhea virus (4,9%)</li> <li>Porcine rotavirus (29,6%)</li> </ul>                     |
| DOZA002M22                | ✓ (77,2%)              |                       |                   |                     |                    | ✓ (3,8%)                  |                             |                      |   |
| DOZA003M22                | ✓ (99,4%)              |                       | ✓ (100%)          |                     |                    | ✓ (7,2%)                  |                             |                      |   |
| DOZA004M22                | ✓ (99,5%)              |                       |                   |                     |                    | ✓ (6,4%)                  |                             |                      |   |
| DOZA005M22                | ✓ (97,6%)              |                       |                   |                     |                    | ✓ (4,7%)                  |                             |                      |   |
| DOZA006M22                | ✓ (99,1%)              |                       |                   |                     |                    | ✓ (13,2%)                 |                             |                      |   |
| DOZA007M22                | ✓ (99,5%)              |                       |                   |                     |                    | ✓ (2,7%)                  |                             |                      |   |
| S460-23                   |                        | ✓ (100%)              | ✓ (94,3%)         |                     |                    | ✓ (1%)                    |                             |                      |   |

Some of the recovered assemblies mapped (Table 3.3) to generally known viruses with low coverage include, white spot syndrome virus, tasmanian devil retrovirus, Semliki Forest virus, human gammaherpesvirus 4, porcine rotavirus and bovine viral diarrhea virus.

In this study, 20 samples were found to be somewhat related to the white spot syndrome virus or something similar. Specifically, isolate WSSV\_CIBA\_002 and a Taiwanese strain (Annexure C). The highest coverage for this sequence was observed in sample OP04-2020/PRL01-2020, reaching 24%. Sample N1775 exhibited a mapped assembly with a coverage of 82.1% to Tasmanian devil retrovirus strains. Additionally, sample 20110039 showed a mapped assembly with a coverage of 6.9% to Semliki Forest virus strains. Sample PRL01-2020 exhibited a sequence coverage of 9.9% to Human gammaherpesvirus 4 strains, representing a relatively low proportion of the entire sequence. Furthermore, sample S2021/06\_0251 displayed a mapped assembly with poor sequence coverage (6.8%) to *Autographacalifronica* nucleopolyhedrovirus strains. Sample DOZA001M22 revealed a mapped assembly with a coverage of 29.6% to porcine rotaviruses, while a poor coverage of 4.9% to bovine viral diarrhea viruses was flagged in the same sample.

### **3.4.2. Phylogenetic analysis**

#### **3.4.2.1. Pigeon torque teno virus**

The phylogenetic analysis for Pigeon torque teno virus (Figure 3.2) based on a partial fragment (539 nt) from 284 to 823 spanning over the *rep* and *cap* gene revealed that four samples (21090443, 20200121\_087\_6102/613923B, 21070306 and 21070476) are closely related to previously documented Pigeon torque teno virus from China during 2017. The small size of the genome and the limited partially sequenced genes available on public accessible databases of this virus resulted in the use of a smaller genetic region to include as much available diversity as possible which limited the phylogenetic analysis to a smaller region. The four samples form distinct clades from each other, with samples 21090443 and 20200121\_087\_6102/613923B grouping together with a bootstrap value of 65% and samples 21070306 and 21070476 grouping together with a bootstrap value of 83%. The remaining sample, S460-23, clustered within a clade and is closely related to PTTV strains documented from Australia in 2018 with a bootstrap value of 77%. Samples 21090443, 20200121\_087\_6102/613923B, 21070306, and 21070476 were closely related to a PTTV strain 11D2FJ2017 (MF576433), while sample S460-23 were closely related to a PTTV strain P18-05523-7-93 (MW286327). Torque teno indri virus (NC\_034978) was used as an outgroup.



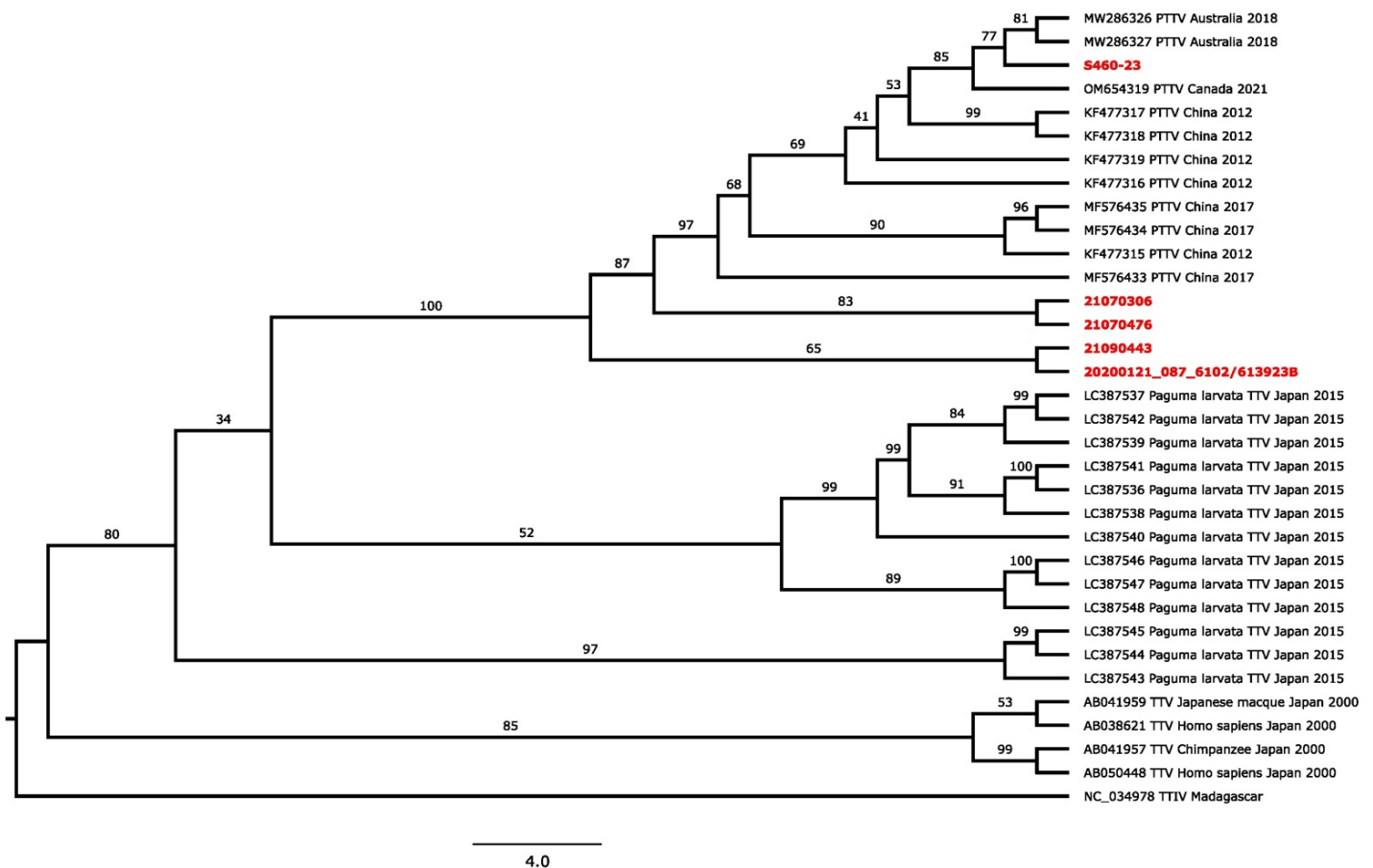


**Figure 3.2:** Maximum likelihood phylogenetic tree of PTTV based on partial genomes spanning over the *rep* and *cap* gene (539 nt) with different species of *Anelloviridae* family. Pigeon torque teno virus isolates generated in this study are highlighted in red font. The trees are rooted and drawn to scale, with branch lengths measured in the number of substitutions per site. Torque teno indri virus was used as an outgroup.

### 3.4.2.2. Avian endogenous retrovirus

Phylogenetic analysis for avian endogenous virus based on a partial genome (1577bp) from 1723 to 3300 spanning over the *gag-env* gene (Figure 3.3) revealed that samples 20100411, 20110039 and S2021/06\_0218 grouped within a general clade of avian endogenous retroviruses sampled from chickens in United Kingdom (UK) and China during 1999, 2010, 2012, 2013 and 2016 with a bootstrap value of 77%. Sample 20100411 clustered together with an AERV isolate SG collected from chickens in China in 2016 with a bootstrap value of only 43%. Samples 20110039 and S2021/06\_0218 established distinct clades from other samples recovered in this study. A human endogenous retrovirus (AJ511660) was used as an outgroup.

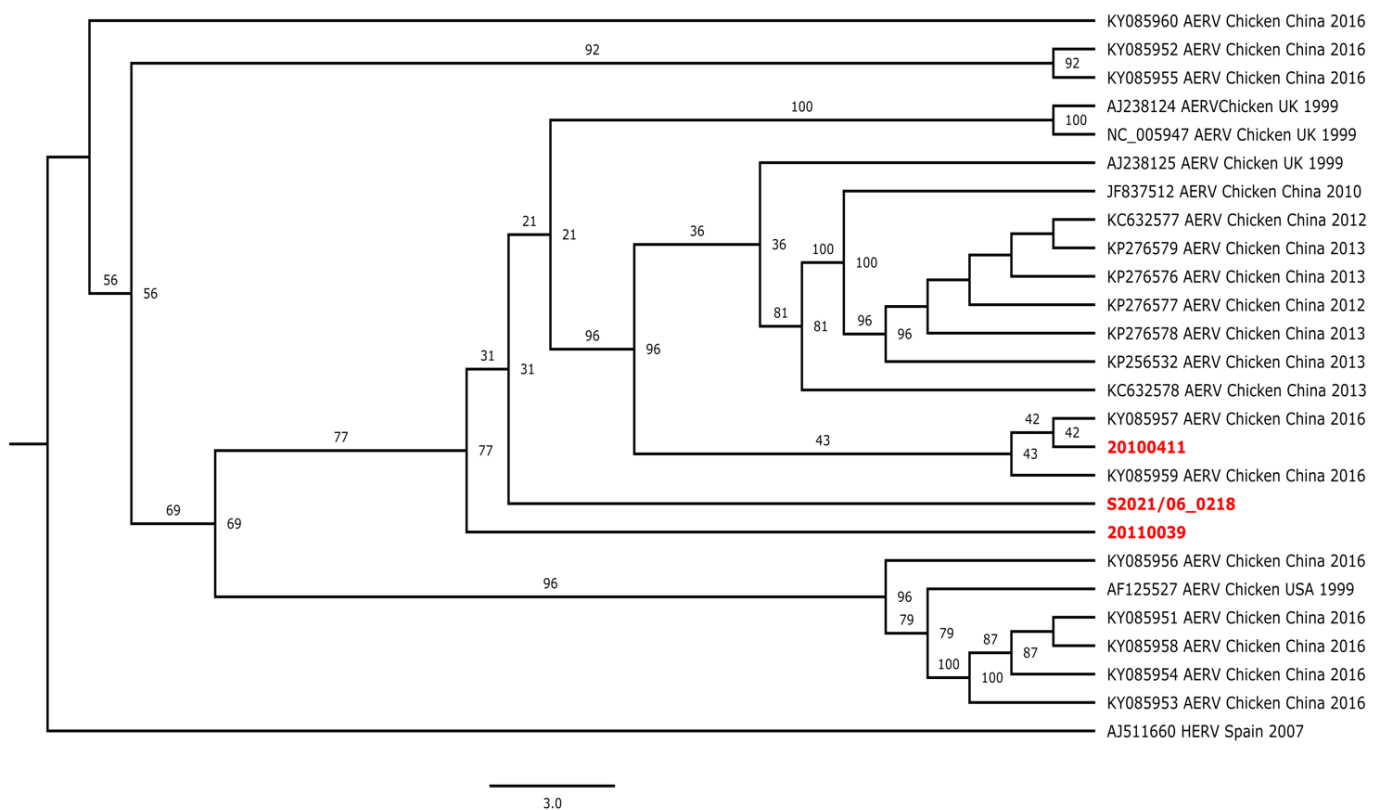


**Figure 3.3:** Maximum likelihood phylogenetic tree of AERV based on partial genomes spanning over the *gag-env* gene (1577bp). Avian endogenous retrovirus isolates generated in this study are highlighted in red font. The trees are rooted and drawn to scale with branch lengths measured in the number of substitutions per site. Human endogenous retrovirus was used as an outgroup.

### 3.5. Discussion and Conclusion

In an effort to gain a better understanding of the virome associated with feral doves and pigeons, numerous novel and previously characterised viruses has been identified. The largest number of viruses identified from the 21 samples in this study belonged to *Retroviridae* although several other viruses were also identified. We identified 8 novel (Autographa californica nucleopolyhedrovirus, Avian myeloblastosis associated virus, Bovine viral diarrhoea virus, Human gammaherpesvirus, Semliki forest virus, Tasmanian devil retrovirus and White spot syndrome virus) and 9 previously (Avian endogenous retro virus, Avian orthoavula virus 1, Infectious bronchitis virus, Pigeon circo virus, Pigeon coronavirus, Pigeon paramyxovirus 1, Pigeon torque teno virus and rotavirus) characterized viruses in pigeons.

Prior to this study, the only viruses previously identified in pigeons and doves in South Africa were Avian orthoavulavirus 1, Pigeon paramyxovirus 1, Influenza A, Pigeon circovirus, and Rotavirus (Abolnik, 2014; Stucker *et al.*, 2015; Abolnik, 2017; Abolnik *et al.*, 2018; Loiko *et al.*, 2018). Avian leukosis virus was previously described in chickens (Simbizi *et al.*, 2021), but not pigeons. Outside of South Africa, only Avian sarcoma virus (Rous sarcoma virus), Pigeon torque teno virus (Torque teno virus), Infectious bronchitis virus, Avian endogenous retroviruses and Pigeon coronavirus (Avian coronavirus) have been detected and characterised in pigeons, however, Avian myeloblastosis associated virus, Human gammaherpes virus, Semliki Forest virus, Autographica californica nucleopolyhedrovirus, Bovine viral diarrhoea virus and Tasmanian devil retrovirus have not been detected and characterised (Gifford *et al.*, 2005; Adebisi and Fagbohun, 2017; Kordadmehr *et al.*, 2017; Martini *et al.*, 2018; Agnihotri *et al.*, 2021).

Viruses not previously described in pigeons worldwide as mentioned, were also identified in the 21 feral pigeon and dove samples, from which the significance of these findings remains unknown. Regarding White spot syndrome virus, a wide range of hosts are susceptible to this virus, including lobsters, crayfish and crabs (Onihary *et al.*, 2021). Some species of seabirds have been reported as potential sources of virus transmission where they have been feeding on infected species and moving those infected species to other places (Onihary *et al.*, 2021). The virus's importance to avian species has yet to be determined, however, it is plausible that avian hosts can contract this virus or something related when they encounter diseased animals or polluted water. Birds can serve as vectors for the transmission of the disease when they scavenge on decapod crustaceans (such as crabs, shrimps, and lobsters) in one location and subsequently release these organisms into ponds (Leu *et al.*, 2008). This activity can potentially

lead to water pollution or make the decapod crustaceans available as scavenging material for other animals, contributing to the disease's spread.

Although numerous retroviruses have been identified in avian species, South Africa does not have native Tasmanian Devils; they are indigenous to Australia. An alternative and more plausible explanation is that viruses closely related to those previously identified in Tasmanian Devils may possess a broader host range than previously documented, extending to other species on different continents. Another alternative could be that the assembly represents a novel virus closely related to Tasmanian devil retrovirus strain DRV2010, but without additional confirmations such as isolations, conclusions like these cannot be drawn. Even though SFV has been linked to illnesses in wild birds, pigeons have not been mentioned as a possible host. Semliki Forest Virus is known to cause infections and illnesses in a wide range of hosts, including humans, animals, wild birds, rodents, domestic animals, and nonhuman primates (James D. Cherry MD *et al.*, 2019). It is currently found in Central and West Africa, parts of Asia and possibly Central and Southern Europe (James D. Cherry MD *et al.*, 2019). Human gammaherpesvirus 4, also known as Epstein-Barr-virus (EBV), known for causing mononucleosis, lymphoma, and nasopharyngeal carcinoma in humans (Kramer, 2019), was detected in the dataset. Although the significance of this virus to bird species remains unclear.

Even though rotaviruses have been identified in pigeons (including RVA, RVD, RVF and RVG), the metagenomics search revealed porcine rotavirus (Lukaszuk and Stenzel, 2020). This occurrence might be explained by the close phylogenetic relationship between porcine and pigeon rotaviruses, as demonstrated by Phan *et al.* in 2013 through a phylogenetic tree analysis based on the VP6 protein of rotaviruses (VP6 is mainly used for classification). Both porcine and pigeons are reservoirs for rotavirus A (Phan *et al.*, 2013). Alternatively, it is plausible that feral pigeons acquired porcine rotavirus from pig farms due to their free-flying nature and frequent presence in agricultural settings (farms). Bovine viral diarrhea is a disease which mainly affects cattle and other ruminants including sheep, goats, domestic pigs, wild boars, and other animal species belonging to the order *Artiodactyla* (Becher *et al.*, 2021). This virus is known to either cause cell death or no cell death and signs of the disease are not always present. The virus's significance to pigeons remains unknown and could be suggested that pigeons contract the virus from direct contact with cattle on farms, as pigeons and doves are frequently observed around feed and water troughs.

However, there is a possibility that families of these above-mentioned viruses exist in pigeons but have not been characterized or identified yet. Alternatively, these viruses might have been acquired incidentally, possibly from animals with which pigeons had direct contact. Therefore, it cannot be assumed that pigeons are necessarily vectors for these viruses; experimental infections and the demonstration of Koch's postulates would be required to establish their role definitively. Other viruses identified in the 21 feral pigeon and dove samples included viruses previously identified in pigeons outside of South Africa (pigeon torque teno virus, infectious bronchitis virus, avian coronavirus, and avian sarcoma virus) and some viruses discovered in South African pigeons including Pigeon paramyxovirus 1 (Avian orthoavula virus), Pigeon circovirus, and various Rotaviruses.

Phylogenetic analysis based on a genetic composition conducted on two of the four viruses previously identified in pigeons—namely, (i) pigeon torque teno virus and (ii) avian endogenous retrovirus—across samples 21070306, 21070476, S2021/06\_0218, 20110039, 20100411, 20200121\_087\_6102B, and S460-23 with a coverage percentage of 95% or higher demonstrated the clustering of the samples from this study within cosmopolitan clades with a widespread distribution across Australia, China, Canada and UK. Although data for Pigeon paramyxovirus 1 and Pigeon circovirus are available, the phylogenetic analysis will be inferred in Chapters 2 and 4.

Torque teno viruses from humans were included in the phylogenetic analysis of PTTV to evaluate whether the origin was zoonosis, as many racing pigeons are handled by humans during flying competitions and travelling, however none of the isolates clustered within the clade including the human torque teno viruses. Torque teno viruses from a masked palm civet (*Paguma larvata*), chimpanzee and Japanese macaque were also included in the study to see if the virus identified in the five samples came from an animal origin other than a pigeon. Torque teno virus strains from chimpanzees, Japanese macaques and homo sapiens showed no sign of relatedness. The torque teno viruses from the masked palm civet constituted a completely distinct clade with a bootstrap value of 52% from the four isolates, indicating no evidence of relatedness to the samples.

A limitation of this thesis lies in the exclusive use of genetic comparison due to the limited reference sequences available in GenBank, neglecting the commonly sequenced regions, which are typically employed in phylogenetic studies given that many viruses are analysed using smaller portions, often major antigens, rather than their entire genomes. Further future research

should consider analysis based on commonly conserved regions to provide a more comprehensive assessment, especially when complete genome sequences are unavailable in GenBank for many viruses. Another limitation of our study was the exclusive reliance on a *de novo* assembly method for identifying virus-specific sequences, as opposed to initially screening for the presence of known viral pathogens in pigeons and doves. This limitation arises from the fact that *de novo* assembly, while valuable for discovering novel viral sequences, may efficiently detect already established viral infections as long as it is sufficiently sequenced. The absence of an initial screening step for known pathogens could potentially overlook crucial insights into the prevalence and impact of recognized viruses in these bird populations. Future research should consider integrating both approaches to provide a more comprehensive understanding of viral infections in pigeons and doves.

Viral discovery activities are critical for gaining a better knowledge of the mechanisms that affect virome structure and the range of host specificity in the avian reservoir. Pigeons may act as reservoirs for many infections, however, it's crucial to recognize that not all findings in research are indicative of actual threats. Many results may be incidental or require further investigation to understand their significance fully. For instance, diseases like Newcastle Disease Virus (NDV) have their distinct strains, each with varying levels of virulence and impact, necessitating in-depth analysis.

The findings ostensibly suggest that viruses previously described in pigeons in other countries have been identified in pigeons in South Africa for the first time. This also suggests that avian organ samples are mostly composed of presumably multi-host generalist viruses and possibly host-specific specialist viruses, both of which are likely to have a role in producing heterogeneity and connection. Further research might establish the importance of these new viruses discovered in feral doves and pigeons. Isolation and characterization of novel viruses discovered in pigeons in South Africa that have not previously been documented must still be established in the future.

## CHAPTER 4

### **Epidemiological Insights into Pigeon Circovirus Variants in South Africa: A Molecular Perspective from 2014 to 2023**

#### **4.1. Introduction**

Pigeon circovirus (PiCV) has been recognized as a significant pathogen in pigeon populations worldwide, affecting both domestic and wild pigeons notably during the summer months between late May and early September (Mankertz, 2008; Stenzel and Konciki, 2017). The first documented PiCV infection in the United States was reported in 1993 by Woods and colleagues, since then, cases of PiCV infection have emerged in numerous countries across Asia, South Africa, America, and Europe (Santos *et al.*, 2020b). The pathogenesis of circovirus infections in pigeons remains a relatively understudied area. Transmission of the virus can occur through both horizontal and vertical routes, where primary transmission occurs through direct contact between hosts that are infected and susceptible (Todd, 2000; Herdt and Pasmans, 2009). The respiratory transmission route is further facilitated by the inhalation of fecal-contaminated substances like feather dust (Silva *et al.*, 2022). Circovirus infections have been observed in a diverse range of hosts, including avian, pig, and mammal species (Todd *et al.*, 2001). Among these hosts, examples encompass canaries, gouldian finches, common starlings, ravens, camels, ducks, geese, swans, sheep, ticks, gulls, and pigeons (Raidal, 2012; Kong *et al.*, 2021). Pigeon circovirus (PiCV), primarily affects pigeons and cause significant health issues in these avian species with a multifactorial syndrome known as young pigeon disease syndrome, characterized by symptoms such as lethargy, anorexia, runting, and poor racing performance (Raidal, 2012). This rapid deterioration in the health of afflicted birds can lead to mortality rates reaching several dozen percent in affected flocks (Stenzel and Konciki, 2017). Circovirus also affects other immune system organs, such as the thymus and spleen, with its genetic material detected in various other body parts, including the liver, kidneys, intestines, brain, and skin (Stenzel and Konciki, 2017). Diagnosing circovirus infections typically involves a histological examination of the bursa, which reveals the characteristic inclusion bodies. To validate this diagnosis, electron microscopy or PCR can be employed (Todd *et al.*, 2001). At present, there is no available vaccine for the prevention of circovirus in pigeons, the sole recourse lies in managing co-occurring infections (Herdt and Pasmans, 2009). The global trade and the sport of pigeon racing have significantly contributed to the widespread distribution of PiCV infection, an observation emphasized by Stenzel *et al.*, in 2012.

However, it is imperative to conduct further investigations to ascertain the prevalence and genetic variability of PiCV strains within South African pigeon populations. Continued research and surveillance efforts are crucial to obtain a more profound insight into the genetic diversity and evolutionary patterns of PiCV in South Africa. Molecular epidemiological studies can elucidate the genetic diversity of PiCV strains circulating in the region, shedding light on whether older strains persist or if new variants have emerged or been introduced.

Chapter 2 had a dual focus. Initially, we sequenced samples from pigeons and doves that had tested positive for Newcastle disease virus at national veterinary diagnostic laboratories, utilizing Ion Torrent technology. Our primary objective was to explore the molecular epidemiology of pigeon paramyxoviruses within the country. Within Chapter 3, our investigation extended to the Ion Torrent data generated earlier, examining these reads and seeking evidence of other viruses through both *de novo* assembly and BLAST analysis. Phylogenetic analysis was conducted to uncover valuable insights into the genetic relationships among these viral entities. In this study, we explored the phylogenetic relationships among PiCV viruses isolated from South African feral doves and pigeons analysed in Chapter 3 with additional suspected PiCV cases spanning the years 2014 to 2023.

#### **4.2. Aims and objectives of this study**

The aim of this chapter was to determine the genetic relationship of pigeon circoviruses (PiCV) collected in South Africa from 2014 to 2023. This study utilised samples in the University's repository and sequence reads generated from Ion Torrent data in Chapter 3.

The objectives were:

- To perform phylogenetic analysis on PiCV data in the UP repository and data generated in Chapter 3.



### 4.3. Materials and Methods

#### 4.3.1. Samples

Samples from the University of Pretoria's repository (n=11) of racing pigeons (*Columba livia domestica*) collected from the Johannesburg region and submitted to the University of Pretoria on 13th October 2014 as cloacal swabs and a racing pigeon sample submitted from the Free State region on 17th February 2023 (n=1) were presently available for analysis (Table 4.1). Sequence data of two samples (21070306 and DOZA003M22) generated in Chapter 3 with a viral metagenomic approach were included in the analysis.

**Table 4.2:** Samples analysed in this study.

| Sample     | Sampling date | Host          | Location <sup>1</sup>   | Sample type <sup>2</sup>                      |
|------------|---------------|---------------|-------------------------|---|
| 9447       | 13 Oct 2014   | Racing pigeon | Johannesburg region, GP | Cloacal swabs                                 |
| 14184      | 13 Oct 2014   | Racing pigeon | Johannesburg region, GP | Cloacal swabs                                 |
| 24978      | 13 Oct 2014   | Racing pigeon | Johannesburg region, GP | Cloacal swabs                                 |
| 24979      | 13 Oct 2014   | Racing pigeon | Johannesburg region, GP | Cloacal swabs                                 |
| 24981      | 13 Oct 2014   | Racing pigeon | Johannesburg region, GP | Cloacal swabs                                 |
| 24982      | 13 Oct 2014   | Racing pigeon | Johannesburg region, GP | Cloacal swabs                                 |
| 24983      | 13 Oct 2014   | Racing pigeon | Johannesburg region, GP | Cloacal swabs                                 |
| 24986      | 13 Oct 2014   | Racing pigeon | Johannesburg region, GP | Cloacal swabs                                 |
| 24991      | 13 Oct 2014   | Racing pigeon | Johannesburg region, GP | Cloacal swabs                                 |
| 24993      | 13 Oct 2014   | Racing pigeon | Johannesburg region, GP | Cloacal swabs                                 |
| 24994      | 13 Oct 2014   | Racing pigeon | Johannesburg region, GP | Cloacal swabs                                 |
| S460-23    | 17 Feb 2023   | Racing Pigeon | Not specified, FS       | Organ pool                                    |
| 21070306   | 15 Jul 2021   | Laughing Dove | Porterville, WC         | Egg-cultured isolate                          |
| DOZA003M22 | 30 May 2022   | Laughing Dove | OP Campus, Pretoria. GP | Gastrointestinal tract/ QH9-2/1 cell cultures |

<sup>1</sup> GP - Gauteng, FS - Free State, OP- Onderstepoort, WC- Western Cape, <sup>2</sup> Egg-cultured isolate (Alantoic fluid)

#### 4.3.2. Sample processing

Cloacal swab samples submitted from racing pigeons were submerged in (Phosphate-Buffered Saline (PBS) upon arrival and preserved at -80 °C until extraction of genetic material for further testing in 2020 due to the unavailability of specific tests for Pigeon Circovirus (PiCV) at the time. During the initial diagnostic phase, the Faculty of Veterinary Science ruled out Newcastle Disease Virus (NDV) infection using their standard diagnostic methods. However, PiCV infection was suspected. However, the recent sample submission from the Free State region

was processed by extracting RNA (section 4.3.3) upon arrival and subsequently stored -80 °C. The detailed processing actions for the samples 21070306 and DOZA003M22 are comprehensively elucidated in Chapter 2 of the study, the consensus sequences that were generated with a viral metagenomic approach from the sequence data in Chapter 3, serves as a pivotal component of the subsequent analysis in this Chapter.

#### **4.3.3. RNA extraction**

Total nucleic acids were extracted from cloacal swabs and an organ pool with a robotic IndiMag 48 platform. An IndiMag<sup>®</sup> Pathogen Kit w/o plastics (384) (Indical Bioscience, Germany) was used according to the manufacturer's recommended procedure. Briefly, Wash Buffer 1 (700 µl), Wash Buffer 2 (700 µl) and Elution Buffer (100 µl) were added into wells 2, 3 and 4 separately. The following master mix was prepared with Buffer VXL (100 µl), Buffer ACB (400 µl), MagAttract Suspension (25 µl) and Carrier RNA (1 µl) from which 500 µl were added into the sample rows alongside 200 µl of the sample and Proteinase K (20 µl). The prepared plates were loaded into the IndiMag 48 with the magnet rod cover strips on the correct positions. Total nucleic acid (100 µl) was removed from the last well and transferred to individually marked 1.5 ml Eppendorf tubes and stored thereafter at -80 °C until further testing.

#### **4.3.4. Whole Transcriptome Amplification for Ion Torrent NGS**

The extracted RNA or total nucleic acids from the samples were utilized to construct transcriptome libraries, employing the Complete Whole Transcriptome Amplification Kit from Sigma-Aldrich, USA. Subsequently, the libraries underwent purification before being dispatched for Ion Torrent Next-Generation Sequencing, a process detailed in section 2.3.7.

#### **4.3.5. Bioinformatic analysis**

The Ion Torrent reads in the form of .bam files were retrieved via FTP from the SU server and imported into CLC Genomic Workbench for the purpose of assembly. Genome assembly was carried out using CLC Genomics Workbench software v11.0.1, employing a hybrid approach that combines both assembly-to-reference and *de novo* assembly methods. During the *de novo* assembly, standard parameters were applied, which included a mismatch cost of 2, an insertion cost of 3, a deletion cost of 3, a length fraction of 0.5, and a similarity fraction of 0.8. The reference sequences for Pigeon circovirus utilized in the assembly-to-reference process were obtained from the Genbank database, specifically MW181985.1 (<https://www.ncbi.nlm.nih.gov/genbank/>). Following the read mapping with parameters of

match score 1, mismatch cost 2, linear gap cost, insertion cost 3, deletion cost 3, length fraction 0.5, similarity fraction 0.8 match score 1, mismatch cost the consensus sequences for each sample were extracted, and subsequently, full or partial sequences were annotated and deposited in the Genbank database.

The PiCV dataset utilised by Wang *et al.*, 2022 was downloaded from GenBank (<https://www.ncbi.nlm.nih.gov/genbank/>) and used for genotype identification. The sequences generated in this study were blasted against the GenBank nucleotide sequence database (<https://www.ncbi.nlm.nih.gov/genbank/>) to retrieve closely-related PiCV sequences from other regions. Multiple sequence alignments were prepared in BioEdit (Hall, 1999) and MAFFT (<https://mafft.cbrc.jp/alignment/server/>) open-source software programs. Phylogenetic trees were reconstructed in IQ tree (<http://iqtree.cibiv.univie.ac.at/>) using the maximum likelihood approach with 1000 bootstrap replicates. The substitution model in IQ tree database was selected as auto, with maximum iterations of 1000, minimum correlation coefficient 0.99, perturbation strength 0.5 and the IQ-TREE stopping rule 100. The phylogenetic trees generated were visualised in FigTree (v1.4.4) (<http://tree.bio.ed.ac.uk/software/figtree/>) and edited in Inkscape (v1.2.2) (<https://inkscape.org>). Suitable outgroups were used for each phylogenetic tree constructed.

## 4.4. Results

### 4.4.1. Collection of samples

A total of 14 suspected cases of PiCV after metagenomic analysis were analysed in this study, consisting of 12 samples obtained from racing pigeons during 2014 and 2023, and 2 samples generated from an in-depth virome analysis in Chapter 3. The field cases gathered from the Johannesburg region specifically involved racing pigeons exhibiting suboptimal performance, raising suspicions of infection. Specific details and information on sampling conditions for sample S460-23 were unavailable.

### 4.4.2. Bioinformatic analysis

Within our Ion Torrent NGS data (Table 4.2), distinct variations in read metrics were apparent among the samples. The total reads exhibited a wide-ranging span, encompassing values from 711,543 bp to 7,751,218 bp, highlighting the diversity in sequencing depth across the dataset. While the average read lengths displayed overall consistency throughout the dataset, a few outliers were identified, with average lengths falling within the range of 57 bp to 179 bp.

The compiled sequence results are displayed in Table 4.3.

**Table 4.2:** Sequence information obtained from samples subjected to Ion Torrent NGS.

| Lab/ sample no. | Bases         | Reads     | Average read length (bp) <sup>1</sup> |
|-----------------|---------------|-----------|---------------------------------------|
| 9447            | 74,325,011    | 1,268,314 | 58                                    |
| 14184           | 68,247,390    | 1,148,834 | 59                                    |
| 24978           | 42,579,858    | 711,543   | 59                                    |
| 24979           | 248,039,145   | 1,494,482 | 165                                   |
| 24981           | 68,376,700    | 1,179,274 | 57                                    |
| 24982           | 69,863,526    | 1,140,354 | 61                                    |
| 24983           | 93,583,499    | 1,582,719 | 59                                    |
| 24986           | 90,349,175    | 1,520,737 | 59                                    |
| 24991           | 63,013,913    | 1,048,496 | 60                                    |
| 24993           | 75,598,182    | 1,214,228 | 62                                    |
| 24994           | 56,915,116    | 917,670   | 62                                    |
| S460-23         | 863,015,521   | 5,198,600 | 166                                   |
| 21070306        | 1,388,058,884 | 7,751,218 | 179                                   |
| DOZA003M22      | 641,668,811   | 4,023,110 | 159                                   |

<sup>1</sup> bp: Base pairs

**Table 4.3 :** Data on consensus sequences and the percentage of recovery for samples processed through Ion Torrent NGS.

| Lab/sample no. | Sample type                                      | Consensus sequence length of Whole genome recovery (nt) <sup>1</sup> |
|----------------|--|--|
| 9447           | Cloacal swabs                                    | 918 (45%)  |
| 14184          | Cloacal swabs                                    | 2031 (99,7%)   |
| 24978          | Cloacal swabs                                    | 2036 (99,9%)   |
| 24979          | Cloacal swabs                                    | 2031 (99,7%)   |
| 24981          | Cloacal swabs                                    | 2031 (99,7%)   |
| 24982          | Cloacal swabs                                    | 2037 (100%)  |
| 24983          | Cloacal swabs                                    | 1966 (96,5%)   |
| 24986          | Cloacal swabs                                    | 2036 (99,9%)   |
| 24991          | Cloacal swabs                                    | 1790 (87,9%)   |
| 24993          | Cloacal swabs                                    | 2034 (99,8%)   |
| 24994          | Cloacal swabs                                    | 2035 (99,9%)   |
| S460-23        | Organ pool                                       | 2014 (98,9%)   |
| 21070306       | Egg-cultured isolate                             | 1450 (71,2%)   |
| DOZA003M22     | Gastrointestinal tract/<br>QH9-2/1 cell cultures | 2020 (99,2%)   |

<sup>1</sup> nt: Nucleotides

#### 4.4.3. Phylogenetic analysis

The phylogenetic tree for Pigeon circovirus relatedness is based on a partial genome (880 nt) from 161 to 1041 spanning over the *rep* gene region (Figure 4.1).

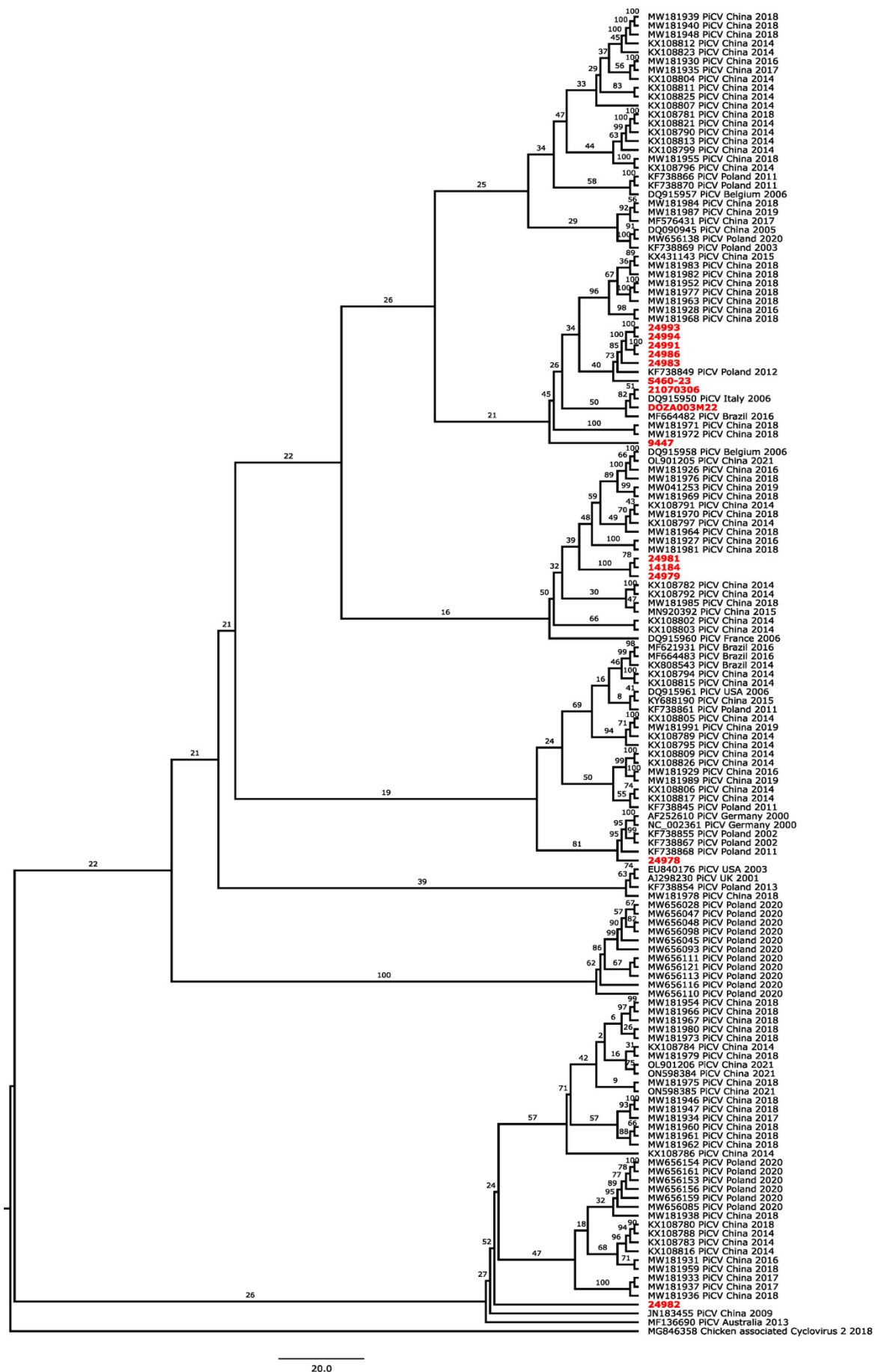


**Figure 4.1:** Maximum likelihood phylogenetic tree of PiCV based on partial genomes spanning over the *rep* gene (880 nt). Pigeon circovirus isolates generated in this study are highlighted in red font. The trees are drawn to scale, with branch lengths measured in the number of substitutions per site. Chicken associated Cyclovirus was used as an outgroup.

Samples 24993, 24994, 24991, 24986, 24983 and S460-23 clustered together with a bootstrap value of 40% and are closely related to a pigeon circovirus strain collected in Poland in 2012. Sample 21070306 and DOZA003M22 formed part of a clade with a bootstrap value of 50% where sample 21070306 is closely related to a pigeon circovirus strain sampled in Italy in 2006 and sample DOZA003M22 is closely related to a pigeon circovirus strain collected in Brazil in 2016. Sample 9447 formed a basal taxon and is closely related to a bigger clade containing pigeon circovirus samples from this study and pigeon circovirus strains sampled in China, Poland, Italy and Brazil in 2006, 2012, 2015, 2016 and 2018. Samples 24981, 14184 and 24979 formed a monophyletic branch with a bootstrap value of 100% and are closely related to a bigger clade containing pigeon circovirus strains collected in Belgium and China in 2006, 2014, 2016, 2018, 2019 and 2021. Sample 24978 formed a basal taxon and is closely related to a bigger clade with a bootstrap value of 81% containing pigeon circovirus strains sampled in Germany and Poland in 2000, 2002 and 2011. Sample 24982 formed a basal taxon with a bootstrap value of 52% and is closely related to a bigger clade containing pigeon circovirus strains collected in China and Poland in 2014, 2016, 2017, 2018, 2020 and 2021. A chicken-associated cyclovirus 2 was used as an outgroup.

For genotype identification of Pigeon circovirus (Figure 4.2), based on a partial genome (536 nt) spanning nucleotides 506 to 1042 of the *cap* gene, isolates used for genotyping based on a previous study by Wang *et al.*, 2022 were downloaded from Genbank. One or more pigeon circovirus isolates were retrieved for each of the nine genotypes, labelled A to I.

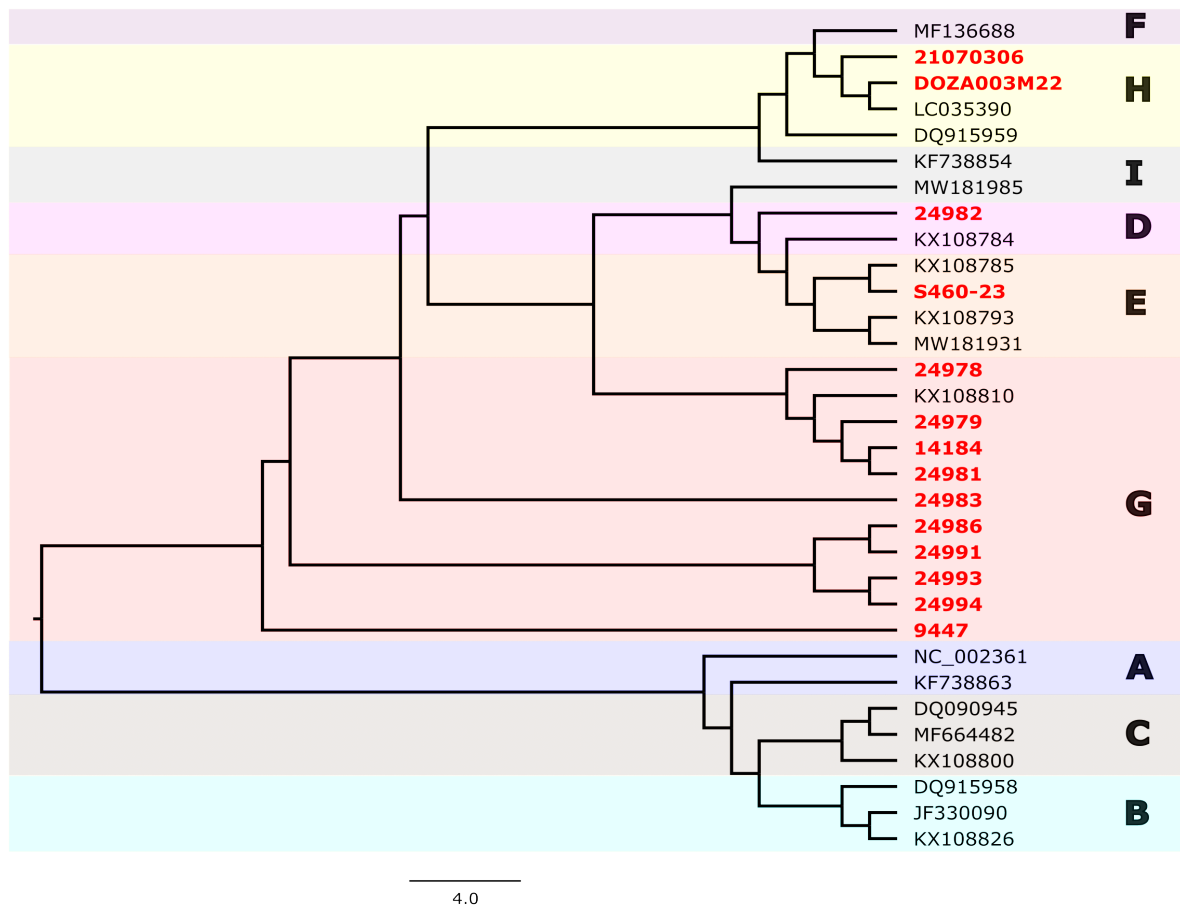


**Figure 4.2:** Dendrogram of the different PiCV genotypes based on a partial fragment of the *cap* gene (536bp) used for genotype classification purposes (Wang *et al.*,2022). The alphabetic letters represent the different genotypes assigned by Wang and co-workers. Pigeon circovirus isolates generated in this study are highlighted in red font. The trees are drawn to scale, with branch lengths measured in the number of substitutions per site.

The dendrogram constructed based on a partial fragment of the *cap* gene revealed that samples DOZA003M22 and 21070306 grouped into genotype H, sample S460-23 into genotype E, sample 24982 into genotype D and samples 24978, 24979, 14184, 24981, 24983, 24986, 24991, 24993, 24994 and 9447 into genotype G.



#### 4.5. Discussion and Conclusion

PiCV viruses were collected from both feral doves and racing pigeons across Gauteng, Free State, and Western Cape regions, spanning the years 2014 and 2021 to 2023. The collection of these virus samples involved a combination of sample submissions and comprehensive virome analyses.

Following the assembly of consensus sequences, among the 14 samples analyzed, only one yielded a complete genome sequence. Ten of these samples managed to recover >96% of the entire genome, while three samples fell short, retrieving <90% of the whole genome. Genotype classification was executed using a dataset based on the *cap* gene sequence, as described by Wang *et al.* in 2022. This dataset facilitated the categorization of PiCV strains into nine distinct genotypes based on the *cap* gene sequence. This approach provided valuable insights into the genetic diversity and evolutionary patterns of PiCV. The results of the genotype classification analysis revealed that ten samples clustered within genotype G, two within genotype H, and the remaining two within genotypes E and D, respectively. Notably, genotypes D and E were primarily composed of sequences obtained from Asia, whereas genotype G encompassed sequences collected from Asia, South America, and Europe. Genotype H, on the other hand, included sequences from Asia, North America, and Oceania. The phylogenetic analysis of the blast results, which relied on a partial fragment of the *rep* gene, revealed that the 14 samples formed six distinct clades. These samples exhibited close genetic relationships with PiCV strains collected from pigeons in various countries, including Belgium, Brazil, China, Germany, Italy, and Poland in different years, spanning from 2000 to 2021.

It's worth noting that one of the main limitations of this study is the relatively limited sample size drawn from various provinces, collecting data from a restricted number of cases across different provinces may not provide a comprehensive representation of the diversity of strains circulating in South Africa. Another notable limitation of this study is that the phylogenetic analysis was performed on a partial segment of the genome that was available, rather than the entire genome. This restricted scope could potentially impact the robustness of the study's conclusions. A comprehensive examination of the entire genome might provide a more accurate and detailed understanding of the genetic diversity and evolutionary dynamics of PiCV in South Africa. While our findings offer valuable insights, the use of partial genome sequences may not capture the full extent of genetic variation, potentially leading to a less comprehensive

interpretation of PiCV's evolutionary patterns and its implications for the sampled pigeon populations.

This study revealed a multitude of PiCV genotypes, indicating ongoing viral evolution and the possible introduction of new strains via international trade and the movement of infected birds. Moreover, the phylogenetic analysis has provided substantial evidence of global clustering among PiCV strains, implying the potential impact of international trading and pigeon racing on the transmission of the virus. The integration of both sample sources has enhanced our understanding of the complex interactions between PiCV and other avian pathogens, shedding light on potential co-infections and their implications. These discoveries make a substantial contribution to the field of molecular epidemiology, enhancing our understanding of PiCV's genetic diversity and the possible dynamics within South Africa, where information has been scarce. This study significantly advances our understanding of PiCV's prevalence and its impact on racing pigeons, underlining the need for further research to address the remaining gaps in our knowledge and to develop more targeted strategies for the detection and management of PiCV infections in avian populations.

## References

- ABDELLA, R., AGGARWAL, M., OKURA, T., LAMB, R. A. & HE, Y. 2020. Structure of a paramyxovirus polymerase complex reveals a unique methyltransferase-CTD conformation. *Proceedings of the National Academy of Sciences*, 117, 4931.
- ABOLNIK, C. (2007) Phylogenetic analysis of pigeon paramyxoviruses isolated in South Africa. Ph.D. Thesis. *University of Pretoria*. Available at: <https://repository.up.ac.za/bitstream/handle/2263/25689/05chapter5.pdf?sequence=6&isAllowed=y> (Accessed: 15 April 2023).
- ABOLNIK, C. 2007. *Molecular epidemiology of Newcastle disease and avian influenza in South Africa*. University of Pretoria.
- ABOLNIK, C. 2014. A current review of avian influenza in pigeons and doves (Columbidae). *Vet Microbiol*, 170, 181-96.
- ABOLNIK, C. 2017. History of Newcastle disease in South Africa. *The Onderstepoort journal of veterinary research*, 84, e1-e7.
- ABOLNIK, C., BISSCHOP, S., GERDES, T., OLIVIER, A. & HORNER, R. 2007. Outbreaks of avian influenza H6N2 viruses in chickens arose by a reassortment of H6N8 and H9N2 ostrich viruses. *Virus Genes*, 34, 37-45.
- ABOLNIK, C., GERDES, G. H., KITCHING, J., SWANEPOEL, S., ROMITO, M. & BISSCHOP, S. P. 2008. Characterization of pigeon paramyxoviruses (Newcastle disease virus) isolated in South Africa from 2001 to 2006. *Onderstepoort Journal of Veterinary Research*, 75, 147-52.
- ABOLNIK, C., HORNER, R. F., BISSCHOP, S. P. R., PARKER, M. E., ROMITO, M. & VILJOEN, G. J. 2004. A phylogenetic study of South African Newcastle disease virus strains isolated between 1990 and 2002 suggests epidemiological origins in the Far East. *Archives of Virology*, 149, 603-619.

ABOLNIK, C., STUTCHBURY, S. & HARTMAN, M. J. 2018. Experimental infection of racing pigeons (*Columba livia domestica*) with highly pathogenic Clade 2.3.4.4 sub-group B H5N8 avian influenza virus. *Vet Microbiol*, 227, 127-132.

ABSALÓN, A. E., CORTÉS-ESPINOSA, D. V., LUCIO, E., MILLER, P. J. & AFONSO, C. L. 2019. Epidemiology, control, and prevention of Newcastle disease in endemic regions: Latin America. *Tropical and Animal Health Production*, 51, 1033-1048.

ADEBIYI, A. I. & FAGBOHUN, A. F. 2017. Infectious Bronchitis Virus in Captured Free-Living, Free-Range and Intensively Reared Birds in Southwest Nigeria. *Folia Veterinaria*, 61, 23-26.

AGNIHOTRI, K., SMITH, C., OAKEY, J. & STORIE, G. 2021. Pigeon adenovirus and pigeon torque teno virus associated with acute multifocal hepatic necrosis in pigeons in Queensland, Australia. *Arch Virol*, 166, 1469-1475.

AKHTAR, S., MUNEER, M. A., MUHAMMAD, K., TIPU, M. Y., RABBANI, M., UL-RAHMAN, A. & SHABBIR, M. Z. 2016. Genetic characterization and phylogeny of pigeon paramyxovirus isolate (PPMV-1) from Pakistan. *Springerplus*, 5, 1295.

AL-KUBATI, A. A. G., HUSSEN, J., KANDEEL, M., AL-MUBARAK, A. I. A. & HEMIDA, M. G. 2021. Recent Advances on the Bovine Viral Diarrhea Virus Molecular Pathogenesis, Immune Response, and Vaccines Development. *Frontiers in Veterinary Science*, 8.

ALDOUS, E. W. & ALEXANDER, D. J. 2001. Detection and differentiation of Newcastle disease virus (avian paramyxovirus type 1). *Avian Pathology*, 30, 117-128.

ALDOUS, E. W., FULLER, C. M., RIDGEON, J. H., IRVINE, R. M., ALEXANDER, D. J. & BROWN, I. H. 2014. The evolution of pigeon paramyxovirus type 1 (PPMV-1) in Great Britain: a molecular epidemiological study. *Transboundary and Emerging Diseases*, 61, 134-9.

ALDOUS, E. W., MYNN, J. K., BANKS, J. & ALEXANDER, D. J. 2003. A molecular epidemiological study of avian paramyxovirus type 1 (Newcastle disease virus) isolates by phylogenetic analysis of a partial nucleotide sequence of the fusion protein gene. *Avian Pathology*, 32, 239-56.

ALEXANDER, D. J. 2000. Newcastle disease and other avian paramyxoviruses. *Rev Sci Tech*, 19, 443-62.

ALEXANDER, D. J. 2009. Ecology and Epidemiology of Newcastle Disease. In: CAPUA, I. & ALEXANDER, D. J. (eds.) *Avian Influenza and Newcastle Disease: A Field and Laboratory Manual*. Milano: Springer Milan.

ALEXANDER, D. J., WILSON, G. W., RUSSELL, P. H., LISTER, S. A. & PARSONS, G. 1985. Newcastle disease outbreaks in fowl in Great Britain during 1984. *Veterinary Record*, 117, 429-34.

ANNAHEIM, D., VOGLER, B. R., SIGRIST, B., VÖGTLIN, A., HÜSSY, D., BREITLER, C., HARTNACK, S., GRUND, C., KING, J., WOLFRUM, N. & ALBINI, S. 2022. Screening of Healthy Feral Pigeons (*Columba livia domestica*) in the City of Zurich Reveals Continuous Circulation of Pigeon Paramyxovirus-1 and a Serious Threat of Transmission to Domestic Poultry. *Microorganisms*, 10.

BARI, F. D., GELAYE, E., TEKOLA, B. G., HARDER, T., BEER, M. & GRUND, C. 2021. Antigenic and Molecular Characterization of Virulent Newcastle Disease Viruses Circulating in Ethiopia Between 1976 and 2008. *Veterinary Medicine (Auckland, NZ)*, 12, 129-140.

BARR, D. A., REECE, R. L., O'ROURKE, D., BUTTON, C. & FARAGHER, J. T. 1988. Isolation of infectious bronchitis virus from a flock of racing pigeons. *Aust Vet J*, 65, 228.

BECHER, P., MOENNIG, V. & TAUTZ, N. 2021. Bovine Viral Diarrhea, Border Disease, and Classical Swine Fever Viruses (Flaviviridae). In: BAMFORD, D. H. & ZUCKERMAN, M. (eds.) *Encyclopedia of Virology (Fourth Edition)*. Oxford: Academic Press.

- BELLO, M. B., YUSOFF, K., IDERIS, A., HAIR-BEJO, M., PEETERS, B. P. H. & OMAR, A. R. 2018. Diagnostic and Vaccination Approaches for Newcastle Disease Virus in Poultry: The Current and Emerging Perspectives. *Biomed Research International*, 2018, 7278459.
- BILAL, E. S. A., ELNASRI, I. M., ALHASSAN, A. M., KHALIFA, K. A., ELHAG, J. I. & AHMED, S. O. 2014. Biological Pathotyping of Newcastle Disease Viruses in Sudan 2008–2013. *Journal of Veterinary Medicine*, 2014, 209357.
- BOROS, Á., NEMES, C., PANKOVICS, P., KAPUSINSZKY, B., DELWART, E. & REUTER, G. 2012. Identification and complete genome characterization of a novel picornavirus in turkey (*Meleagris gallopavo*). *J Gen Virol*, 93, 2171-2182.
- BREITBART, M., DELWART, E., ROSARIO, K., SEGALÉS, J., VARSANI, A. & ICTV REPORT, C. 2017. ICTV Virus Taxonomy Profile: Circoviridae. *Journal of General Virology*, 98, 1997-1998.
- BROWN, I. H. 2000. Brown, I. H. The epidemiology and evolution of influenza viruses in pigs. *Vet. Microbiol.* 74, 29-46. *Veterinary microbiology*, 74, 29-46.
- BUCKO, M. & GIEGER, S. 2019. Newcastle disease (Avian paramyxovirus serotype 1). USGS National Wildlife Health Center 2019.
- BWALA, D. G., FASINA, F. O. & DUNCAN, N. M. 2015. Avian poxvirus in a free-range juvenile speckled (rock) pigeon (*Columba guinea*). *J S Afr Vet Assoc*, 86, e1-e4.
- CALNEK, D. S., MAZZELLA, L., ROSER, S., ROMAN, J. & HART, C. M. 2003. Peroxisome proliferator-activated receptor gamma ligands increase release of nitric oxide from endothelial cells. *Arterioscler Thromb Vasc Biol*, 23, 52-7.
- CANTÍN, C., HOLGUERA, J., FERREIRA, L., VILLAR, E. & MUÑOZ-BARROSO, I. 2007. Newcastle disease virus may enter cells by caveolae-mediated endocytosis. *Journal of General Virology*, 88, 559-569.

CARRANZA, J., POVEDA, J. B. & FERNÁNDEZ, A. 1986. An Outbreak of Encephalitis in Pigeons (*Columba livia*) in the Canary Islands (Spain). *Avian Diseases*, 30, 416-420.

CATTOLI, G., SUSTA, L., TERREGINO, C. & BROWN, C. 2011. Newcastle disease: a review of field recognition and current methods of laboratory detection. *Journal of Veterinary Diagnostic Investigation*, 23, 637-56.

CAVANAGH, D. 2007. Coronavirus avian infectious bronchitis virus. *Vet Res*, 38, 281-97.

CHANG, H., FENG, S., WANG, Y., LI, F., SU, Q., WANG, B., DU, J. & HE, H. 2020. Isolation and Pathogenic Characterization of Pigeon Paramyxovirus Type 1 via Different Inoculation Routes in Pigeons. *Front Vet Sci*, 7, 569901.

CHANG, H., FENG, S., WANG, Y., LI, F., SU, Q., WANG, B., DU, J. & HE, H. 2020. Isolation and Pathogenic Characterization of Pigeon Paramyxovirus Type 1 via Different Inoculation Routes in Pigeons. *Frontiers in Veterinary Science*, 7, 569901.

CHAVES HERNÁNDEZ, A. J. 2014. Poultry and Avian Diseases. In: VAN ALFEN, N. K. (ed.) *Encyclopedia of Agriculture and Food Systems*. Oxford: Academic Press.

CHOI, K. S., LEE, E. K., JEON, W. J. & KWON, J. H. 2010. Antigenic and immunogenic investigation of the virulence motif of the Newcastle disease virus fusion protein. *Journal of Veterinary Sciences*, 11, 205-11.

CHOWDHARY, M., NASHIRUDDULLAH, N., ABROL, R., SOOD, S., RAHMAN, S., AHMED, J. & MAQBOOL, R. 2020. Newcastle Disease and their Pathology in Fowls Affected with Genotype XIII and Pigeons with Genotype II. *International Journal of Current Microbiology and Applied Sciences*, 9, 3800-3810.

COETZEE, L. 1980, 'An evaluation of immunity and protection against Newcastle disease', MMedVet thesis, Faculty of Veterinary Science, University of Pretoria.

CROSS, G. 1995. Paramyxovirus-1 infection (Newcastle disease) of pigeons. *Seminars in Avian and Exotic Pet Medicine*, 4, 92-95.

DASH, H. R. & DAS, S. 2018. Chapter 4 - Molecular Methods for Studying Microorganisms From Atypical Environments. *In: GURTLER, V. & TREVORS, J. T. (eds.) Methods in Microbiology*. Academic Press.

DAUM, I., FINSTERBUSCH, T., HÄRTLE, S., GÖBEL, T. W., MANKERTZ, A., KORBEL, R. & GRUND, C. 2009. Cloning and expression of a truncated pigeon circovirus capsid protein suitable for antibody detection in infected pigeons. *Avian Pathology*, 38, 135-141.

DE ALMEIDA, R. S., HAMMOUMI, S., GIL, P., BRIAND, F.-X., MOLIA, S., GAIDET, N., CAPPELLE, J., CHEVALIER, V., BALANÇA, G., TRAORÉ, A., GRILLET, C., MAMINIAINA, O. F., GUENDOUZ, S., DAKOUO, M., SAMAKÉ, K., BEZEID, O. E. M., DIARRA, A., CHAKA, H., GOUTARD, F., THOMPSON, P., MARTINEZ, D., JESTIN, V. & ALBINA, E. 2013. New Avian Paramyxoviruses Type I Strains Identified in Africa Provide New Outcomes for Phylogeny Reconstruction and Genotype Classification. *PLOS ONE*, 8, e76413.

DE BENEDICTIS, P., SCHULTZ-CHERRY, S., BURNHAM, A. & CATTOLI, G. 2011. Astrovirus infections in humans and animals—molecular biology, genetic diversity, and interspecies transmissions. *Infection, Genetics and Evolution*, 11, 1529-1544.

DE KLERK, G. & PIENAAR, H. 2022. *Animal Disease Reporting Manual* [Online]. Available: <https://www.nda.agric.za/vetweb/Epidemiology/Reporting%20forms/Disease%20reporting%20%20manual%205Apr2016.pdf> [Accessed].

DEOL, P., KATTOOR, J. J., SIRCAR, S., GHOSH, S., BÁNYAI, K., DHAMA, K. & MALIK, Y. S. 2017. Avian Group D Rotaviruses: Structure, Epidemiology, Diagnosis, and Perspectives on Future Research Challenges. *Pathogens* [Online], 6.

DEPARTMENT OF AGRICULTURE, L. R. A. R. D. 2022a. *Disease database* [Online]. Available: <https://www.dalrrd.gov.za/Branches/Agricultural-Production-Health-Food-Safety/Animal-Health/Epidemiology/diseasedatabase> [Accessed 5 November 2022].



DEPARTMENT OF AGRICULTURE, L. R. A. R. D. 2022b. *Disease reporting summaries* [Online]. Available: <https://www.dalrrd.gov.za/Branches/Agricultural-Production-Health-Food-Safety/Animal-Health/Epidemiology/mapsdisease> [Accessed 10 November 2022].

DESSELBERGER, U. 2014. Rotaviruses. *Virus Res*, 190, 75-96.

DEY, S., CHELLAPPA, M. M., GAIKWAD, S., KATARIA, J. M. & VAKHARIA, V. N. 2014. Genotype Characterization of Commonly Used Newcastle Disease Virus Vaccine Strains of India. *PLOS ONE*, 9, e98869.

DIEL, D. G., DA SILVA, L. H. A., LIU, H., WANG, Z., MILLER, P. J. & AFONSO, C. L. 2012. Genetic diversity of avian paramyxovirus type 1: Proposal for a unified nomenclature and classification system of Newcastle disease virus genotypes. *Infection, Genetics and Evolution*, 12, 1770-1779.

DIMITROV, K. M., ABOLNIK, C., AFONSO, C. L., ALBINA, E., BAHL, J., BERG, M., BRIAND, F. X., BROWN, I. H., CHOI, K. S., CHVALA, I., DIEL, D. G., DURR, P. A., FERREIRA, H. L., FUSARO, A., GIL, P., GOUJGOULOVA, G. V., GRUND, C., HICKS, J. T., JOANNIS, T. M., TORCHETTI, M. K., KOLOSOV, S., LAMBRECHT, B., LEWIS, N. S., LIU, H., LIU, H., MCCULLOUGH, S., MILLER, P. J., MONNE, I., MULLER, C. P., MUNIR, M., REISCHAK, D., SABRA, M., SAMAL, S. K., SERVAN DE ALMEIDA, R., SHITTU, I., SNOECK, C. J., SUAREZ, D. L., VAN BORM, S., WANG, Z. & WONG, F. Y. K. 2019. Updated unified phylogenetic classification system and revised nomenclature for Newcastle disease virus. *Infection, Genetics and Evolution*, 74, 103917.

DIMITROV, K. M., LEE, D.-H., WILLIAMS-COPLIN, D., OLIVIER, T. L., MILLER, P. J. & AFONSO, C. L. 2016. Newcastle Disease Viruses Causing Recent Outbreaks Worldwide Show Unexpectedly High Genetic Similarity to Historical Virulent Isolates from the 1940s. *Journal of clinical microbiology*, 54, 1228-1235.

DOERFLER, W. 1996. Adenoviruses. In: BARON, S. (ed.) *Medical Microbiology*. Galveston (TX): University of Texas Medical Branch at Galveston, Copyright © 1996, The University of Texas Medical Branch at Galveston.

DOMAŃSKA-BLICHAZ, K., MIŁEK-KRUPA, J. & PIKUŁA, A. 2021. Diversity of Coronaviruses in Wild Representatives of the Aves Class in Poland. *Viruses*, 13.

DORTMANS, J. C. F. M., KOCH, G., ROTTIER, P. J. M. & PEETERS, B. P. H. 2011. Virulence of newcastle disease virus: what is known so far? *Veterinary Research*, 42, 122.

DUAN, X., ZHANG, P., MA, J., CHEN, S., HAO, H., LIU, H., FU, X., WU, P., ZHANG, D., ZHANG, W., DU, E. & YANG, Z. 2014. Characterization of genotype IX Newcastle disease virus strains isolated from wild birds in the northern Qinling Mountains, China. *Virus Genes*, 48, 48-55.

DUCHATEL, J. & SZELESZCZUK, P. 2011. Young pigeon disease syndrome. *Medycyna Weterynaryjna*, 67, 291-294.

DUCHATEL, J. P., TODD, D., SMYTH, J. A., BUSTIN, J. C. & VINDEVOGEL, H. 2006. Observations on detection, excretion and transmission of pigeon circovirus in adult, young and embryonic pigeons. *Avian Pathology*, 35, 30-34.

DZOGBEMA, K. F. X., TALAKI, E., BATAWUI, K. B. & DAO, B. B. 2021. Review on Newcastle disease in poultry. *International Journal of Biological and Chemical Sciences*, 15, 773-789.

EHLERS SMITH, Y. C., MASEKO, M. S. T., SOSIBO, M., DLAMINI, P. V., THOBEKA GUMEDE, S., NGCOBO, S. P., TSOANANYANE, L., ZUNGU, M. M., EHLERS SMITH, D. A. & DOWNS, C. T. 2021. Indigenous knowledge of South African bird and rangeland ecology is effective for informing conservation science. *Journal of Environmental Management*, 284, 112041.

ETRIWATI, RATIH, D., HANDHARYANI, E. & SETIYANINGSIH, S. 2017. Pathology and immunohistochemistry study of Newcastle disease field case in chicken in Indonesia. *Veterinary World*, 10, 1066-1071.

FADIJI, A. E. & BABALOLA, O. O. 2020. Metagenomics methods for the study of plant-associated microbial communities: A review. *Journal of Microbiological Methods*, 170, 105860.

- FEI, Y., LIU, X., MU, J., LI, J., YU, X., CHANG, J., BI, Y., STOEGER, T., WAJID, A., MUZYKA, D., SHARSHOV, K., SHESTOPALOV, A., AMONSIN, A., CHEN, J., DING, Z. & YIN, R. 2019. The Emergence of Avian Orthoavulavirus 13 in Wild Migratory Waterfowl in China Revealed the Existence of Diversified Trailer Region Sequences and HN Gene Lengths within this Serotype. *Viruses*, 11, 646.
- FRANÇOIS, S. & PYBUS, O. G. 2020. Towards an understanding of the avian virome. *Journal of General Virology*, 101, 785-790.
- FULLER, C. M., BRODD, L., IRVINE, R. M., ALEXANDER, D. J. & ALDOUS, E. W. 2010. Development of an L gene real-time reverse-transcription PCR assay for the detection of avian paramyxovirus type 1 RNA in clinical samples. *Archives of Virology*, 155, 817-23.
- GANAR, K., DAS, M., SINHA, S. & KUMAR, S. 2014. Newcastle disease virus: current status and our understanding. *Virus research*, 184, 71-81.
- GHEDIN, E., SENGAMALAY, N. A., SHUMWAY, M., ZABORSKY, J., FELDBLYUM, T., SUBBU, V., SPIRO, D. J., SITZ, J., KOO, H., BOLOTOV, P., DERNOVOY, D., TATUSOVA, T., BAO, Y., ST GEORGE, K., TAYLOR, J., LIPMAN, D. J., FRASER, C. M., TAUBENBERGER, J. K. & SALZBERG, S. L. 2005. Large-scale sequencing of human influenza reveals the dynamic nature of viral genome evolution. *Nature*, 437, 1162-1166.
- GHOSH, A., MEHTA, A. & KHAN, A. M. 2019. Metagenomic Analysis and its Applications. *In: RANGANATHAN, S., GRIBSKOV, M., NAKAI, K. & SCHÖNBACH, C. (eds.) Encyclopedia of Bioinformatics and Computational Biology*. Oxford: Academic Press.
- GIFFORD, R., KABAT, P., MARTIN, J., LYNCH, C. & TRISTEM, M. 2005. Evolution and distribution of class II-related endogenous retroviruses. *Journal of virology*, 79, 6478-6486.
- GONDA, M. A. 1999. Bovine Immunodeficiency Virus (Retroviridae). *In: GRANOFF, A. & WEBSTER, R. G. (eds.) Encyclopedia of Virology (Second Edition)*. Oxford: Elsevier.

GYURANECZ, M., FOSTER, J. T., DÁN, Á., IP, H. S., EGSTAD, K. F., PARKER, P. G., HIGASHIGUCHI, J. M., SKINNER, M. A., HÖFLE, U., KREIZINGER, Z., DORRESTEIN, G. M., SOLT, S., SÓS, E., KIM, Y. J., UHART, M., PEREDA, A., GONZÁLEZ-HEIN, G., HIDALGO, H., BLANCO, J. M. & ERDÉLYI, K. 2013. Worldwide phylogenetic relationship of avian poxviruses. *Journal of Virology*, 87, 4938-51.

HALL, T. A. BioEdit: a user-friendly biological sequence alignment editor and analysis program for Windows 95/98/NT. Nucleic acids symposium series, 1999. Oxford, 95-98.

HANSON, R. P. & SPALATIN, J. 1978. Thermostability of the hemagglutinin of Newcastle disease virus as a strain marker in epizootologic studies. *Avian Diseases*, 22, 659-65.

HARRACH, B. 2014. Adenoviruses: General Features. Reference Module in Biomedical Sciences. Elsevier.

HARRIS, D. J. & OGLESBEE, B. L. 2006. Chapter 169 - Avian Infectious Diseases. In: BIRCHARD, S. J. & SHERDING, R. G. (eds.) *Saunders Manual of Small Animal Practice (Third Edition)*. Saint Louis: W.B. Saunders.

HE, Y., LU, B., DIMITROV, K. M., LIANG, J., CHEN, Z., ZHAO, W., QIN, Y., DUAN, Q., ZHOU, Y., LIU, L., LI, B., YU, L., DUAN, Z. & LIU, Q. 2020. Complete Genome Sequencing, Molecular Epidemiological, and Pathogenicity Analysis of Pigeon Paramyxoviruses Type 1 Isolated in Guangxi, China during 2012-2018. *Viruses*, 12.

HERCZEG, J., WEHMANN, E., BRAGG, R. R., TRAVASSOS DIAS, P. M., HADJIEV, G., WERNER, O. & LOMNICZI, B. 1999. Two novel genetic groups (VIIb and VIII) responsible for recent Newcastle disease outbreaks in Southern Africa, one (VIIb) of which reached Southern Europe. *Archives of Virology*, 144, 2087-2099.

HERDT, P. D. & PASMANS, F. 2009. 15 - Pigeons. In: TULLY, T. N., DORRESTEIN, G. M., JONES, A. K. & COOPER, J. E. (eds.) *Handbook of Avian Medicine (Second Edition)*. Edinburgh: W.B. Saunders.

HINES, N. L. & MILLER, C. L. 2012. Avian Paramyxovirus Serotype-1: A Review of Disease Distribution, Clinical Symptoms, and Laboratory Diagnostics. *Veterinary Medicine International*, 2012, 708216.

HOFFMANN, B., BEER, M., REID, S. M., MERTENS, P., OURA, C. A., VAN RIJN, P. A., SLOMKA, M. J., BANKS, J., BROWN, I. H., ALEXANDER, D. J. & KING, D. P. 2009. A review of RT-PCR technologies used in veterinary virology and disease control: sensitive and specific diagnosis of five livestock diseases notifiable to the World Organisation for Animal Health. *Veterinary Microbiology*, 139, 1-23.

HOLMES, E. C. 2010. The Evolution and Emergence of RNA Viruses. *Emerging Infectious Diseases*, 16.

HONNAY, O. 2008. Genetic Drift. In: FATH, B. (ed.) *Encyclopedia of Ecology (Second Edition)*. Oxford: Elsevier.

HUGHES, A. L., IRAUSQUIN, S. & FRIEDMAN, R. 2010. The evolutionary biology of poxviruses. *Infection, Genetics and Evolution*, 10, 50-9.

HÜPPI, L., RUGGLI, N., PYTHON, S., HOOP, R., ALBINI, S., GRUND, C. & VÖGTLIN, A. 2020. Experimental pigeon paramyxovirus-1 infection in chicken: evaluation of infectivity, clinical and pathological manifestations and diagnostic methods. *Journal of General Virology*, 101, 156-167.

HURLEY, S., EDEN, J., BINGHAM, J., RODRIGUEZ, M., NEAVE, M., JOHNSON, A., HOWARD-JONES, A., KOK, J., ANAZODO, A., MCMULLAN, B., WILLIAMS, D., WATSON, J., SOLINAS, A., KIM, K. & RAWLINSON, W. 2023. Fatal Human Neurologic Infection Caused by Pigeon Avian Paramyxovirus-1, Australia. *Emerging infectious diseases*, 29, 2482-2487.

HUSSAIN, T., MANZOOR, S., WAHEED, Y., TARIQ, H. & HANIF, K. 2012. Phylogenetic analysis of torque teno virus genome from Pakistani isolate and incidence of co-infection among HBV/HCV infected patients. *Virology Journal*, 9, 320.

JAGANATHAN, S., OOI, P. T., PHANG, L. Y., ALLAUDIN, Z. N. B., YIP, L. S., CHOO, P. Y., LIM, B. K., LEMIERE, S. & AUDONNET, J.-C. 2015. Observation of risk factors, clinical manifestations and genetic characterization of recent Newcastle Disease Virus outbreak in West Malaysia. *BMC Veterinary Research*, 11, 219.

JAMES D. CHERRY MD, M., GAIL J. HARRISON MD, SHELDON L. KAPLAN MD, MD, W. J. S. & PETER J. HOTEZ MD, P. 2019. Alphaviruses. Feigin and Cherry's Textbook of Pediatric Infectious Diseases.

JOHNE, R., FERNÁNDEZ-DE-LUCO, D., HÖFLE, U. & MÜLLER, H. 2006. Genome of a novel circovirus of starlings, amplified by multiply primed rolling-circle amplification. *Journal of General Virology*, 87, 1189-1195.

JOHNSTON, K. M. & KEY, D. W. 1992. Paramyxovirus-1 in feral pigeons (*Columba livia*) in Ontario. *The Canadian Veterinary Journal*, 33, 796.

KÄÄRIÄINEN, L., TAKKINEN, K., KERÄNEN, S. & SÖDERLUND, H. 1987. Replication of the genome of alphaviruses. *Journal of Cell Science Supplement*, 7, 231-50.

KAJON, A. E., WEINBERG, J. B. & SPINDLER, K. R. 2019. Adenoviruses. Reference Module in Biomedical Sciences. Elsevier.

KALETA, E. Paramyxoviruses in free-living and captive birds-a brief account. Workshop on avian paramyxoviruses, 1992. Germany: Rauischholzhausen, 29.

KANG, S. T., WANG, H. C., YANG, Y. T., KOU, G. H. & LO, C. F. 2013. The DNA virus white spot syndrome virus uses an internal ribosome entry site for translation of the highly expressed nonstructural protein ICP35. *Journal of Virology*, 87, 13263-78.

KAPIKIAN, A. Z. & SHOPE, R. E. 1996. Rotaviruses, Reoviruses, Coltiviruses, and Orbiviruses. In: BARON, S. (ed.) Medical Microbiology. Galveston (TX): University of Texas Medical Branch at Galveston, Copyright © 1996, The University of Texas Medical Branch at Galveston.

KASCHULA, V., CANHAM, AS, DIESEL, AM & COLES, J. 1946. Newcastle disease in Natal. *Journal of the South African Veterinary Association*, 17, 1-14.

KASTELIC, M., PŠENIČNIK, I., GREGURIĆ GRAČNER, G., ČEBULJ KADUNC, N., LINDTNER KNIFIC, R., SLAVEC, B., KRAPEŽ, U., VERGLES RATAJ, A., ZORMAN ROJS, O., PULKO, B., RAJŠP, M., MLAKAR HRŽENJAK, N. & DOVČ, A. 2021. Health Status and Stress in Different Categories of Racing Pigeons. *Animals : an open access journal from MDPI*, 11, 2686.

KHALIFEH, A., KRABERGER, S., DZIEWULSKA, D., VARSANI, A. & STENZEL, T. 2021. A Pilot Study Investigating the Dynamics of Pigeon Circovirus Recombination in Domesticated Pigeons Housed in a Single Loft. *Viruses*, 13.

KHAN, J. S., PROVENCHER, J. F., FORBES, M. R., MALLORY, M. L., LEBARBENCHON, C. & MCCOY, K. D. 2019. Chapter One - Parasites of seabirds: A survey of effects and ecological implications. *In: SHEPPARD, C. (ed.) Advances in Marine Biology*. Academic Press.

KHORDADMEHR, M., FIROUZAMANDI, M., ZEHTAB NAJAFI, M. & SHAHBAZI, R. 2017. Naturally Occurring Co-infection of Avian Leukosis Virus (subgroups A-E) and Reticuloendotheliosis Virus in Green Peafowls (*Pavo muticus*). *Revista Brasileira de Ciência Avícola*, 19, 609-614.

KING, A. M. Q., ADAMS, M. J., CARSTENS, E. B. & LEFKOWITZ, E. J. 2012. Family - Circoviridae. *Virus Taxonomy*. San Diego: Elsevier.

KLUGE, E. 1964. Newcastle disease and its control in South Africa. *Bulletin of the Office International des Epizooties*, 62, 897-902.

KOEPPEL, K. N., KEMP, L. V., MAARTENS, L. H. & THOMPSON, P. N. 2020. Immunogenicity of Newcastle Disease Vaccine in Southern Ground-hornbill (*Bucorvus leadbeateri*). *Journal of Avian Medicine and Surgery*, 34, 229-236.

KOFSTAD, T. & JONASSEN, C. M. 2011. Screening of Feral and Wood Pigeons for Viruses Harboring a Conserved Mobile Viral Element: Characterization of Novel Astroviruses and Picornaviruses. *PLOS ONE*, 6, e25964.

KONG, Y., YAN, C., ZHANG, G., CAI, Y., HE, B. & LI, Y. 2021. Detection of pigeon circoviruses in ticks of sheep and camels in Inner Mongolia, China. *bioRxiv*, 2021.06.09.447674.

KRAMER, J. A. 2019. Chapter 13 - Diseases of the Gastrointestinal System. *In*: MARINI, R., WACHTMAN, L., TARDIF, S., MANSFIELD, K. & FOX, J. (eds.) *The Common Marmoset in Captivity and Biomedical Research*. Academic Press.

KUHN, J. H., ABE, J., ADKINS, S., ALKHOVSKY, S. V., AVŠIČ-ŽUPANC, T., AYLLÓN, M. A., BAHL, J., BALKEMA-BUSCHMANN, A., BALLINGER, M. J., KUMAR BARANWAL, V., BEER, M., BEJERMAN, N., BERGERON, É., BIEDENKOPF, N., BLAIR, C. D., BLASDELL, K. R., BLOUIN, A. G., BRADFUTE, S. B., BRIESE, T., BROWN, P. A., BUCHHOLZ, U. J., BUCHMEIER, M. J., BUKREYEV, A., BURT, F., BÜTTNER, C., CALISHER, C. H., CAO, M., CASAS, I., CHANDRAN, K., CHARREL, R. N., KUMAR CHATURVEDI, K., CHOOI, K. M., CRANE, A., DAL BÓ, E., CARLOS DE LA TORRE, J., DE SOUZA, W. M., DE SWART, R. L., DEBAT, H., DHEILLY, N. M., DI PAOLA, N., DI SERIO, F., DIETZGEN, R. G., DIGIARO, M., DREXLER, J. F., DUPREX, W. P., DÜRRWALD, R., EASTON, A. J., ELBEAINO, T., ERGÜNAY, K., FENG, G., FIRTH, A. E., FOOKS, A. R., FORMENTY, P. B. H., FREITAS-ASTÚA, J., GAGO-ZACHERT, S., LAURA GARCÍA, M., GARCÍA-SASTRE, A., GARRISON, A. R., GASKIN, T. R., GONG, W., GONZALEZ, J.-P. J., DE BELLOCQ, J., GRIFFITHS, A., GROSCHUP, M. H., GÜNTHER, I., GÜNTHER, S., HAMMOND, J., HASEGAWA, Y., HAYASHI, K., HEPOJOKI, J., HIGGINS, C. M., HONGŌ, S., HORIE, M., HUGHES, H. R., HUME, A. J., HYNDMAN, T. H., IKEDA, K., JIĀNG, D., JONSON, G. B., JUNGLEN, S., KLEMPA, B., KLINGSTRÖM, J., KONDŌ, H., KOONIN, E. V., KRUPOVIC, M., KUBOTA, K., KURATH, G., LAENEN, L., LAMBERT, A. J., LĚ, J., LI, J.-M., LIU, R., LUKASHEVICH, I. S., MACDIARMID, R. M., MAES, P., MARKLEWITZ, M., MARSHALL, S. H., MARZANO, S.-Y. L., MCCAULEY, J. W., MIRAZIMI, A., et al. 2023. Annual (2023) taxonomic update of RNA-directed RNA polymerase-encoding negative-sense RNA viruses (realm Riboviria: kingdom Orthornavirae: phylum Negarnaviricota). *Journal of General Virology*, 104.



KUIKEN, T., BREITBART, M., BEER, M., GRUND, C., HÖPER, D., VAN DEN HOOGEN, B., KERKHOFFS, J. H., KROES, A. C. M., ROSARIO, K., VAN RUN, P., SCHWARZ, M., SVRAKA, S., TEIFKE, J. & KOOPMANS, M. 2018. Zoonotic Infection With Pigeon Paramyxovirus Type 1 Linked to Fatal Pneumonia. *The Journal of Infectious Diseases*, 218, 1037-1044.

KUIKEN, T., BUIJS, P., VAN RUN, P., VAN AMERONGEN, G., KOOPMANS, M. & VAN DEN HOOGEN, B. 2017. Pigeon paramyxovirus type 1 from a fatal human case induces pneumonia in experimentally infected cynomolgus macaques (*Macaca fascicularis*). *Veterinary Research*, 48, 80.

KUMAR, K. V., SHEKHAR, M. S., OTTA, S. K., KARTHIC, K., KUMAR, J. A., GOPIKRISHNA, G. & VIJAYAN, K. K. 2018. First Report of a Complete Genome Sequence of White spot syndrome virus from India. *Genome Announcements*, 6, e00055-18.

LAMB, K. D., PERRING, A. E., SAMSET, B., PETERSON, D., DAVIS, S., ANDERSON, B. E., BEYERSDORF, A., BLAKE, D. R., CAMPUZANO-JOST, P., CORR, C. A., DISKIN, G. S., KONDO, Y., MOTEKI, N., NAULT, B. A., OH, J., PARK, M., PUSEDE, S. E., SIMPSON, I. J., THORNHILL, K. L., WISTHALER, A. & SCHWARZ, J. P. 2018. Estimating Source Region Influences on Black Carbon Abundance, Microphysics, and Radiative Effect Observed Over South Korea. *Journal of Geophysical Research: Atmospheres*, 123, 13,527-13,548.

LEU, J. H., TSAI, J. M. & LO, C. F. 2008. White Spot Syndrome Virus. In: MAHY, B. W. J. & VAN REGENMORTEL, M. H. V. (eds.) *Encyclopedia of Virology (Third Edition)*. Oxford: Academic Press.

LI, J., MENG, F., LI, W., WANG, Y., CHANG, S., ZHAO, P. & CUI, Z. 2018. Characterization of avian leukosis virus subgroup J isolated between 1999 and 2013 in China. *Poultry Science*, 97, 3532-3539.

LISTER, S., ALEXANDER, D. & HOGG, R. 1986. Evidence for the presence of avian paramyxovirus type 1 in feral pigeons in England and Wales. *The Veterinary Record*, 118, 476-479.

LIU, X. F., WAN, H. Q., NI, X. X., WU, Y. T. & LIU, W. B. 2003. Pathotypical and genotypical characterization of strains of Newcastle disease virus isolated from outbreaks in chicken and goose flocks in some regions of China during 1985-2001. *Archives of Virology*, 148, 1387-403.

LOIKO, M., JUNQUEIRA, D., VARELA, A. P. M., TOCHETTO, C., SCHEFFER, C. M., LIMA, D., MOREL, A., CERVA, C., PAIM, W., MAYER, F. & ROEHE, P. 2018. Columbidae circoviruses detected in free ranging pigeons from Southern Brazil: insights on PiCV. *Archives of Virology*, 163, 1-8.

ŁUKASZUK, E. & STENZEL, T. 2020. Occurrence and Role of Selected RNA-Viruses as Potential Causative Agents of Watery Droppings in Pigeons. *Pathogens* (Basel, Switzerland), 9, 1025.

LUMEIJ, J. T. & STAM, J. W. E. 1985. Paramyxovirus disease in racing pigeons. *Veterinary Quarterly*, 7, 60-65.

MACLACHLAN, N. J. & DUBOVI, E. J. 2017. Chapter 13 - Circoviridae and Anelloviridae. In: MACLACHLAN, N. J. & DUBOVI, E. J. (eds.) *Fenner's Veterinary Virology (Fifth Edition)*. Boston: Academic Press.

MANKERTZ, A. 2008. Circoviruses. In: MAHY, B. W. J. & VAN REGENMORTEL, M. H. V. (eds.) *Encyclopedia of Virology (Third Edition)*. Oxford: Academic Press.

MANKERTZ, A., HATTERMANN, K., EHLERS, B. & SOIKE, D. 2000. Cloning and sequencing of columbid circovirus (CoCV), a new circovirus from pigeons. *Archives of Virology*, 145, 2469-2479.

MANSOUR, S. M. G., ELBAKREY, R. M., MOHAMED, F. F., HAMOUDA, E. E., ABDALLAH, M. S., ELBESTAWY, A. R., ISMAIL, M. M., ABDIEN, H. M. F. & EID, A. A. M. 2021. Avian Paramyxovirus Type 1 in Egypt: Epidemiology, Evolutionary Perspective, and Vaccine Approach. *Frontiers in Veterinary Science*, 8.

MANZIN, A., MALLUS, F., MACERA, L., MAGGI, F. & BLOIS, S. 2015. Global impact of Torque teno virus infection in wild and domesticated animals. *Journal of Infection in Developing Countries*, 9, 562-70.

MARLIER, D. & VINDEVOGEL, H. 2006. Viral infections in pigeons. *The Veterinary Journal*, 172, 40-51.

MARTINI, M. C., CASERTA, L. C., DOS SANTOS, M., BARNABÉ, A. C. S., DURÃES-CARVALHO, R., PADILLA, M. A., SIMÃO, R. M., RIZOTTO, L. S., SIMAS, P. V. M., BASTOS, J. C. S., CARDOSO, T. C., FELIPPE, P. A. N., FERREIRA, H. L. & ARNS, C. W. 2018. Avian coronavirus isolated from a pigeon sample induced clinical disease, tracheal ciliostasis, and a high humoral response in day-old chicks. *Avian Pathology*, 47, 286-293.

MATLOCK, B. 2015. Assessment of nucleic acid purity. *Technical Note*, 52646, 1-2.

MEGAHED, M. M., MOHAMED, W. K. & HASSANIN, O. A Complex Genetic Diversity of Newcastle Disease Virus (Ndv) In Africa Continent: An Updated Review. 2020.

MILLER, P. J. 2014. Newcastle Disease in Poultry. *MSD Veterinary Manual*. New Jersey, USA: Merck Sharp & Dohme Corp.

MOLINI, U., AIKUKUTU, G., KHAISEB, S., CATTOLI, G. & DUNDON, W. G. 2018. Phylogenetic Analysis of Pigeon Paramyxoviruses Type-1 Identified in Mourning Collared-doves (*Streptopelia decipiens*) in Namibia, Africa. *Journal of Wildlife Diseases*, 54, 601-606.

MOLINI, U., AIKUKUTU, G., KHAISEB, S., CATTOLI, G. & DUNDON, W. G. 2017. First genetic characterization of newcastle disease viruses from Namibia: identification of a novel VIIk subgenotype. *Archives in Virology*, 162, 2427-2431.

MONNE, I., BEATO, M. S., CAPUA, I. & MANDOLA, M. 2006. Pigeon paramyxovirus isolated from a robin in Italy. *The Veterinary record*, 158, 384.

MOSER, L. & SCHULTZ-CHERRY, S. 2008. Astroviruses. *In: MAHY, B. W. J. & VAN REGENMORTEL, M. H. V. (eds.) Encyclopedia of Virology (Third Edition)*. Oxford: Academic Press.

NAIR, V. 2022. Chapter 17 - Tumors of the avian immune system. *In: KASPERS, B., SCHAT, K. A., GÖBEL, T. W. & VERVELDE, L. (eds.) Avian Immunology (Third Edition)*. Boston: Academic Press.

NAVEEN, K. A., SINGH, S. D., KATARIA, J. M., BARATHIDASAN, R. & DHAMA, K. 2013. Detection and differentiation of pigeon paramyxovirus serotype-1 (PPMV-1) isolates by RT-PCR and restriction enzyme analysis. *Tropical Animal Health and Production*, 45, 1231-6.

NOOIJ, S., SCHMITZ, D., VENNEMA, H., KRONEMAN, A. & KOOPMANS, M. P. G. 2018. Overview of Virus Metagenomic Classification Methods and Their Biological Applications. *Frontiers in Microbiology*.

OBANDA, V., MICHUKI, G., JOWERS, M. J., RUMBERIA, C., MUTINDA, M., LWANDE, O. W., WANGORU, K., KASIITI-ORENGO, J., YONGO, M. & ANGELONE-ALASAAD, S. 2016. COMPLETE GENOMIC SEQUENCE OF VIRULENT PIGEON PARAMYXOVIRUS IN LAUGHING DOVES (*STREPTOPELIA SENEGALENSIS*) IN KENYA. *Journal of Wildlife Diseases*, 52, 599-608.

ODEND'HAL, S. 1983. Avian Leukosis Virus. *In: ODEND'HAL, S. (ed.) The Geographical Distribution of Animal Viral Diseases*. Academic Press.

OGALI, I. N., OKUMU, P. O., MUNGUBE, E. O., LICHOTI, J. K., OGADA, S., MORAA, G. K., AGWANDA, B. R. & OMMEH, S. C. 2020. Genomic and Pathogenic Characteristics of Virulent Newcastle Disease Virus Isolated from Chicken in Live Bird Markets and Backyard Flocks in Kenya. *International Journal of Microbiology*, 2020, 4705768.

OGALI, I. N., WAMUYU, L. W., LICHOTI, J. K., MUNGUBE, E. O., AGWANDA, B. & OMMEH, S. C. 2018. Molecular Characterization of Newcastle Disease Virus from Backyard Poultry Farms and Live Bird Markets in Kenya. *International Journal of Microbiology*, 2018, 2368597.

ONIHARY, A. M., RAZANAJATOVO, I. M., RABETAFIKA, L., BASTARAUD, A., HERAUD, J. M. & RASOLOFO, V. 2021. Genotype Diversity and Spread of White Spot Syndrome Virus (WSSV) in Madagascar (2012-2016). *Viruses*, 13.

Oosthuizen M, 1979, *The history of the South African poultry association*, World's Poultry Science Association, South African Branch, Honeydew, South Africa.

PALGEN, J. L., JURGENS, E. M., MOSCONA, A., POROTTO, M. & PALERMO, L. M. 2015. Unity in diversity: shared mechanism of entry among paramyxoviruses. *Progress in Molecular Biology and Translational Science*, 129, 1-32.

PANDA, A., HUANG, Z., ELANKUMARAN, S., ROCKEMANN, D. D. & SAMAL, S. K. 2004. Role of fusion protein cleavage site in the virulence of Newcastle disease virus. *Microbial Pathogenesis*, 36, 1-10.

PAYNE, S. 2017a. Chapter 14 - Family Astroviridae. *In: PAYNE, S. (ed.) Viruses*. Academic Press.

PAYNE, S. 2017b. Chapter 23 - Family Orthomyxoviridae. *In: PAYNE, S. (ed.) Viruses*. Academic Press.

PAYNE, S. 2017c. Chapter 30 - Other Small DNA Viruses. *In: PAYNE, S. (ed.) Viruses*. Academic Press.

PAYNE, S. L. 2017d. Family Coronaviridae. *Viruses*, 149 - 158.

PEEPLES, M. E. 1988. Newcastle Disease Virus Replication. *In: ALEXANDER, D. J. (ed.) Newcastle Disease*. Boston, MA: Springer US.

PEETERS, B. & KOCH, G. 2021. Newcastle Disease Virus (Paramyxoviridae). *In: BAMFORD, D. H. & ZUCKERMAN, M. (eds.) Encyclopedia of Virology (Fourth Edition)*. Oxford: Academic Press.

PERBAL, B. 2008. Avian myeloblastosis virus (AMV): only one side of the coin. *Retrovirology*, 5, 49.

PEREIRA, M. R., MACHADO, L. C., DE OLIVEIRA CARVALHO, R. D., DE LIMA CAVALCANTI, T. Y. V., DA SILVA FILHO, G. B., DE SOUSA LIMA, T., FONSECA, S. M. C., DE ASSIS LEITE SOUZA, F., DA LUZ WALLAU, G., DE SOUZA MENDONÇA, F. & DE OLIVEIRA FRANCA, R. F. 2022. Identification of a Virulent Newcastle Disease Virus Strain Isolated from Pigeons (*Columbia livia*) in Northeastern Brazil Using Next-Generation Genome Sequencing. *Viruses*, 14, 1579.

PESTKA, D., STENZEL, T. & KONCICKI, A. 2014. Occurrence, characteristics and control of pigeon paramyxovirus type 1 in pigeons. *Polish Journal of Veterinary Science*, 17, 379-84.

PHAN, T. G., VO, N. P., BOROS, Á., PANKOVICS, P., REUTER, G., LI, O. T., WANG, C., DENG, X., POON, L. L. & DELWART, E. 2013. The viruses of wild pigeon droppings. *PLoS One*, 8, e72787.

PIENAAR, A. C. & CILLIERS, J. 1987. The isolation of a paramyxovirus from pigeons in South Africa.

POLLARD, B. & MARAIS, E. J. 1983. Pigeon herpesvirus confirmed in South Africa. *Journal of the South African Veterinary Association*, 54, 247-8.

QIU, X., MENG, C., ZHAN, Y., YU, S., LI, S., REN, T., YUAN, W., XU, S., SUN, Y., TAN, L., SONG, C., LIAO, Y., DING, Z., LIU, X. & DING, C. 2017. Phylogenetic, antigenic and biological characterization of pigeon paramyxovirus type 1 circulating in China. *Virology Journal*, 14, 186.

RAIDAL, S. R. 2012. Chapter 39 - Avian Circovirus and Polyomavirus Diseases. *In: MILLER, R. E. & FOWLER, M. (eds.) Fowler's Zoo and Wild Animal Medicine*. Saint Louis: W.B. Saunders.

REHAN, M. H., ASLAM, A., KHAN, M. I., ABID, M., HUSSAIN, S., UMBER, J., ANJUM, A. & HUSSAIN, A. 2019. Potential Economic Impact of Newcastle Disease Virus Isolated from Wild Birds on Commercial Poultry Industry of Pakistan: A Review. *Hosts and Viruses*.

RIDKY, T. W. & LEIS, J. 2013. Chapter 48 - Rous Sarcoma Virus Retropepsin and Avian Myeloblastosis Virus Retropepsin. In: RAWLINGS, N. D. & SALVESEN, G. (eds.) *Handbook of Proteolytic Enzymes (Third Edition)*. Academic Press.

ROBINSON, D., LIU, J. L., JONES, D., BRUNOVSKIS, P., QIAN, Z., ISFORT, R., TILLOTSON, J. K., LEE, L., WITTER, R., SALTER, D., CRITTENDEN, L., HUGHES, S. & KUNG, H. J. 1997. Avian leukemias and lymphomas: interplay between retroviruses and herpesviruses. *Leukemia*, 11 Suppl 3, 176-8.

ROIZMAN, B. & THAYER, N. 2001. Herpesvirus Family: Herpesviridae [Online]. Available: <http://stdgen.northwestern.edu/stdgen/bacteria/hhv2/herpes.html> [Accessed 12 February 2023].

ROSARIO, K., BREITBART, M., HARRACH, B., SEGALÉS, J., DELWART, E., BIAGINI, P. & VARSANI, A. 2017. Revisiting the taxonomy of the family Circoviridae: establishment of the genus Cyclovirus and removal of the genus Gyrovirus. *Archives of Virology*, 162, 1447-1463.

ROUX, S., MATTHIJNSSENS, J. & DUTILH, B. E. 2021. Metagenomics in Virology. *Encyclopedia of Virology*, 133-140.

RUBBENSTROTH, D., ULRICH, R., WYLEZICH, C., RAUTENSCHLEIN, S., BEER, M. & MOHR, L. 2020. First experimental proof of Rotavirus A (RVA) genotype G18P[17] inducing the clinical presentation of 'young pigeon disease syndrome' (YPDS) in domestic pigeons (*Columba livia*). *Transboundary and Emerging Diseases*, 67, 1507-1516.

RYU, W.-S. 2017. Chapter 17 - Retroviruses. In: RYU, W.-S. (ed.) *Molecular Virology of Human Pathogenic Viruses*. Boston: Academic Press.

SAHINDOKUYUCU, I., TURKMEN, M. B., SUMER, T., ELHAG, A. E., ALCIGIR, M. E., YAZICI, Z., BARRY, G., GULBAHAR, M. Y. & KUL, O. 2022. First detection and molecular characterisation of a pigeon aviadenovirus A and pigeon circovirus co-infection associated with Young Pigeon Disease Syndrome (YPDS) in Turkish pigeons (*Columba livia domestica*). *Veterinary Medicine and Science*, 8, 139-149.

SAMAL, S. K. 2008. Paramyxoviruses of Animals. In: MAHY, B. W. J. & VAN REGENMORTEL, M. H. V. (eds.) *Encyclopedia of Virology (Third Edition)*. Oxford: Academic Press.

SAND, P. H. Commodity or Taboo? International Regulation of Trade in Endangered Species. 2001.

SANDIKLI, M. S. 2021. Newcastle disease. *Ceva Poultry*.

SANTOS, H. M., CHEN, C. C., TSAI, C.-Y., HSISH, Y. C., CHUNG, F. C., TYAN, Y.-C., TAYO, L. L. & CHUANG, K. P. 2020a. Influence of pigeon interferon alpha (PiIFN- $\alpha$ ) on pigeon circovirus (PiCV) replication and cytokine expression in *Columba livia*. *Veterinary Microbiology*, 242, 108591.

SANTOS, H. M., TSAI, C.-Y., CATULIN, G. E. M., TRANGIA, K. C. G., TAYO, L. L., LIU, H.-J. & CHUANG, K. P. 2020b. Common bacterial, viral, and parasitic diseases in pigeons (*Columba livia*): A review of diagnostic and treatment strategies. *Veterinary Microbiology*, 247, 108779.

SILVA, B. B. I., URZO, M. L. R., ENCABO, J. R., SIMBULAN, A. M., LUNARIA, A. J. D., SEDANO, S. A., HSU, K. C., CHEN, C. C., TYAN, Y. C. & CHUANG, K. P. 2022. Pigeon Circovirus over Three Decades of Research: Bibliometrics, Scoping Review, and Perspectives. *Viruses*, 14.

SIMBIZI, V., MOERANE, R., RAMSAY, G., MUBAMBA, C., ABOLNIK, C. & GUMMOW, B. 2021. A study of rural chicken farmers, diseases and remedies in the Eastern Cape province of South Africa. *Preventive Veterinary Medicine*, 194, 105430.



SNOECK, C. J., DUCATEZ, M. F., OWOADE, A. A., FALEKE, O. O., ALKALI, B. R., TAHITA, M. C., TARNAGDA, Z., OUEDRAOGO, J. B., MAIKANO, I., MBAH, P. O., KREMER, J. R. & MULLER, C. P. 2009. Newcastle disease virus in West Africa: new virulent strains identified in non-commercial farms. *Archives in Virology*, 154, 47-54.

SNOECK, C. J., OWOADE, A. A., COUACY-HYMANN, E., ALKALI, B. R., OKWEN, M. P., ADEYANJU, A. T., KOMOYO, G. F., NAKOUNÉ, E., LE FAOU, A. & MULLER, C. P. 2013. High genetic diversity of Newcastle disease virus in poultry in West and Central Africa: cocirculation of genotype XIV and newly defined genotypes XVII and XVIII. *Journal of Clinical Microbiology*, 51, 2250-60.

STENZEL, T. & KONCICKI, A. 2017. The epidemiology, molecular characterization and clinical pathology of circovirus infections in pigeons - current knowledge. *Veterinary Quarterly*, 37, 166-174.

STENZEL, T., DZIEWULSKA, D., TYKAŁOWSKI, B., SMIALEK, M. & KONCICKI, A. 2012. Epidemiological investigation of selected pigeon viral infections in Poland. *The Veterinary record*, 171.

STENZEL, T., PIASECKI, T., CHRZĄSTEK, K., JULIAN, L., MUHIRE, B. M., GOLDEN, M., MARTIN, D. P. & VARSANI, A. 2014. Pigeon circoviruses display patterns of recombination, genomic secondary structure and selection similar to those of beak and feather disease viruses. *Journal of General Virology*, 95, 1338-1351.

STERN, A. & ANDINO, R. 2016. Chapter 17 - Viral Evolution: It Is All About Mutations. In: KATZE, M. G., KORTH, M. J., LAW, G. L. & NATHANSON, N. (eds.) *Viral Pathogenesis (Third Edition)*. Boston: Academic Press.

STONE, N. P., DEMO, G., AGNELLO, E. & KELCH, B. A. 2019. Principles for enhancing virus capsid capacity and stability from a thermophilic virus capsid structure. *Nature Communications*, 10, 4471.

STUCKER, K. M., STOCKWELL, T. B., NYAGA, M. M., HALPIN, R. A., FEDOROVA, N., AKOPOV, A., NGOVENI, H., PEENZE, I., SEHERI, M. L., MPHABLELE, M. J. &

WENTWORTH, D. E. 2015. Complete genomic sequence for an avian group G rotavirus from South Africa. *Genome Announcements*, 3.

SUSTA, L., MILLER, P. J., AFONSO, C. L. & BROWN, C. C. 2011. Clinicopathological characterization in poultry of three strains of Newcastle disease virus isolated from recent outbreaks. *Veterinary Pathology*, 48, 349-60.

SWAYNE, D. & BROWN, I. H. 2021. Newcastle disease (Infection with Newcastle disease virus). In: ANYNOUMUS (ed.) *Manual of Diagnostic Tests and Vaccines for Terrestrial Animals 2021*. World Organisation for Animal Health.

SYKES, J. E. & RANKIN, S. C. 2013. Isolation in Cell Culture. *Canine and Feline Infectious Diseases*, 2 - 9.

TAKIMOTO, T., TAYLOR, G. L., CONNARIS, H. C., CRENNELL, S. J. & PORTNER, A. 2002. Role of the hemagglutinin-neuraminidase protein in the mechanism of paramyxovirus-cell membrane fusion. *Journal of virology*, 76, 13028-13033.

TATE, J. E. & BRESEE, J. S. 2012. 240 - Astroviruses. In: LONG, S. S. (ed.) *Principles and Practice of Pediatric Infectious Diseases (Fourth Edition)*. London: Elsevier.

THAM, M. L., YUSOFF, K., OTHMAN, S. & CHIA, S. L. 2019. V protein, the virulence factor across the family Paramyxoviridae: a review. *Asia Pacific Journal of Molecular Biology and Biotechnology*.

TODD, D. 2000. Circoviruses: immunosuppressive threats to avian species: a review. *Avian Pathology*, 29, 373-94.

TODD, D., FRINGUELLI, E., SCOTT, A. N. J., BORGHMANS, B. J., DUCHATEL, J. P., SHIVAPRASAD, H. L., RAIDAL, S. R., ABADIE, J. X., FRANCIOSINI, M. P. & SMYTH, J. A. 2008. Sequence comparison of pigeon circoviruses. *Research in Veterinary Science*, 84, 311-319.

TODD, D., WESTON, J. H., SOIKE, D. & SMYTH, J. A. 2001. Genome Sequence Determinations and Analyses of Novel Circoviruses from Goose and Pigeon. *Virology*, 286, 354-362.

TUTHILL, T. J., GROPELLI, E., HOGLE, J. M. & ROWLANDS, D. J. 2010. Picornaviruses. *Current Topics on Microbiology and Immunology*, 343, 43-89.

VERECKEN, M., HERDT, P. & DUCATELLE, R. 1998. Adenovirus infections in pigeons: A review. *Avian pathology : Journal of the World Veterinary Poultry Association*, 27, 333-8.

VIBIN, J., CHAMINGS, A., COLLIER, F., KLAASSEN, M., NELSON, T. M. & ALEXANDERSEN, S. 2018. Metagenomics detection and characterisation of viruses in faecal samples from Australian wild birds. *Scientific Reports*, 8, 8686.

VIDOVSKY, M. Z., KAPITÁNY, S., GELLÉRT, Á., HARRACH, B., GÖRFÖL, T., BOLDOGH, S. A., KOHL, C., WIBBELT, G., MÜHLDORFER, K., KEMENESI, G., GEMBU, G.-C., HASSANIN, A., TU, V. T., ESTÓK, P., HORVÁTH, A. & KAJÁN, G. L. 2023. Detection and genetic characterization of circoviruses in more than 80 bat species from eight countries on four continents. *Veterinary Research Communications*, 47, 1561-1573.

WAFAA, A. A. E.-G. 2023. Pigeon Paramyxovirus-1 Infection and the Public Health Importance: A Review Article. *Veterinarija ir Zootechnika*, 81, 23-32.

WAN, C., CHEN, C., CHENG, L., SHI, S., FU, G., LIU, R., CHEN, H., FU, Q. & HUANG, Y. 2018. Detection of novel adenovirus in sick pigeons. *Journal of Veterinary Medical Science*, 80, 1025-1028.

WANG, H.-Y., WU, M.-C., CHEN, H.-W., LAI, Y.-C., HUANG, W.-H., CHANG, H.-W., JENG, C.-R., CHENG, C.-H., WANG, P.-J., LAI, Y.-H. & CHANG, Y.-C. 2023. Isolation, full sequence analysis, and in situ hybridization of pigeon paramyxovirus-1 genotype VI.2.1.1.2.2 from oriental turtle doves (*Streptopelia orientalis*). *Poultry Science*, 102, 102974.

WANG, H., GAO, H., JIANG, Z., SHI, L., ZHAO, P., ZHANG, Y. & WANG, C. 2022. Molecular detection and phylogenetic analysis of pigeon circovirus from racing pigeons in Northern China. *BMC Genomics*, 23, 290.

WANG, J., LIU, H., LIU, W., ZHENG, D., ZHAO, Y., LI, Y., WANG, Y., GE, S., LV, Y., ZUO, Y., YU, S. & WANG, Z. 2015. Genomic Characterizations of Six Pigeon Paramyxovirus Type 1 Viruses Isolated from Live Bird Markets in China during 2011 to 2013. *PLOS ONE*, 10, e0124261.

WANG, P., LI, M., LI, H., LIN, L., SHI, M., GU, Z., GAO, Y., HUANG, T., MO, M., WEI, T. & WEI, P. 2020. Full-length cDNA sequence analysis of 85 avian leukosis virus subgroup J strains isolated from chickens in China during the years 1988-2018: coexistence of 2 extremely different clusters that are highly dependent upon either the host genetic background or the geographic location. *Poultry Science*, 99, 3469-3480.

WEI, T., DENG, Q., LI, H., PAN, C., ZHAI, G., YUAN, Y., CHENG, E., ZHANG, Y., MO, M., HUANG, T. & WEI, P. 2018. Molecular characterization of two novel sub-sublineages of pigeon paramyxovirus type 1 in China. *Archives of Virology*, 163, 2971-2984.

WERNER, O., RÖMER-OBBERDÖRFER, A., KÖLLNER, B., MANVELL, R. J. & ALEXANDER, D. J. 1999. Characterization of avian paramyxovirus type 1 strains isolated in Germany during 1992 to 1996. *Avian Pathology*, 28, 79-88.

WHITLEY, R. J. 1996. Herpesviruses. In: BARON, S. (ed.) *Medical Microbiology*. Galveston (TX): University of Texas Medical Branch at Galveston, Copyright © 1996, The University of Texas Medical Branch at Galveston.

WILLE, M., SHI, M., KLAASSEN, M., HURT, A. C. & HOLMES, E. C. 2019. Virome heterogeneity and connectivity in waterfowl and shorebird communities. *ISME journal*, 13, 2603-2616.

WISEMAN, A., BERMAN, E. M. & KLEMENT, E. 2018. Risk factors for Newcastle disease in broiler farms in Israel. *Preventive Veterinary Medicine*, 149, 92-97.

WOODS, L., LATIMER, K., BARR, B., NIAGRO, F., CAMPAGNOLI, R., NORDHAUSEN, R. & CASTRO, A. 1993. Circovirus-Like Infection in a Pigeon. *Journal of veterinary diagnostic investigation : official publication of the American Association of Veterinary Laboratory Diagnosticians, Inc*, 5, 609-12.

WOOLHOUSE, M. E. & GOWTAGE-SEQUERIA, S. 2005. Host range and emerging and reemerging pathogens. *Emerging Infectious Diseases*, 11, 1842-7.

WOŹNIAKOWSKI, G. J., SAMOREK-SALAMONOWICZ, E., SZYMAŃSKI, P., WENCEL, P. & HOUSZKA, M. 2013. Phylogenetic analysis of Columbid herpesvirus-1 in rock pigeons, birds of prey and non-raptorial birds in Poland. *BMC Veterinary Research*, 9, 52.

XIE, P., CHEN, L., ZHANG, Y., LIN, Q., DING, C., LIAO, M., XU, C., XIANG, B. & REN, T. 2020. Evolutionary Dynamics and Age-Dependent Pathogenesis of Sub-Genotype VI.2.1.1.2.2 PPMV-1 in Pigeons. *Viruses*, 12, 433.

XIE, P., CHEN, L., ZHANG, Y., LIN, Q., DING, C., LIAO, M., XU, C., XIANG, B. & REN, T. 2020. Evolutionary Dynamics and Age-Dependent Pathogenesis of Sub-Genotype VI.2.1.1.2.2 PPMV-1 in Pigeons. *Viruses*, 12, 433.

XUE, C., XU, X., YIN, R., QIAN, J., SUN, Y., WANG, C., DING, C., YU, S., HU, S., LIU, X., CONG, Y. & DING, Z. 2017. Identification and pathotypical analysis of a novel VIk sub-genotype Newcastle disease virus obtained from pigeon in China. *Virus Research*, 238, 1-7.

YIN-MURPHY, M. & ALMOND, J. W. 1996. Picornaviruses. In: BARON, S. (ed.) *Medical Microbiology*. Galveston (TX): University of Texas Medical Branch at Galveston, Copyright © 1996, The University of Texas Medical Branch at Galveston.

YU, H., GRASSMANN, C. W. & BEHRENS, S. E. 1999. Sequence and structural elements at the 3' terminus of bovine viral diarrhea virus genomic RNA: functional role during RNA replication. *Journal of Virology*, 73, 3638-48.

- YUAN, L., HENSLEY, C., MAHSOUB, H. M., RAMESH, A. K. & ZHOU, P. 2020. Microbiota in viral infection and disease in humans and farm animals. *Progress in molecular biology and translational science*, 171, 15-60.
- YUAN, P., SWANSON, K. A., LESER, G. P., PATERSON, R. G., LAMB, R. A. & JARDETZKY, T. S. 2011. Structure of the Newcastle disease virus hemagglutinin-neuraminidase (HN) ectodomain reveals a four-helix bundle stalk. *Proceedings of the National Academy of Sciences*, 108, 14920.
- YUSOFF, K. & TAN, W. S. 2001. Newcastle disease virus: Macromolecules and opportunities. *Avian Pathology*, 30, 439-455.
- ZEGHDOUDI, M., AOUN, L., MERDACI, L. & BOUZIDI, N. 2017. Epidemiological features and pathological study of avian leukosis in turkeys' flocks. *Veterinary World*, 10, 1135-1138.
- ZHANG, Z., DAI, W., WANG, S. & DAI, D. 2015. Epidemiology and genetic characteristics of pigeon circovirus (PiCV) in eastern China. *Archives of Virology*, 160, 199-206.
- ZHANG, Z., ZHUANG, L., DAI, W., MAO, H. & DAI, D. 2013. Complete genome sequence of a novel pigeon torque teno virus in China. *Genome Announcements*, 1.
- ZHAO, W., ZHU, A. L., YUAN, C. L., YU, Y., ZHU, C. X., LAN, D. L., YANG, Z. B., CUI, L. & HUA, X. G. 2011. Detection of astrovirus infection in pigeons (*Columbia livia*) during an outbreak of diarrhoea. *Avian Pathology*, 40, 361-5.
- ZHOU, Z., QIU, Y. & GE, X. 2021. The taxonomy, host range and pathogenicity of coronaviruses and other viruses in the Nidovirales order. *Animal Diseases*, 1, 5.
- ZHU, F., TWAN, W.-H., TSENG, L.-C., PENG, S.-H. & HWANG, J.-S. 2019. First detection of white spot syndrome virus (WSSV) in the mud shrimp *Austinopecten edulis* in Taiwan. *Scientific Reports*, 9, 18572.

ZHU, W., DONG, J., XIE, Z., LIU, Q. & KHAN, M. I. 2010. Phylogenetic and pathogenic analysis of Newcastle disease virus isolated from house sparrow (*Passer domesticus*) living around poultry farm in southern China. *Virus Genes*, 40, 231-5.

ZHUANG, Q., LIU, S., ZHANG, X., JIANG, W., WANG, K., WANG, S., PENG, C., HOU, G., LI, J., YU, X., YUAN, L., WANG, J., LI, Y., LIU, H. & CHEN, J. 2020. Surveillance and taxonomic analysis of the coronavirus dominant in pigeons in China. *Transboundary and Emerging Diseases*, 67, 1981-90.

## Appendix A



### agriculture, land reform & rural development

Department:  
Agriculture, Land Reform and Rural Development  
REPUBLIC OF SOUTH AFRICA

Directorate Animal Health, Department of Agriculture, Land Reform & Rural Development  
Private Bag X138, Pretoria 0001

Enquiries: Ms Marna Laing • Tel: +27 12 319 7532 • Fax: +27 12 319 7470 • E-mail: [MarnaL@dalrrd.gov.za](mailto:MarnaL@dalrrd.gov.za)

Reference: 12/11/1/1/8 (2280 LH)

Prof Celia Abolnik  
Department of Production Animal Studies, Poultry Section  
Faculty of Veterinary Science, University Pretoria  
Old Soutpan Road  
Onderstepoort, Pretoria  
Tel: 0824271190  
E-mail: [celia.abolnik@up.ac.za](mailto:celia.abolnik@up.ac.za)

Dear Prof Celia Abolnik,

#### **RE: PERMISSION TO DO RESEARCH IN TERMS OF SECTION 20 OF THE ANIMAL DISEASES ACT, 1984 (ACT NO 35 OF 1984)**

Your application dated 14 January 2022, received by us on 17 January 2022, requesting permission under Section 20 of the Animal Disease Act, 1984 (Act No. 35 of 1984) to perform a research project or study, refers. I am pleased to inform you that permission is hereby granted to perform the following study, with the following conditions:

#### **Conditions:**

1. This permission does not relieve the researcher of any responsibility which may be placed on him by any other act of the Republic of South Africa;
2. This permission is given upon finding the biosecurity of the research project as described to be acceptable to DALRRD;
3. The research project is approved as per the application form dated 14 January 2022 and the correspondence thereafter. Written permission from the Director: Animal Health must be obtained prior to any deviation from the conditions approved for this research project under this Section 20 permit. Please apply in writing to [MarnaL@dalrrd.gov.za](mailto:MarnaL@dalrrd.gov.za);
4. If required, an application for an extension must be made by the responsible researcher at least one month prior to the expiry of this Section 20 permit. Please apply in writing to [MarnaL@dalrrd.gov.za](mailto:MarnaL@dalrrd.gov.za);
5. No part of this research project may begin until the valid ethical approval has been obtained in writing from the relevant South African authority;

SUBJECT: S20 PERMISSION FOR: Molecular epidemiology of pigeon paramyxoviruses (PPMV) in South Africa



6. The following samples may be used as part of this study: Samples currently in the University of Pretoria's repository, as well as new samples submitted to the poultry section for diagnosis and/or sequencing during the study period;
7. Virus isolation and harvesting of tissue samples may only be performed in the Poultry Research Unit BSL 3 facility, and may only be moved to the Poultry Research Laboratory for RNA extraction and molecular testing after inactivation;
8. Samples must be packaged and transported in accordance with International Air Transport Association (IATA) requirements and/or the National Road Traffic Act, 1996 (Act No. 93 of 1996);
9. All potentially infectious material utilised or generated during or by the research project is to be destroyed at completion of the study;
10. Only a waste disposal company registered for the disposal of biohazardous waste may be used for the removal of all potentially infectious waste from the research project; Records must be kept for five years for auditing purposes;
11. Only RNA extracts may be stored under access control in the Poultry Research Laboratory, as per the application form; Virus isolates may only be stored under access control in the Poultry Research Unit BSL 3 facility;
12. DNA amplification products may be sent to the following sequencing service providers: Inqaba Biotech (Pty) Ltd and Stellenbosch University Central Analytical Facility;
13. Stored samples may not be outsourced for research without prior written approval from the Director: Animal Health. Should samples be used for further research, written approval from the Director: Animal Health must be obtained prior to start of project

**Title of research/study:** Molecular epidemiology of pigeon paramyxoviruses (PPMV) in South Africa

**Researcher:** Prof Celia Abolnik

**Institutions:** University of Pretoria, Faculty of Veterinary Science, Department of Production Animal Studies

**Permit Expiry date:** 28 February 2025

**Our ref Number:** 12/11/1/1/8 (2280 LH)

**Your ref:**

Kind regards,



**DR. MPHOMAJA**  
**DIRECTOR OF ANIMAL HEALTH**

**Date:**

2022-02-15

**SUBJECT:** S20 PERMISSION FOR: Molecular epidemiology of pigeon paramyxoviruses (PPMV) in South Africa

## Appendix B



Faculty of Veterinary Science  
Animal Ethics Committee

13 May 2022

### Approval Certificate New Application

**AEC Reference No.:** REC013-22  
**Title:** Molecular epidemiology of pigeon paramyxoviruses (PPMV) in South Africa  
**Researcher:** Ms MC Hayes  
**Student's Supervisor:** Prof C Abolnik

Dear Ms MC Hayes,

The **New Application** as supported by documents received between 2022-02-15 and 2022-05-03 for your research, was approved by the Animal Ethics Committee on its quorate meeting of 2022-05-03.

Please note the following about your ethics approval:

1. The use of species is approved:

| Species   | Number |
|---|--------|
| Birds (wild) - Feral pigeons and doves                      | 50     |
| Samples   | Number |
| Dead bird samples (Samples from live animals)               | 50     |
| Organ pool, alantoic fluid (Stored- Historic/Retrospective) | 18     |

2. Ethics Approval is valid for 1 year and needs to be renewed annually by 2023-05-13.
3. Please remember to use your protocol number (REC013-22) on any documents or correspondence with the AEC regarding your research.
4. Please note that the AEC may ask further questions, seek additional information, require further modification, monitor the conduct of your research, or suspend or withdraw ethics approval.
5. **All incidents** must be reported by the PI by email to Ms Marleze Rheeder (AEC Coordinator) within 3 days, and must be subsequently submitted electronically on the application system within 14 days.
6. The committee also requests that you record major procedures undertaken during your study for own-archiving, using any available digital recording system that captures in adequate quality, as it may be required if the committee needs to evaluate a complaint. However, if the committee has monitored the procedure previously or if it is generally can be considered routine, such recording will not be required.

#### Ethics approval is subject to the following:

- The ethics approval is conditional on the research being conducted as stipulated by the details of all documents submitted to the Committee. In the event that a further need arises to change who the investigators are, the methods or any other aspect, such changes must be submitted as an Amendment for approval by the Committee.

Room 6-13, Arnold Theiler Building, Onderstepoort  
Private Bag X04, Onderstepoort 0110, South Africa  
Tel +27 12 529 8434  
Fax +27 12 529 8321  
Email: marleze.rheeder@up.ac.za

Fakulteit Veeartsenykunde  
Lefapha la Diseense tsa Bongakadirulwa

We wish you the best with your research.

Yours sincerely



**Prof V Naidoo**  
**CHAIRMAN: UP-Animal Ethics Committee**

---

Room 6-13, Arnold Theiler Building, Onderstepoort  
Private Bag X04, Onderstepoort 0110, South Africa  
Tel +27 12 529 8434  
Fax +27 12 529 8321  
Email: marleze.rheeder@up.ac.za

Fakulteit Veeartsenykunde  
Lefapha la Diseanse tša Bongakadiriwa

## **Appendix C**

Link on Figshare: [10.6084/m9.figshare.24994856](https://www.figshare.com/entries/10.6084/m9.figshare.24994856)

## Appendix D



## agriculture, land reform & rural development

Department:  
Agriculture, Land Reform and Rural Development  
REPUBLIC OF SOUTH AFRICA

### CERTIFICATE OF COMPLIANCE

This is to certify that:

**University of Pretoria**

**Poultry Research Unit (PRU) BSL3**

DAH Compliance Number:

**DAH-CQ06**

is a DAH Compliant Animal Quarantine BSL3 Facility

provided that all DAH conditions and requirements are complied with.

The facility complies with the requirements of Procedure Manual: Laboratory/Facility

Biosafety and Biosecurity including Biobanks and Vector Protection and

FORM: DAH AF BSL3.

A handwritten signature in black ink, appearing to read 'M. Majo', written over a horizontal line.

**Director: Animal Health**

Initial DAH Compliance Date: 2014-05-23

Certificate Commences: 2022-11-18

Certificate Expires: 2024-11-18

